New Insights into Transport Phenomena Involved in Carbonated Water Injection: Effective Mathematical Modeling Strategies

By

© Cleverson Ebeagbor Esene

A thesis submitted to the School of Graduate Studies
In partial fulfillment of the requirements for the degree of

Doctor of Philosophy

Faculty of Engineering and Applied Science

Memorial University of Newfoundland

August 2019

St. John's, Newfoundland, Canada

Dedication

This work is dedicated to my father and all my siblings for all their immense support while I was growing up and even until date.

Specially, I will like to also dedicate this to my mother, Lucy Ebague Esene whom I barely knew as she passed away when I was a kid. I will never forget every teacher that taught me and every student whom I taught during this memorable journey which felt good all-way.

I will never forget my best friend Joseph Isiwele who passed away in his late teen. Thank you for being an ever-lasting influence in my life and I still miss you.

More importantly to my future wife and family. I have left a path for you and a light to lead your way.

I hope you win!

Abstract

Carbonated water injection (CWI) is a promising enhanced oil recovery (EOR) method that provides an efficient and a more environmentally friendly alternative to meet the ever-increasing demand for energy. An additional benefit from the implementation of CWI is the storage of anthropogenic CO_2 and this has made it even more attractive. Over the years, several attempts have been made to model CWI as an EOR process but have been of very little success due to the underlying assumptions used or the modelling strategy. There are several multi-physics involved during CWI and to have an accurate model to investigate CWI, these physics need to be adequately captured. In this thesis, we have attempted to model CWI adequately by using more realistic and practical assumptions to present a novel modeling strategy. This thesis shows our research in a manuscript-based format which is presented in each chapter as major contributions. Firstly, a comprehensive review of CWI where the behavior of fluids, fluid-rock interactions and challenges associated with CWI technique have been thoroughly discussed. Secondly, the modelling investigation to capture the critical salinity which plays an important role in EOR techniques for sandstones and carbonate as well as the solubility of CO_2 during CWI is presented. Thirdly, a 3-D modeling method to investigate CWI which considers important terms such as gravity, non-instantaneous equilibrium, heterogeneity, anisotropy and well orientation is presented. Fourthly, a 1-D core modelling approach which considers the reaction term and rock dissolution in an improved attempt to capture CWI is presented. Finally, a deterministic approach is presented to effectively predict oil recovery factor based on pattern recognition and artificial intelligence. To facilitate this, the use of artificial neural network (ANN), least square support vector machine (LSSVM) modelling and gene expression programming (GEP) are adopted.

Acknowledgments

I would like to express my gratitude to my supervisor Dr Sohrab Zendehboudi whose guidance, patience, willingness and positive actions saw me through my doctoral program at the Memorial University of Newfoundland. I will like to extend my warmest appreciation to my co-supervisors Dr Amer Aborig and Dr Hodjat Shiri for providing positive input and encouragement towards my research with extended greetings to Dr Nima Rezaei, Dr Lesley James, and Dr Steve Butt.

I would like to appreciate the friendship of Oyinka Lawson, Tari Orubide, Oyeaka Mabu, Ruaa Fadul, Shirley Swamidas , Esiro Anarvhe , Kasia Jas, Shirley Erijo, Peter Gulliver, Valerie Parrot and so many friends whose name I have not mentioned. Your positive actions kept my head up in this journey. To everyone I played soccer with, laughed with or at some point crossed my path is indeed given credit for been part of this incredible and memorable journey.

Finally, the financial assistance offered by Equinor (formerly Statoil) Canada, Memorial University (NL, Canada), Natural Sciences and Engineering Research Council of Canada (NSERC), and InnovateNL (formerly RDC) is greatly acknowledged.

.

Table of Contents

List of Tables

List of Figures

Chapter 1 **Introduction**

In an oil reservoir, production is primarily associated with natural depletion which precedes the use of secondary recovery methods such as water flooding to further recover the remaining oil in place. As the demand of energy continually increases, the need to reduce the oil volumes left behind during primary and secondary recovery methods increases. The contribution of crude oil to the world's energy supply is estimated to be 26.3% in 2035[1]. Hence, enhanced oil recovery methods are constantly been applied to oil reservoirs to recover more oil to meet ever increasing energy demands. Due to the added benefit of CO_2 storage and simplicity of implementation, CO_2-EOR methods are been frequently sort after. Several CO_2-EOR methods such as pure CO_2 injection, water alternating gas (WAG), simultaneous water alternating gas (SWAG) have proven to be quite efficient in field scales but they are associated with several draw backs upon their implementation. Poor oil sweeping efficiency is reported during the oil displacement process due to high mobility of CO_2 compared to oil, and due to gravity segregation (override) because of a large difference between the densities of CO_2 and oil. These challenging phenomena are dominant in pure CO_2 injection, WAG and SWAG which lead to a high residual oil saturation and an early CO_2 breakthrough. Carbonated water injection (CWI) is an efficient oil recovery technique to further reduce residual oil saturation [2]. The major problems normally associated with water flooding and CO_2 injection can be mitigated by implementing CWI as an enhanced oil recovery technique [2-8]. In carbonated water injection, CO_2 and water are both injected as single-phase fluid and provides and piston like displacement due to low mobility ratio because of the similarities between the density of the displacing fluid (carbonated water) and the displaced fluid oil. CWI was first introduced as an improved oil recovery approach in the late 1940s. It is recognized as a promising EOR alternative and since CO_2 is more soluble in water compared to other common gases, it becomes the preferred gas. The availability of CO_2 makes CWI a viable option for onshore and offshore reserves. In comparison with the conventional water injection (WI), higher incremental oil recovery is expected from the CWI technique. The oil recovery increase is mainly attributed to the CO_2 mass transfer from the carbonated water (CW) to the oil phase, causing the oil phase to become more mobilized. The dissolved CO_2 in the oil phase enhances the mobility of the oil (M_o) and due to the oil swelling and reduction in both oil viscosity and interfacial tension (IFT), there is an overall reduction in residual oil saturation. Due to the nature of carbonated water

injection and its associated multi physics, the modelling aspects as an efficient EOR method have not been successful. After a comprehensive review of CWI as an efficient EOR method, especially in the modelling aspects. The drawbacks or inaccuracies of existing models spark the interest for this research because of several physics that have been overlooked and the modelling approaches and assumptions that have been adopted. Some of the overlooked physics are; (1) assumption of an instantaneous equilibrium in the modelling approach which has caused over prediction of recovery factor when compared to experimental data (2) The exclusion of gravity term during the modelling approach (3) the exclusion of reaction term, (4) the exclusion of diffusion and dissolution term. With the exclusion of these physics, the existing models do not entirely capture the phenomena that exist during CWI which current study attempts to address.

1.1 **Objectives of research**

The objective of this research is to develop a model that captures the entire physics that exist during carbonated water injection. This objective is divided into 4 sub-objectives

- Perform a comprehensive review of CWI to cover its important aspects/features such as displacement mechanisms, and recovery performance at various conditions/properties during CWI
- Investigate the critical water salinity that gives the best recovery factor. This is important because the solubility of CO_2 in water is largely affected by salinity. This salinity will be a base case and give better insights optimum solubility of CO_2 towards modeling CWI.
- Develop a 3-D model to capture important aspects such as gravity, heterogeneity and anisotropy, well placement and orientation, and the effect of operational parameters in the field scale
- Develop a 1-D model to capture reaction term, rock dissolution, diffusion and the effect of operational parameters in the laboratory core scale
- Develop statistical models (Artificial Neural Network, Least Square Vector Machine and Gene Expression Programming) to investigate CWI in terms of pattern recognition by relaxing its complex Multiphysics

1.2 **Organisation of thesis**

This thesis is written as a manuscript (paper based) and the outlines of this thesis are presented below;

Chapter 2 presents a comprehensive review of carbonated water injection for enhanced oil recovery. The chapter reviews thoroughly, vital aspects of carbonated water injection in terms of fluid- fluid interaction, fluid rock interactions, practical and theoretical challenges, carbon capture, modelling approach and experimental approach during the CWI for EOR.

This chapter is published in the Journal of Fuel 237 (2019)1086-1107

Chapter 3 presents a modelling investigation of low salinity water injection in sandstone and carbonates. The chapter investigates the determination of critical salinity for an optimum performance in terms of EOR for sandstone and carbonates and this salinity also gives an idea to model the solubility of CO_2 in water during CWI

This chapter is published in the Journal of Fuel 232 (2018)362-373

Chapter 4 presents a modeling strategy to investigate carbonated water injection for EOR and CO_2 sequestration. This chapter presents a novel modelling strategy to investigate CWI considering important aspects such as gravity, heterogeneity anisotropy, well orientation as well as the effect of operational parameters during CWI.

This chapter is published in the Journal of Fuel 252 (2019)710-721

Chapter 5 presents core scale tests and computational modeling of carbonated water injection. This chapter captures the reaction term as a part of complex physics during carbonated water injection to consider the effect of rock dissolution as well as the effect of operational parameters during CWI

This chapter is submitted to the Journal of Fuel

Chapter 6 presents a deterministic approach to predict the recovery performance of carbonated water injection. This chapter uses Artificial Neural Network (ANN) Modeling, Least Square Support Vector Machine (LSSVM) and Gene Expression Programming (GEP) to model CWI.

This chapter is submitted to the Journal of Molecular Liquids

References

1. Foroozesh J.,Jamiolahmady M.,Sohrabi M., Mathematical modeling of carbonated water injection for EOR and CO_2 storage with a focus on mass transfer kinetics. Fuel, 2016. **174**: p. 325-332.
2. Esene C.,Rezaei N.,Aborig A.,Zendehboudi S., Comprehensive review of carbonated water injection for enhanced oil recovery. Fuel, 2019. **237**: p. 1086-1107.
3. Riazi M.,Jamiolahmady M.,Sohrabi M., Theoretical investigation of pore-scale mechanisms of carbonated water injection. Journal of Petroleum Science and Engineering, 2011. **75**(3): p. 312-326.
4. Ghedan S. G., Global laboratory experience of CO_2-EOR flooding, in In: SPE/EAGE reservoir characterization and simulation conference. 12-19 October 2009, Society of Petroleum Engineer: Abu Dhabi.
5. Kulkarni M. M. R., Dandina N., Experimental investigation of miscible and immiscible water-alternating-gas (wag) process performance. Journal of Petroleum Science and Engineering, 2005. **48**(1): p. 1-20.
6. Mosavat N.,Torabi F., Micro-optical analysis of carbonated water injection in irregular and heterogeneous pore geometry. Fuel, 2016. **175**: p. 191-201.
7. Mosavat N.,Torabi F., Performance of secondary carbonated water injection in light oil systems. Industrial & Engineering Chemistry Research, 2014. **53**(3): p. 1262-1273.
8. Mosavat N.,Torabi F., Application of CO_2-saturated water flooding as a prospective safe CO_2 storage strategy. Energy Procedia, 2014. **63**: p. 5619-5630.

Chapter 2 **Comprehensive Review of Carbonated Water Injection for EOR and CO_2 Sequestration**

ABSTRACT

Carbonated water injection (CWI) is a promising enhanced oil recovery (EOR) technique in which the dissolved CO_2 can transfer to the oil phase to improve the oil mobility, and to cause oil swelling, both enhancing the sweep efficiency. In addition to serving as an EOR method, CWI promotes a high storage capacity for geological CO_2 storage. A number of laboratory tests and field applications have confirmed the effectiveness of this recovery process. This paper provides a comprehensive review of CWI to cover its important aspects/features such as displacement mechanisms, and recovery performance at various conditions/properties. In this paper, carbonated water injection process and the properties of CO_2-brine-oil systems are described. The influences of petrophysical properties, fluid properties, and operational parameters on the performance of CWI are also thoroughly addressed. The pore-scale investigations available in the literature are discussed to unveil the fundamental mechanisms of transport phenomena in CWI. The previous modelling/simulation conducted by several researchers are briefly explained where the main findings, advantages, and disadvantages of the proposed models are reported. The theoretical and practical challenges associated with the implementation of CWI process are presented. The additional benefits of CO_2 storage capacity are also highlighted by reviewing some real cases in the open sources. Studying a large number of experimental and modeling works on CWI, this review is aimed to further understand the CWI process and to provide helpful tips/guidelines for researchers and engineers who focus on theoretical and practical prospects of CWI operations.

Keywords: Carbonated Water Injection; Enhanced Oil Recovery; Displacement Mechanisms; Pore-Scale; Implementation Guideline

2.1 **Introduction**

Since the discovery of oil in the Creek Pennsylvania in 1859, the demand for oil as a primary source of energy has continuously increased, while the hydrocarbon reservoirs are being depleted over time. The reservoir depletion has motivated researchers to develop novel and efficient

improved oil recovery methods to maximize the oil recovery factor while fulfilling the energy market demand. After the primary recovery stage, the amount of oil that remains in the reservoir is about 75 % original oil in place (OOIP) for light oil, 95 % OOIP for heavy oil, and 100 % OOIP for tar sands. The target recovery factor for EOR processes is estimated to be 45 % OOIP for light oil, 90 % OOIP for heavy oil, and 100 % OOIP for tar sands [1]. Gas injection (GI) is a common EOR technique with application to conventional light oil reservoirs, in which a gas (usually CO_2) is continuously injected to recover the that is oil trapped in the reservoir [2]. The injected CO_2 may be miscible or immiscible with the reservoir hydrocarbons, depending on the thermodynamic and operating conditions [3]. CO_2 injection is usually conducted to recover a part of the residual oil that is left after water injection (WI). GI has been proven as a successful recovery method which has been investigated extensively and applied in several fields [4]. However, poor oil sweeping efficiency is reported during the displacement process due to high mobility of CO_2 compared to oil, and also due to gravity segregation (override) because of a large difference between the densities of CO_2 and oil. These challenging phenomena in pure CO_2 injection lead to a high residual oil saturation and an early CO_2 breakthrough. To overcome these problems during the pure CO_2 injection, various recovery approaches such as water alternating gas (WAG), simultaneous water alternating gas (SWAG), CO_2 foam flooding, and carbonated water injection (CWI) were developed (and applied) at laboratory, pilot, and field scales, while the gas injection is still used in oil production because of its simplicity [5].

CWI was first introduced as an improved oil recovery approach in the late 1940s. It is recognized as a promising EOR alternative, since CO_2 is more soluble in water compared to other common gases. The availability of CO_2 makes CWI a viable option for onshore and offshore reserves. In comparison with the conventional water injection (WI), higher incremental oil recovery is expected from the CWI technique. The oil recovery increase is mainly attributed to the CO_2 mass transfer from the carbonated water (CW) to the oil phase, causing the oil phase to become more mobilized. The dissolved CO_2 in the oil phase enhances the mobility of the oil (M_o) due to the oil swelling and reduction in both oil viscosity and interfacial tension (IFT), leading to a lower residual oil saturation. Results of the sand-pack experiments show that the residual oil saturation can be further reduced up to 15 % of pore volume (PV) if CWI is applied after WI. Several studies are conducted on CWI in sand-packs and core samples at different operating conditions [6-11]. They reported that the oil RF improvement by CWI is in the range of 2 % to 30 % [6]. In the secondary

recovery mode of CWI, a 40 % reduction in the residual oil saturation after the WI was measured during the experiments, which is in agreement with the range of 33 % to 48 % reported by Marfarlane et al. [7] based on the core flood experiments, using Bradford crude oil. In the secondary implementation of CWI, in the K&S field project in Oklahoma, an oil recovery of 43 % was reported [8]. This recovery performance was greater, compared to the recovery factor of 33 %, using conventional WI [8]. In the tertiary recovery mode, CWI process provides a 31 % reduction in the residual oil saturation after WI, based on the experimental work. This shows a good agreement with the coreflooding tests using the Bradford oil where an oil recovery improvement of 14 % to 47 % was attained [7]. CWI has several advantages compared to its competing EOR processes such as CO_2 injection, WAG, and SWAG because CWI leads to a better areal and microscopic sweep efficiency. In water flooded reservoirs, CWI can alleviate the adverse effects of high water saturation and water shielding because of the mixing between CW and resident water [9-11]. This mixing favors the dissolution of CO_2 and propagates the oil swelling. However, in direct CO_2, WAG, and SWAG injection, it has been confirmed that the time scale for CO_2 diffusion in the oil can be longer due to low sweep efficiency and gravity segregation [12-14]. CO_2 storage is an additional benefit during CWI process because CO_2 is dissolved into water and oil; the volume of free gas phase in the reservoir might not be considerable. Thus, CWI has a potential to provide a safe storage strategy which also contributes to a reduction in the level of greenhouse gas in the atmosphere.

There have been several experimental and numerical studies on CWI in the recent years to understand the involved microscopic and macroscopic production mechanisms [9-24]. The first reported commercial application of CWI was in 1958 (during the K&S project in the US). Since then, numerous successful studies of the CWI for EOR has been reported [11-15]. However, the effects of heterogeneities, fracture characteristics, mass transfer coefficient, non-equilibrium thermodynamic behaviors, pore structure, and injection-production well configuration on CWI performance have not been systematically investigated.

Oil swelling has been found to considerably contribute to the total oil recovery during CWI and its effects on EOR are studied in the literature [9, 12, 13]. Flow of fluids in the reservoir during CWI is strongly affected by the CO_2 mass transfer across the phases, which leads to the variations in the fluids properties, especially viscosity, interfacial tension and density [14]. The CO_2 is known

to alter the wettability of reservoirs. The effects of oil viscosity reduction and fluid-rock wettability alteration during the CWI have been studied in several research works [12, 15, 16]. It was concluded that these two phenomena act as important recovery mechanisms during CWI, affecting the displacement process and consequently oil recovery. During the CWI, there is a higher potential of CO_2 storage, compared to pure CO_2 injection. It was also found that the shrinkage rate is considerably faster than the swelling rate [17, 6, 18].

Mathematical models and simulation tools have been developed to study the mechanisms of CO_2 dissolution in water and to simulate the CWI process where the equilibrium state of CO_2 was assumed to be instantaneous [19, 20, 18, 21, 21]. An excellent match between the modeling results and real data is not yet materialized. The commercial simulators tend to overestimate the total recovery factor by 10 % when simulating CWI recovery processes [22, 23, 6]. In all CWI experimental and modelling studies, they agree on the wettability alterations through fluid-rock interactions, reduction in oil viscosity, oil swelling, and overall reduction of the residual oil saturation, which contribute to an increase in total oil recovery. However, there are still discussions on why there are disparities between the experimental and modelling results while conducting CWI simulation runs. The difference between predicted and real behaviors is attributed to the assumption of complete mixing and thermodynamic equilibrium in the conventional simulation techniques, and inappropriate models for relative permeability and capillary pressure [22, 24]. Moreover, the overall effects of gravity and diffusion have not been comprehensively explored to capture the main production and transport phenomena mechanisms in real field scenarios. Most studies have also overlooked the possible formation of carboxylic acid and its reactive contribution to the fluid-fluid and fluid -rock characteristics especially in carbonate reservoir cases.

Practical and theoretical issues can arise during the CWI application for the oil recovery processes. One of the issues, occurring during CWI is the preparation of carbonated water, where thousands of hydrophobic micro-hollow fibers are required to dissolve CO2 gas into water at elevated pressures [10]. Other challenges might be corrosion, scale formation, and asphaltene precipitation around the wellbore region (which strongly depends on the lithology and geochemistry of the reservoir), water weakening effect, and high capital, operating, and maintenance costs.

Though there are several reviews on CO_2 injection, WAG, LSWAG, and SWAG enhanced oil recovery strategies in the open sources, there is no comprehensive review paper on CWI technique

for oil recovery. As CWI is considered as a promising alternative for EOR with field applications, it appears to be a suitable replacement for CO_2 injection, WAG, and SWAG as an enhanced oil recovery process since it lessens major problems; including, early gas breakthrough, poor areal sweep efficiency, and gravity override [25, 24, 26]. Highlighting the advantages of CWI, it seems vital to obtain a deep and insightful knowledge about this recovery approach. The objective of this paper is to provide a proper description/understanding of the CWI process, its applications, key mechanisms (e.g., fluid-fluid interactions, rock-fluid interactions, phase change, and wettability alterations), pros and cons, challenges, and new advances, where several previous experimental and modeling investigations are discussed.

The paper is structured as follows. After the introduction section, this paper offers an overview of the CWI process in session 2. The characteristics and thermodynamic behaviors of the CO_2 and brine/oil/CO_2 systems are described in section 3. The effects of petrophysical properties, fluid properties, and operational parameters on the CWI process/performance are discussed in sessions 4, 5, and 6 respectively. Section 7 addresses the main recovery mechanisms through discussions on the pore scale studies. Session 8 represents the influence of CWI on fluid properties. Modeling and simulation studies are reported and discussed in session 9. Practical and theoretical challenges of CWI are addressed in session 10. The CO_2 storage capacity of CWI is discussed in session 11. Finally, concluding remarks about CWI are presented, based on the research works available in the literature.

2.2 **Process Overview of Carbonated Water Injection**

In the carbonated water injection (CWI) process, carbon dioxide (CO_2) is dissolved into the water phase before injecting into the reservoir. The dissolved CO_2 will transfer from the water phase to the oil phase due to the chemical potential difference of the CO_2 in two phases (as a driving force) [27]. This interphase mass transfer reduces the oil viscosity, lowers the oil-water interfacial tension (IFT), and causes oil swelling, which will be responsible for the reconnection of isolated residual oil ganglia, mobilizing the trapped oil (after WI) to be produced. These mechanisms will then result in a higher oil recovery factor upon CWI [28]. The increased oil mobility due to the oil viscosity reduction by CO_2 dissolution (in oil) is one of the main advantages of the CWI process, which is in favor of enhanced oil sweeping efficiency.

Figure 2.1 compares CO_2 injection (Figure 2.1a)) and CWI (Figure 2.1(b)) in terms of their sweeping efficiency and their sweeping patterns. In Table 2.1(a), CO_2 injection is shown to be more prone to the gravity and capillarity instabilities. The presence of heterogeneities such as fractures or regions of large-scale heterogeneities are expected to intensify these problems. As it is expected, better oil sweeping efficiency, more stable displacement front, delayed water breakthrough, and less viscous fingering are observed during the displacement process in CWI (Table 2.1 (b)).

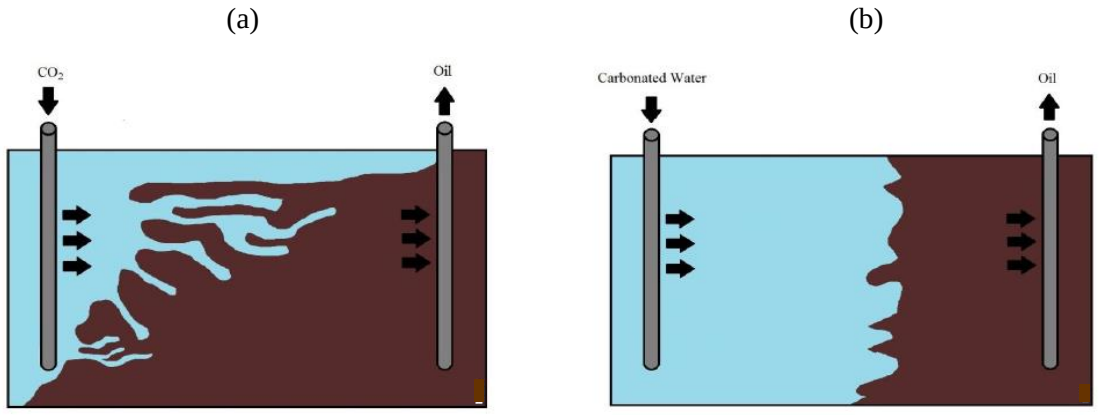

Figure 2.1: Schematic cartoon of enhanced oil recovery process by (a) continuous CO_2 injection and (b) carbonated water injection. The brown color represents oil and the blue color represents the injected fluids; including CO_2 and carbonated water (modified after [29]).

The oil swelling itself leads to a greater relative permeability to oil [29]. The oil mobility enhancement, carbonated water-oil (CW-O) interfacial tension reduction, and oil swelling phenomena are affected by the concentration of CO_2 in the oil, which is controlled by the solubility at reservoir conditions and the rate of CO_2 mass transfer across the interface (and also in the oil phase) [6]. These factors are influenced by the reservoir properties and operating conditions. In addition to the oil viscosity reduction, CW-O IFT reduction, and oil swelling upon dissolution of CO_2 in the oil, there is another advantage associated with CWI when compared to WI. In CWI, there is a potential for CO_2 ex-solution upon pressure drop because of the difference in the volume

of CO_2 in the liquid and gas phases. The gas ex-solution causes expansion, which will serve as an additional driving force for the increased oil recovery in comparison with WI [2].

For CWI to be effective (compared to WF), the CO_2 mass transfer from water to oil will be essential. The simulation results by Shu [30] (presented in Figure 2.2) demonstrate the evolution of CO_2 distribution curves near the carbonated water-oil (CW-O) interface in the absence of a porous medium for Bakken crude oil, where the operating temperature and pressure were 20 ˚C and 17 MPa, respectively. It can be observed that the mass transfer of CO_2 from water to the oil phase occurs close to the interface between the carbonated water (CW) and oil. This phenomenon causes the CO_2 concentration to decline from its initial value near the interface in the CW phase; however, it increases in the oil phase. Over time, the CO_2 will diffuse in the oil phase. It can be observed from Figure 2.2 that for the specific crude oil used in this investigation, the thickness of interfacial region (that is affected by the CO_2 mass transfer across the CW-O interface) is about 3 cm in the water phase and about 1 cm in the oil phase after 30 hours, which is due to higher viscosity of oil, compared to CW (~2.2 cP at 20 ˚C). The dissolution of CO_2 in the oil phase will cause oil swelling and shrinkage of water phase, which can be noticed through the interface movement.

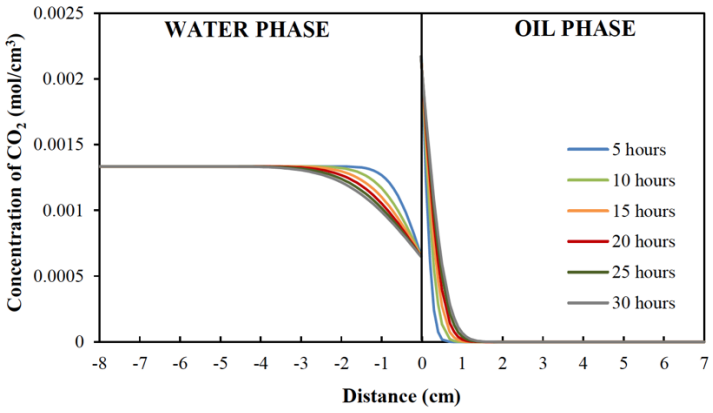

Figure 2.2: Concentration change in water and oil phases due to the inter-phase mass transfer from the carbonated water to the oil phase at 16.56 MPa and 20 ˚C [30].

A recognized technology to prepare CWI is the use of gas infusion generator. In this technique, the ground water pressurized remediation optimizer (GWPRO) is capable of infusing a high amount of dissolved gas into liquids at elevated pressures. It employs a hydrophobic micro-hollow fibre to provide a high mass transfer efficiency because of the large surface area that exists between

the water and gas phases. Hence, this strategy produces a water phase with a high dissolved gas concentration [29].

The CO_2 weight concentration of 2 % to 5 % is required to prepare the CW that is injected at a particular temperature and pressure to assure flow of single CW phase in the porous medium. After CW contacts the oil phase, the asphaltene precipitation may occur as a result of CO_2 transfer from CW to the oil, depending on the asphaltene precipitation/deposition phase envelope for the CO_2-crude oil system [31]. Another concern in handling CW is associated with its corrosive nature due to the formation of carbonic acid (H_2CO_3) when CO_2 dissolves into water. The carbonic acid accelerates corrosion of carbon steel materials, adding higher expenses to the CWI project.

2.3 **Properties of CO_2 and Brine/ Oil Systems**

2.3.1 Properties of Pure CO_2

Phase behavior. The triple and critical points for pure CO_2 are identified at (-56.4 ˚C, 0.52 MPa) and (31.1 ˚C and 7.38 MPa), respectively [32]. A practical phase diagram for pure CO_2 with application to hydrocarbon reservoirs is given by van der Meer, as depicted in Figure 2.3, in which the typical range of reservoir conditions is also highlighted [32]. Referring to CO_2 utilization in the EOR methods, CO_2 normally behaves as a gas at the standard/normal conditions of temperature and pressures (STP). When its operating conditions such as temperature and pressure are both increased above the critical point, it adopts properties (e.g., density, viscosity, and compressibility), replicating a gas phase and a liquid phase. For instance, it can expand to fill its container like a gas; however, it possesses a density as that of a liquid. More specifically, CO_2 behaves as a supercritical fluid above its critical temperature 31.10 °C and critical pressure 7.39 MPa. The physical properties of CO_2 such as density, viscosity, and compressibility are found to be strongly dependent on the operating pressure and temperature [33]. CO_2 is usually utilized either as a gas or a supercritical fluid, depending on the operating conditions and implication objective [29].

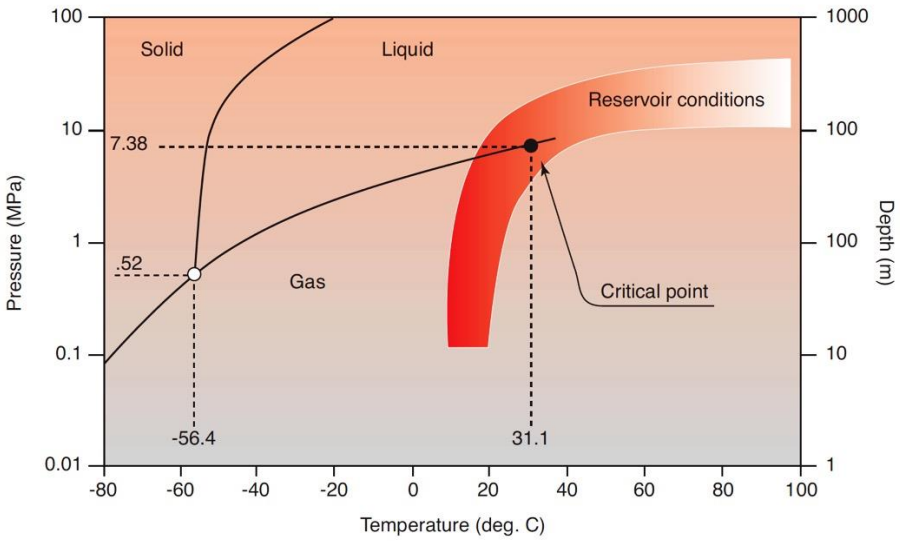

Figure 2.3: Triple-point phase diagram of CO_2 and typical range of reservoir conditions [32].

2.3.2 Properties of CO_2-Brine Systems

Solubility of CO_2 in brine. Compared to other common reservoir gases, CO_2 has an exceptionally higher solubility in the brine phase, which is shown Figure 2.4 (modified after [29]). The dissolved CO_2 (aq) can react with water and dissociate to form HCO_3^- and CO_3^{2-}; these reactions are among important reasons for higher solubility. The equilibrium quantities of CO_2, HCO_3^-, and CO_3^{2-} are governed by Le Chateliers' principle. In general, the solubility of CO_2 in brine is affected by temperature, pressure, brine salinity, and pH [34]. Alkalinity influences the equilibrium conditions. Above a pH value of 8.3, CO_2 (aq) will completely dissociate to form HCO_3^- and CO_3^{2-} ions [35]. Therefore, the dissolution of ions from reservoir into CW can also change the equilibrium conditions, and further complicate the problem.

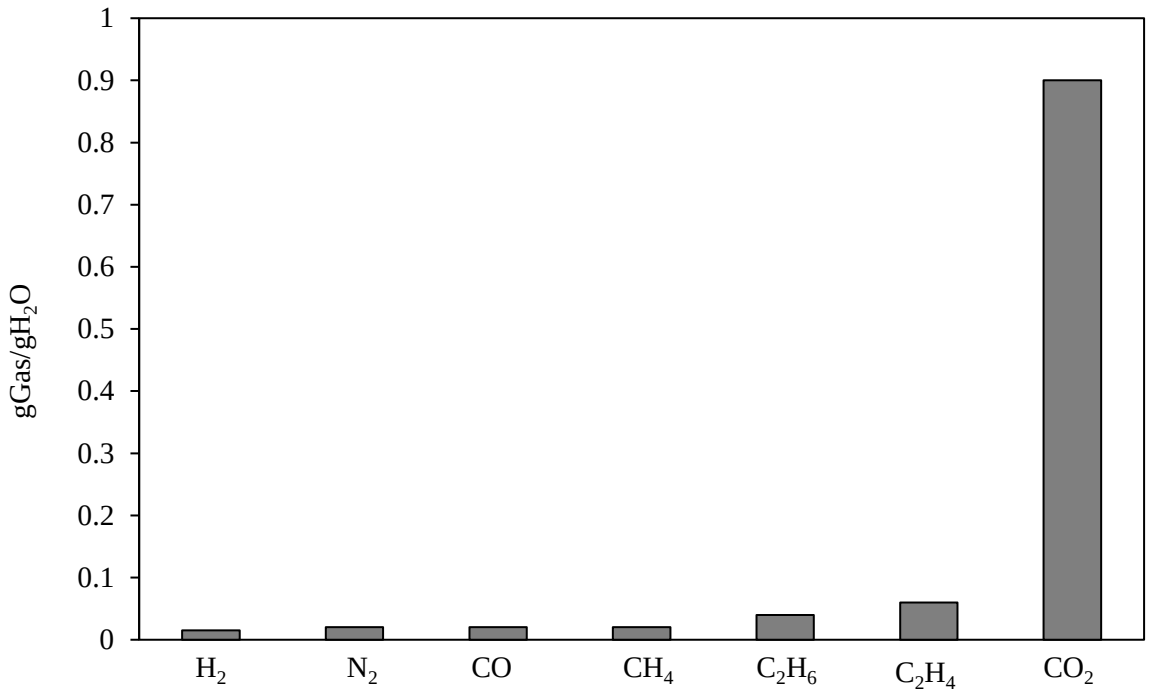

Figure 2.4: Solubility of different gases in pure water (modified after [29]).

A correlation was proposed by Yih-Bor et al. [36] that can be used to estimate the solubility of CO_2 in the water phase, implying that the CO_2 solubility is a function of pressure, temperature, and salinity of brine. Experimental works on measurements of CO_2 solubility in water are extensive. Table 2.1 summarizes a part of the experimental studies conducted so that it shows the solubility of CO_2 in pure water and brine (NaCl solution) at various temperatures and pressures.

Table 2.1: Experimental data on the solubility of carbon dioxide in pure water and in NaCl solutions [37].

Aqueous phase	Salinity (mol/kg H_2O)	Temperature range (°C)	Pressure range (bar)	Ref.
Pure water	0	12–100	30–800	[38]
		101–120	30–700	[39]
		71	100–1000	[40]
		15–260	6.9–202.7	[41]
		110–260	100–700	[42]
		250–350	200–3500	[43]
		100–200	3–80	[44]

		200–330	98–490	[45]
		20–30	5–30	[46]
		0–100	10–90	[47]
		10–30	1–20	[48]
		30–80	10-39	[49]
		50–200	1–54	[50]
		50–100	100–800	[51]
		15–93	7–203	[52]
		10–70	10–160	[53]
		50	Up to 200	[54]
		-29–25	6.9–137.9	[55]
		50–75	101–152	[56]
		70–148	Up to 200	[57]
NaCl solution	0–2	172–330	16–93	[58]
	0–6	50–400	30–266	[59]
	0–6	40–160	1–100	[60]
	0–3	0–25	1	[61]
	0–6	25–150	48	[62]
	0–4	25–75	48	[63]
	0.1–4	0–40	1	[64]
	0–6	40–160	2–96	[65]
	0–0.2	80–200	1–100	[66]
	0–3	25	1	[67]
	1–4.3	135–527	30–2800	[68]
	0–4.3	150–250	100–1400	[69]
	0.4–5.1	15–35	1	[70]
	0.01–0.06	5–65	0.49–0.84	[71]
	0.52–4	40–120	7–92	[72]
	1–3	50–100	Up to 200	[73]
	0–6	50–150	Up to 150	[74]
	1–6	50–150	Up to 200	[75]

2.5–4	50–150	Up to 180	[76]
0.01–0.03	30–60	100–120	[77]
0–5	50–140	50–400	[78]

Table 2.1 reveals a higher CO_2 solubility in pure water, compared to brine solution. Experimental data on the solubility of CO_2 in multivalent brines are also available in the literature [10, 79], which is not presented in Table 2.1 for brevity. Figure 2.5 describes the effect of temperature and pressure on the solubility of CO_2 in pure water in the temperature range of 373 -473 K and the pressure range of 0 - 100 MPa. As it is clear from Figure 2.5, an increase in the pressure leads to a higher solubility, while a decrease in the solubility with temperature is noticed because of the increase in the kinetic energy of the fluid. Furthermore, the solubility is more affected by pressure at lower pressure and lower temperature values [80]. In Figure 2.5, the scatter points are from the experimental data reported by Yan et al [80] and the solid lines represent the magnitudes of the solubility predicted by Peng Robinson equation of state (PR-EOS) from the Søreide-Whitson model [81].

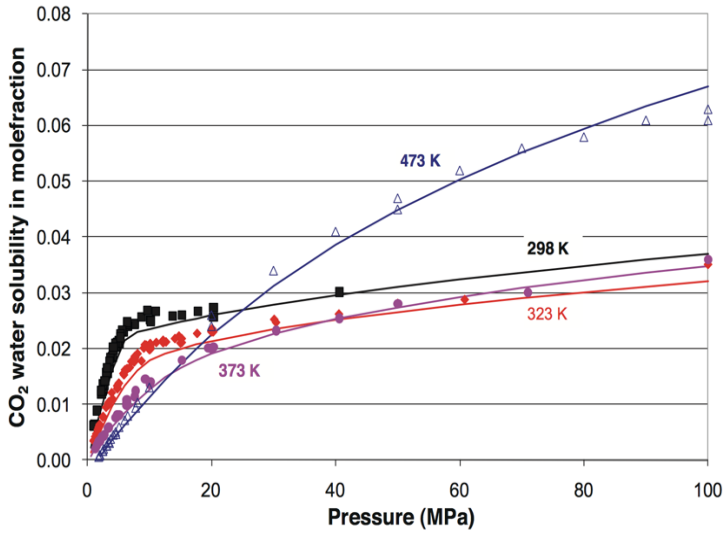

Figure 2.5: CO_2 solubility in pure water as a function of temperature and pressure (scatter points) [80] . Solid lines are obtained based on the solubility values estimated from the Søreide-Whitson model using PR-EOS [81].

The CO_2-water solubility was investigated in a systematic research work within the temperature range of 323-413 K and pressure range of 5-40 MPa, where Zhao et al. studied the effects of

salinity (in wt % and in molality) on CO_2 solubility, considering monovalent ions (e.g., NaCl and KCl) and divalent ions ($MgCl_2$, $CaCl_2$, and Na_2SO_4) in water [82]. The impact of multivalent salt on solubility of CO_2 in water at 323 K and 15 MPa is presented in Figure 2.6, where different salinity conditions are considered [82]. Based on their results, the effect of salts on the solubility of CO_2 in water is more pronounced at lower pressures [82]. At the same level of salt ionic strength (mol/kg), the salts influence the magnitude of CO_2 solubility in the following order: KCl<$CaCl_2$<$MgCl_2$<NaCl<Na_2SO_4; however, when the salinity is considered in weight percent of salt in aqueous solutions, the salts will affect the CO_2 solubility in a different order: KCl<NaCl<$CaCl_2$<$MgCl_2$<Na_2SO_4 [82].

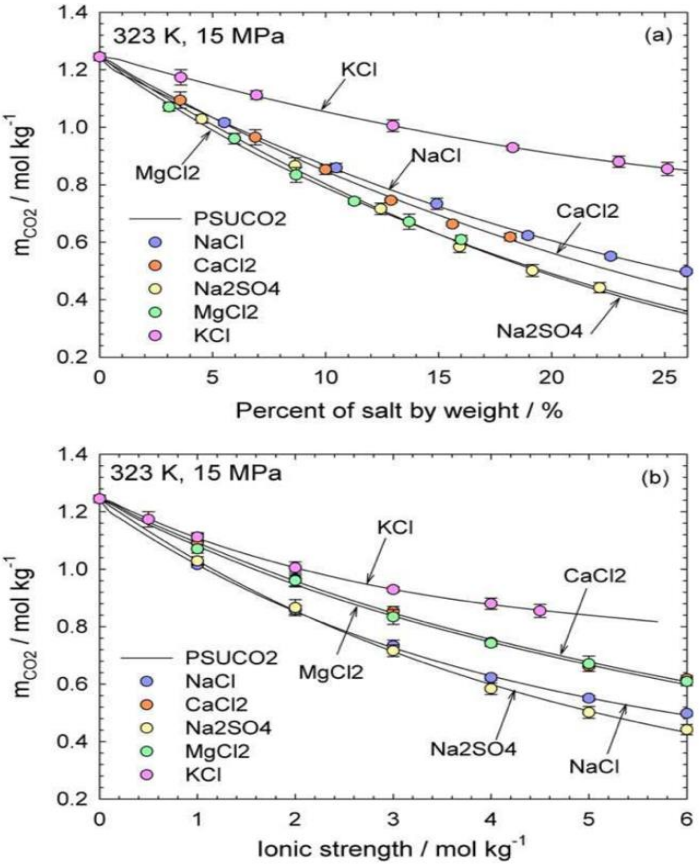

Figure 2.6: Effect of different salts on the solubility of CO_2 in water (in terms of molality of CO_2 in aqueous solutions) at 323 K and 15 MPa versus (a) salt weight percent and (b) ionic strength (mol/kg). Experimental data are shown with markers [82].

One of the main factors affecting the solubility of CO_2 in the aqueous solution is the charge density of ions in the presence of salts, leading to a change in the arrangement of the water molecules [83].

Small ions with a high charge density (kosmotropes) can strongly interact with the water molecules (compared to the water molecules with themselves) to become strongly hydrated. Hence, the kosmotropes can cause the molecules in the aqueous phase to be more organized [83], decreasing the solubility of the gas in the aqueous solution. Larger ions with a small surface charge (chaotropes) generally have weak interactions with water molecules. Thus, they are weakly hydrated. These ions will cause the molecules in the aqueous phase to be more disordered. Therefore, they increase the solubility of the gas in the solution [83].

Phase behavior of CO_2-brine systems. The P-x phase diagram for CO_2–H_2O system is demonstrated in Figure 2.7 [79]. The black isotherms show bubble point curves for the H_2O–rich phase, which is saturated with CO_2. The red isotherms represent the dew point curves for the CO_2-rich phase, which is saturated with H_2O. The solid lines are based on the data from Peng-Robinson-Stryjek-Vera EOS with Wang-Sandler mixing rules (PRSV-WS) EOS [79] and the scatter points are the measured equilibrium data [43, 69, 44]. As it is illustrated in Figure 2.7, the phase equilibrium data predicted for the CO_2-rich phase are less accurate than those for the water-rich phase. Li and Firoozabadi [10] concluded that the cross-association between H_2O and CO_2 molecules will influence the phase equilibria, which is more important in the CO_2-rich phase system than that in the water-rich phase. This is confirmed by the results reported in Figure 2.7.

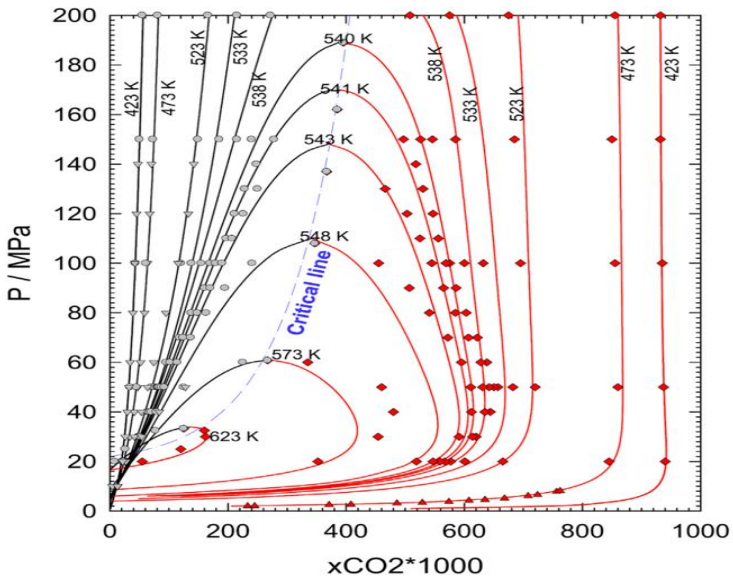

Figure 2.7: Pressure-mole fraction phase diagram for CO_2-H_2O binary systems [79].The black isotherms (left to critical line) are the bubble point curves for H_2O-rich phase saturated with CO_2

and the red isotherms (right to critical line) are the dew point curves for CO_2-rich phase saturated with H_2O. The solid lines are the estimated phase equilibria data based on Peng-Robinson-Stryjek-Vera EOS with Wang-Sandler mixing rules [79]. The experimental data are shown with scatter data points [43, 69, 44].

Viscosity of CO_2-brine system. An early work on the viscosity of CW as a function of CO_2 concentration was conducted in 1969 by Tumasyan et al. [84], in which the viscosity of CW was found to increase with CO_2 concentration. Yokoyama et al. [85] performed experiments at temperatures of 273, 276, and 278 K and at the pressure range of 0.1 MPa to 30 MPa. They reported that the viscosity of the aqueous solutions increases with the CO_2 content at a constant temperature and pressure. The combined effects of temperature and CO_2 concentration on the viscosity of CW are illustrated in Figure 2.8, based on the experimental work conducted by Bando et al. [86]. In their tests, the pressure was 20 MPa and the NaCl salinity varies from 0 wt % (pure water) to 3 wt% [86]. It was found that the viscosity of saturated CW lowers with temperature and salinity. It confirms that a higher salinity leads to a smaller CO_2 solubility in water, which is in an agreement with the output of the research work carried out by Yokoyama et al. [85]. It was also concluded that the viscosity of CW decreases with CO_2 concentration. According to Figure 2.8, the impact of salinity on the viscosity is less pronounced at higher temperatures. Moreover, the viscosity of CW is more affected by temperature when it holds low values.

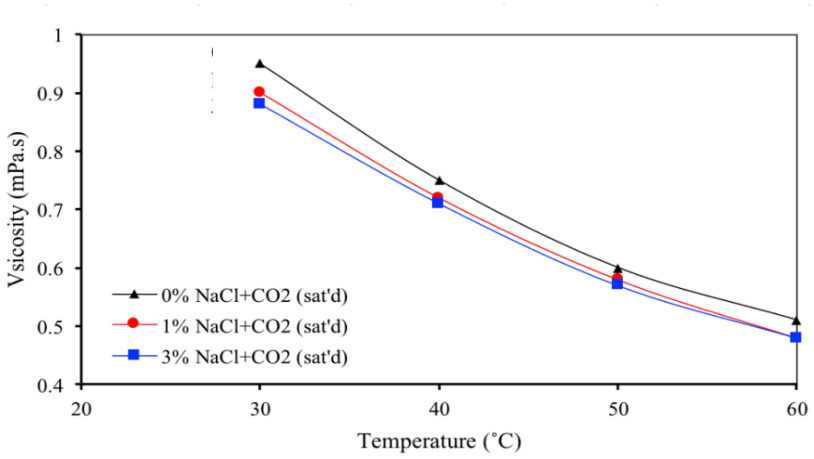

Figure 2.8: Viscosity of saturated mixture of brine (NaCl) and CO_2 at 20 MPa as a function of temperature [86].

Uchida et al. [87] showed that the viscosity of carbonated brine depends on time, temperature, and pressure through applying the dynamic scattering method. They concluded that the viscosity of brine–CO_2 mixture increases with time until a thermodynamic equilibrium condition is attained. It was also found that the solubility is higher at higher pressures and lower temperatures; the viscosity of brine increases with increasing CO_2 content [88].

Diffusion coefficient of CO_2 in brine. The diffusion of CO_2 from the water phase to the oil phase is an important feature of CWI for enhanced oil recovery, which can be controlled by the CO_2-brine diffusion coefficient [88]. The diffusion coefficient of CO_2 in brine is a function of temperature, pressure, salinity, and salt composition, which may be correlated to the viscosity of the liquid [89]. In the presence of a porous medium, the effective diffusivity will be also dependent on the porosity and tortuosity [89]. As measurement of tortuosity is difficult, it can be obtained from empirical correlations such as Archie [90]. A general form of diffusion coefficient for CO_2/water in porous media may be written as follows:

$$D_{eff,CO2,W} = D_0\left[\frac{T}{T_s} - 1\right]^m f^n \qquad (2.1)$$

where D_0, T_s, and m introduce the parameters of the diffusion coefficients of CO_2 in pure water, and n is the Archie's exponent. The values of D_0, T_s, and m are found to be 13.942×10^{-9} (m^2/s), 227 K, and 1.7094, respectively for the CO_2-water systems. The value of n is between 1.3 and 4.5 [90].

The diffusivity of CO_2 in the bulk water phase may be correlated to the solvent viscosity as given below [89]:

$$D_{CO2,W} = D_0\eta^m \qquad (2.2)$$

where η stands for the solvent viscosity. For pure water, the values of parameters D_0 and m were obtained to be 2.831×10^{-6} (m^2/s) and -1.0743, respectively [89]. The effect of pressure on the diffusion coefficient of CO_2-water systems seems to be small [89, 91], [91]. Sell et al. [91] investigated the diffusion coefficient of CO_2 in water and NaCl brine inside a microfluidic chip at 26 ˚C and a pressure of 5 to 50 bar. They did not observe a significant pressure effect in this pressure range. They found the diffusion coefficient of CO_2 in pure water to be $(1.86\pm0.26)\times10^{-9}$ m^2/s, which decreases as a power law correlation with salinity in the range of (0 to 5) M NaCl. At

5 M NaCl salinity, the diffusion coefficient was one-third of that of the pure water at the same temperature. The experimental diffusion coefficient values from the bulk and microfluidics systems were in a good agreement with those obtained from molecular dynamics simulations [92]. A comprehensive modeling study and review of the CO_2 diffusion coefficient in water is available by Mutoru et al. in the literature[93].

Interfacial tension of CO_2-brine systems. The interfacial tension of CO_2 with pure water and different brines was experimentally investigated by Bachu and Bennion [94] within wide ranges of pressure (2-27 MPa), temperature (20-125 ˚C), and salinity (0-334000 mg/l) using single and multivalent salts. They introduced the following general empirical correlation to determine the interfacial tension (γ) as a function of temperature (T), pressure (P) and salinity (S) [94]:

$$g = A(T,S)P^{-B(T,S)} \qquad (2.3)$$

In Equation (3), A and B are the variables, which are functions of both temperature and salinity. A recent research work on CO_2-brine interfacial tension with application to the geological storage of CO_2 is given by Pereira et al. [95]. Their experimental data covered the temperatures and pressures up to 423 K and 69.51 MPa, respectively, using NaCl, KCl, and $CaCl_2$ salts with an ionic strength up to 2.7 ml/kg. Employing the density gradient theory, the objective function was estimated theoretically, showing an acceptable accuracy in terms of statistical analysis.

2.4 Properties of CO_2-Oil Systems

Solubility of CO_2-oil system. The solubility of CO_2 in oil is an important parameter in CWI that governs the production rate of oil. In 1964, Simon and co-workers [96] suggested a correlation to determine the solubility of CO_2 in the oil phase as a function of temperature and pressure, based on their experimental data. Systematic experiments were conducted, using seven different crude oils and two refined oils with API gravity values, ranging from 11-33 [96]. They have measured the solubility of CO_2 in these nine different oil samples at various temperature and pressure conditions. An early set of the experiments was also performed, using different oils with various API gravity values to investigate the temperature and pressure effects on the solubility of CO_2 in the oil. They also measured the swelling factor of CO_2 in the oil phase and the viscosity change of dead oil with CO_2 dissolution [97]. Orr et al. conducted a systematic analysis of the CO_2-oil equilibrium phase behavior from the stationary and displacement experiments (slim tube and

continuous multiple contact) within a wide range of operating conditions [98, 99, 99, 98]. A review of CO_2-oil properties with application to CO_2 capture and storage is given by Sasaki et al. [100].

Interfacial tension of CO_2-oil system. Several experimental studies in the recent years have investigated the influences of temperature and pressure on the interfacial tension of CO_2 with brine and oil with application to enhanced oil recovery by CO_2 injection and CWI. A recent study by Yang et al. [101] was conducted to measure the IFT of CO_2 with Shangli crude oil in a broad range of temperature up to 412 K and pressure up to 45 MPa, using the pendant drop method. The experimental results show that the IFT decreases with increasing temperature, pressure, and CO_2 content in the oil. For example, by increasing the CO_2 content in the oil phase from (0 to 65) mol% at 27 MPa, the IFT decreased from 53.07 mN/m to 34.79 mN/m [101]. The rate of change in IFT with pressure is more influenced at a lower temperature in the range of 45 to 139˚C. Moreover, they observed that the IFT variation undergoes a transition behaviour with pressure at the minimum miscible pressure (MMP), beyond which the rate of decrease in IFT with pressure is minimal. For example, the MMP was found to be 26.4 MPa at 412 K for a specific crude oil with CO_2. The IFT reduction with pressure is thus significant up to this pressure as it can be observed in Figure 2.9 [101]. There is a transition point at 19.15 MPa at which the IFT is as low as 3 to 5 mN/m.

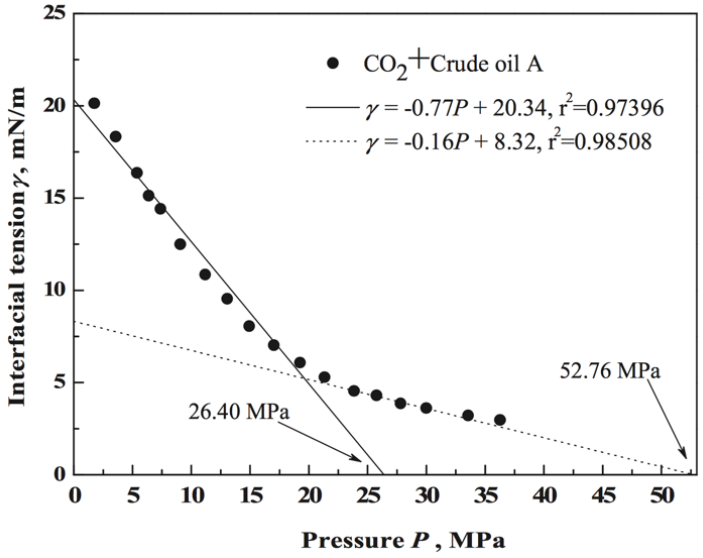

Figure 2.9 : Correlation of IFT with pressure for CO_2-oil (Shengli crude oil) at 412 K. The transition point at 26.4 MPa is the MMP for this crude oil [101].

The experimental measurements of CO_2-oil IFT at reservoir conditions are also found elsewhere [102, 103].

Diffusion coefficient of CO_2-oil system. In an early work, McManamey et al. [104] developed a correlation that can be used to estimate the CO_2 diffusion coefficient in an oil as a function of oil viscosity (at 25 ˚C and 50 ˚C):

$$D_{CO2,O} = 1.41' 10^{-10} h_o^{-0.47} \quad (2.4)$$

where η_O denotes the oil viscosity in Pa. s and $D_{CO2,O}$ refers to the CO_2 diffusion coefficient in oil with an unit of m^2/s. This equation can exhibit various industrial applications because it relates the diffusion coefficient to the viscosity in a simple way [105]. A review of the diffusion coefficient of CO_2 in different crude oils based on a variety of experimental and simulation studies is given by Zheng et al. [106] where it can provide useful tips while implementing enhanced oil recovery processes through CO_2 injection and CWI.

Oil swelling in CO_2-oil system. Oil swelling is found to be an important mechanism in recovering the disconnected oil ganglia in processes such as CO_2 injection, CO_2-WAG, and CWI. Upon swelling, the disconnected oil ganglia may become connected with the adjacent ganglia and attain a higher mobility. The oil swelling factor may be determined from volume measurements of the oil phase when exposed to CO_2 at different temperatures and pressures, using PVT cell, pendant drop, or/and microfluidic chips. It might also be obtained from an equation of state in combination with a transport model for CO_2 diffusion in the oil. The swelling factor is affected by various parameters such as pressure, temperature, oil properties (e.g., viscosity and composition), and the CO_2 solubility [107] . An empirical correlation was proposed by Welker et al. [108] to obtain the swelling factor of different crude oils, as provided below:

$$SF = 1 + \left[\frac{0.35 R_s}{1000} \right] \quad (2.5)$$

where SF represents the swelling factor (ratio of oil volume to that at atmospheric pressure and test temperature), and R_s symbolizes the solubility of CO_2 in oil in scf/bbl. Chung et al. used four different crude oils with a solubility in the range 0-1000 scf/bbl. They noticed an excellent agreement between the experimental data and the results obtained from the empirical correlation

introduced by Welker and Dunlop [107]. As it is demonstrated in Figure 2.10, recent studies [109, 110] show a maximum in the swelling factor with equilibrium pressure at different temperatures, after which the swelling factor decreases significantly; this maximum swelling factor becomes smaller at higher temperatures and is shifted to a higher equilibrium pressure with temperature [110]. Having a maximum point in the swelling factor curve is explained by the extraction of lighter cuts of the crude oil as the pressure reaches that value corresponding to the maximum swelling factor [109, 110]. Perhaps, the proximity of critical condition of the gas phase (mainly CO_2) may also justify such a behavior.

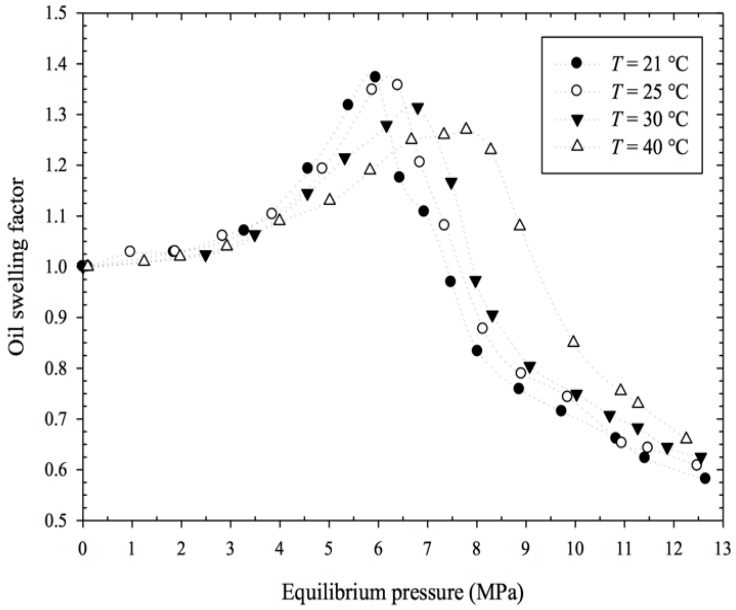

Figure 2.10 : Swelling factor versus equilibrium pressure at different temperatures for a light crude oil [110].

2.5 **Properties of CO_2-brine-oil systems**

Interfacial tension of CW-oil. When CO_2 does not exsolve as a separate free gas, the IFT of CW-oil contributes to the efficiency of CWI. The IFT measurements of CW-crude oil at reservoir conditions are available in the literature [111, 112]. As it is expected, the IFT of carbonated brine with oil is less than that of brine-oil, using similar fluids because of CO_2 effects. In addition, an increase in temperature and pressure causes a reduction in the IFT of CW-oil [112]. The effect of salinity is more complex in the literature. [112] Comparing the IFT of CW-oil using seawater and formation brine, lower IFT was obtained for the formation brine due to lower CO_2 content (due to

higher salinity), where the salinity of formation brine was about 3 times of that of the seawater. The combined effects of ions in low salinity water and CO_2 content in the CW at reservoir conditions were investigated using NaCl, KCl, KI, $MgCl_2$, $CaCl_2$, Na_2SO_4, $MgSO_4$, and K_2SO_4 [111]. A minimum IFT was observed with the concentration of these salts, which occurred between 1500-2000 ppm [111]. The maximum reduction in IFT at the reservoir condition was observed with 2000 ppm K_2SO_4, in which the IFT decreased by 48 %. The maximum reduction in IFT was recorded between 4-48 % with these salts. As a controversial point, they noticed an increase in the IFT with temperature for all salts, at 1500 psig and the temperature range of 40-80 ˚C [111] , which is not justified as it is not in an agreement with results of Honarvar et al. [112].

Partition coefficient of CO_2: This coefficient is a parameter, which is used to show how CO_2 is partitioned between the CW and oil phases. Partition coefficient of CO_2 is defined as the ratio of concentration of CO_2 in the oil phase to that in the water (CW) phase, as follows:

$$K_{CO_2,OW} = \frac{C_{CO_2,O}}{C_{CO_2,W}} \qquad (2.6)$$

in which, $K_{CO2,OW}$ denotes the oil-water partition coefficient of CO_2; $C_{CO2,O}$ is the concentration of CO_2 in the oil phase, and $C_{CO2,W}$ represents the concentration of CO_2 in the CW phase. Both pressure and temperature affect the partition coefficient of CO_2. This parameter may be used to simplify the modeling aspect of mass transfer of CO_2 from CW to oil phase [113]. As demonstrated in Figure 2.11, the partition coefficient of CO_2 decreases with pressure, but increases with temperature. Furthermore, the change in the partition coefficient with pressure is more pronounced at higher temperatures as it may be observed in Figure 2.11. At a room temperature (20 ˚C), the partition coefficient of CO_2 in the pressure range of 4-22 MPa is almost constant at about 3.4 [113], meaning that the concentration of CO_2 in the oil phase at equilibrium is 3.4 times of that in the CW.

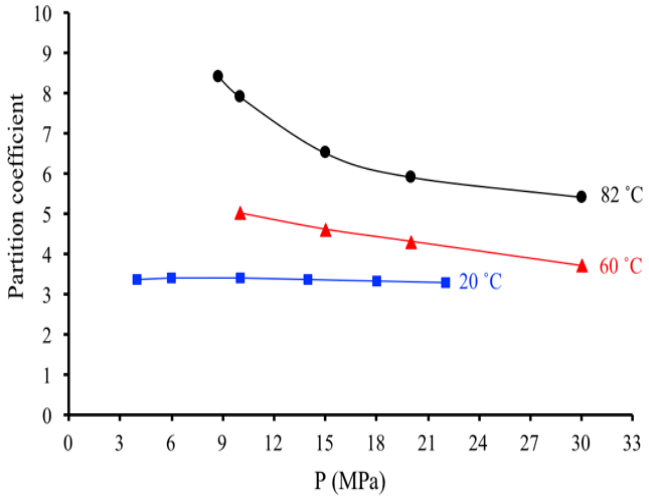

Figure 2.11: Partition coefficient of CO_2 between oil and carbonated water phases versus pressure. The experimental data at 20 ˚C is taken from [112], the data at 60 ˚C is taken from [113], and the data at 82 ˚C is obtained from [114].

2.6 **Effects of Petrophysical Properties on Cwi Performance**

The research investigations on carbonated water injection process as an enhanced oil recovery method under various reservoir conditions are limited. The interactions between the injected CW and reservoir rock can lead to various chemical reactions, especially in carbonates. The reactions will influence the fluid-flow and oil recovery mechanisms of reactive transport in porous media. Upon the reactions, the mechanical properties of the reservoir will be affected, resulting in the loss of reservoir formation integrity [116]. The performance of CWI under different reservoir conditions; including reservoir permeability and wettability will be discussed in this section.

2.6.1 Heterogeneity

A series of experiments were performed, using CWI in a heterogenous sandstone core to investigate how the heterogeneity affects the performance of CWI with an insight on RF [17]. In this study, the porous system had an absolute permeability of 98.73 mD and a porosity of 17.68 %. A crude oil with an API gravity of 20.8 and a brine with a salinity 54647 ppm of ionic constituents of (Na^+ 16844, Ca^{2+} 664, Mg^{2+} 2279, SO_4^{2-} 3560, Cl^- 31107 and HCO_3^{-1} 193) were

used at operating conditions of 2000 psi and 100 ^{o}F where the injection rate was 5 cm^3/h. Based on their observations, it was found that after injecting only 0.21 pore volume (PV) of brine, there was a water breakthrough, which was attributed to the presence of high permeable layer in the rock. The ultimate recovery factor of 35 % was also reported, which was improved additionally by 10 % when CWI was implemented in the tertiary mode. This significant extra oil recovery by CWI reveals that heterogeneity do not derail the performance of CWI in the tertiary mode, particularly when the performance of the conventional water flooding in the same reservoir is usually poor. In another experimental study, the effect of fracture geometry on the performance of the carbonated water injection (CWI) in the presence of gravity was carried out by Mahdavi and James [117]. A heterogenous micromodel (20 cm × 3.5cm) with fractures was designed with a porosity of 38 % and a permeability of 400 D. An oil with an API gravity of 29.8 and a viscosity of 6.8 cP was utilized in this research study where the operating pressure, temperature, and injection rate were 305 psi, 21^{o}C, and 0.0024 cm^3/min, respectively. They systematically investigated the displacement pattern and residual oil saturation distribution in the experimental tests. The visualization results of their study to present the saturation distribution are demonstrated in Figure 2.12.

(a)

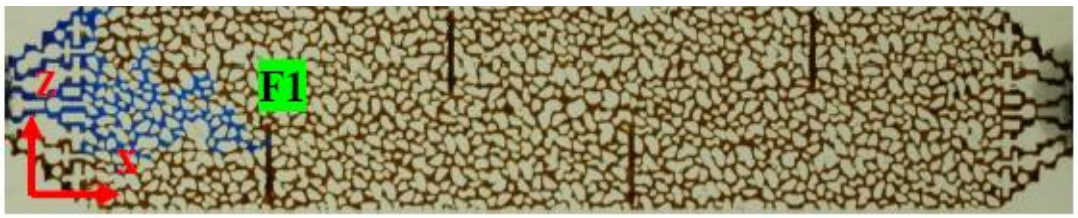

(b)

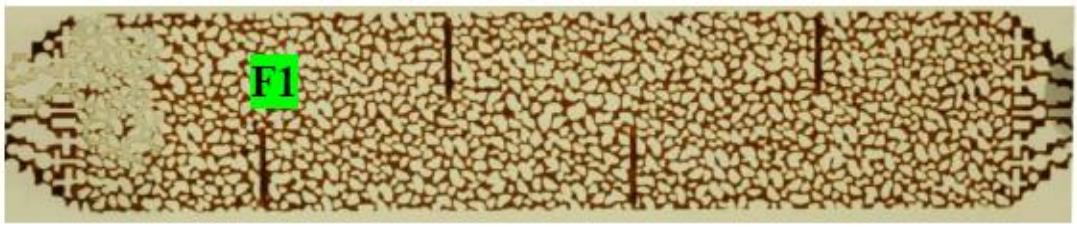

Figure 2.12 : Saturation distribution pattern for (a) WF and (b) CWI in a fractured medium in the presence of gravity [117].

It can be seen from Figure 2.12(a) that after 0.05 PV of the injected brine, the fluid distribution pattern near the fracture (F1) exhibits the fingering phenomenon due to the high permeability of the fracture zone, leading to a 9.2 %-recovery. However, in Figure 12(b) which is the case of CWI, the fluid distribution in the fracture and matrix was more even distributed with 14.9 % oil recovery after 0.05 PV of injected CW. This experimental investigation also shows that the overall performance of CWI (as a viable EOR method) is not considerably affected by the heterogeneities such as fractures and vugs in a porous medium.

2.6.2 Wettability

Sohrabi et al. conducted an experimental study, which investigates the influence of wettability on the CWI performance, using two Clashach cores; one was naturally water-wet and the other was treated to become mixed-wet by ageing it in the crude oil phase [118]. Permeabilities of the cores were 1300 mD and 850 mD, respectively; the values of the porosity were 0.185 and 0.165, respectively. The operating conditions of the tests were 38 ˚C and 2000 psig with an injection rate of 20 cm^3/h. The cores were initially saturated with decane as the oil phase with a viscosity of 0.82 cP. Their production results are presented in Figure 2.13(a) and (b).

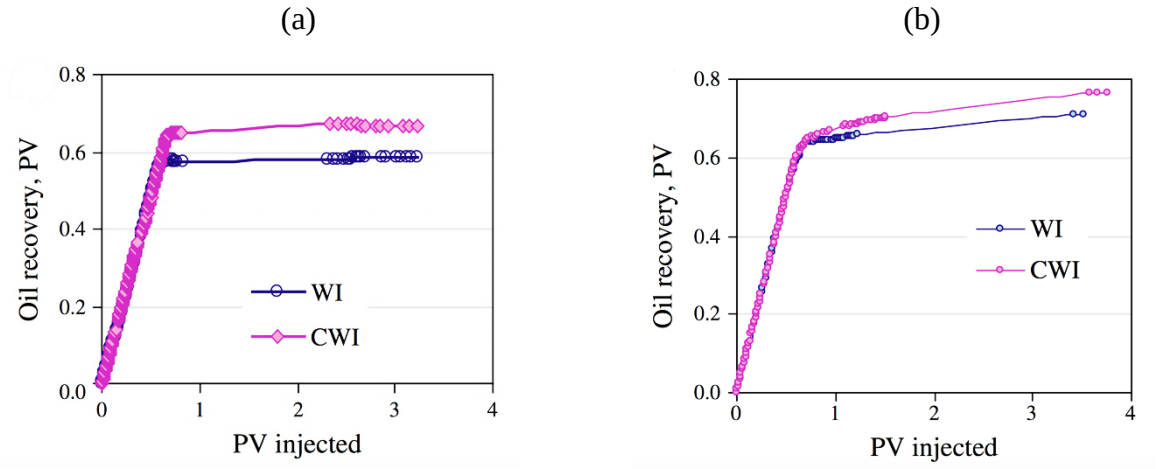

Figure 2.13: Comparing recovery factor for CWI and water injection (WI) at 38 ˚C and 2000 psig for (a) mixed-wet and (b) water-wet cores [118].

The impact of the core wettability on the CWI performance was assessed in terms of the oil recovery factor, which was compared to WI as a baseline. The ultimate oil recovery upon WI was found to be 59.5 % PV in the mixed-wet core and 71.0 % PV in the water-wet core [118]. After

applying the secondary recovery by CWI, the ultimate oil recovery increased by 11.8 % in the mixed-wet core and by 7.7 % in the water-wet core (compared to WI), as depicted in Figure 2.13(b) [118]. Therefore, it was concluded that the CWI improves the oil recovery–compared to WI–slightly better in the mixed-wet media, compared to that in the water-wet media. The reason for this behavior in the mixed-wet core was hypothesized by the presence of continuous oil-wet paths of appreciable lengths in the mixed-wet rock that causes better oil connectivity as it allows film flow of the oil along the wetting phase even at a low oil saturation [119]. This connectivity is expected to be further enhanced by the oil swelling mechanism, thus contributing to a better oil recovery [120].

The effect of wettability on the performance of CWI was also studied through a simulation study performed using E300 [121]. Two sandstone cores were used for this investigation; including a water-wet system with a permeability and a porosity of (1300 mD, 0.19) and a mixed-wet medium with a permeability and a porosity of (850 mD, 0.16). The cores were initially saturated with decane with a viscosity of 0.83 cP under the operating conditions of 38 ^{o}C initial temperature, 136. 1 atm pressure, and 20 cm^3/h injection rate. In this research work, their results were validated by the real data so that a good agreement was noticed when the modeling and core flooding results of recovery factors, total oil production, and differential pressure were compared. Based on their research investigation, the secondary CWI led to about 60 % oil recovery for water-wet core and 65 % in the mixed -wet case at the breakthrough condition. The CWI yielded an additional 6 % ultimate recovery oil recovery for a water-wet core [121]. In the case of the mixed wet-core, CWI resulted in 68 % oil recovery at breakthrough, which was 13% more than WF recovery factor at the breakthrough; but it yielded only additional 1 % as the ultimate recovery factor. It was concluded that CWI has a better performance in mixed water-wet rocks, compared to the water-wet rocks; however, no explanation was given as a reason for this trend [121]. CWI was also applied for the oil-wet cores in an experimental investigation by Ruidiaz et al. [122]. Dolomite and limestone cores were used, which were extracted from Silurian Devonian formation, Pennsylvania, USA, and Morro do Chaves Formation at the Sergipe-Alagoas Basin, Brazil, respectively. The rock properties varied between 7 % and 21 % for the porosity and 10 mD to 400 mD for the absolute permeability. A crude oil with an API density of 28 and a viscosity of 6.4 cP was utilized where the tests were operated at a pressure of 2500 psi and a temperature of 64 ^{o}C. The dolomite and limestone cores were subjected to CWI with the sea water salinity of 35,000 ppm NaCl. It

was reported that the oil recovery for limestone at breakthrough is 48 % and the ultimate recovery is about 49 %, while the limestone case led to a recovery factor of about 10 % at breakthrough and an ultimate recovery of about 28 %. It was also found that the wettability of both cores may alter towards a more neutral wet condition. Another experimental study was also carried out using a carbonate system by Kilybay et al. [123]. According to the core flooding results, quaternary CWI resulted in 5.7 % to 13.6 % additional oil after the smart water injection.

2.7 Effects of Fluid Properties on CWI Performance

The performance of CWI also depends on the physical properties of the CW and crude oil. In this section, the effects of CW salinity, CO_2 content, and crude oil density and viscosity on the performance of CWI will be discussed.

2.7.1 Effect of CW Salinity

The effect of CW salinity on the CWI performance was studied by Sohrabi et al. [120] in an experimental investigation using a reservoir core, which was water-wet with a permeability and a porosity of 4580 mD and 0.350 %, respectively; where a crude oil with a viscosity of 145 cP was utilized in the experiments. To examine the impact of CW salinity on CWI performance, the case of CW salinity of 1 % (0.8 % wt of NaCl and 0.2% wt $CaCl_2.6H_20$) at the test condition of 2500 psig and 38 ^oC was compared in terms of recovery factor with the case of CW salinity of 3.2 % (2.6 % wt of NaCl and 0.6 % wt $CaCl_2.6H_20$) at the test condition of 2000 psig and 38 ^oC, as described in Figure 2.14. In the experiments, the effect of CW salinity was studied in the tertiary mode, which followed after the water injection process. It can be seen from Figure 2.14 that 3.2 % saline carbonated water improves the secondary recovery by an additional 4 % compared to 1% saline carbonated water, which increases the secondary recovery by an additional 11 %.

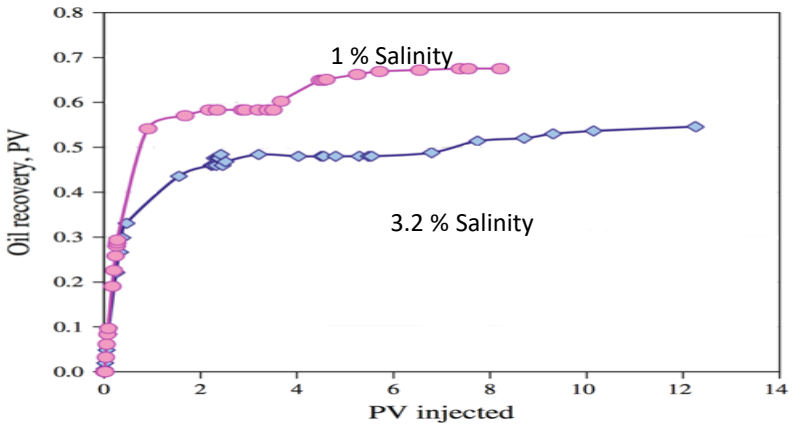

Figure 2.14 : Comparison of oil recovery factor using tertiary CWI with high salinity (3.2 % salinity, 2000 psig) and low salinity (1 % salinity, 2500 psig) brines at 38 ˚C in water-wet reservoir core [120].

2.7.2 Effect of CO_2 Content

The effect of CO_2 content or carbonation level (CL) was observed in an experimental study by Mosavat [29] for a homogenous sand-pack flooding set-up with a permeability of 4074 mD and a porosity of 0.27 using a crude oil sample from Bakken formation in Saskatchewan Canada with a viscosity of 2.76 mPa.s. For this investigation, two different types of CW were prepared by dissolving CO_2 in water to attain the carbonation level of 100 % and 50 %, respectively, under the operating conditions of 4.1 MPa and 25 ^{o} C and an injection rate of 1 cm^3/min. In this research study, it was found that the oil recovery increases proportionally to the carbonation level during the test. According to the experimental findings, the ultimate recovery factor was reduced from 68.8 % to 66.8 % when the carbonation level was decreased from CL = 100 % to 50 %.

The effect of CO_2 content/carbonation level was also investigated in a simulation study of CWI using Eclipse 300 by Ahmadi et al. [124] for an Iranian oil reservoir with a viscosity of 0.2109 mPa.s measured at the bubble point condition. The initial reservoir pressure and temperature were reported to be 63.2 MPa and 421 K, respectively. The reservoir bubble point was 40 MPa, GOR was 276.6 m^3/m^3, and the oil API gravity of 39 was reported for this simulation study. The simulation approach was conducted using an injection rate of 0.0505 m^3/s and an injection pressure of 68.9 MPa. The performance of CWI in terms of oil recovery was examined using the concentration of 0.8, 1.6, and 3.2 mol % CO_2 in solvent for a constant injection rate of 0.0505

m^3/s. It was observed that the ultimate oil recovery increases by 32.3 %, 34.5 %, and 40.6 % respectively for the CO_2 concentrations reported above. Thus, it was concluded that the recovery factor of a CWI process with a higher CO_2 dissolved is more than that with a lower carbonation level or CO_2 concentration. In other words, increasing CO_2 concentrations results in a greater CWI recovery factor.

2.7.3 Effect of Oil Properties

One of the first CWI related research in Shell was conducted in 1960's by van Dijke [125]. In this study, a series of sand pack experiments were performed at 104 ºF and various pressures using oils with different viscosities (e.g., 10.7 cP and 57.4 cP). The recombined live oil with 35 cP viscosity was also tested where the injection rate was 15 PV/d. It was noticed that the recovery increases by 4.5 % PV and 13 % PV at 5 PV injection rate for 10.7 cP and 57.4 cP oils, respectively, implying the carbonated water flood performs better for more viscous oil [125].

The effect of oil viscosity on the performance of CWI was experimentally investigated by Sohrabi et al. at pore scale, using a glass micro-model [126]. They conducted the experiments at a pressure of 2000 psia and a temperature of 100.4 ºF. A mineral oil with a viscosity of 16.5 cP (under the experimental conditions) and nC_{10} with a viscosity of 0.8 cP were used to study the performance of CWI. The flooding tests were conducted at 24 PV/d and the total cumulative volume of 144 PVs was injected in the experiments. The performance of CWI was evaluated for the viscous oil (16.5 cP) and light oil (0.8 cP). For the viscous oil, the secondary CWI reduced that oil saturation and yielded an additional recovery of 11.8 % when compared to WI. However, for the light oil (0.8 cP), the secondary CWI yielded additional 32.7 %, compared to WI. The higher recovery experienced for the light oil during this experiment was attributed to a higher oil swelling and coalescence in the oil, compared to the viscous oil. The higher swelling factor for the light oil, compared to viscous oil, is directly related to a higher CO_2 solubility in the lighter oil [126]. The finding of this study is in contradiction with the results, which were reported by van Dijke [125]. In another experimental study of CWI on heavy oil conducted by Afra et al. [127], 28 % to 49 % additional oil recovery were attained during heavy oil production upon implementation of CWI after WF. It was also concluded that CWI is an efficient EOR technology even for heavy oil production.

2.8 **Effect of Operational Parameters on CWI Performance**

The efficiency of CWI during an EOR process depends on operational parameters such as temperature, pressure, and injection rate, which will be discussed in the following subsections.

2.8.1 Effect of Pressure

A series of CWI tests with brine (saturated with CO_2) were performed by Mosavat et al. [6] using the sand pack model with a permeability ranging from 4011 mD to 6715 mD and a porosity within the range of 0.27 to 0.28. A light crude oil of 44 ° API and 2.76 mPa.s viscosity was utilized in this research study with an injection rate of 1 cm^3/min, a temperature of 25 °C, and a pressure in the range of 0.4 MPa to 10.3 MPa in order to investigate the effect of the operating pressure on the recovery factor. The results of their experiments for CWI in the secondary and tertiary modes are illustrated in Figure 2.15(a) and 2.15(b), respectively.

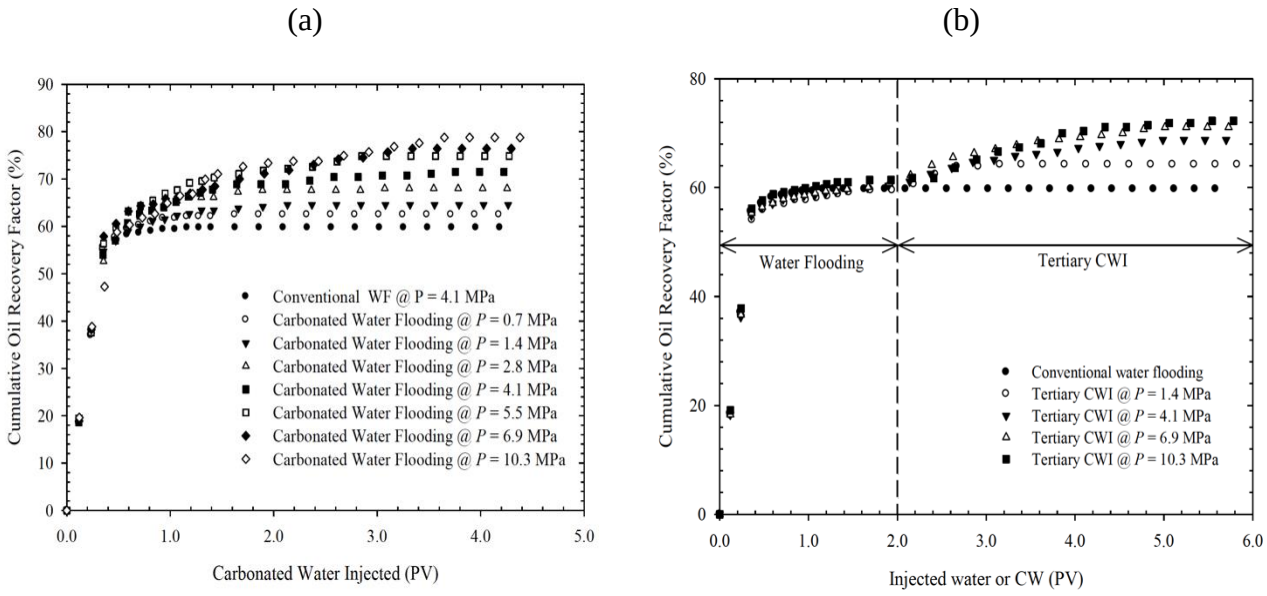

Figure 2.15: Effect of pressure on the performance of: (a) secondary CWI, and (b) tertiary CWI processes, conducted at the room temperature of 25 ˚C [29].

The ultimate recovery factor for the conventional WI at 4.1 MPa was reported to be 59.74 % (see Figure 2.15(a)). The relative increase in the oil recovery factor during secondary CWI (compared to conventional WI) varied from 2.74 % at 0.7 MPa to 19.02 % at 10.3 MPa, where the temperature was 25 °C. In the tertiary mode, as shown in Figure 15(b), an increase in the operating pressure at 25 °C increases the recovery factor additionally by 11.77 % at 1.4 MPa to 12.52 % at 10.3 MPa,

when compared to the conventional water flooding scenario. This extra oil recovery, which was observed at a higher operating pressure, was due to a higher CO_2 solubility in water, leading to further performance enhancement of the carbonated water injection operation [29]. The impact of operating pressure on the performance of CWI was also investigated by Fathollahi et al. [128] in a core flooding experimental study. A water- wet core with a permeability of 57 mD and a porosity of 0.18 was employed in their research work. The fluids including n-decane of 0.92 cP and a synthetic brine with an NaCl salinity of 35000 ppm were used where the operating conditions were 2000 psi and 30 ^oC. The performance of CWI was evaluated by increasing the operating pressure from 2000 psi to 3500 psi for both secondary and tertiary EOR scenarios. It was noticed that in the secondary mode of CWI, an increase in the operating pressure from 2000 psi to 3500 psi yields an increase in the ultimate recovery factor from 42.73 % to 44.39 % and an improvement in the recovery from 4.85 % to 8.63 % when compared to the conventional water flooding with a recovery factor of 37.88 % [128]. In the tertiary mode, increasing the operating pressure from 2000 psi to 3500 psi led to an improvement in the ultimate recovery factor from 39.39 % to 40 %, which is not appreciable [128].

2.8.2 Effect of Temperature

Using a sand pack porous system, Mosavat [29] investigated the effect of temperature on the recovery performance of CWI at 4.1 MPa and two different temperature values of 25 ^oC and 40 ^oC. Their experimental results are presented in Figure 2.16 in which the oil production (primary vertical axis) and CO_2 production (secondary vertical axis) data are plotted versus pore volume injection at two different temperatures.

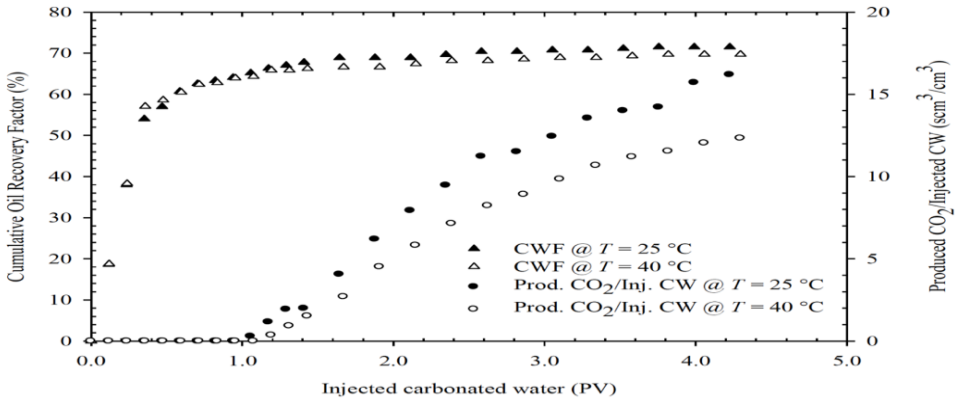

Figure 2.16 : Effect of temperature on recovery of oil and CO_2 production by CWI at 4.1 MPa, conducted in sand-packs at 25 ^oC and 40 ^oC [29].

As depicted in Figure 2.16, the breakthrough RF for both 25 ^{o}C and 40 ^{o}C was 55 %; but after injecting about 4 PV of carbonated water, the ultimate recovery at 25 ^{o}C was 68 %, while it was 65 % at 40 ^{o}C. This observation is justified by the reduced CO_2 solubility while injecting more carbonated water at a higher temperature (40 ^{o}C), which in turn reduces the performance of CWI. In Figure 2.16, the amount of produced CO_2 lowers from 16.5 scm^3/cm^3 at 25 ^{o}C to 12.5 scm^3/cm^3 at 40 ^{o}C after 4 PV of injected carbonated water (CW). This is because, at lower temperature causing greater CO_2 solubility, the CW holds more CO_2, which can be subsequently stored and produced in the pore spaces of the porous media. A mathematical modelling was conducted by Yang et al. [3] to study the effect of temperature on CWI performance with focus on IFT of the three-component liquid-liquid system using an oil with a viscosity of 0.009 mPa.s. In this modelling work, a core with a permeability of 1×10^{-12} m^2 and a porosity of 0.18 was used. The relative permeability curves were modelled using the Corey's equation, where the operating conditions including a pressure of 3.1 MPa and temperatures of 80 and 250 ˚C were considered. In this study, the IFT relationship with temperature for a three-component liquid -liquid system was assumed to be linear; hence the total cumulative oil production was 3250 m^3 at 80 ^{o}C. At 250 ^{o}C, the total cumulative oil production increased to 3500 m^3 after 200 days due to the IFT reduction. This outcome contradicts that of Mosavat [29]. It seems that CO_2 dissolution as the dominant mechanism in the oil production has not been accurately captured in the modelling work. Even though there is a IFT reduction during CWI, it is mainly attributed to the transfer of CO_2 from CW to the oil phase (not only temperature effect).

2.8.3 Effect of Injection Rate

A sand pack experimental set-up was used by Mosavat [29] to assess the influence of injection rate on CWI performance using a light crude oil of 44 ^{o} API and 2.76 mPa.s, where the ranges of permeability and porosity were 4011 mD - 6715 mD and 0.27 - 0.28, respectively. The performance of CWI in terms of recovery factor was investigated using different injection rates of 0.5 cm^3/min and 1 cm^3/min at a constant pressure of 4.1 MPa. Their research results show that at lower injection rate (0.5 cm^3/min) the recovery factor at the breakthrough was 56 %, while the ultimate recovery was 72 % for this injection rate. However, for the higher flow rate (1 cm^3/min) at a constant pressure of 4.1 MPa, the recovery factor at breakthrough and ultimate recovery were 54 % and 68 %, respectively. It was later explained that a higher recovery factor is achieved at a lower injection rate (0.5 cm^3/min) due to a longer contact time between CWI and the oil, which

allows a greater amount of CO_2 transfer across the phases [29]. Table 2.2 reports the specifications/conditions of the research work performed by Ahmadi et al. [124], which compares oil recovery of CWI at different injection rates (2 to 4 cm^3/h) and different CO_2 concentrations in the CW (0 to 3.2 mol%) in a water -wet core. In their study, the core permeability and porosity were in the range of 30 to 1500 mD and 0.08 to 0.11, respectively; where a live oil with a bubble point viscosity of 0.2109 mPa.s and a brine of 75000 ppm salinity of NaCl were considered. Other operating conditions were the initial pressure and temperature of 62.2 MPa and 415 K, respectively. It was found that an increase in the injection rate from 2 to 4 cm^3/h at a constant concentration of 0.8 mol% CO_2 increases the ultimate oil recovery factor from 40.9 % to 47.7 %. However, their experimental findings contradict the results attained in the experiments performed by Mosavat [29]. A numerical field scale simulation was also conducted by Ahmadi et al. [124] to predict the production history of an Iranian oil reservoir under CWI operation using ECLIPSE 300 compositional simulator.

Table 2.2: Effect of injection rate and CO_2 concentration on CWI performance [124].

Scale	Injection rate (cm^3/h)	Ultimate RF (% hydrocarbon pore volume or HCPV)			
		CO_2 concentration (mol %)			
		0	0.8	1.6	3.2
Core	2	38.2	40.9	43.7	48.7
	4	n/a	47.7	50.1	60.0
Field	3.03×10^6	30.7	32.3	34.5	40.6
	6.06×10^6	n/a	23.7	24.8	25.9

The initial reservoir pressure and temperature were 63.2 MPa and 421 K. An oil with an API gravity of 39 and a GOR of 276.6 m^3/m^3 was used in their simulation investigation. Different injection rates of 3.03 $\times10^6$ cm^3/h to 6.06 $\times10^6$ cm^3/h were taken into account to evaluate the performance of CWI. The results presented in Table 2 imply that at 3.3×10^6 cm^3/h and at 0.8 mol % of CO_2, the ultimate recovery factor was 32.3 %. At the same concentration of CO_2, when the injection rate was increased to 6.06 $\times10^6$ m^3/h, the ultimate recovery decreased to 23.7 %. For a field scale, this decrease in the recovery factor due to an increase in injection rate can be attributed to water coning; because the production wells are shut-off when the water cut reaches to 50 %,

leading to the recovery reduction. However, this is not a concern in the core scale as the water coning is not experienced in the core flooding runs [124].

2.9 **Pore Scale Aspects of Carbonated Water Injection**

Due to the successful performance of CWI in EOR projects, researchers are motivated to investigate the pore-scale mechanisms of CWI to explain the mechanisms responsible for the recovery enhancement. In this section, the pore-scale numerical and experimental studies of CWI will be addressed. These CWI pore-scale mechanisms involve the pore-scale observations on CO_2 diffusion to the oil phase, oil swelling, wettability alteration, CO_2 exsolution, CWI sweeping pattern, and pore-scale flow mechanisms in the micro-model. The pore-scale aspect of the CO_2 diffusion in the oil phase was investigated in some studies [129, 130]. For instance, a one-dimensional model was developed by Grogan et al. [129], which focused on simulating the swelling of residual oil by CO_2 diffusion through an intermediate water phase. The diffusion rate was calculated and the model results were compared to those determined from the laboratory micromodel and core flood experiments. It was concluded that CO_2 diffusion plays an influential role in the mobilization of residual oil ganglia after WF. By allowing sufficient time, the diffusion of CO_2 into oil ganglia and the oil swelling can increase their mobility, which enhances the oil production. Another numerical 1-D model was developed by Muller and Lake [130],where the CO_2 diffusion coefficients in water and oil were considered to be 3.6×10^{-9} m^2/s and 5.6×10^{-9} m^2/s under a reservoir temperature of 327 K and a pressure of 13.1 MPa, respectively. The numerical model was used to simulate the diffusion of CO_2 into the oil and the diffusional extraction of oil components by CO_2. According to their investigation, it was observed that CO_2 diffusion causes swelling, while extraction of the oil components causes the oil to be shrank. Their results showed that the two dimensionless parameters, which influence the oil production, are the ratio of the stagnant water to oil volumes and the solvent (CO_2) equilibrium constant at the phase boundaries. It was concluded that the diffusion coefficient of CO_2 has a minor effect on the ultimate oil production. This finding is different from the outcome of the work by Grogans et al. [129]. There are also numerous laboratory studies, focusing on the pore-scale aspect of CWI. Several fluid flow experiments were conducted on CWI using a high-pressure micro-model of porosity of 62 %, for n-decane of 16.47 cP at a pressure of 2000 psia and a temperature of 38 ^oC [2]. It was found that the main pore-scale mechanisms of the oil recovery by CWI are the oil swelling and coalescence of isolated oil ganglia, which results in fluid redistribution and consequently increases

the mobility of the residual oil. An interesting phenomenon in this research investigation was the gas nucleation subsequent to depressurizing of the porous system from 2000 psia to the pressures of 431 psia and 429 psia. This pressure reduction appreciably affected the production process, leading to an additional oil recovery [2]. As demonstrated in Figure 2.17 (gas positions indicated by red arrows 1 to 5), CO_2 gas exsolves from the solution due to depressurization of the micro model, based on Figure 2.18(a) to (f). It was also observed that the gas tends to move towards the bigger pores because of its wettability character as a non-wetting phase and less capillary pressure. The additional oil recovery attained from the gas growth (as a result of pressure depressurization) was not reported in the research work; however, it seems to be the main phenomenon, which is responsible for additional oil recovery during CWI [2].

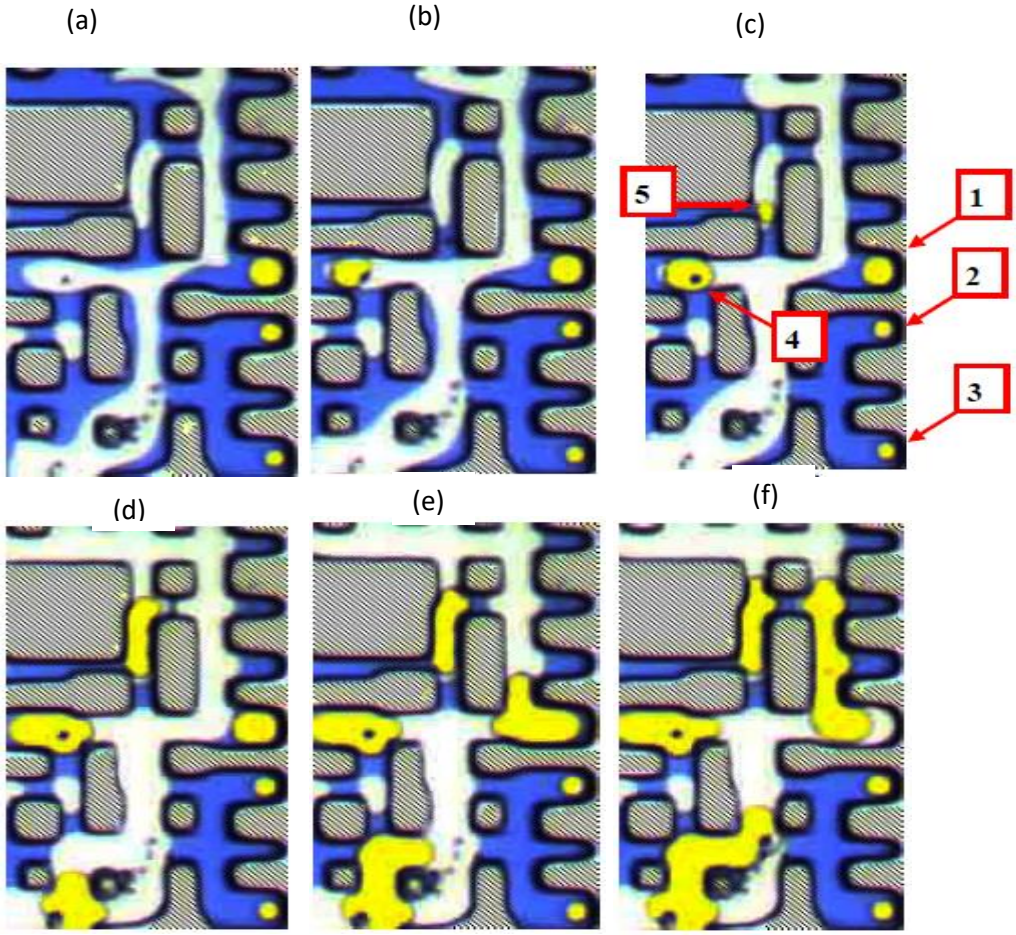

Figure 2.17:Gas nucleation occurrence at 431 psi to 429 psi [2].

Another interesting pore-scale aspect of the CWI related to CO_2 exsolution to form a free gas phase was also explored by Alizadeh et al. [131]. They studied the impact of in-situ CO_2 exsolution in CWI on the oil recovery. According to a micro computed tomography (CT) visualization of the pore spaces in CWI, it was found that as the pressure drops, it leads to formation of a new CO_2 gas phase in the CW solution, as depicted in Figure 2.18 [131]. It was observed that when the oil droplets are contacted with the free CO_2 gas, a thick layer of oil, which is placed between the brine and free CO_2, is displaced towards the production outlet along with the moving free gas (CO_2 clusters). A significant re-connection by CO_2 gas of the trapped oil was also noticed, while experiencing CO_2 exsolution in the CW solution due to the spreading of oil films during the CWI [131] .

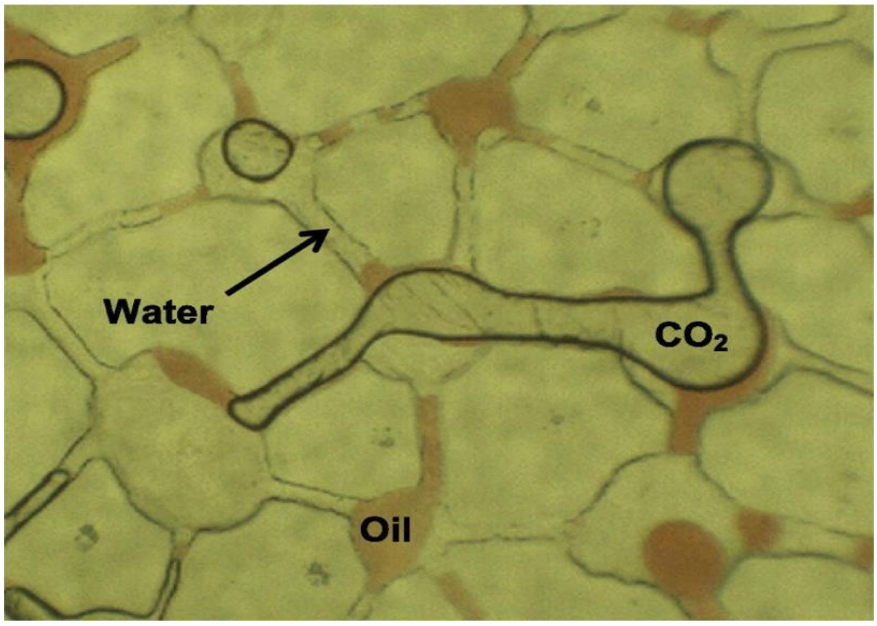

Figure 2.18: Pore-scale displacement of oil (brown), water (transparent), and exsolved CO_2 (transparent enclosed phase with a thick border line) during CWI process [131].

The formation of the free gas causes expansion due to the difference between the density of CO_2 in the solution and that in the free gas phase. The expansion will serve as an additional driving force for enhanced oil recovery. Moreover, when the saturation of exsolved CO_2 exceeds the critical gas saturation in the micro-model, the gas slug can attain enough mobility to flow in the porous medium; if the oil can spread on the brine phase in the presence of exsolved CO_2, a film of oil will be carried with the gas phase towards the production well. Thus, the oil spread on CO_2 will

also serve as another mechanism for enhancement of oil recovery. This oil recovery mechanism was explained by Chatzis [132] for oil production in the form of oil films around rising bubbles in water-wet glass micro-models.

In another CWI experimental work performed by Mosavat et al. [15], the wettability alteration, contact angle analysis, and residual oil trapping mechanisms during CWI strategy were investigated. Figure 2.19(a) to (d) present the saturation distribution in the micromodel after the water flooding, secondary CWI, tertiary CWI (after 5 PVI), and the extension of tertiary CWI (after 20 PVI). In Figure 2.19, the brown phase is oil, the blue phase is CW, and the white areas are the solid glass grains. It was found that the wettability trapping due to the relatively oil-wet nature of the micromodel is dominant during the water flooding process. Compared to the water flooding, less wettability trapping was observed during the secondary CWI. This phenomenon is the main reason why the secondary CWI can improve the oil recovery from oil-wet reservoirs through modifying the wettability of the formation from oil-wet to mixed or water-wet condition. In their conclusion, the wettability alteration was believed to be initiated by diffusion of CO_2 from the brine into the oil ganglia. It was also reported that the secondary CWI recovers additional 9.4 % oil while in the tertiary mode, additional 7.3 % was recovered when compared to the water flooding operation. It was also concluded that once CO_2 molecules reach the rock surface (in contact with the oil droplet), the molecules start replacing the hydrocarbon molecules that are adsorbed on the surface. This gradual replacement causes the rock surface to shift its wettability towards the water-wet condition. Hence, the beneficial role of CWI in improving the recovery of the original oil in place is through altering the wettability of the reservoir toward the water-wet condition.

(a) (b)

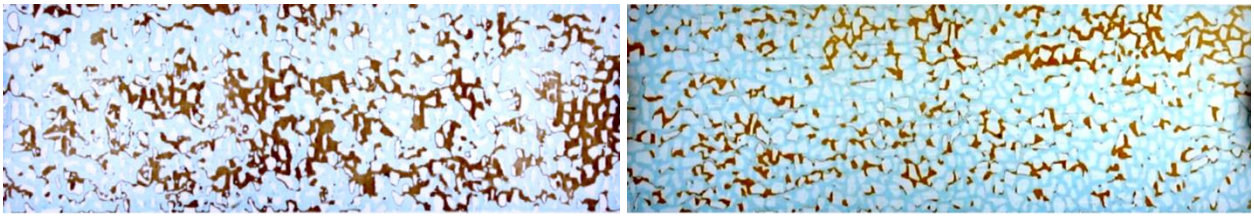

(c) (d)

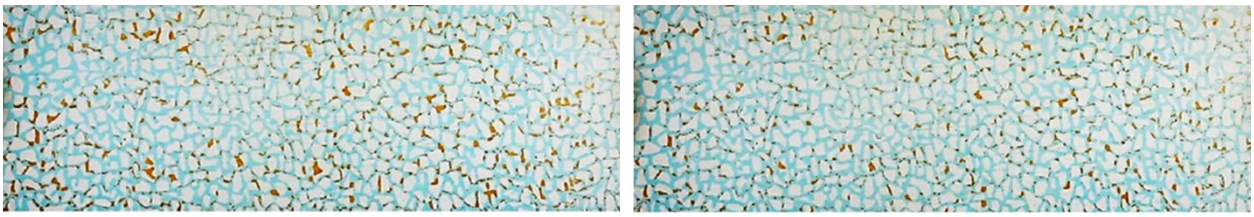

Figure 2.19: Pore-scale observation of saturation distributions in the micromodel: (a) at the end of waterflooding, (b) at the end of secondary CWI, (c) at the end of tertiary CWI after 5 PV, and (d) at the end of extended tertiary CWI after 20 PV [15].

Mosavat et al. [15] reported that the residual oil during CWI is in the form of films of oil on the surface of micro-model pore spaces, the interception of oil droplets (that were created by snap-off mechanism), and the oil bypassed in the pore spaces, as observed in Figure 2.20 [15].

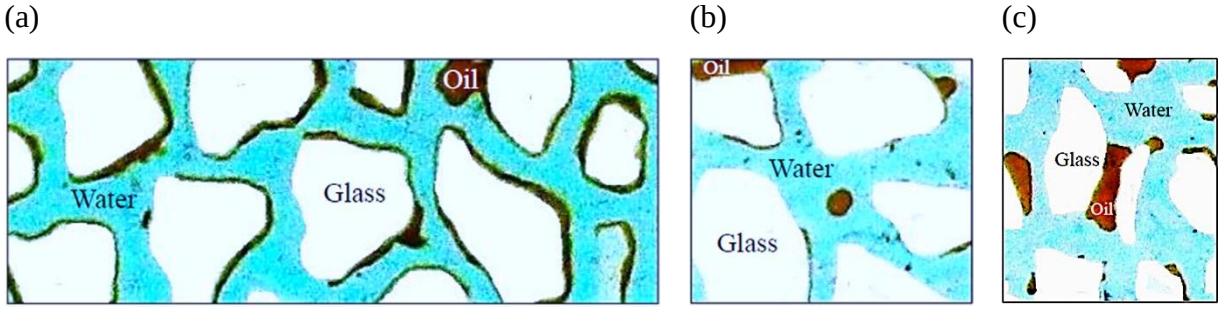

Figure 2.20: Pore-scale mechanisms of oil trapping after CWI process by: (a) a wetting film, (b) interception of oil droplet formed by snap-off, and (c) oil by-passed in pores [15]

One of their interesting observations was the residual oil in the form of continuous film of oil on the surface of grains (as seen in Figure 2.20(a)). The micro-model was originally oil-wet; however, after being in contact with CWI, the wettability alteration to oil phase in some areas of the micromodel was noticed. CO_2 is known to change the wettability. The work by Chiquet et al. [133] might be referred to obtain further understanding on the effects of CO_2 on the wettability of reservoir rock. A portion of the trapped oil in the dead-end pores was found to be trapped even

after 20 PVI (in CWI); however, a part of the residual oil trapped as oil ganglia was mobilized and eventually produced in CWI, as depicted in Figure 2.20(c).

When CW is injected into the micromodel, CO_2 molecules transfer from brine to the residual oil phase and gradually modify the oil–solid interactions at the micromodel surface. As a result, the wettability changes from oil-wet to water-wet condition, which greatly assists the residual oil detachment from the grains [15]. Wettability alteration is believed to be initiated by diffusion of CO_2 from the brine phase into the oil ganglia, which ultimately leads to improvement of the residual oil mobility.

An experimental investigation was performed by Mahdavi and James [117] to assess the influence of the fracture geometry on the performance of CWI. A fracture with a vertical orientation in a porous medium (e.g., micromodel) was fabricated to perform the tests at a pressure of 6.89 MPa and a temperature of 21 ^{o}C, where the oil viscosity was 6.8 cP, the overall micromodel permeability was 400 D, and the injection rate was 0.0024 cm^3/min. It was reported that a good sweep efficiency is attained by the carbonated water injection, compared to the water injection, even in the presence of fracture. According to their investigation, a recovery factor of 14.9 % was obtained after injecting 0.05 PV of CW, while only 9.2 % oil recovery were achieved in the WF process for the same amount of injected PV. Based on the displacement visualization patterns, it was observed that even in the presence of fractures, CWI exhibits a stable and better sweep, compared to the WF scenario.

A summary of the experimental studies (cores, sand-packs, and micro-models) is shown in Table 2.3 where the research works are organized chronologically. Four key columns namely; 1) CWI operating conditions, 2) oil sample, 3) porous media, and 4) CWI recovery data are included in Table 2.4. The improvement of oil recovery through both secondary and tertiary applications of CWI (compared to conventional water flooding) is highlighted in Table 4.

Table 2.3: Summary of experimental studies on CWI.

CWI operating conditions					Oil phase		Porous media			Ultimate recovery (%HCPV)			Ref
										WI	CWI		
T (°C)	P (psia)	Salinity (%wt)	CO_2 content (% wt)	Injection rate (cm^3/h)	Type	μ (cP)	K (mD)	Wettability*	Type§		Secondary	Tertiary	
38	2000	0	5	0.01	decane	0.83	n/a		MM	38	n/a	51	[2]
38	2000	0	5	0.01	synthetic	16.5	n/a		MM	n/a	n/a	35	[118]
38	2000	0	5	0.008	crude	145	n/a		MM	32	n/a	41	[134]
38	2000	1	5	20	decane	0.80	1300	WW	CF	69	73	n/a	[118]
38	2000	1	5	20	synthetic	81	n/a	WW	CF	50	53	n/a	
38	2000	1	5	20	decane	0.80	850	MW	CF	59	68	n/a	
38	2500	3.5	4.5	5	crude	154	4580	WW	CF	59	68	n/a	
38	2500	3.5	4.5	5	crude	8.5	1123	WW	CF	48.5	55.5	53	
25	104.7	n/a	2	0.2	mineral oil	n/a	89	WW	CF	40	n/a	74	[131]
25	104.7	n/a	2	3	mineral oil	n/a	88	WW	CF	35	n/a	75	
40	614.7	0	3	4	dead oil	70.7	3500	WW	SP	41	85	63	[135]
25	594.6	2	3	1	crude	2.7	5610	WW	SP	60	71	67	[6]
38	1998	1	5	20	n-decane	0.83	1300	WW	CF	60	70	n/a	[121]
38	1998	1	5	20	n-decane	0.83	850	MW	CF	55	67	n/a	
38	2500	3.5	sat	6	dead crude	31	n/a	WW	CF	34	n/a	62	[136]
37	2500	3.5	sat	1	North Sea oil	289	3580		CF	55	n/a	69	[137]
38	614.7	n/a	sat	10	dead oil	20	22	WW	SP	42	63	90	[138]
100	350	n/a	sat	30	crude (UAE)	n/a	1.5	OW	CF	54.3	n/a	63.7	[123]
100	350	n/a	sat	30	crude (UAE)	n/a	8.2	OW	CF	67.2	69.3	71.2	
100	350	n/a	sat	30	crude (UAE)	n/a	20.2	OW	CF	57.4	63	62.4	
38	2500	n/a	2	5	Live oil	31.2	n/a	WW	MM	25	35	n/a	[139]
142	6900	7.5	0.8, 1.6	2	crude (Iran)	0.21 (Pb)	30-150	OW	CF	30-39	40	n/a	[124]

* WW = water-wet; MW = mixed-wet; OW = oil-wet

§ CF = coreflood; MM = micromodel; SP = sandpack; sat = saturated

2.10 **Effects of CWI on Reservoir Fluid and Rock Properties**

As CO_2 moves from water into the oil phase, it normally makes changes on the physical properties of the reservoir fluids and various characteristics of the rock. The changes to crude oil and formation brine properties such as density, viscosity, and interfacial tension, rock permeability, rock porosity, and rock wettability during CWI are reported in the open sources [88].

2.10.1 Crude Oil Density and Viscosity Variation

The effect of CWI on oil properties such as density and viscosity has not been systematically studied yet. However, it is clear that the density and viscosity of oil will alter during CWI similar to what happens in pure CO_2 injection operation, but not to the same extent. To investigate the variation of the oil density during the CWI process, a series of experiments were conducted by Jones et al. [140] to determine the oil viscosity, oil density, saturation, and swelling factor at three different values of temperature; namely, 75 ^{o} F, 140 ^{o} F, and 200 ^{o} F. For each temperature, measurements were carried out for 11 pressure steps ranging from 200 psi to 5000 psi. Different oil samples with an API gravity ranging from 10 to 17 were utilized. It was concluded that the presence of CO_2 may increase or decrease the oil density, depending on temperature, pressure, and oil type; the density of heavy oil systems was found to be significantly reduced with the addition of CO_2 (at temperatures of 140 ^{o} F and 200 ^{o} F). An experimental study to investigate Wilmington oil viscosity versus pressure at different isothermal conditions of 75 ^{o} F, 140 ^{o} F, and 200 ^{o} F was performed, where the results are presented in Figure 2.21 [140]. It was found in all cases that the viscosity of the oil in the absence of CO_2 increases as the pressure increases, while the viscosities of the oil with CO_2 in the solution decrease as the pressure increases.

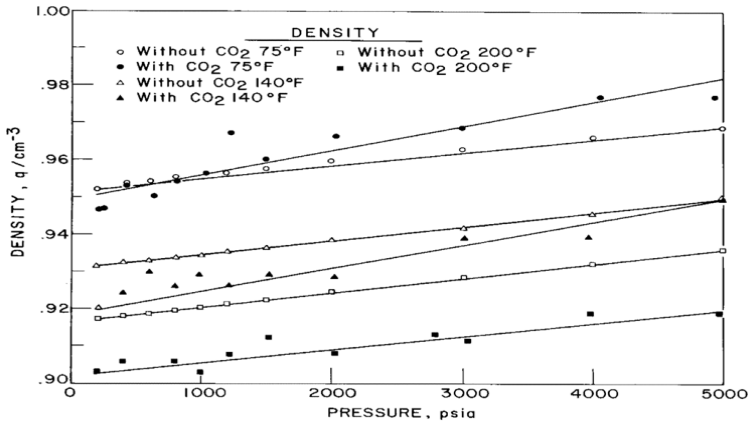

Figure 2.21: Density of Wilmington Oil at 75 ° F, 140 ^{o} F, and 200 ^{o} F [140].

Viscosity of heavy oil systems was significantly reduced at temperatures of 75 ^{o}F, 140 ^{o}F and 200 ^{o}F with the addition of CO_2 [140]. Barrufet et al. [141] also presented some experimental data for the viscosity of Decane/CO_2 mixtures for various temperatures and CO_2 concentrations. The experimental results show that by increasing the temperature and CO_2 concentration, the viscosity of crude oil is lowered [88].

2.10.2 Variation of Reservoir Rock Properties

A microscopic observation on the effect of CWI on the reservoir rock was made by Riazi through a static treatment (e.g., no flow)[142], as depicted in Figure 2.22. The dissolution of CO_2 in water can form a carbonic acid, leading to dissolution of reservoir rock [143]. Figure 2.22 was obtained from scan electron microscopy (SEM) on a sample of sandstone before and after exposure to CWI. It was observed that the sandstone is corroded by bicarbonates due to prolonged exposure to CWI for 2 weeks at the process conditions of 2000 psi and 38 ^{o}C.

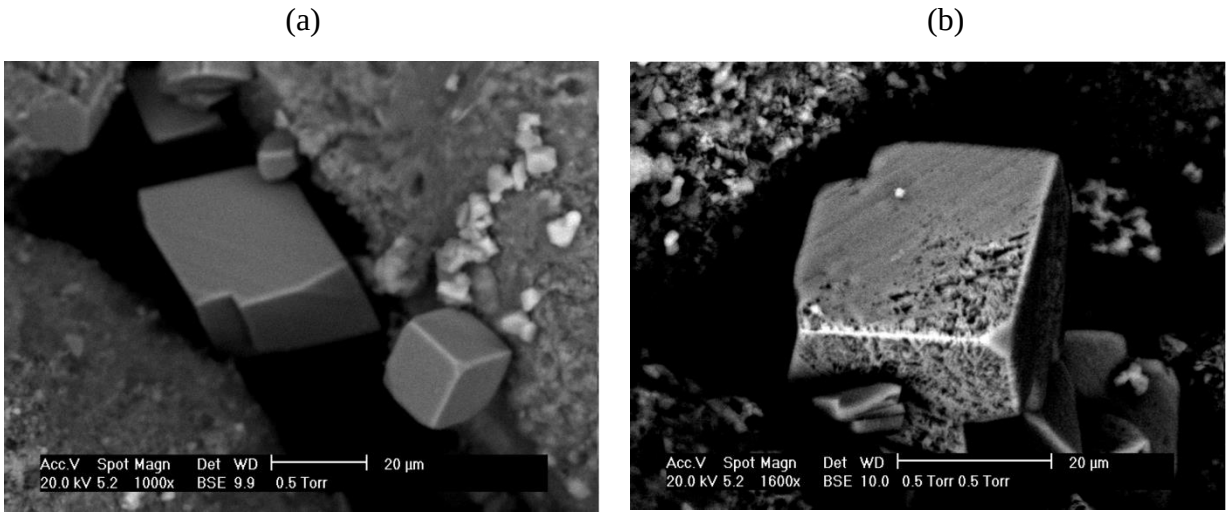

Figure 2.22: Scan electron microscopy pictures of a sandstone (a) before and (b) after contact with CWI for 2 weeks at a pressure of 2000 psi and a temperature of 38 ^{o}C [143].

The effect of CWI on the permeability and porosity was studied in an experimental set-up using a dolomite core [144]. The experimental run was conducted using a core with a porosity and a permeability of 15.905 % and 252 mD, respectively, at an operating temperature of 70 ^{o}C, where the pressure varied from 7500 psi to 8500 psi and the injection rate was 2 cm^3/min. The injected fluid contained 21.5 % CO_2 and a synthetic sea water where the salinity was 38,000 ppm. X-ray

computed tomography (CT) provided the image acquisition to evaluate how porosity was changed through the test where the permeability was calculated using Darcy's Law, and the pressure drop values were determined by employing the pressure transducers. The results of their investigation are illustrated in Figure 2.23.

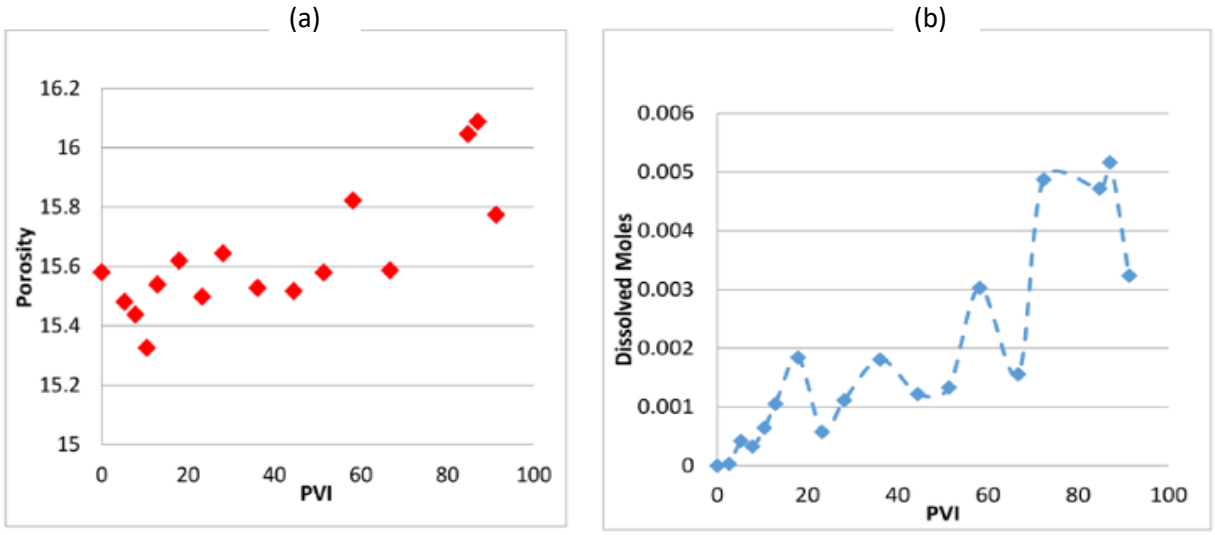

Figure 2.23: Effect of CW on (a) porosity and (b) amount of dissolved moles of dolomite in CWI core flooding tests at 70 ˚C (modified after [144]).

An increasing trend of porosity up to 16.15 % was observed in Figure 2.23(a), which is attributed to dissolution of rock due to the reaction of the carbonic acid with the rock surface. They also supported their conclusion through presenting Figure 2.23(b), which shows an increase in moles of dissolved dolomite with a number of PVI. This confirms that the porosity increase is as a result of an increase in the number of moles of dolomite being dissolved during CWI during the experiment. No appreciable change in the rock permeability was noticed in the tests.

2.11 **Modeling and Simulation Investigations of CWI**

The CWI process is not a mature EOR technique. Hence, the modeling/simulation studies of CWI are not extensive. One of the problems with simulating CWI approach is lack of enough experimental data for prediction of important parameters (relative permeability and swelling factor) and model validation. The first mathematical model to simulate CWI was developed by De Nevers [19], which was based on the Buckley–Leveret theory to predict the CWI performance. In this model, the capillary and gravity effects were ignored and the model was able to incorporate the effect of oil viscosity reduction and oil swelling due to carbon dioxide transfer to the reservoir oil. Based on the results attained from this model, it was concluded that viscosity reduction is the dominant factor and the oil swelling has a lower contribution to the oil recovery improvement. The main assumption of this model was that the pressure remains constant throughout the reservoir or/and the pressure is high enough so that there is no free gas which is rare in practice. About 10 years later, a 2-D dynamic three-phase flow mathematical model was developed by Dixon et al. [145]. They extended the black oil formulation to include the solubility of CO_2 in water so that the developed approach was able to investigate the important aspects (e.g., displacement mechanisms and recovery factor) of CWI and CO_2 flooding in a Berea sandstone core at 1300 psia and 125 ^oF. The implicit method was used for discretization of the pressure equation. The saturation equation was also discretized explicitly and both equations were solved by the iterative method proposed by Douglas and Rachford [146]. They did not show the performance of CWI (CO_2 saturated water) in terms of rock type, fluid properties, and process conditions; however, the model was able to simulate four runs of CO_2 slugs/relative amount of CO_2 (150, 300, 356, and 450 cm^3/cm^3). The results imply that the recovery of original oil in place increases with an increase in the relative amount of injected CO_2 to 52%, 63%, 65%, and 70%, respectively. A compositional simulator being able to simulate CO_2 dissolution in the water phase during CO_2 injection projects was developed by Mansoori [20]. The Soave-Redlich-Kwong (SRK) equation of state was used in the model for phase equilibrium calculations and for estimating CO_2 solubility in water and fluids density. The finite difference form of the flow equations was used, resulting in an implicit oil pressure and explicit overall grid block composition system. The model was utilized to simulate 1-D and 2-D displacement processes with bottom hole pressures of 1900 psi and 1750 psi for injection and production wells, respectively [20]. The discretized sets of equations were solved using the Newton's method until convergence was achieved. The injection scheme used in the

model consisted of 0.05 PV of CO_2 separated by three water slugs of 0.05 PV. In the developed 3-dimensional model, the objective of the simulation runs was to investigate the effect of CO_2 solubility in water on oil recovery. Based on the simulation results, it was found that about 10 % of the injected CO_2 are dissolved into water and the higher the solubility of CO_2 in water the higher oil recovery is achieved. A 3-D three-phase compositional model to simulate CO_2 flooding processes was presented by Chang et al. [18], where CO_2 dissolution in the water phase was considered. An oil with a viscosity of 0.7 cP and a brine phase with 10 wt % salinity were used in the modeling work. The oil and gas densities and their fugacities were modeled by SRK equation of state; the gravity and capillary terms were also included in the model. The governing equations were discretized by the finite difference and the implicit pressure explicit saturation (IMPES) method was used in formulating the Jacobian matrix. For a typical case, the injection rate was 7500 stb/d with the pressures of 4500 psia and 5000 psia assigned for the injection and production wells, respectively [18]. It was also assumed that phases would reach the thermodynamic equilibrium, instantaneously. The Gaussian elimination method was applied to solve the equations to obtain the main variables such as pressure and saturation. A commercial simulator (E300) was employed by Kechut et al. [24] to simulate a series of carbonated water flood experiments. It was concluded that E300 over-predicts the oil recovery, compared to the experimental data for all core-flood tests. They explained that the over-prediction is due to the assumption of instantaneous equilibrium condition that was included in the commercial compositional simulator; it was argued that the instantaneous equilibrium between CO_2 and water or/and complete mixing assumptions would not be feasible in real CWI cases. A 1-D mathematical model was developed by Foroozesh et al. [22] which included the mass transfer term to capture the mixing process of CO_2 in water. The fully implicit technique was combined with the Newton–Raphson iterative method to solve the equations. In their work, the oil–water relative permeability functions were defined based on the Corey's correlations [147]. Capillary pressure curve was defined based on the Brooks-Corey correlation [147] .The proposed model was used to simulate the oil recovery in a sandstone core and a water-wet Clashach core, which were originally saturated with decane. In the research work, the gravity term was ignored. The injection rate used for this model was 20 cm^3/h, where the CO_2 concentration was 5 % wt , having 10,000 ppm brine in the injected CW. The developed model was validated with their experimental data and a close match was observed for the total oil production (recovery factor and cumulative recovery) and differential pressure. An enhanced

numerical simulation with application to CWI in core flooding experiments was later developed [148]. The model was employed to forecast the average gas saturation in the core. They then used the saturation distribution to tune the thermodynamic EOS for phase behavior. The oil-water and gas-oil relative permeability functions/curves were adjusted to match the results of the core flood experiments. The Baker's model [149] was used to define the oil-relative permeability curves. The homogenous core was utilized to be saturated with an oil with a viscosity of 1.41 cP. A constant bottom hole pressure and an injection rate of 2500 psi and 5 cm^3/h, respectively, were considered in the simulation. The modeling strategy was implemented to obtain the cumulative oil production, water production, and CO_2 production, implying a good agreement between the modeling outputs and the experimental results from CWI core flooding tests [29].

Table 2.4 lists a summary of the CWI modelling investigations. Table 2.4 is organized chronologically; including three main columns namely; CWI operating parameter, oil sample, and model characteristics. For all the studies summarized in this table, finite difference method of discretization is used, and the effect of capillary pressure is neglected in all models.

Table 2.4: Summary of mathematical modelling studies on CW.

CWI operating parameter					Oil sample		Model									
T (ºC)	P (psia)	Salinity (%wt)	CO_2 content (%wt)	Injection rate (cm^3/h)	Type	μ (cP)	Dimension	Discretization	EoS	Form	Oil model	P_c included	k_r model	K (mD)	Application/Remarks	Ref
25	1300	10	2.2	0.0012	crude	2.2	2D	Finite difference	n/a	n/a	Compositional	n/a	n/a	200	CWI, CO_2 flooding Computation time =0.000317 s/(iteration. grid)	[150]
		10			crude	0.7	3D	Finite difference	SRK	IMPES	Compositional	n/a	n/a	n/a	Effect of CO_2-water solubility on oil recovery by CO_2 flooding and CWI	[20]
38	4500	10	n/a	0.006	live	0.7	3D	Finite difference	SRK	IMPES	Compositional	n/a	n/a	n/a	CO_2 flooding and CO_2 solubility in water in CWI	[18]
37	2500	3.5	n/a	1	North Sea	145	1D	Finite difference	PR	n/a	Compositional	n/a	Corey	4580	Modeling CWI and CO_2 storage.	[137]
38	1998	1	5	20	decane	0.83	1D	Finite difference	PR	n/a	Black oil	n/a	Corey	1300	Mass transfer coefficient and wettability effects on RF in CWI.	[121]
38	2500	3.5	n/a	5	crude	31.5	1D	Finite difference	PR	n/a	Compositional	n/a	Baker	n/a	CWI with CO_2 exsolution potential.	[139]
140	6690	7.5	0.8	3.0	crude (Iran)	0.21	3D	Finite difference	PR	n/a	Compositional	n/a	n/a	335	Modeling CWI at field and core scales.	[124]

2.12 Practical Challenges in CWI

The main applications of CWI are in enhanced oil recovery, remediation, and carbon sequestration operations. The common practical challenges with the CWI implication for enhanced oil recovery operations include preparation process of CW, corrosion, scale formation/ asphaltene precipitation (around the wellbore region), water weakening effect, and high capital, operating, and maintenance costs [29].

2.12.1 CW Preparation

It is a fairly difficult task to prepare the CW at large scales and under desired pressure and temperature conditions. One of the well-known technologies to produce carbonated water is the gas infusion generator that uses thousands of hydrophobic micro-hollow fibres to dissolve CO_2 gas into water at elevated pressures. There are some safety concerns and high total costs to design and operate the carbonated water preparation processes [10, 151, 29].

2.12.2 Corrosion

Another serious issue that can be associated with CWI is corrosion of the process facilities due to the formation of carbonic acid (H_2CO_3) as a result of CO_2 dissolution in water. The acid promotes corrosion of carbon steel, and therefore demands corrosion-resistant materials such as stainless steel for safe operation, which will increase the capital and operating expenses. The important factors governing the dissolution process are the partial pressure of CO_2 in the gas phase, temperature, pH of CW, water salinity, and velocity of the fluids in the pipelines and wells [152]. The De Waard-Milliam's equation is usually used to predict the corrosion rate of carbon steel in terms of the partial pressure of CO_2, temperature, and injection rate [152]. It should be noted that as the carbonated water flows through the formation, it becomes saturated with bicarbonates, and loses its acidic nature and reactivity. Despite the concern that carbonic acid may cause localized corrosion of steel [153], no evidence of corrosion in the production wells and flow lines was reported in the first commercial K&S carbonated water flood project [154]. Referring to the impact of carbonated water on equipment during a CWI pilot test performed by the Amoco production company in the Slaughter field (Texas), it was found that stainless steel and aluminum bronze materials experience no deterioration during the pilot tests [26].

2.12.3 Scale Formation and Asphaltene Precipitation

It is well-known that the injection of CO_2 in oil reservoirs can lead to scale formation and precipitation of asphaltene, which is a sticky substance that clogs the formation pores and production equipment [155,156]. Even though the CO_2 is completely dissolved in water at the operating pressures in the CWI process, CO_2 can exist in a free phase under certain thermodynamic conditions, where the operating pressure drops below the minimum miscibility pressure. Hence, the occurrence likelihood of similar phenomena such as scale formation and asphaltene precipitation, which normally happen during pure CO_2 injection, are fairly high.

2.12.4 Water Weakening Effect

The water weakening effect refers to the deformation of reservoir layers (especially for chalk layers) during water flooding. This effect causes several issues; including, reservoir compaction and seabed subsidence [157]. The effect of carbonated water on the rock/fluid interaction has been studied by several researches [158,159]. It was found that the mechanical strength of high porosity rocks especially chalk formation is affected by using carbonated water. This water weakening effect is enhanced due to increased dissolution of chalk in the presence of CO_2 [160].

2.12.5 High Capital, Operating, and Maintenance Cost

CWI has been proven as a viable enhanced oil recovery method, though economic aspects of the process might be a serious concern. For instance, high total costs for drilling, CW preparation, pressure pumps, well completion, and operation and maintenance stages are expected during field implementation of CWI.

2.13 CO_2 Storage Capacity of CWI

Global warming has raised the awareness of societies and it has been linked to a considerable increase in the level of greenhouse gases in the atmosphere. CO_2 alone is responsible for about 72 % of the total greenhouse gas emissions [161]. In 2015, the International Panel on Climate Change (IPCC) agreed on a reduction in the level of CO_2 in the atmosphere. A 14 % share in CO_2 reduction was considered through carbon capture and storage strategy [162]. CWI has the potential to store CO_2 in geological formations, while recovering oil. Thus, CO_2 storage is a secondary benefit achieved from employing the CWI process. This benefit remains as a key asset of CWI, compared to other EOR processes. Several simulation and experimental studies have been carried out to investigate this carbon sequestration potential [17-29, 134]. A numerical simulation and

experimental investigation of CWI was performed by Nor et al. [134] on a core with a permeability of 4580 mD, a porosity of 0.35 %, and under operating conditions of 2500 psig, 100 ^{o}F, and 1 cm^3/h injection rate. It was reported that 3857 scm^3 of CO_2 are injected in the secondary mode and 45 % (1754 scm^3) of the injected CO_2 are stored after this period. CWI in the tertiary mode was also investigated. It was found that after injecting 4000 scm^3, about 51 % (2043 scm^3) of injected CO_2 are stored. In the sand pack flooding experiments conducted by Mosavat [29], it was observed that CO_2 accumulates during the CWI operation, and it is stored in the porous medium after 1 PVI. The results are presented in Figure 2.25 for the pressure range of 0.7 MPa to 10.3 MPa [29]. After 1 PVI, the amount of CO_2 stored in the porous medium is stabilized for the rest of the injection process. The reason for this trend is that the porous medium has reached its maximum capacity and no more CO_2 can be dissolved in oil or stored in the pore spaces, considering the operating pressure, temperature, and salinity. As it is expected, at a higher pressure, the storage capacity of a porous medium in capturing CO_2 increases, which is due to increased solubility of CO_2 in water.

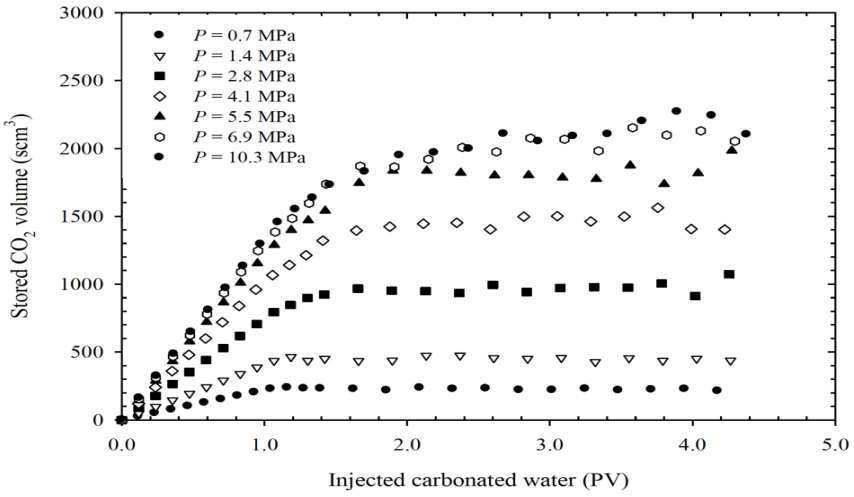

Figure 2.24: Cumulative CO_2 storage capacity by CWI process at 25 ˚C and different pressures [29].

A mathematical model of carbonated water injection for EOR and CO_2 storage was used to estimate the CO_2 storage [25]. A water-wet sandstone core with a permeability and a porosity of 1300 mD and 0.19, respectively, was used under operating conditions of 20 cm^3/h injection rate, 136. 1 atm pressure, and a temperature of 38 ^{o}C. The model predicted that 100 % of injected CO_2 are stored in the porous system before breakthrough, while the storage capacity declines after the

breakthrough. It was also found that at the end of the simulation period, 44 % of injected CO_2 are stored in the core. In a core-flooding experiment, the potential of CO_2 storage during CWI was investigated [17]. A sandstone core with a permeability and a porosity of 98.73 mD and 17.68 %, respectively, was employed. A crude oil with an API gravity of 20.8^o and a synthetic brine with a salinity of 54 647 ppm were also used for this experiment under the test conditions of 2500 psi, 100 ^{o}F, and injection rate of 5 cm^3/h. It was concluded that after the secondary CWI, about 47.5% of the injected CO_2 are stored inside the core and 44 % of the injected CO_2 are stored after tertiary CWI.

2.14 **Conclusions**

CWI has been a proven EOR technique since it was first introduced in the 1940s with an additional benefit of CO_2 storage. It further enhances oil recovery in both secondary and tertiary modes, compared to conventional water flooding. Due to the nature of CW (as a single-phase fluid comprising of water and CO_2), it gives a stable front, and better sweep efficiency in comparison to other alternative EOR methods such as WI, CO_2 injection, WAG, and SWAG. Several experimental research works have focused on the pore scale, micro scale, and macro scale mechanisms of CWI to understand the process and to obtain optimal conditions for achieving high recovery factor. Many mathematical modelling, simulation, and optimization studies have also been carried out to conduct systematic parametric sensitivity analysis for design, scale-up, and optimization purposes. Although extensive studies on the theoretical and practical aspects of CWI have been carried out, no comprehensive review on CWI is available in the literature. In this review paper, the effects of important variables on CWI performance (fluid properties, reservoir properties, and operating conditions) are extensively studied and summarized for the field, experimental, and modelling approaches of CWI. A large number of previous research investigations are well reported and the key technical and practical challenges associated with CWI are presented. The following important conclusions as drawn based on this review.

- Although CWI is assumed to be a single-phase injection of completely dissolved CO_2 in water, the effect of gas exsolution can occur as the pressure drops. This phenomenon will provide an additional energy for the displacement of oil along the gas growth path, leading to an additional oil recovery.

- CO_2 concentration, brine salinity, injection pressure, temperature, and injection rate are important operating conditions that notably affect the performance of the CWI process. Wettability is another key factor which controls the overall performance of the CWI process.
- There is a limited leakage of CO_2 because CW is injected as a single phase fluid and the operating pressures is lower than the fracture pressure of the reservoir rocks.
- The reservoir heterogeneity does not reduce the performance of CWI as CW was able to sustain a stable front even along the fractured channels or zones.
- Existing mathematical models of CWI have difficulties to successfully match the experimental oil recovery data so that the absolute error percentage is about 10 %, implying a fairly big difference between the modeling results and real data. This is attributed to the fact that instantaneous and complete mixing of CO_2 and water is assumed during model development. Lack of proper correlations/curves for capillary pressure and relative permeabilities can also lead to prediction errors.
- Mathematical models that appropriately capture all of the underlying physical and chemical phenomena of CWI processes such as dissolution, gravity, hysteresis and 3-D spatial orientation have not been yet developed.
- Although there is a formation of carbonic acid (H_2CO_3) because of CO_2 dissolution in water during CWI operation, corrosion of the flow lines and production wells has not been reported in real cases.
- Implementation of CWI may alter the petrophysical properties (porosity and permeability) of the porous medium, core, or/and reservoir. It is found that the porosity increases due to dissolution caused by carbonic acid, especially for dolomite and limestone rocks.
- There is no comprehensive investigation on the impact of reservoir properties on CWI performance in the literature. It seems that further experimental and modeling investigations are required to fill this knowledge gap.
- The occurrence of asphaltene precipitation during CWI operations has not been highlighted in several research works, while it is expected to occur during the CO_2 exsolution resulted from the pressure drop.

- CO_2 storage capacity appears to be an additional benefit during the implementation of CWI. There are a large number of research and industrial projects ongoing in the area of carbon management where CWI is proposed for EOR and CO_2 sequestration purposes.

Acknowledgements

The financial assistance offered by Memorial University (NL, Canada), Natural Sciences and Engineering Research Council of Canada (NSERC), InnovateNL (formerly RDC), and Statoil Canada is greatly acknowledged.

Nomenclatures

Acronyms

API	American Petroleum Institute
bbl	Barrel
BT	Break Through
cP	centi Poise
CW	Carbonated Water
CWI	Carbonated Water Injection
CT	Computed Tomography
CWF	Carbonated Water Flood
CF	Core Flood
EoS	Equation of State
EOR	Enhanced Oil Recovery
E300	ECLIPSE300
GI	Gas Infusion
HCPV	Hydro-Carbon Pore Volume
IMPES	Implicit Pressure, Explicit Saturation
IFT	Inter Facial Tension
IPPC	International Panel on Climate Change
K_r	Relative permeability
LSWAG	Low salinity SWAG
MPa	Mega Pascal
mD	milli Darcy
MW	Mixed wet
MMP	Minimum Miscibility Pressure
n/a	Not applied
OOIP	Original Oil Initially in Place
OW	Oil Wet
PVI	Pore Volumes Injected
PV	Pore Volume
psi	Pounds per square inch
P_c	Capillary Pressure
ppm	Parts per million

PVT	Pressure Volume and Temperature.
PR	Peng-Robinson
Ref	Reference
RF	Recovery Factor
R_s	Solubility of CO_2 in oil
SWAG	Simultaneous Water Alternating Gas
SRK	Soave-Redlich-Kwong
STP	Standard Temperature and Pressure
SEM	Scan Electron Microscopy
SP	Sand Pack
scf	Standard cubic feet
sat	Saturated
SF	Swelling Factor
UT	Ultimate
WW	Water Wet
WAG	Water Alternating Gas
WI	Water Injection
WF	Water Flood
wt	weight

Variables

C	Equilibrium concentration
D	Diffusion coefficient
h	hour
K	Partition coefficient
K	Permeability
M	Molality
P	Pressure
q	Volumetric flow rate
S	Salinity
T	Temperature
x	composition

Greek letters

ρ	Mass density
μ	Viscosity
Φ	Porosity
ω	Mass fraction of phase
η	Solvent viscosity
γ	Interfacial tension

Subscripts

eff	Effective

w	Water
o	Oil
CO_2	Carbon dioxide

Superscripts

A	constant
B	constant
m	constant
n	Archie's coefficient

References

[1] Thomas, a., polymer flooding, in chemical enhanced oil recovery (ceor) - a practical overview. 2016, intechs.

[2] Riazi, m., m. Sohrabi, and m. Jamiolahmady, experimental study of pore-scale mechanisms of carbonated water injection. Transport in porous media, 2010. **86**(1): p. 73-86.

[3] Yang h, lesly james and thormod johansen, carbonated water injection for eor in one dimensional flow with constant pressure boundaries, st johns, 2013.

[4] Ghedan, s.g., global laboratory experience of co_2-eor flooding, in spe/eage reservoir characterization and simulation conference. 2009, society of petroleum engineers.

[5] Kulkarni, m.m. and d.n. rao, experimental investigation of miscible and immiscible water-alternating-gas (wag) process performance. Journal of petroleum science and engineering, 2005. **48**(1-2): p. 1-20.

[6] Mosavat, n. And f. Torabi, application of co_2-saturated water flooding as a prospective safe co2 storage strategy. Energy procedia, 2014. **63**: p. 5408-5419.

[7] Marfarlane r.m and j. N. Breston, oil recovery from cores when flooded with carbonated water and liquid co_2, 1952.

[8] Hickok, c.w. and h.j. ramsay, case histories of carbonated waterfloods in dewey-bartlesville field, in spe secondary recovery symposium. 1962, society of petroleum engineers.

[9] Riazi, m., et al., oil recovery improvement using co_2-enriched water injection, in europec/eage conference and exhibition. 2009, society of petroleum engineers.

[10] Li, z. And a. Firoozabadi, cubic-plus-association equation of state for water-containing mixtures: is "cross association" necessary? Aiche journal, 2009. **55**(7): p. 1803-1813.

[11] Ireland, s., et al., mathematical modelling of carbonated water injection including mass transfer kinetics, in proceedings of spe reservoir characterisation and simulation conference and exhibition. 2013, society of petroleum engineers.

[12] M. Sohrabi, n. Kechut and m. Jamiolahmady, safe storage of co_2 together with improved oil recovery by co_2 enriched water injection, 2011.

[13] Y. Eric, t. Erika, v. Osvair and j. Euclides, study of petrophysical properties alteration during carbonated water injection, brazil, 2015.

[14] Mosavat, n. And f. Torabi, performance of secondary carbonated water injection in light oil systems. Industrial & engineering chemistry research, 2013. **53**(3): p. 1262-1273.

[15] Mosavat, n. And f. Torabi, micro-optical analysis of carbonated water injection in irregular and heterogeneous pore geometry. Fuel, 2016. **175**: p. 191-201.

[16] Tavakolian, m., et al., significant improvement in oil recovery and co2 storage by carbonated water injection (cwi), in third eage co2 geological storage workshop. 2012, eage publications bv.

[17] Seyyedi, m, s. Mehran and s. Adam, quantification of oil recovery efficiency, co2 storage potential, and fluid-rock interactions by cwi in heterogeneous sandstone oil reservoirs, 2017.

[18] Chang, y, b. Coats and j. Nolen, a compositional model for co2 floods including co2 solubility in water, spe, 1998.

[19] De nevers, a calculation method for carbonated waterflooding, journal of society of petroleum engineers, 1964.

[20] Mansoori, j. Compositional modelling of co2 flooding and the effect of co2 solubility in water, spe, 1982.

[21] Embid, s. And o. Rivas, simulation of miscible displacement with interphase mass transfer resistance. Spe advanced technology series, 1994. **2**(01): p. 161-168.

[22] Foroozesh, j. And m. Jamiolahmady, simulation of carbonated water injection coreflood experiments: an insight into the wettability effect. Fuel, 2016. **184**: p. 581-589.

[23] Kechut, n.i., et al., tertiary oil recovery and co2 sequestration by carbonated water injection (cwi), in spe international conference on co2 capture, storage, and utilization. 2010, society of petroleum engineers.

[24] Sohrabi, m., et al., coreflooding studies to investigate the potential of carbonated water injection as an injection strategy for improved oil recovery and co2 storage. Transport in porous media, 2011. **91**(1): p. 101-121.

[25] Ireland, s., et al., mathematical modelling of carbonated water injection including mass transfer kinetics, in proceedings of spe reservoir characterisation and simulation conference and exhibition. 2013, society of petroleum engineers.

[26] Blackford, t.a., carbonated waterflood implementation and its impact on material performance in a pilot project, in spe annual technical conference and exhibition. 1987, society of petroleum engineers.

[27] Green, d and r. A. Dawe, enhanced oil recovery, vol. Spe textbook series, richardson tx, 1998.

[28] Steffens, a. Modelling and laboratory study of carbonated water flooding, netherlands, 2010.

[29] Mosavat, n. Utilization of carbonated water injection(cwi) as a means of improved oil recovery in light oil systems: pore scale mechanism and recovery evaluation, regina, 2014.

[30] Shu, g. Improvement of carbon dioxide eor in water-wet reservoirs by using active carbonated water, calgary, 2016.

[31] Zendehboudi, s., et al., asphaltene precipitation and deposition in oil reservoirs – technical aspects, experimental and hybrid neural network predictive tools. Chemical engineering research and design, 2014. **92**(5): p. 857-875.

[32] Van der meer, b., carbon dioxide storage in natural gas reservoir. Oil & gas science and technology, 2005. **60**(3): p. 527-536.

[33] Whitson, c and m. R. Brule, phase behaviour, texas: spe, 2000.

[34] Konrad, k and d. Bird, introduction to geochemistry, 1995.

[35] Manahan, s environmental chemistry, 2017.

[36] Yih-bor, c, coats, b. And j. Nolen, a compostional model for co_2 floods including co2 floods including co_2 solubility in water, spe, 1998.

[37] Portier, s. And c. Rochelle, modelling co2 solubility in pure water and nacl-type waters from 0 to 300 °c and from 1 to 300 bar. Chemical geology, 2005. **217**(3-4): p. 187-199.

[38] Wiebe, r and v. L. Gaddy, the solubility in water of carbon dioxide at 50°, 75° and 100° at pressures to 700 atm, 1939.

[39] Prutton, c.f and r. L. Savage, the solubility of carbon dioxide in calcium chloride–water solutions at 75, 100, 120 °c and high pressures, 1945.

[40] Dihma, a and g. Morrachini, solubility of light hydrocarbons and their mixtures in pure water under high pressure, 1998.

[41] Gillepsie,c and g. Wilson, vapor–liquid and liquid–liquid equilibria: water–carbon dioxide., texas, 1982.

[42] Takenouchi, s. And g.c. kennedy, the binary system h 2 o-co 2 at high temperatures and pressures. American journal of science, 1964. **262**(9): p. 1055-1074.

[43] Todheide, k and e. Franck, das zweiphasengebiet und die kritische kurve im system kohlendioxid-wasser bis zu drucken von 3500 ba, 1963.

[44] Muller,g.e, das dampf-flüssigkeitsgleichgewicht des ternären systems ammoniak–kohlendioxid–wasser bei hohen wassergehalten im bereich zwischen 373 und 473 kelvin, 1988.

[45] Malinin, s.d and savalyeva, the solubility of co_2 in nacl and $cacl_2$ solutions at 25, 50 and 75 °c under elevated co_2 pressures, 1972.

[46] Kritschewsky,i r, s. M. N and a. A. V, combined solubility of gases in liquids under pressure: i. Solubility of carbon dioxide in water from its mixtures with hydrogen of 20 and 30°c and total pressure of 30kg/cm2, amsterdam: elservier science, 2003.

[47] Zel'vinskii,y.d and k. Zhurn, measurements of carbon dioxide solubility in water, 1937.

[48] Bartholome, e and h. Friz, solubility of co_2 in water, germany, 1956.

[49] Matouš, j. Sobr and j. Novak, solubility of carbon dioxide in water at pressures up to 40 atm, czech: elservier science, 1969.

[50] Zawisza, a. And b. Malesinska, solubility of carbon dioxide in liquid water and of water in gaseous carbon dioxide in the range 0.2-5 mpa and at temperatures up to 473 k. Journal of chemical & engineering data, 1981. **26**(4): p. 388-391.

[51] Tarzimanov, a and r. Shagiakhmetov, measurements of co_2 solubility in water up to 60 mpa, 1982.

[52] Gillespie, p.c and g. M. Wilson, vapor-liquid and liquid-liquid equilibria: water-methane, water-carbon dioxide, water-hydrogen sulfide, water-npentane, water-methane-npentane, 1982.

[53] Oleinik,p.m, method of evaluating gases in liquids and volumetric properties of solutions under pressure, 1986.

[54] Nakayama, t., et al., high pressure liquid・liquid equilibria for the system of water, ethanol and 1,1-difluoroethane at 323.2 k. Fluid phase equilibria, 1987. **38**(1-2): p. 109-127.

[55] Song, k.y and r. Kobayashi, water content of co_2 in equilibrium with liquid water and/or hydrates., 1987.

[56] D'souza, r, j. R. Patrick and a. S. Teja, high pressure phase equilibria in the carbon dioxide -n-hexadecane and carbon dioxide -water systems, richmond, 1988.

[57] Sako, t., et al., phase equilibrium study of extraction and concentration of furfural produced in reactor using supercritical carbon dioxide. Journal of chemical engineering of japan, 1991. **24**(4): p. 449-455 .

[58] Ellis, a.j and r. M. Golding, the solubility of carbon dioxide above 100 °c in water and in sodium chloride solutions, 1963.

[59] Drummond,s.e, boiling and mixing of hydrothermal fluids: chemical effects on mineral precipitation, pennsylvannia, 1981.

[60] Rumpf, and maurer, an experimental and theoretical investigation on the solubility of carbon dioxide in aqueous solutions of strong electrolytes, 1993.

[61] Harned, h.s. and r. Davis, the ionization constant of carbonic acid in water and the solubility of carbon dioxide in water and aqueous salt solutions from 0 to 50°. Journal of the american chemical society, 1943. **65**(10): p. 2030-2037.

[62] Malinin,s and n. Kurovskaya, the solubility of co_2 in chloride solutions at elevated temperatures and co_2 pressures, 1975.

[63] Malinin, s.d and kurovskaya, the solubility of co_2 in nacl and $cacl_2$ solutions at 25, 50 and 75 °c under elevated co_2 pressures, 1972.

[64] Markham, a.e. and k.a. kobe, the solubility of carbon dioxide and nitrous oxide in aqueous salt solutions. Journal of the american chemical society, 1941. **63**(2): p. 449-454.

[65] H. Nicolaisen, phase equilibria in aqueous electrolyte solutions, denmark, 1994.

[66] Nighswander, j.a., n. Kalogerakis, and a.k. mehrotra, solubilities of carbon dioxide in water and 1 wt. % sodium chloride solution at pressures up to 10 mpa and temperatures from 80 to 200.degree.c. Journal of chemical & engineering data, 1989. **34**(3): p. 355-360.

[67] Onda, k., et al., salting-out parameters of gas solubility in aqueous salt solutions. Journal of chemical engineering of japan, 1970. **3**(1): p. 18-24.

[68] M. Gehrig, phasengleichgewichte und pvt-daten ternarer mischungen aus wasser, kohlendioxid und natriumchlorid bis 3 kbar and 550 °c, 1980.

[69] Takenouchi, s. And g.c. kennedy, the solubility of carbon dioxide in nacl solutions at high temperatures and pressures. American journal of science, 1965. **263**(5): p. 445-454.

[70] Yasunishi, a. And f. Yoshida, solubility of carbon dioxide in aqueous electrolyte solutions. Journal of chemical & engineering data, 1979. **24**(1): p. 11-14.

[71] Zheng, d.-q., t.-m. Guo, and h. Knapp, experimental and modeling studies on the solubility of co2, chc1f2, chf3, c2h2f4 and c2h4f2 in water and aqueous nacl solutions under low pressures. Fluid phase equilibria, 1997. **129**(1-2): p. 197-209. S under low pressures, ediburgh, 1997.

[72] Kiepe, j., et al., experimental determination and prediction of gas solubility data for co2+ h2o mixtures containing nacl or kcl at temperatures between 313 and 393 k and pressures up to 10 mpa. Industrial & engineering chemistry research, 2002. **41**(17): p. 4393-4398.

[73] Koschel, d., et al., enthalpy and solubility data of co2 in water and nacl(aq) at conditions of interest for geological sequestration. Fluid phase equilibria, 2006. **247**(1-2): p. 107-120.

[74] Zhao, h., et al., carbon dioxide solubility in aqueous solutions of sodium chloride at geological conditions: experimental results at 323.15, 373.15, and 423.15 k and 150 bar and modeling up to 573.15 k and 2000 bar. Geochimica et cosmochimica acta, 2015. **149**: p. 165-189.

[75] Messabeb, h., et al., experimental measurement of co2 solubility in aqueous nacl solution at temperature from 323.15 to 423.15 k and pressure of up to 20 mpa. Journal of chemical & engineering data, 2016. **61**(10): p. 3573-3584.

[76] Hou, s.-x., g.c. maitland, and j.p.m. trusler, phase equilibria of (co2+h2o+nacl) and (co2+h2o+kcl): measurements and modeling. The journal of supercritical fluids, 2013. **78**: p. 78-88.

[77] Bando, s., et al., solubility of co2in aqueous solutions of nacl at (30 to 60) °c and (10 to 20) mpa. Journal of chemical & engineering data, 2003. **48**(3): p. 576-579.

[78] Yan, w., s. Huang, and e.h. stenby, measurement and modeling of co2 solubility in nacl brine and co2–saturated nacl brine density. International journal of greenhouse gas control, 2011. **5**(6): p. 1460-1477.

[79] Zhao, h. And s.n. lvov, phase behavior of the co2–h2o system at temperatures of 273–623 k and pressures of 0.1–200 mpa using peng-robinson-stryjek-vera equation of state

with a modified wong-sandler mixing rule: an extension to the co2–ch4–h2o system. Fluid phase equilibria, 2016. **417**: p. 96-108.

[80] Yan, w., s. Huang, and e.h. stenby, measurement and modeling of co2 solubility in nacl brine and co2–saturated nacl brine density. International journal of greenhouse gas control, 2011. **5**(6): p. 1460-1477.

[81] Søreide, i. And c.h. whitson, peng-robinson predictions for hydrocarbons, co2, n2, and h_2s with pure water and naci brine. Fluid phase equilibria, 1992. **77**: p. 217-240.

[82] Zhao, h., r.m. dilmore, and s.n. lvov, experimental studies and modeling of co2solubility in high temperature aqueous cacl2, mgcl2, na2so4, and kcl solutions. Aiche journal, 2015. **61**(7): p. 2286-2297.

[83] Collins, k.d., charge density-dependent strength of hydration and biological structure. Biophysical journal, 1997. **72**(1): p. 65-76.

[84] Tumasyan, a, v. Panteleev and g. Meinster, influence de l'anhydride carbonique sur les proprietes physiques du petrole et de l'eau, 1969.

[85] Yokoyama, c., j. Takei, and a. Kumagai, erratum to paper: viscosity of mixtures of indole containing 2-methylnaphthalene and isoquinoline under pressure. High temperatures-high pressures, 2001. **33**(3): p. 345-346.

[86] Bando, s., et al., viscosity of aqueous nacl solutions with dissolved co2at (30 to 60) °c and (10 to 20) mpa. Journal of chemical & engineering data, 2004. **49**(5): p. 1328-1332.

[87] Uchida, t., et al., viscosity of aqueous co2solutions measured by dynamic light scattering. Journal of chemical & engineering data, 2003. **48**(5): p. 1225-1229.

[88] Hasanvand, m.z., et al., geological storage of carbon dioxide by injection of carbonated water in an iranian oil reservoir: a case study. Journal of petroleum science and engineering, 2013. **111**: p. 170-177.

[89] W. Lu, h. Guo, i. Chou, r. Burruss and l. Lanlan, determination of diffusion coefficients of carbon dioxide in water between 268 and 473 k in a high-pressure capillary optical cell with in situ raman spectroscopic measurements, 2013.

[90] Lu, w., et al., determination of diffusion coefficients of carbon dioxide in water between 268 and 473k in a high-pressure capillary optical cell with in situ raman spectroscopic measurements. Geochimica et cosmochimica acta, 2013. **115**: p. 183-204.

[91] Sell, a., et al., measurement of co2 diffusivity for carbon sequestration: a microfluidic approach for reservoir-specific analysis. Environmental science & technology, 2012. **47**(1): p. 71-78.

[92] Lv, j., k. Ren, and y. Chen, co2 diffusion in various carbonated beverages: a molecular dynamics study. The journal of physical chemistry b, 2018. **122**(5): p. 1655-1661.

[93] Mutoru, j.w., a. Leahy-dios, and a. Firoozabadi, modeling infinite dilution and fickian diffusion coefficients of carbon dioxide in water. Aiche journal, 2010. **57**(6): p. 1617-1627.

[94] Bachu, s. And d.b. bennion, interfacial tension between co2, freshwater, and brine in the range of pressure from (2 to 27) mpa, temperature from (20 to 125) °c, and water salinity from (0 to 334 000) mg·l−1. Journal of chemical & engineering data, 2009. **54**(3): p. 765-775.

[95] Pereira, l.m.c., et al., interfacial tension of co_2 + brine systems: experiments and predictive modelling. Advances in water resources, 2017. **103**: p. 64-75.

[96] Simon, r. And d.j. graue, generalized correlations for predicting solubility, swelling and viscosity behavior of co2 -crude oil systems. Journal of petroleum technology, 1965. **17**(01): p. 102-106.

[97] Welker, j.r., physical properties of carbonated oils. Journal of petroleum technology, 1963. **15**(08): p. 873-876.

[98] Orr, f.m., a.d. yu, and c.l. lien, phase behavior of co2 and crude oil in low-temperature reservoirs. Society of petroleum engineers journal, 1981. **21**(04): p. 480-492.

[99] Orr, f.m., m.k. silva, and c.-l. Lien, equilibrium phase compositions of co2/crude oil mixtures-part 2: comparison of continuous multiple-contact and slim-tube displacement tests. Society of petroleum engineers journal, 1983. **23**(02): p. 281-291. Displacement tests, 1983.

[100] Sasaki, k, yuichi, o. Chanmoly and h. Kono, co2 solubility characteristics of crude oils related to carbon capture and utilization (ccu).

[101] Yang, z, liu, x, z. Hua, y. Ling, m. Li, m. Lin and z. Dong, et al., interfacial tension of co 2 and crude oils under high pressure and temperature. Colloids and surfaces a: physicochemical and engineering aspects, 2015. **482**: p. 611-616.

[102] Yang, d., p. Tontiwachwuthikul, and y. Gu, interfacial tensions of the crude oil + reservoir brine + co2systems at pressures up to 31 mpa and temperatures of 27 °c and 58 °c. Journal of chemical & engineering data, 2005. **50**(4): p. 1242-1249.

[103] Sun, c.-y. And g.-j. Chen, measurement of interfacial tension for the co2injected crude oil + reservoir water system. Journal of chemical & engineering data, 2005. **50**(3): p. 936-938.

[104] Mcmanamey, w.j. and j.m. woollen, the diffusivity of carbon dioxide in some organic liquids at 25° and 50°c. Aiche journal, 1973. **19**(3): p. 667-669.

[105] Grogan, a.t. and w.v. pinczewski, the role of molecular diffusion processes in tertiary co2 flooding. Journal of petroleum technology, 1987. **39**(05): p. 591-602.

[106] Zheng, s. And d. Yang, experimental and theoretical determination of diffusion coefficients of co2-heavy oil systems by coupling heat and mass transfer. Journal of energy resources technology, 2016. **139**(2): p. 022901.

[107] F. Chung, r. Jones and h. Nguyen, measurements and correlations of the physical properties of co2-heavy crude oil mixtures, 1988.

[108] Welker, j.r., physical properties of carbonated oils. Journal of petroleum technology, 1963. **15**(08): p. 873-876.

[109] Abedini, a. And f. Torabi, on the co2 storage potential of cyclic co2 injection process for enhanced oil recovery. Fuel, 2014. **124**: p. 14-27.

[110] Mosavat, n., a. Abedini, and f. Torabi, phase behaviour of co2–brine and co2–oil systems for co2 storage and enhanced oil recovery: experimental studies. Energy procedia, 2014. **63**: p. 5631-5645.

[111] Khaksar manshad, a., et al., effects of water soluble ions on interfacial tension (ift) between oil and brine in smart and carbonated smart water injection process in oil reservoirs. Journal of molecular liquids, 2016. **223**: p. 987-993.

[112] Honarvar, b., et al., experimental investigation of interfacial tension measurement and oil recovery by carbonated water injection: a case study using core samples from an iranian carbonate oil reservoir. Energy & fuels, 2017. **31**(3): p. 2740-2748.

[113] Shu, g., et al., mass transfer of co2 in a carbonated water–oil system at high pressures. Industrial & engineering chemistry research, 2016. **56**(1): p. 404-416.

[114] Daniel,r, natural barriers formed in the region of hydrocarbon reservoirs, 1972.

[115] Baliant,v, methode de prevision du comportement d'un gisement d'huile balaye par du gaz carbonique, 1972.

[116] Ott, h, co_2 reactive transport in limestone flow regimes,fluid flow and mechanical rock properties, international symposium of the society of core analyst, 2013.

[117] Sedigheh,m and a. J. Lesley, investigation of water flooding and carbonated water injection in a fractured porous media, 2017.

[118] Sohrabi, m., et al., coreflooding studies to investigate the potential of carbonated water injection as an injection strategy for improved oil recovery and co2 storage. Transport in porous media, 2011. **91**(1): p. 101-121.

[119] Salathiel, r.a., oil recovery by surface film drainage in mixed-wettability rocks. Journal of petroleum technology, 1973. **25**(10): p. 1216-1224.

[120] Sohrabi, m ,kechut, n. I, riazi, m. And mahmoud jamiolahmady, "coreflooding studies to investigate the potential of carbonated water injection as an injection strategy," chemical engineering research and design, vol. 89, 2011.

[121] Foroozesh, j. And m. Jamiolahmady, simulation of carbonated water injection coreflood experiments: an insight into the wettability effect. Fuel, 2016. **184**: p. 581-589.

[122] Ruidiaz, e.m., a. Winter, and o.v. trevisan, oil recovery and wettability alteration in carbonates due to carbonate water injection. Journal of petroleum exploration and production technology, 2017. **8**(1): p. 249-258.

[123] Kilybay, a., et al., hybrid eor technology: carbonated water-smart water flood improved recovery in oil wet carbonate formation: part-ii, in spe oil and gas india conference and exhibition. 2017, society of petroleum engineers..

[124] Ahmadi, m.a., et al., effect of operational parameters on the performance of carbonated water injection: experimental and numerical modeling study. The journal of supercritical fluids, 2016. **107**: p. 542-548.

[125] Van dijke,c, carbonated water flood, 1965.

[126] M. Sohrabi, m. Riazi, s. Jamiolahmady, s. Ireland and c. Brown, mechanisms of oil recovery by carbonated water injection, 2009.

[127] Shokri afra, m. Bahaloo, b. Rostami, laboratory investigation of oil viscosity effect during carbonated water injection: comparison of secondary and tertiary recovery. The canadian journal of chemical engineering, 2018. Solution for heavy oil production, 2018.

[128] Fathollahi, a. And b. Rostami, carbonated water injection: effects of silica nanoparticles and operating pressure. The canadian journal of chemical engineering, 2015. **93**(11): p. 1949-1956.

[129] Grogan, a.t. and w.v. pinczewski, the role of molecular diffusion processes in tertiary co2 flooding. Journal of petroleum technology, 1987. **39**(05): p. 591-602.

[130] Muller, t. And l.w. lake, theoretical study of water blocking in miscible flooding. Spe reservoir engineering, 1991. **6**(04): p. 445-451.

[131] Alizadeh, a.h., et al., multi-scale experimental study of carbonated water injection: an effective process for mobilization and recovery of trapped oil. Fuel, 2014. **132**: p. 219-235.

[132] Chatzis i, mobilization of residual oil mechanisms seen in micromodels, 2011.

[133] Chiquet, p., d. Broseta, and s. Thibeau, wettability alteration of caprock minerals by carbon dioxide. Geofluids, 2007. **7**(2): p. 112-122.

[134] Kechut, n.i., m. Sohrabi, and m. Jamiolahmady, experimental and numerical evaluation of carbonated water injection (cwi) for improved oil recovery and co2 storage, in spe europec/eage annual conference and exhibition. 2011, society of petroleum engineers.

[135] Dong, y., et al., an experimental investigation of carbonated water flooding, in spe annual technical conference and exhibition. 2011, society of petroleum engineers. Denver colorado, 2011.

[136] Sohrabi, m., et al., a thorough investigation of mechanisms of enhanced oil recovery by carbonated water injection, in spe annual technical conference and exhibition. 2015, society of petroleum engineers.

[137] Kechut, n.i., et al., tertiary oil recovery and co2 sequestration by carbonated water injection (cwi), in spe international conference on co2 capture, storage, and utilization. 2010, society of petroleum engineers.

[138] Dong, y., et al., an experimental investigation of carbonated water flooding, in spe annual technical conference and exhibition. 2011, society of petroleum engineers.

[139] Al mesmari, a., p. Mahzari, and m. Sohrabi, modelling formation of a new fluid phase during carbonated water injection, in international petroleum technology conference. 2016, international petroleum technology conference.

[140] Miller, j.s. and r.a. jones, a laboratory study to determine physical characteristics of heavy oil after co2 saturation, in spe/doe enhanced oil recovery symposium. 1981, society of petroleum engineers.

[141] Barrufet, m.a., a. Bacquet, and g. Falcone, analysis of the storage capacity for co sequestration of a depleted gas condensate reservoir and a saline aquifer, in canadian international petroleum conference. 2009, petroleum society of canada.

[142] Riazi, m., m. Jamiolahmady, and m. Sohrabi, theoretical investigation of pore-scale mechanisms of carbonated water injection. Journal of petroleum science and engineering, 2011. **75**(3-4): p. 312-326.

[143] Riazi, m., m. Sohrabi, and m. Jamiolahmady, experimental study of pore-scale mechanisms of carbonated water injection. Transport in porous media, 2010. **86**(1): p. 73-86.

[144] Nunez, r., et al., investigation of dissolution effects on dolomite porous media under carbonated water injection cwi, in abu dhabi international petroleum exhibition & conference. 2017, society of petroleum engineers.

[145] Ramesh, a.b. and t.n. dixon, numerical simulation of carbonated waterflooding in a heterogeneous reservoir, in spe symposium on numerical simulation of reservoir performance. 1973, society of petroleum engineers. A heterogeneous reservoir, texas, 1973.

[146] Douglas, j. And h.h. rachford, on the numerical solution of heat conduction problems in two and three space variables. Transactions of the american mathematical society, 1956. **82**(2): p. 421.

[147] Brooks, r.h. and a.t. corey, hydraulic properties of porous media and their relation to drainage design. Transactions of the asae, 1964. **7**(1): p. 0026-0028.

[148] Al mesmari, a., p. Mahzari, and m. Sohrabi, an improved methodology for simulating oil recovery by carbonated water injection: impact of compositional changes, in spe annual technical conference and exhibition. 2016, society of petroleum engineers.

[149] Baker, l.e., three-phase relative permeability correlations, in spe enhanced oil recovery symposium. 1988, society of petroleum engineers.

[150] Ramesh, a.b. and t.n. dixon, numerical simulation of carbonated waterflooding in a heterogeneous reservoir, in spe symposium on numerical simulation of reservoir performance. 1973, society of petroleum engineersn a heterogeneous reservoir, texas, 1973.

[151] Riazi, m., m. Jamiolahmady, and m. Sohrabi, theoretical investigation of pore-scale mechanisms of carbonated water injection. Journal of petroleum science and engineering, 2011. **75**(3-4): p. 312-326.

[152] De waard, c. And d.e. milliams, carbonic acid corrosion of steel. Corrosion, 1975. **31**(5): p. 177-181.

[153] Browning, d.r., co2 corrosion in the anadarko basin, in spe deep drilling and production symposium. 1984, society of petroleum engineers.

[154] Hickok, c.w., r.j. christensen, and h.j. ramsay, progress review of the k&s carbonated waterflood project. Journal of petroleum technology, 1960. **12**(12): p. 20-24.

[155] Spencer, m , p. Briskeby and l. Christensen, petroleum geoscience in norden exploration, production and organization., 2008.

[156] Madland, m.v., et al., the influence of co_2 gas and carbonate water on the mechanical stability of chalk. Journal of petroleum science and engineering, 2006. **51**(3-4): p. 149-168.

[157] Oliver, j, k. Schure and peters, trends in global co2 and total greenhouse gas emissions., 2017.

[158] Ipcc, climate change 2014: mitigation of climate change, 2015.

[159] Kumar, s. And a. Mandal, a comprehensive review on chemically enhanced water alternating gas/co 2 (cewag) injection for enhanced oil recovery. Journal of petroleum science and engineering, 2017. **157**: p. 696-715.

[160] Mashid and robiah, application of super critcal anti solvent in drugs, 2011.

[161] Basic concepts in enbanced oil recovery processes (critical reports on applied chemistry volume 33). Edited by m. Bavière elsevier applied science,. Isbn 1–85166–617–6. Polymer international, 1992. **28**(3): p. 256-256.

[162] Zhang, y., et al., effect of capillary pressure and salinity on co 2 solubility in brine aquifers. International journal of greenhouse gas control, 2017. **57**: p. 26-33.

[163] Yang, d. And y. Gu, interfacial interactions of crude oil-brine-co2 systems under reservoir conditions, in spe annual technical conference and exhibition. 2004, society of petroleum engineers.

[164] Yang, d., p. Tontiwachwuthikul, and y. Gu, interfacial tensions of the crude oil + reservoir brine + co2systems at pressures up to 31 mpa and temperatures of 27 °c and 58 °c. Journal of chemical & engineering data, 2005. **50**(4): p. 1242-1249.

[165] Martin,j, additional oil production through flooding with carbonated water, 1951.

[166] Johnson, m, lab experiments with carbonated water and liquid carbondioxide as recovery agents, 1952.

[167] Jarrel, c. Fox and s. Webb, practical aspects of co2 flooding, 2002.

[168] Mosavat, n. And f. Torabi, experimental evaluation of the performance of carbonated water injection (cwi) under various operating conditions in light oil systems. Fuel, 2014. **123**: p. 274-284.

[169] Kokal, s.l. and s.g. sayegh, phase behavior and physical properties of co2-saturated heavy oil and its constitutive fractions: experimental data and correlations. Journal of petroleum science and engineering, 1993. **9**(4): p. 289-302.

[170] Holm, l.w. and v.a. josendal, mechanisms of oil displacement by carbon dioxide. Journal of petroleum technology, 1974. **26**(12): p. 1427-1438.

[171] Bessières, d., h. Saint-guirons, and j.-l. Daridon, volumetric behavior of decane + carbon dioxide at high pressures. Measurement and calculation. Journal of chemical & engineering data, 2001. **46**(5): p. 1136-1139.

[172] Zúñiga-moreno, a., l.a. galicia-luna, and f.f. betancourt-cárdenas, compressed liquid densities and excess volumes of co2+thiophene binary mixtures from 313 to 363k and pressures up to 25mpa. Fluid phase equilibria, 2005. **236**(1-2): p. 193-204.

[173] Lohrenz, j., b.g. bray, and c.r. clark, calculating viscosities of reservoir fluids from their compositions. Journal of petroleum technology, 1964. **16**(10): p. 1171-1176. Compositions, 1964.

[174] Hebach, a., a. Oberhof, and n. Dahmen, density of water + carbon dioxide at elevated pressures: measurements and correlation. Journal of chemical & engineering data, 2004. **49**(4): p. 950-953.

[175] Bijeljic, b.r., a.h. muggeridge, and m.j. blunt, effect of composition on waterblocking for multicomponent gasfloods, in spe annual technical conference and exhibition. 2002, society of petroleum engineers.

[176] Martin , additional oil production through flooding with carbonated water, 1951.

[178] Holm, l.w. and v.a. josendal, mechanisms of oil displacement by carbon dioxide. Journal of petroleum technology, 1974. **26**(12): p. 1427-1438.

[179] Van dijke, carbonated water flood, shell internal research report, 1965.

[180] Grigg, r. And r. Svec, co2 transport mechanisms in co2/brine coreflooding, in proceedings of spe annual technical conference and exhibition. 2006, society of petroleum engineers.

[181] Seyyedi, m., et al., quantification of oil recovery efficiency, co 2 storage potential, and fluid-rock interactions by cwi in heterogeneous sandstone oil reservoirs. Journal of molecular liquids, 2018. **249**: p. 779-788.

[182] Spencer, m, p. Briskeby and l. Christensen, petroleum geoscience in norden exploration, production and organization., 2008.

[183] Martin, additional oil production through flooding with carbonated water, 1951.

[184] Dong, y., et al., an experimental investigation of carbonated water flooding, in spe annual technical conference and exhibition. 2011, society of petroleum engineers.

[185] Yokoyama, c., j. Takei, and a. Kumagai, erratum to paper: viscosity of mixtures of indole containing 2-methylnaphthalene and isoquinoline under pressure. High temperatures-high pressures, 2001. **33**(3): p. 345-346.

[186] Müller, g., e. Bender, and g. Maurer, das dampf-flüssigkeitsgleichgewicht des ternären systems ammoniak-kohlendioxid-wasser bei hohen wassergehalten im bereich zwischen 373 und 473 kelvin. Berichte der bunsengesellschaft für physikalische chemie, 1988. **92**(2): p. 148-160.

[187] Orr, f.m. and m.k. silva, equilibrium phase compositions of co2/hydrocarbon mixtures part 1: measurement by a continuous multiple-contact experiment. Society of petroleum engineers journal, 1983. **23**(02): p. 272-280.

[188] Orr, f.m. and c.m. jensen, interpretation of pressure-composition phase diagrams for co2/crude-oil systems. Society of petroleum engineers journal, 1984. **24**(05): p. 485-497.

[189] Vazquez, d. And g.a. mansoori, identification and measurement of petroleum precipitates. Journal of petroleum science and engineering, 2000. **26**(1-4): p. 49-55.

[190] Buckley, j.s., et al., asphaltene precipitation and solvent properties of crude oils. Petroleum science and technology, 1998. **16**(3-4): p. 251-285.

[191] Sayegh, s.g., et al., rock/fluid interactions of carbonated brines in a sandstone reservoir: pembina cardium, alberta, canada. Spe formation evaluation, 1990. **5**(04): p. 399-405.

[192] Korsnes ,r. I, m. V .madland and h. Hildebrand, enhanced chemical weakening of chalk due to injection of co2 enriched water, 2008.

Chapter 3 **Modelling Investigation of Low Salinity Water Injection for EOR: Effect of Na^+ and SO_4^{2-}**

ABSTRACT

Low salinity water injection (LSWI) has gained great attention as a promising enhanced oil recovery (EOR) method with numerous advantages (e.g., economic and environmental aspects), compared to other conventional chemical EOR methods. For the past two decades, several laboratory studies have been performed by researchers to understand the main pore-scale mechanisms of oil displacement during LSWI; however, further experimental and modeling research works are required to comprehend the LSWI governing mechanisms. The focus of this paper is to investigate important aspects such as oil recovery mechanisms, oil-water wettability alterations, changes in pH of formation water, and mineral reaction (dissolution/precipitation) which occur during LSWI in sandstones and carbonates. To explore the effect of ion-exchange, a compositional model is developed with the aid of laboratory data by Computer Modelling Group (CMG) where Na^+ and SO_4^{2-} are used as interpolants to model LSWI in sandstones and carbonates cores respectively.

***Keywords**:* Low Salinity Water Injection (LSWI), Precipitation and Dissolution, Ionic-Exchange, Sandstones, Carbonates, Oil Recovery Factor.

3.1 **Introduction**

Post-primary oil production drive may leave behind up to 85% of the proven reserves in a petroleum formation. Water flooding can reduce the amount of oil saturation to nearly 60% and low salinity water injection (LSSWI) may produce an extra 15% so that about 40% of the residual oil can be recovered [1,2]. It appears that LSSWI is becoming one of the most popular enhanced oil recovery (EOR) technique, based on the literature [3–9]. This is probably due to the low cost associated with its implementation when compared to other EOR techniques. Low salinity water is referred to smart water, ion-engineered water, and advanced ion management water in various research studies by many researchers; however, the methodology and mechanisms behind the increase in oil recovery remain the same [9,10]. The mechanisms responsible for the increased oil recovery have been identified to be wettability alteration, double layer expansion, multicomponent ionic exchange, fines migration, and mineral dissolution [3,6,8–19]. However, the dominant mechanisms for the oil recovery increase still remain a subject of debate among researchers. The above mechanisms alter the rock-brine-oil equilibrium from its inherent state so that they might modify important properties such as permeability and wettability to improve the oil recovery. Wettability alteration appears to be the most widely accepted dominant mechanism for low salinity water injection [4,7,13,18–24].

These are a few mathematical modeling on LSWI in the open sources where contradictions and vital limitations are found in them. For instance, Altahir et al. [25] studied the LSWI strategy in carbonates in core-flood experiments by considering the improved oil recovery and pH increase; however they did not take into consideration the changes in the composition of the rock [25]. Vajihi et al. [26] also investigated LSWI oil recovery and residual oil saturation in core-flood where ions exchange and effect of the flowrate were not discussed in their work [26]. Didier et al. [27] suggested that pH is the key factor in wettability alteration in Fontainebeau and Ottawa sandstones. The results show that oil adhesion occurs at pH values of higher than 6 – 8. Other research works concluded that the oil adhesion experiences at pH values lower than 6 – 8 (for instance, a pH of 4) [27]. In another work, Al-Shalabi and Sepehrnoori [9] suggest that more modeling research works need to be conducted in carbonates than sandstones because it is assumed that the mechanisms that controls the wettability alteration in sandstone is known – clay, but the mechanism is not known in carbonates.

The composition and salinity of the low salinity water are not constant and universal in all formations across the world. Hence, systematic studies need to be carried out to determine the optimum salinity and concentration of the selected low salinity water. During laboratory investigation of sandstone and carbonate cores, as the salinity of the LSWI is reduced, there is an increase in the oil recovery; however, after a certain threshold value, there is no significant increase in the oil recovery upon further reduction of salinity in the LSWI process. This suggests that there is an optimum salinity and concentration for the various formations under LSWI. It was observed that the optimum salinity can range for sandstones, a reduction in LSWI salinity of up to 100% to give salinities as low 100 to 2000 ppm is possible [28,29], but for carbonates, 50% reduction in LSWI salinity yields LSWI of 1000 to 5000 ppm [6,8,12,15,30,31] for effective low salinity water injection schemes.

A balance of adsorption capacity, cation exchange capacity, and pH window for clay is necessary to evaluate the effectiveness of LSWI in sandstones [17]. In core flood experiments conducted by Zhang and Morrow [2], up to 33% increase was observed in Berea sandstone which contained clay, while no significant increase was observed in clay-free Berea sandstone when the brine with 1% salinity was injected. In sandstones with kaolinite clay, fines migration due to the desorption of kaolinite clay from the mixed-wet sandstone surface is suggested as the mechanism responsible for the increased oil recovery by LSWI [32]. An increase in the injection pressure and a reduction in permeability are often accompanied with the increased oil recovery in core flood experiments [33,34]. There are a limited number of research investigations on the formation damage during LSWI in the open sources [35]. Typical pH values of 4-6 are attainable in sandstone reservoirs; the pH in the formation increases as the low salinity water is injected in formations due to cation exchange of the effluent and clay anion surfaces; however, a pH value greater than 10 is seldom encountered due to the inherent CO_2 in the hydrocarbon-bearing formations, which acts as a pH buffer [32]. During laboratory investigation of LSWI, the concentration of divalent ions such as Ca^{2+} and Mg^{2+} in the effluent were lowered, leading to an increase in oil recovery; however, when the cores were pre-flushed with NaCl to remove the divalent ions, there was no significant oil recovery [32]. The ions contribute to the electric surface charge and an electric double layer is formed. The expansion of the electric double layer has also been suggested as the dominant mechanism that considerably affects the oil recovery over the LSWI process [30,36]. This can be measured by the zeta potential of the surface.

More than half of the proven oil reserves are found in carbonates. Efficient exploitation and recovery of these reserves are challenging due to the low permeability and porosity of the porous system, particularly the matrix blocks [6]. The dominant mechanism in carbonates may be attributed to the wettability alteration of the mixed to oil-wet formations to more water-wet formations, leading to a higher oil production. Monovalent and divalent ions that alter the rock-brine equilibrium are referred to potential determining ions and the mechanism behind their alteration in the formation is known as a multicomponent ionic exchange. Austad et al. [16] investigated the effect of seawater salinity on oil recovery in the Ekofisk field as a highly fractured carbonate reservoir. The surface charge is positive with Ca^{2+} in equilibrium with the formation brine at a pH value of 7-8. Ekofisk seawater has a Ca^{2+} ion concentration less than half of the formation brine concentration. When the seawater is injected into the formation, Ca^{2+} is desorbed from the surface into the injected water to balance the rock-brine equilibrium; but the desorption alters the rock-oil equilibrium. The negatively charged carboxylic components ($R\text{-}COO^-$) attached to the Ca^{2+} are desorbed, leading to an increase in the crude oil mobility and eventually an increase in the amount of oil recoverable. SO_4^{2-} ions can also promote the desorption of carboxylic oil components from the carbonate surface by adsorbing Ca^{2+} to produce $CaSO_4$ [13,20,37–39]. Enhanced oil recovery is also attributed to the rock dissolution [40,25,41], though Austad et al. [42] suggested that the rock dissolution is not necessary for increased oil recovery based on a series of experimental runs. The initial wettability, salinity, ions present, and wetting phase are the critical parameters that influence wettability alteration, production mechanism, and oil recovery. In the laboratory scale in the absence of Ca^{2+} and Mg^{2+}, an increase in SO_4^{2-} concentration of the injected fluid fails to improve the oil recovery, implying that divalent potential determining cations are needed to improve oil recovery through SO_4^{2-} adsorption [16,43–45]. Based on the literature, there are no numerical studies to discuss about the production behaviour/trend of LSWI in carbonates and sandstones. To the best of our knowledge, the effects of mineral dissolution and precipitation have not been numerically investigated in the previous related research works. Wettability alteration appears to be the dominant mechanism for LSWI; however there have not been sufficient number of numerical compositional studies in the literature to validate this claim because of the difficulty to entirely capture ion exchange by most commercial simulators. Other phenomena, which occur during LSWI, such as the change in the local pH in the formation water, ionic-exchange, and mineral reactions (in carbonates) have not been studied adequately.

In this paper, a compositional simulation model was built employing the CMG-GEM module to study the effect of concentration of sodium ion (Na+) and sulfate (SO_4^{2-}) in sandstones and carbonates, respectively. The first step is to build a fluid model with CMG-Winprop such that the fluid properties such as saturation pressure, gas/oil ratio, formation volume factor, relative oil volume, and oil density are tuned to match the available experimental data for the reservoir fluids. Then, the matched fluid model is imported into a 1-D generic reservoir and the initial ionic compositions of the brine are provided from the laboratory analysis. The simulation model uses Na+ and SO_4^{2-} ions for ion exchange in sandstone reservoir and carbonate reservoir, respectively. Na^+ and SO_4^{2-} concentrations in the sandstone and carbonate are altered to find the impact of the ion concentration on pH, mineral precipitation and dissolution, and oil recovery.

3.2 **Theoretical Analysis: Ion Exchange in LSWI**

There is a chemical equilibrium between the ionic concentration of the connate water or the initial formation water and the ions which are adsorbed onto the clay surface in the reservoir [47]. Figure 3.1 shows a typical representation of clay mineral, ionic bridge, oil and typical ions to describe the important interaction mechanisms in LSWI

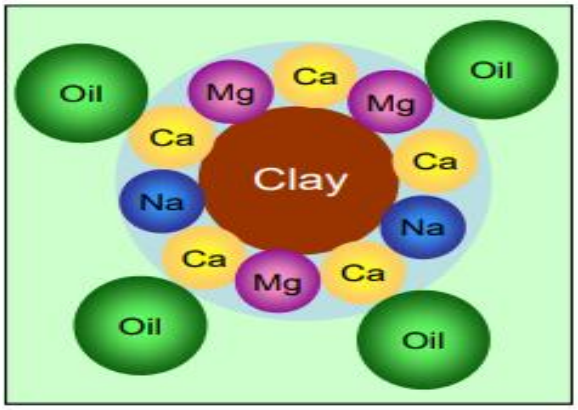

Figure 3.1: Schematic representation of clay mineral, ionic bridge, oil and typical ions to describe the important interaction mechanisms in LSWI (Modified after Lager et al. [32])

The polar oil components are bound to the clay surface in the presence of an ionic bridge which lies between the actual clay and oil. This makes the rock preferentially oil wet as shown in Figure 3.1 in a molecular level. Once the low salinity water is injected, it causes the ion exchange between

the monovalent ions and divalent ions (e.g., Na exchanging with Ca). During this ionic exchange, the oil is released from the divalent ions and becomes producible. This reduces the overall residual oil saturation and causes a shift in wettability to more water wet rock.

Injecting water with an ionic concentration, which is different from the original formation water, causes a chemical reaction and an ionic exchange. There are two typical ionic exchange reactions which can occur during LSWI. The reactions involve the alkali and alkali earth metals particularly sodium, calcium, and magnesium as given below [47].

$$Na^+ + \frac{1}{2}(Mg - X_2) \rightleftharpoons (Na - X) + \frac{1}{2}Mg^{2+} \tag{3.1}$$

$$Na^+ + \frac{1}{2}(Ca - X_2) \rightleftharpoons (Na - X) + \frac{1}{2}Ca^{2+} \tag{3.2}$$

where X represents the clay mineral in the reservoir rocks. The above reactions are reversible, implying that the monovalent ions are exchanged with divalent ions during LSWI. For instance, Na^+ is taken by the exchanger and Ca^{2+}/Mg^{2+} are freed to represent the forward reactions (see Equations (1) and (2)). In this case, the oil initially bounded on Ca and Mg (as shown in Figure 3.1) is released, causing the rock surface to become more water wet. Similar to the chemical reactions, ion-exchange reactions can be defined by the equilibrium constant as represented by the following expression:

$$K_{Na/Ca} = \frac{\left[a\left(Ca^{2+}\right)\right]^{0.5} a(Na-X)}{a(Na^+)[a(Ca-X_2)]^{0.5}} \tag{3.3}$$

$$K_{Na/Mg} = \frac{\left[a\left(Mg^{2+}\right)\right]^{0.5} a(Na-X)}{a(Na^+)[a(Mg-X_2)]^{0.5}} \tag{3.4}$$

in which, *a* stands for the activity. The activity of i^{th} component (a_i) is related to the activity coefficient (γ_i) through the following equation:

$$a_i = \gamma_i m_i \tag{3.5}$$

where m_i refers to the molality of component *I* in mol/kg.

Substituting Equation (3.5) into Equations (3.3) and (3.4) results in Equations (3.6) and (3.7) to determine the equilibrium constant, as shown below:

$$K_{Na/Mg} = \frac{\left[m\left(Mg^{2+}\right)\right]^{0.5} m(Na-X)}{m(Na^{+})\,[m(Mg-X_2)]^{0.5}} \quad x \quad \frac{\left[\left(\gamma\, Mg^{2+}\right)\right]^{0.5} \gamma(Na-X)}{\gamma(Na^{+})\,[\gamma(Mg-X_2)]^{0.5}} \tag{3.6}$$

$$K_{Na/Ca} = \frac{\left[m\left(Ca^{2+}\right)\right]^{0.5} m(Na-X)}{m(Na^{+})\,[m(Ca-X_2)]^{0.5}} \quad x \quad \frac{\left[\left(\gamma\, Ca^{2+}\right)\right]^{0.5} \gamma(Na-X)}{\gamma(Na^{+})\,[\gamma(Ca-X_2)]^{0.5}} \tag{3.7}$$

The activity coefficient of sodium and calcium ions in the aqueous phase can be calculated by the Debye-Huckel model or by the B-dot model; however, the evaluation of the activity coefficient of Na-X, Ca-X_2 and Mg-X_2, which correspond to Na^+, Ca^{2+} and Mg^{2+} on the exchanger surface, is not an easy task. Therefore, the selectivity coefficient is used by CMG instead of the equilibrium constant, as introduced by Equations (3.8) and (3.9):

$$K'_{Na/Mg} = \frac{\left[m\left(Mg^{2+}\right)\right]^{0.5} \zeta(Na-X)}{m(Na^{+})\,[\zeta(Mg-X_2)]^{0.5}} \quad x \quad \frac{\left[\left(\gamma\, Mg^{2+}\right)\right]^{0.5}}{\gamma(Na^{+})} \tag{3.8}$$

$$K'_{Na/Ca} = \frac{\left[m\left(Ca^{2+}\right)\right]^{0.5} \zeta(Na-X)}{m(Na^{+})\,[\zeta(Ca-X_2)]^{0.5}} \quad x \quad \frac{\left[\left(\gamma\, Ca^{2+}\right)\right]^{0.5}}{\gamma(Na^{+})} \tag{3.9}$$

ζ(Na-X), ζ(Ca-X_2), and ζ(Mg-X_2) stand for the equivalent fraction of $Na^+/Ca^{2+}$and Na^+/Mg^{2+} on the exchanger, respectively. The selectivity coefficient, which is a function of operational conditions, is used, since they can be measured unlike equilibrium constants which are thermodynamic variables. Hence, $K'_{Na/Ca}$ and $K'_{Na/Mg}$ are estimated using the experimental measurements. Appelo, et al. [48] reported the selectivity coefficient between Na^+ and many ions which are used in the CMG simulation package.

In CMG-GEM, all component moles are represented as moles per grid block volume. The total moles of Na-X, Ca-X_2, and Mg-X_2 in a grid block are $VN_{Na\text{-}X}$, $VN_{ca\text{-}X2}$, and $VN_{Mg\text{-}X2}$, respectively; where V is the grid block volume. For any value of cation exchange capacity in the grid block, the following equation needs to be satisfied

$$VN_{Na\text{-}X} + VN_{ca\text{-}X2} + VN_{Mg\text{-}X2} = V\phi(CEC) \tag{3.10}$$

In a control volume (see Figure 3.2), the material balance equation for the ion of charge i^+ that includes ion exchange with an exchanger X in the aqueous phase is expressed by Equation (3.11);

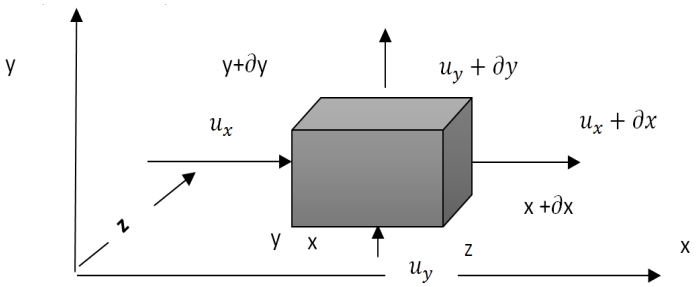

Figure 3.2 : A control volume/element of a 3-D flow in directions x, y, and z

$$\Delta T^{u}_{aq} y^{u}_{iw} \left(\Delta P^{n+1} + -\rho^{u}_{aq} g \Delta h\right) + \Sigma \Delta D^{u}_{iaq} \Delta y^{u}_{iaq} + VR^{n+1}_{i,aq} + VR^{n+1}_{i,mn} + q^{n+1}_{i} - \frac{V}{\Delta t}\left(\left(N^{n+1}_{i,aq} - N^{n+1}_{i-x}\right) - \left(N^{n}_{i,aq} - N^{n}_{i-x}\right) = 0, \tag{3.11}$$

Where T = Transmissibility; y = mole fraction, P = pressure, g = acceleration due to gravity, h = height, D= Diffusivity, V = grid block volume, R = reaction rate, q = injection, $VR^{n+1}_{j,aq}$ = Intra aqueous reaction rate, $VR^{n+1}_{j,mn}$ = Mineral dissolution/precipitation, n + 1 = implicit time step for grid block, u = explicit time step for grid block, N = Number of moles of mineral and *i =1 …n^{th}* represents the number of components.

Running CMG, the governing equations are solved simultaneously along with the phase, chemical, and ion-exchange equations through using the Newton's method.

3.3 Model Development

This section illustrates the main steps to obtain the fluid and rock properties and to conduct the modeling simulations using CMG

3.3.1 Fluid Behavior Modeling

To create a fluid model used for the simulation of LSWI, various steps should be taken (see Figure 3.3). Fluid composition given in Tables 3.1 and 3.2 is first used to build an EOS model using Peng Robinson equation of state to represent the original reservoir fluid. The EOS model is then tuned against the experimental data of Constant composition expansion (CCE), Constant volume depletion (CVD), and Differential liberation (DL) after which a flash process of the reservoir fluid at standard condition of 60^{o}F and 14.7psia is simulated. A good match is obtained between the experimental and modelled fluid properties. Figure 3.3 depicts the flow chart to illustrate how the fluid model is built for this simulation.

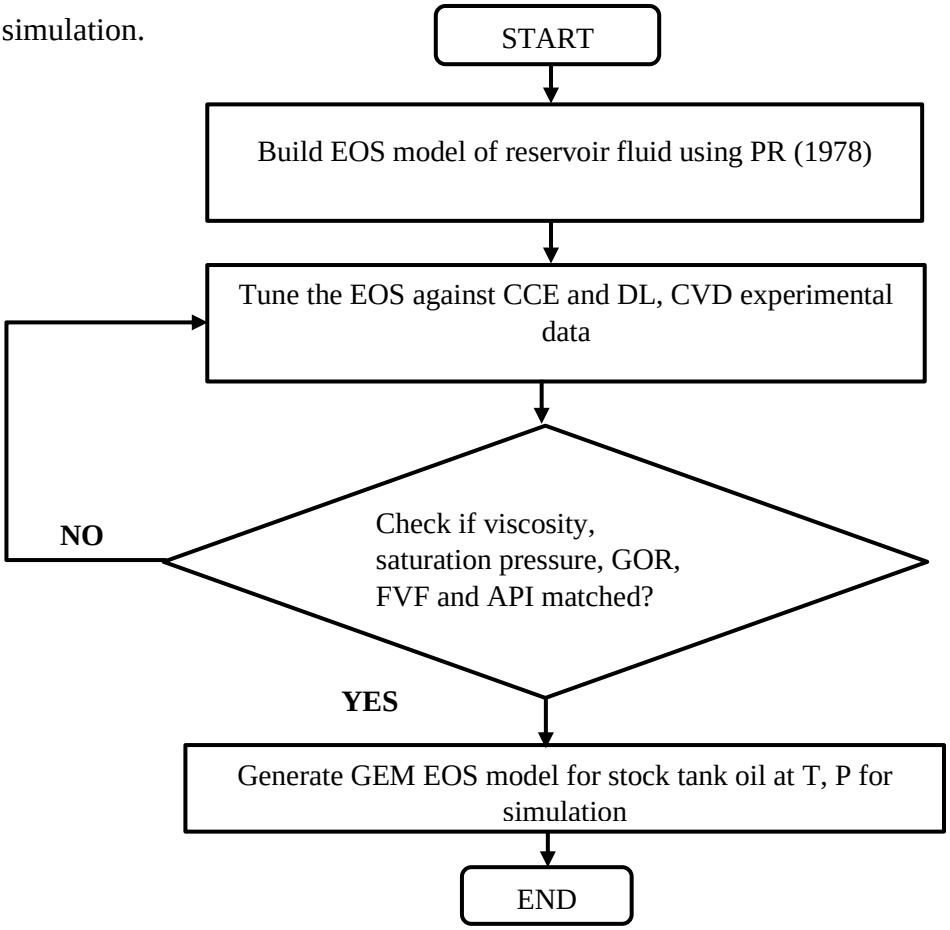

Figure 3.3: Flowchart to prepare the EOS fluid model

PVT Data. Laboratory experiments were conducted for Saturation Pressure, Constant Composition Expansion test and Differential Liberation test. From the laboratory experiments, the

total Gas Oil Ratio (GOR), Saturation Pressure, Formation Volume Factor (FVF) and API Gravity are 247 scf/stb, 740 Psi, 1.18, 40.0 respectively. The oil viscosity used for this study is 0.65 cP measured at bubble point. These experiments were added to the CMG - Winprop model to obtain an idea of how close the current EoS is to modelling the observed fluid behavior. The supplied data for reservoir oil fluid compositions/heavy fractions, separator test results, constant composition test results, differential liberation test results are all used for tuning the EoS to match the fluid behavior. The fluid compositions and the laboratory heavy fraction analysis utilized in this study are provided in Table 3.1 and Table 3.2 which are available in Computer modelling Group, 2017 [46].

Table 3.1: Black oil composition [46].

Component	Mole %
CO_2	0.1183
N_2	0.0016098
C_1	0.1154103
C_2	0.060058
C_3	0.0647635
i-C_4	0.0221657
n-C_4	0.047551
i-C_5	0.0328152
n-C_5	0.0370254
C_6	0.065135

Table 3.2: Laboratory heavy fraction analysis for C7 – C30+ [46].

Components	Mole, %	Molecular	Specific
C7	0.084205	91.931365	0.7400
C8	0.098941	103.11563	0.74659
C9	0.078385	113.43017	0.8129
C10	0.051514	132.0084	0.7937
C11	0.031329	147	0.7930
C12	0.021299	161	0.8040
C13	0.019318	175	0.8150
C14	0.014488	190	0.8260
C15	0.013374	206	0.8360
C16	0.010649	222	0.8430
C17	0.00904	237	0.8510
C18	0.009659	251	0.8560
C19	0.008173	263	0.8610

C20	0.005325	275	0.8660
C21	0.003963	291	0.8710
C22	0.00322	300	0.8760
C23	0.002353	312	0.8810
C24	0.001981	324	0.8850
C25	0.001857	337	0.8880
C26	0.001857	349	0.8920
C27	0.001981	360	0.8960
C28	0.002105	372	0.8990
C29	0.002105	382	0.9020
C30+	0.064516	400	0.9700

Peng Robinson equation of state is employed to construct the fluid model through using the fluid compositions where the regression procedure on experimental constant composition expansion, constant volume depletion, differential liberation, and separator test is carried out. Figure 4 shows the phase envelope to characterize the fluid used in this modeling/simulation work.

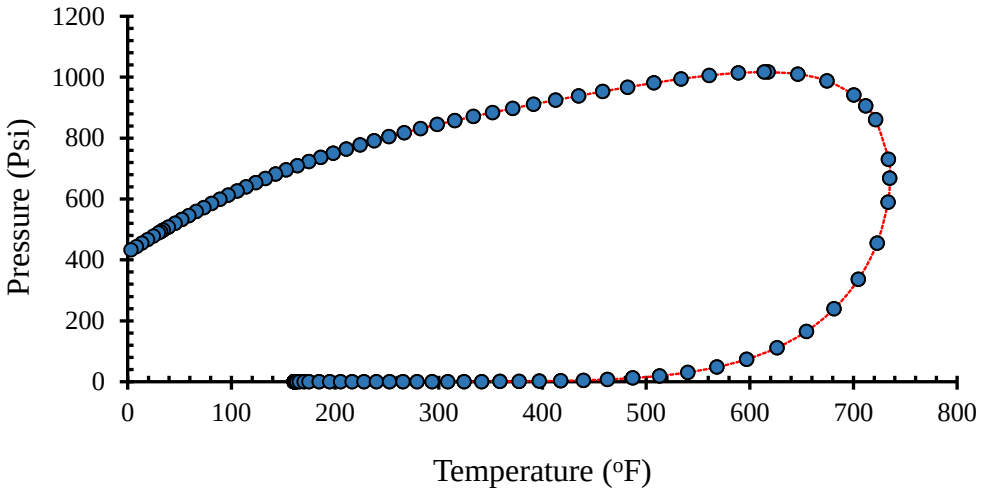

Figure 3.4: Pressure-temperature (P-T) diagram of the modelled reservoir fluid.

The comparison between the initial GOR, final GOR and the experimental data is shown in Figure 5 (after regression).

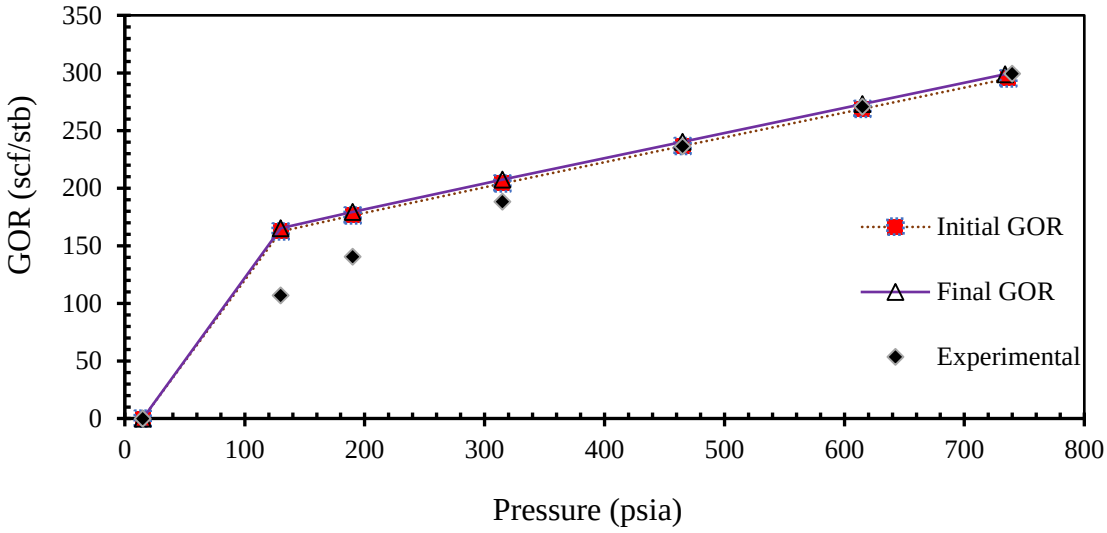

Figure 3.5: Comparison of measured gas oil ratio (GOR), initial GOR (before tuning), and final GOR (after tuning)

As can be seen in Figure 3.5, an improvement is achieved to match the experimental GOR by tuning the Pc and Tc of the heavier components during regression procedure. The similar comparisons between the experimental and the final parameter for the fluid are shown in Figure 3.6 for the relative oil volume and Figure 3.7 for the saturation pressure. Based on the comparison (showing relatively small error), it can be concluded that the modelled fluid behaves the same as the real reservoir fluid.

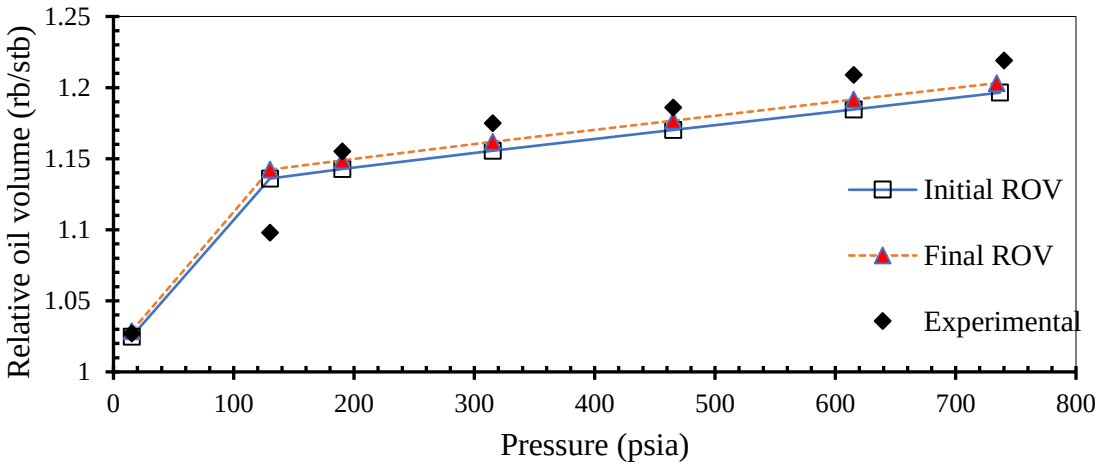

Figure 3.6 : Comparison of measured relative oil volume (ROV), initial ROV (before tuning) and final ROV (after tuning)

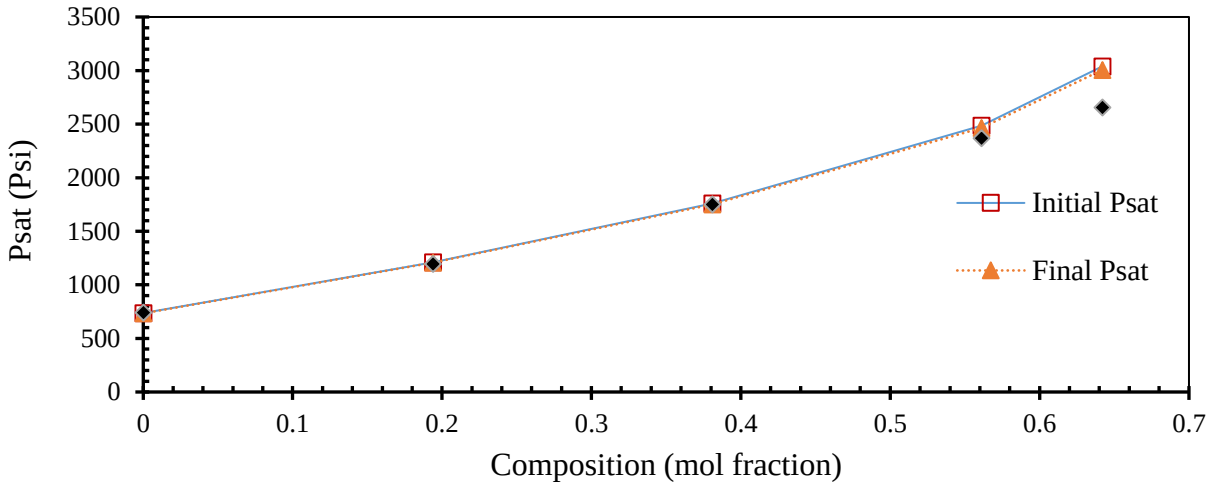

Figure 3.7: Comparison of measured Psat, initial Psat (before tuning) and final Psat (after tuning)

Tuning the EOS model to attain a good matching between the modeling results and available experimental data, Table 3.3 shows the reduction in error percentage (through comparing the values before and after tuning) for a part of important fluid properties used in this research work. This final error reduction percentage between the before and after tuning results shows that a valid match has been obtained through the regression analysis carried out using the Winprop EoS module in CMG.

Table 3.3: Experimental and modelled fluid properties

Property/Data	Experimental	Before tuning	After tuning	Error reduction
Psat, psi	740.0000	740.040	736.70	0.4 %
GOR, scf/stb	247.000	247.000	248.881	0.4 %
FVF, bbl/stb	1.180	1.140	1.159	1.3 %
API	40.000	41.000	40.009	0.25

The main source of error is through Plus fraction splitting of the grouped/lumped heavy carbon fractions. Through the lumping of the carbon fractions, technique such as Kays mixing rule is employed to determine the resultant properties such as critical temperature, critical pressure, acentric factor, and mole fraction. This process is accompanied with a degree of error which is unassociated with pure and single carbon number.

3.3.2 Reservoir Modeling

We consider a 1-D model to simulate a core flood displacement test with CMG-GEM compositional simulator. The steps taken to build the compositional generic reservoir model for LSWI simulation are represented in a flowchart as demonstrated in Figure 3.8.

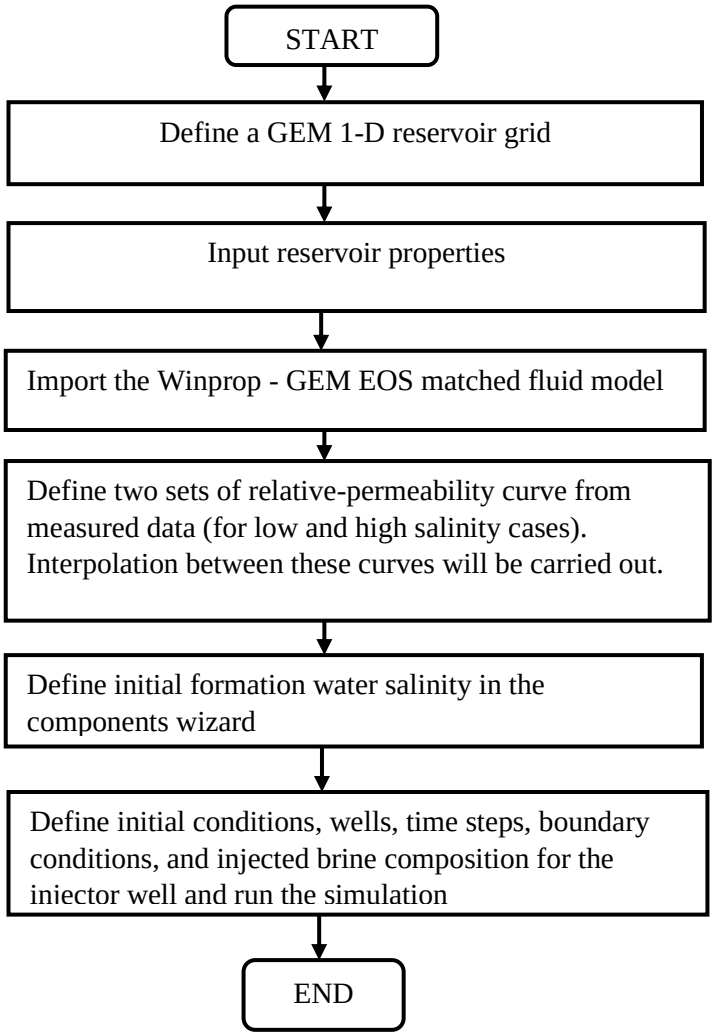

Figure 3.8: A simple approach to develop GEM reservoir compositional model for LSWI

A core of length 2.87 ft and a diameter of 0.1228 ft is considered to replicate the core dimensions used for a water flood experiment conducted by CMG [46]. The total grid of 50 is used in the I-direction and 1grid in J and K directions. The reservoir porosity is 0.24. The matrix permeability (k_m) and fracture permeability (k_f) are 11.43 mD and 1000 mD, respectively. Figure 3.9 shows a schematic representation of the 1-D compositional generic model which is built in CMG-GEM to study important aspects of LSWI.

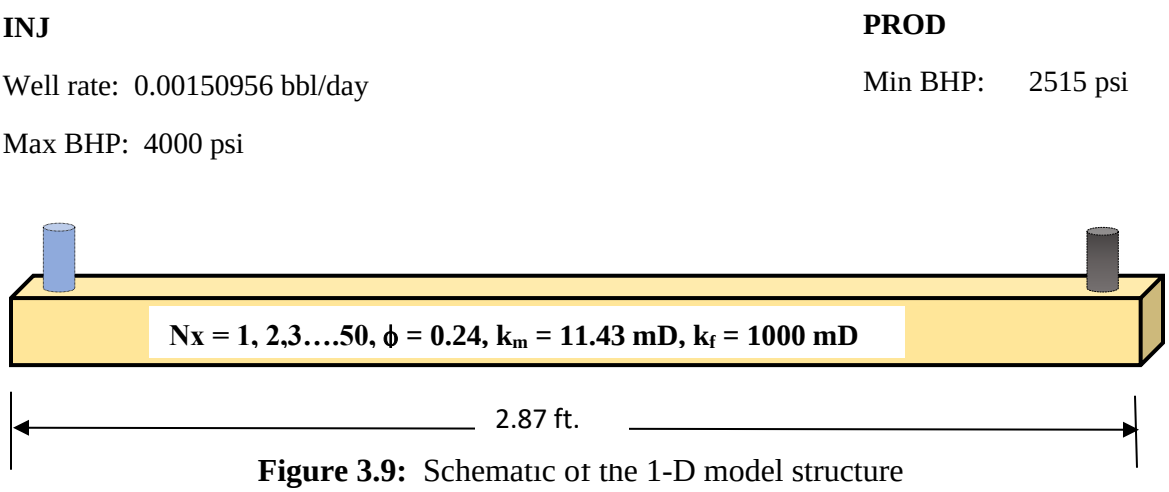

Figure 3.9: Schematic of the 1-D model structure

The injector well is constrained by an injection flow rate of 0.00150956 bbl/day and by a maximum bottom hole flowing pressure (BHP) of 4000 psi. A minimum BHP of 2515 psi is considered for the producer well. The finite difference method is used (as a mathematical strategy) by CMG to discretize the conservation mass or/and momentum equations of the oil and water/brine phases during the LSWI process. The mass balance equations are written for the fracture and matrix domains which are discretized in an adaptive-implicit manner for each grid block. The equations are then solved interactively by CMG where the primary constraints are used for the convergence purpose.

Input Data. To construct a 1-D numerical reservoir model, the model properties, which were used by Computer modelling Group for their experimental investigation of 1-D laboratory core flood, were employed in the current simulation work. Reservoir properties (for sandstone and carbonate) and the laboratory end-point relative permeability data are tabulated in Table 3.4 and Table 3.5, respectively. Also the plot of the resultant relative permeability versus water saturation used for this study is shown in Figure 3.10

Table 3.4: Model properties [46]

Parameter	Field unit	SI unit
Initial Reservoir pressure	2515 psi	17.23 x 10^{-6} N/m^2
Permeability	11.43 mD (Matrix)	1.12 x 10^{-14} m^2
Matrix Porosity	0.24	0.24
Fracture porosity	1.00	1.00
Initial oil saturation	0.80	0.80
Connate Water saturation	0.20	0.20
Cross sectional area	0.01185ft^2	0.00110m^2
Grid thickness	0.10888 ft	0.01011m

Table 3.5: Laboratory end-point relative permeability data [46]

Description/Parameter	Value
Endpoint saturation: Connate water	0.20
Endpoint saturation : Residual oil	0.29
Endpoint saturation : Irreducible oil for	0.37
Endpoint saturation : critical gas	0.03
Relative permeability at connate water	0.30
Relative permeability at irreducible oil	0.20
Exponent for calculating Krow	3.00

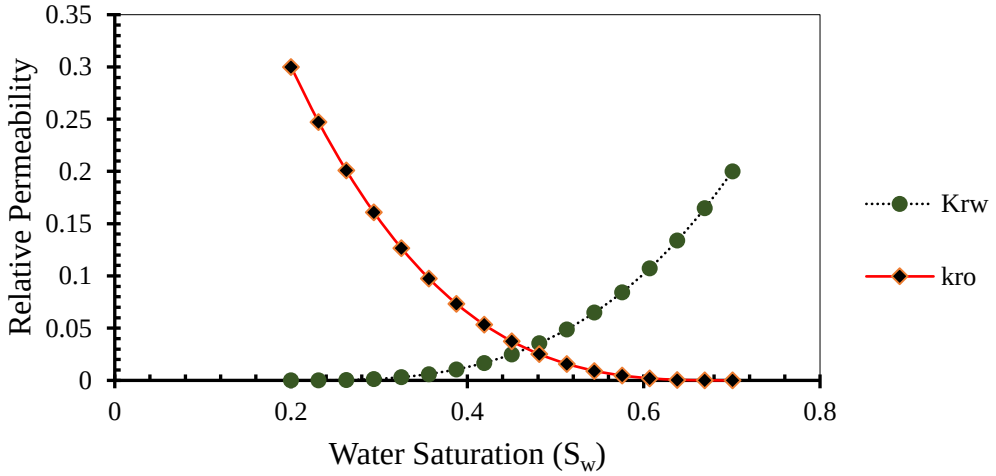

Figure 3.10: Relative Permeability curve

Brine Water Analysis. This section presents the laboratory water analysis of the formation water with total dissolved salt of 245980 ppm as listed in Table 3.6 (as a part of the input date in the simulator). The total Na^+ and SO_4^{2-} ions originally present in the formation water are 68520 ppm

and 612 ppm, respectively. Figure 3.11 illustrates the simulation runs to study the effect of Na^+ and SO_4^{2-} on the oil recovery in the sandstone and carbonate.

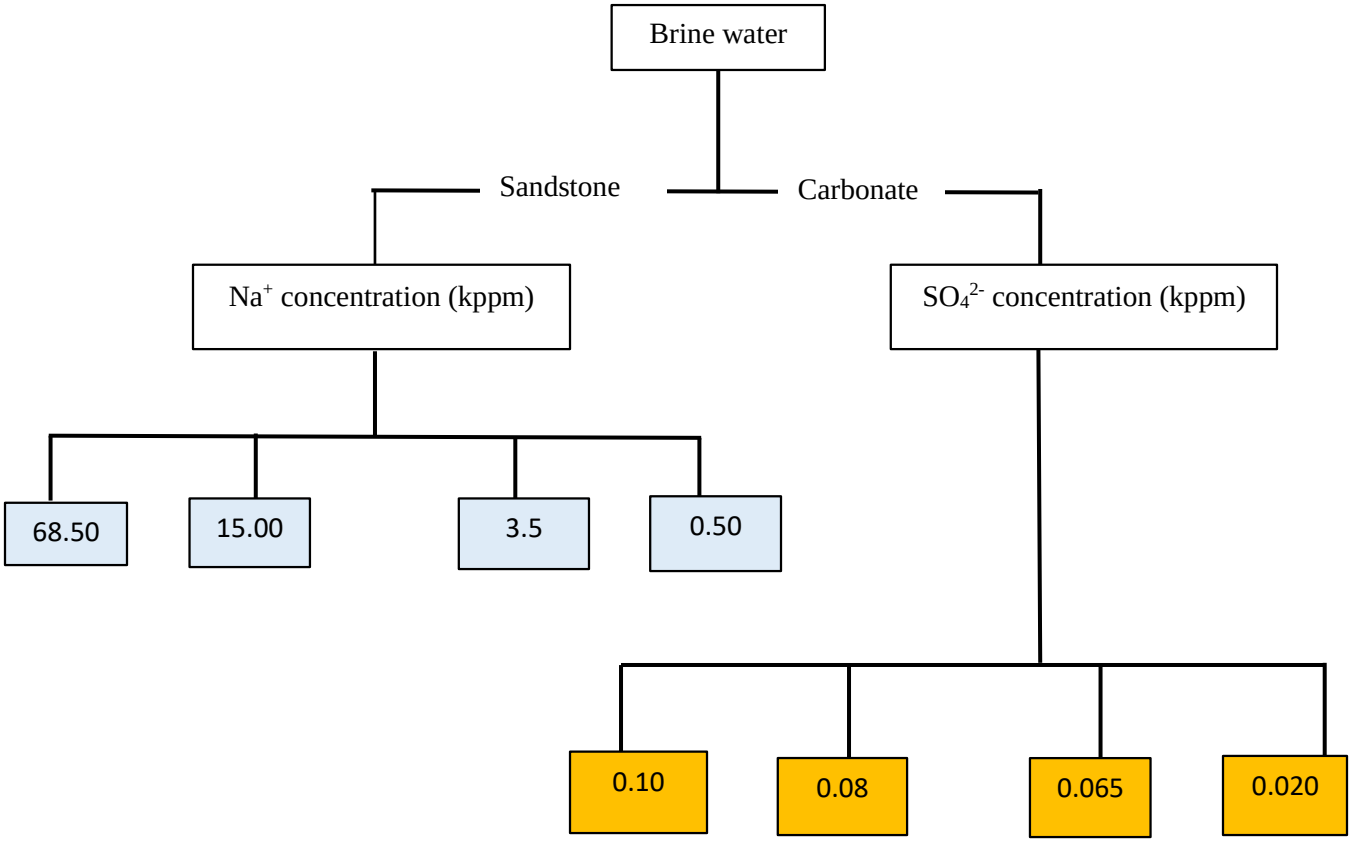

Figure 3.11: Design of simulation runs to understand the impact of Na^+ and SO_4^{2-} in the LSWI process

Table 3.6: Initial laboratory formation water compositions/mineral volume fractions [46]

Component/ ion		Formation water
Calcium	Ca^{2+}	18492 ppm
Magnesium	Mg^{2+}	2320 ppm
Strontium	Sr^{2+}	1880 ppm
Sodium	Na^{+}	68520 ppm
Potassium	K^{+}	4050 ppm
Barium	Ba_2^{+}	2.5 ppm
Bicarbonate	HCO_3^{-}	0
Carbonates	CO_3^{2}-	0
Chloride	Cl^{-}	150060 ppm
Sulphate	SO_4^{2-}	612 ppm
Hydroxide	H^{+}	0
Boron	Br_2^{+}	43.7 ppm
Total dissolved salts (TDS)		245980 ppm
pH		5.22
Volume fraction of calcite		0.5
Volume fraction of dolomite		0.5

Boundary and Initial Conditions. There are two types of boundary condition implemented by CMG for the solution of PDE's; namely, Newman and Dirchelet (or fixed pressure) boundary conditions. These boundary conditions are the set of constraints (primary and secondary) which are defined as the input into the simulator in terms of BHP and well flow rates. The initial brine compositions and the measured relative permeability for the high and low salinity conditions are defined as a set into CMG and the interpolation will be carried out for the salinity values between the limits.

Although CMG model has been validated with the experimental data and the results have been also compared with other commercial simulators such as PHREEQC, concluding the model is suitable or applicable as a tool for the study of LSWI, it is only capable of modelling low salinity water injection in sandstones by using Na^{+} as an interpolant between the low salinity relative permeability curve and high salinity relative permeability curve. Only Ca^{2+} or SO_4^{2-} can be used as an interpolant for modelling in carbonates. Hence, the complexities of ion exchange during this process cannot be effectively captured.

Modelling Wettability Alteration

The effect of wettability alteration during low salinity water injection is modelled by the shifting of relative permeability curves. Typically, two sets of relative permeability curves are defined in this study as input to represent high salinity (625000 Kppm) and low salinity conditions (1 Kppm) as shown in Figure 3.12. Interpolation between these two curves is usually carried out by the interpolant. The interpolant is the equivalent ionic fraction on the rock surface and these relative permeability curves are usually measured from the laboratory experiments [46] which serve as input during numerical modelling.

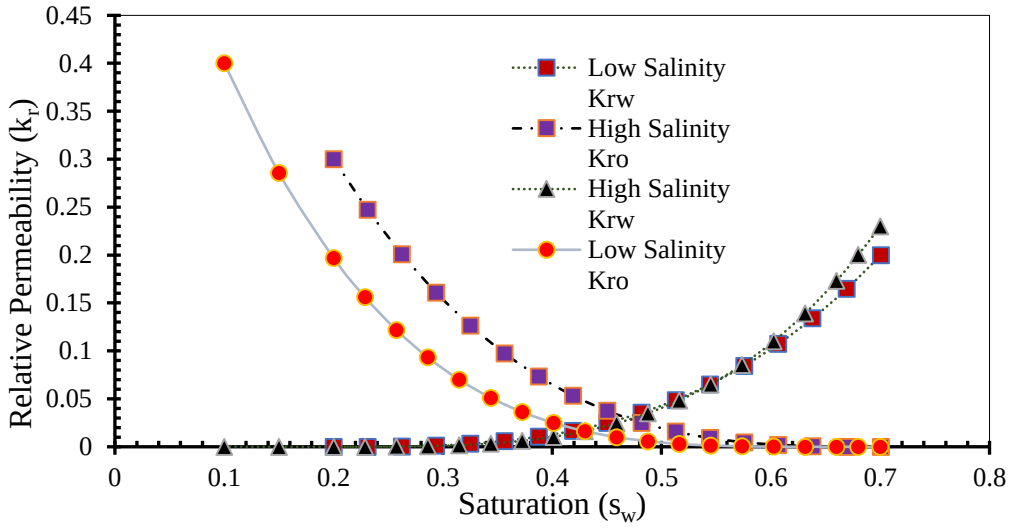

Figure 3.12: Experimental high and low Salinity relative permeability curves [46].

3.4 Results and Discussion

This section presents the main results obtained from LSWI simulation runs, with focus on the important mechanisms/phenomena during the recovery process.

Effect of LSWI on Oil Recovery in Sandstone and Carbonate.

Figure 13 shows the effect of pore volume of LSWI on recovery factor for the sandstone reservoir at various concentrations of Na^+ ions where the Na^+ concentrations of 68.52 kppm,15.00 kppm, 3.50 kppm, and 0.50 kppm are examined.

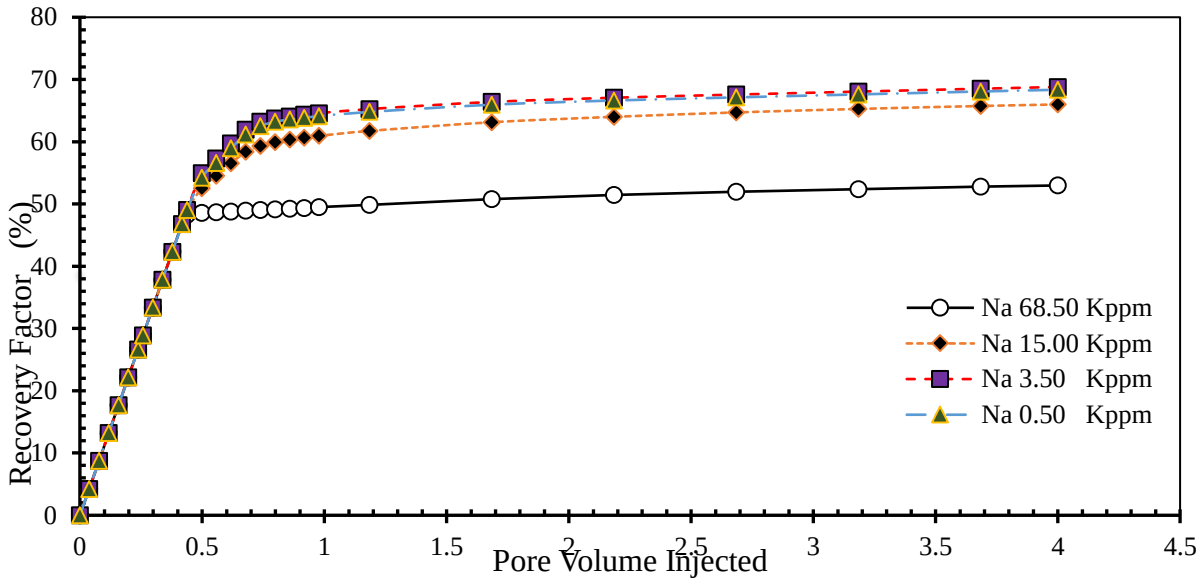

Figure 3.13: Oil recovery versus injected pore volume and Na^+ concentration

It is observed that the ultimate oil recovery factor increases from 51 % to 68 % by decreasing Na^+ concentration in the injected brine from 68.52 kppm to 0.5 kppm after injecting 4.0 pore volumes of brine into the reservoir. Indeed, the highest recovery factor is attained with a concentration of 3.5 kppm for Na^+.

Further decrease of Na^+ concentration below 3.5 Kppm provides no improvement in the oil recovery as illustrated in Figure 3.14 which shows the ultimate recovery factor after 4.0 injected PV. Further reduction in the Na^+ concentration does not lead to further increment in the ultimate oil recovery due to the subsequent reductions of Na^+ ions in the injected brine. As the Na^+ concentration in the injected brine is reduced, the brine-rock equilibrium is altered and Na^+ on the surface of the formation must be desorbed thereby releasing the formation Na^+ to balance the equilibrium state. This desorption of Na^+ from the sandstone surface leads to a replacement by a divalent ion to attain a new ionic bridge equilibrium state. This phenomenon causes the polar oil components attached to divalent ion to be released. At a certain point in the reduction Na^+ in the injection brine, there will be no more free ions on the formation surface to balance the reduction of Na^+ in the effluent. At this point, a further reduction in Na^+ will not lead to higher oil recovery. In our simulations, this occurred at 3.5 Kppm.

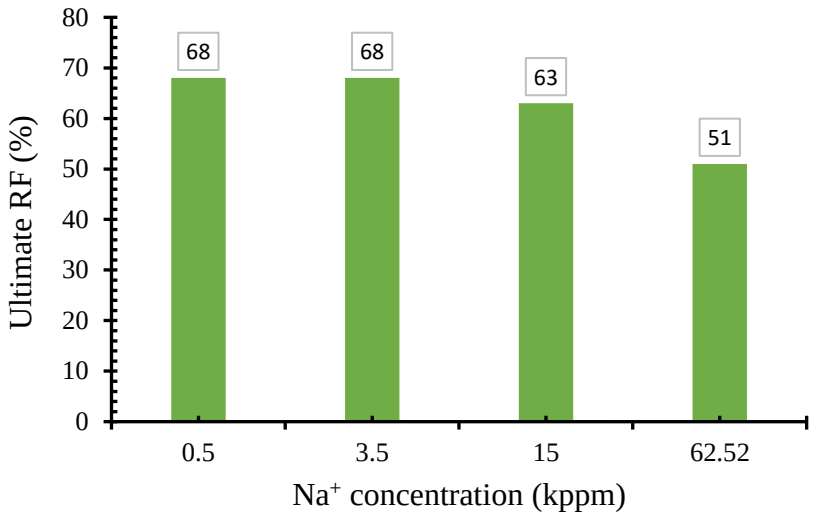

Figure 3.14: Final oil recovery for different Na+ concentration in the sandstone case

The impact of concentration of SO_4^{2-} ions on the oil recovery in the carbonate is investigated where the SO_4^{2-} concentration varies from 0.02 kppm to 0.10 kppm, as demonstrated in Figure 3.15. It is observed that the ultimate recovery increases from 53.4% to 66 % if the concentration of SO_4^{2-} in the injected brine lowers from 0.1 kppm to 0.02 kppm where 4 pore volumes of injected brine are used in the LSWI.

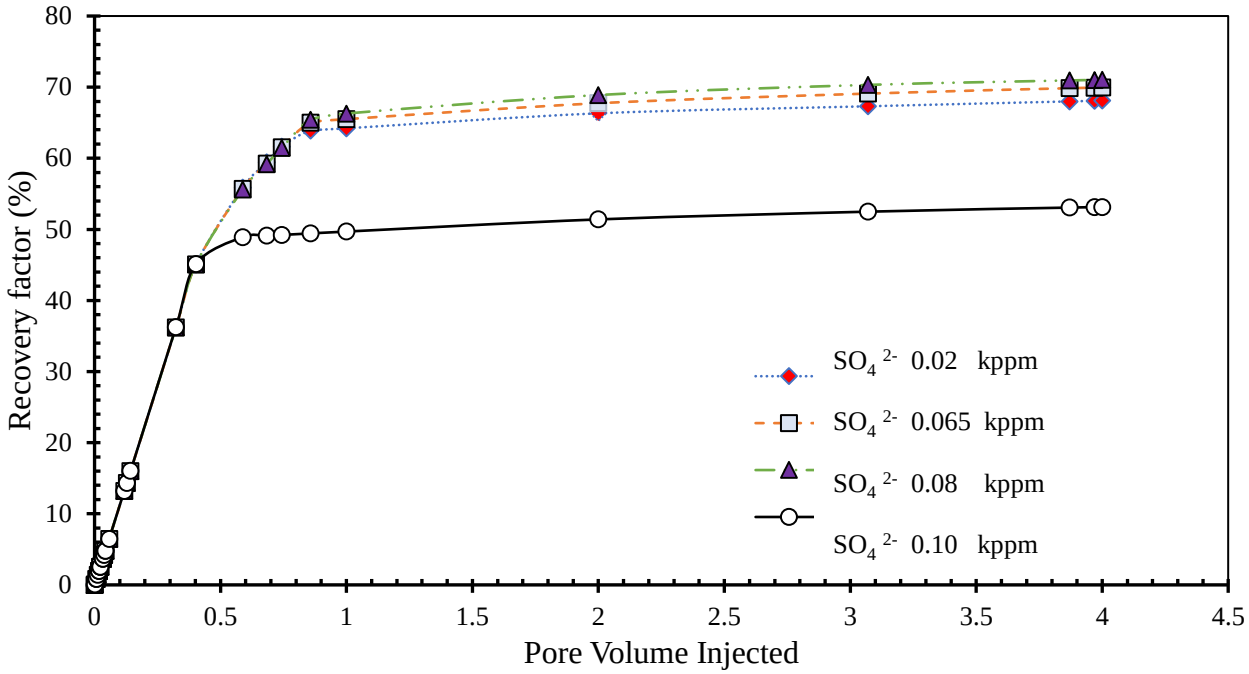

Figure 3.15 : Oil recovery factor by altering $S0_4^{2-}$ concentration

As clear from Figure 3.16 which shows the ultimate recovery factor, the variation of RF with SO_4^{2-} concentration does not follow a similar trend as observed in sandstone. As depicted in Figure 3.15, RF increases when SO_4^{2-} concentration decreases from 0.1 kppm to 0.08 kppm; however, the recovery factor decreases if the SO_4^{2-} concentration lowers further after 0.08 kppm. This observation has been debatable by many researchers. According to the experimental investigation conducted by (Chinedu , 2008) on the effect of rock wettability on oil recovery for secondary and tertiary oil recovery process, it was reported that there is a critical low salinity at which injecting SO_4^{2-} gives the highest increase in contact angle. Hence, there is a critical salinity that yields the optimum oil recovery. The critical salinity in this study is 0.08kppm.

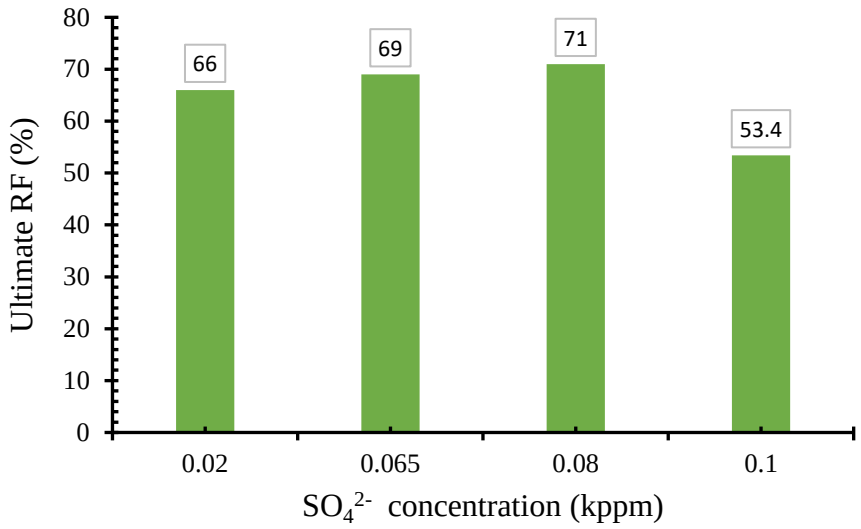

Figure 3.16: Ultimate oil recovery versus the magnitude of SO_4^{2-} concentration

According to Figure 3.15, a sensitivity analysis is required to determine the optimum concentration of SO_4^{2}- that offers the highest ultimate oil recovery in the carbonate. In this research work, the optimum SO_4^{2-} concentration is 0.08 Kppm, as the highest ultimate oil recovery of 72% is attained at this concentration after 4.0 pore volumes of injected brine. Further reduction in the concentration yields lower recovery factor as depicted in Figure 3.15.

Effect of LSWI on pH. For sandstone, the initial pH of formation water increases after 2.5 days under LSWI operation. The increase in the local pH is because more proton ions are released during the exchange of monovalent ion of Na^+ and Ca-X_2, leading to the release of Ca^{2+} ions in the formation water. In this study, the local pH during LSWI for sandstone varies from 5 to 9, 5 to 8, and 5 to 7.13 for 3.5 kppm, 15 kppm, and 62.52 kppm of Na^+ concentration respectively, as shown in Figure 3.17.

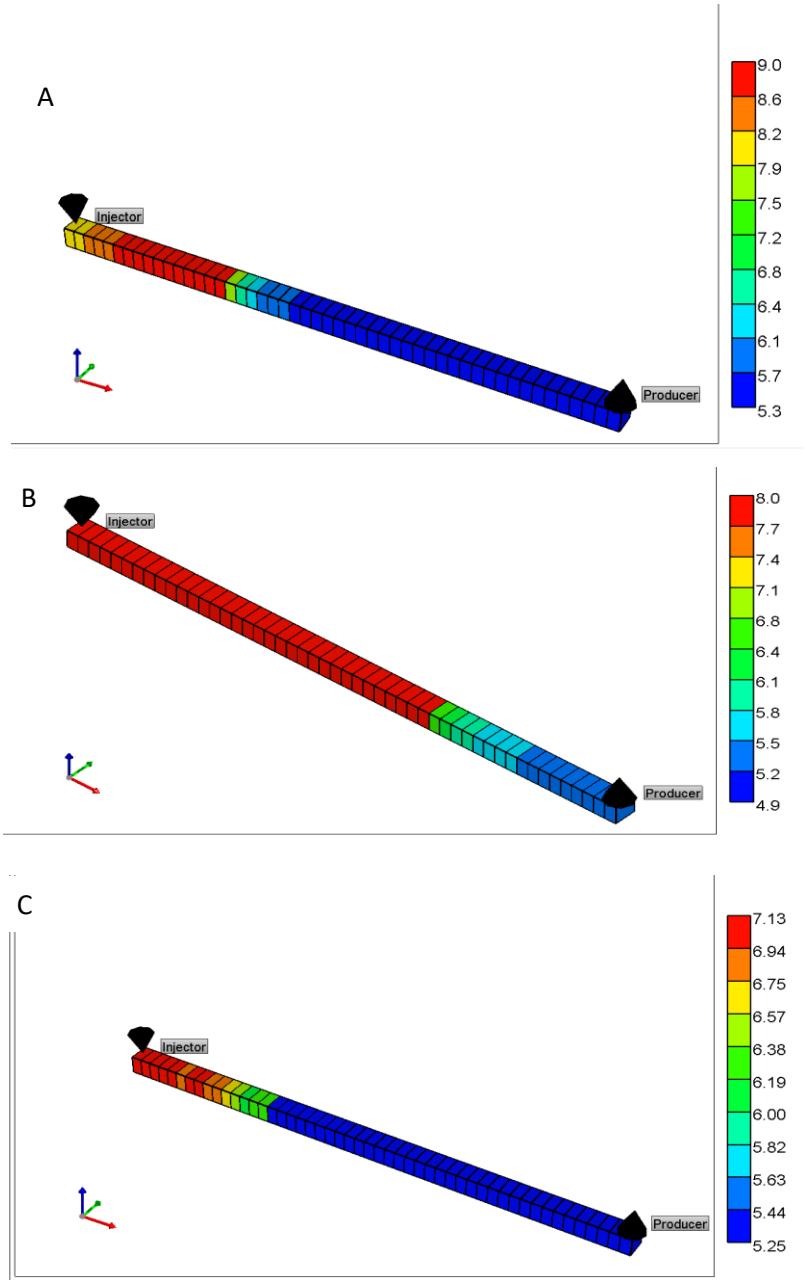

Figure 3.17 : 3D representation of pH change in sandstone for A(3.5 kppm), B(15 kppm), and C (62.52 kppm).

Figure 3.18 shows a variation of pH with Na^+ concentration for the sandstone case. It is observed that there is a gradual increase in the pH while decreasing the salinity. As the Na^+ concentration in the injected brine is reduced, there is an ionic exchange between a monovalent ion and a divalent ion which are mainly between Na^+ and $Ca\text{-}X_2$ or Na^+ and $Mg\text{-}X_2$ respectively. This phenomenon

will cause a release of Na^+ into the injected brine and formation water in other to attain a new ionic equilibrium. The release of Na^+ with protons ions will cause an increase in the local pH of the formation. In this study, the local pH during LSWI for sandstone varies from (5 to 9), (5 to 8), and (5 to 7.13) for 3.5 kppm, 15 kppm and 62.52 kppm of Na^+ concentration respectively as shown in Figure 3.18. It can also be observed that the lower the salinity of Na^+ concentration in the injected brine, the higher the increase in the local pH because more Na^+ will be released from formation water to remedy this deficiency and this will in turn increase the pH.

This increase in pH during LSWI contributes to the overall effective mechanism of increasing the recovery factor in sandstone, because the injected water behaves like an alkaline solution which is capable of decreasing the interfacial tension between oil and water phases.

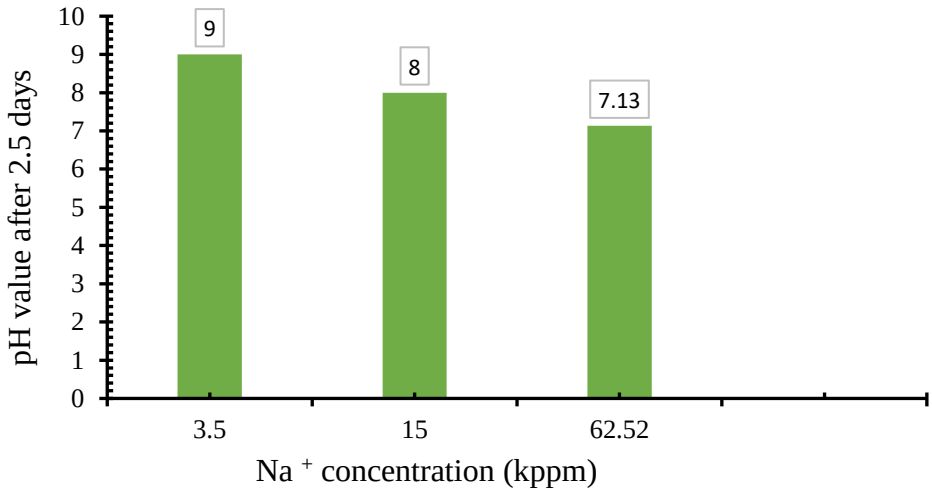

Figure 3.18 : pH change in sandstone versus Na^+ concentration

For the carbonate case as shown in Figures 3.19 and 3.20, there is no increase in the pH even though there is also a release of proton ions during ion exchange. This is due to the fact that an increased solubility of CO_2 (liberated from $CaCO_3$) in the aqueous phase is experienced with decreasing the salinity which results in the formation of a weak acid and bicarbonates of HCO_3^{2-} . This will cancel the proton effect according to the following reaction as shown in Equation (3.18), where the bicarbonates act as a buffer.

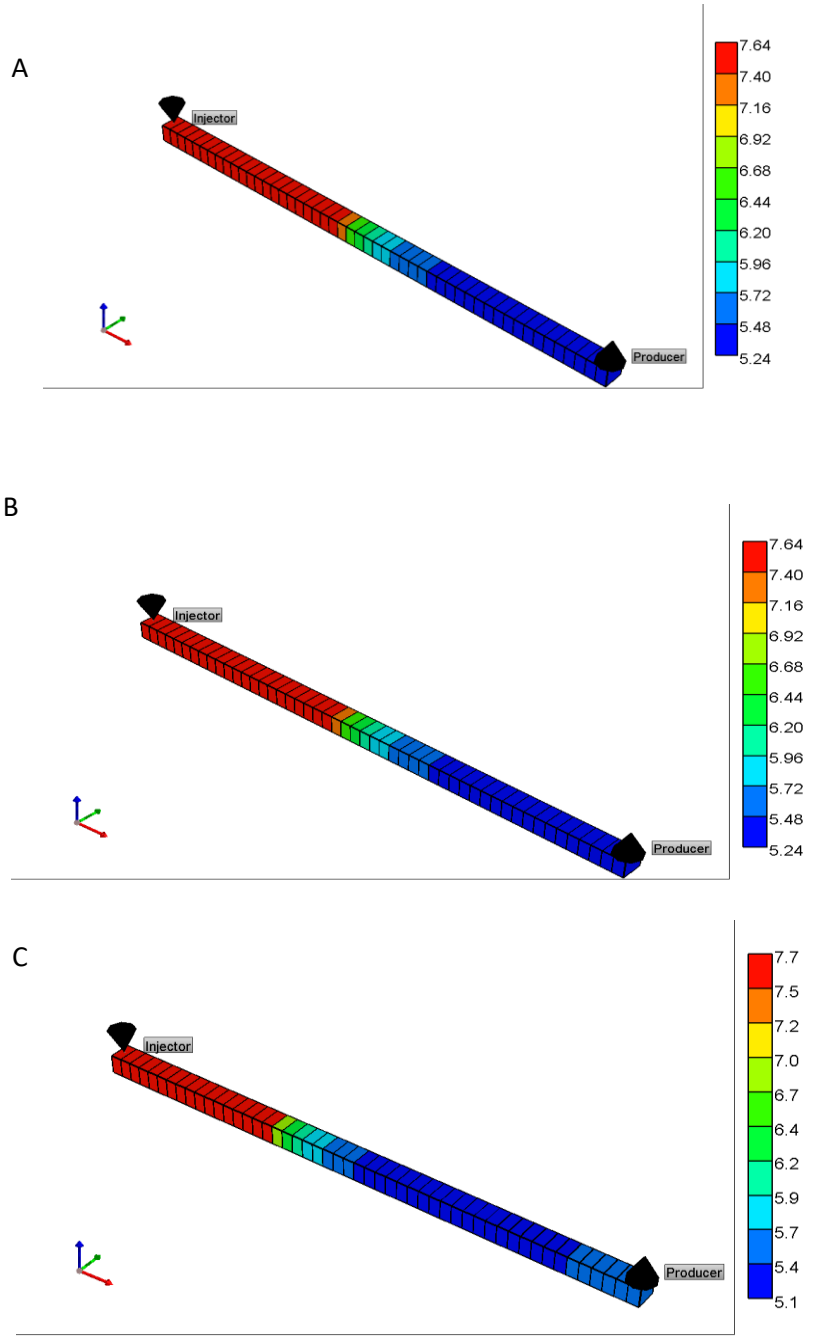

Figure 3.19: 3D representation of pH change in carbonate for A (0.1 kppm), B (0.08 kppm), and C (0.065 kppm)

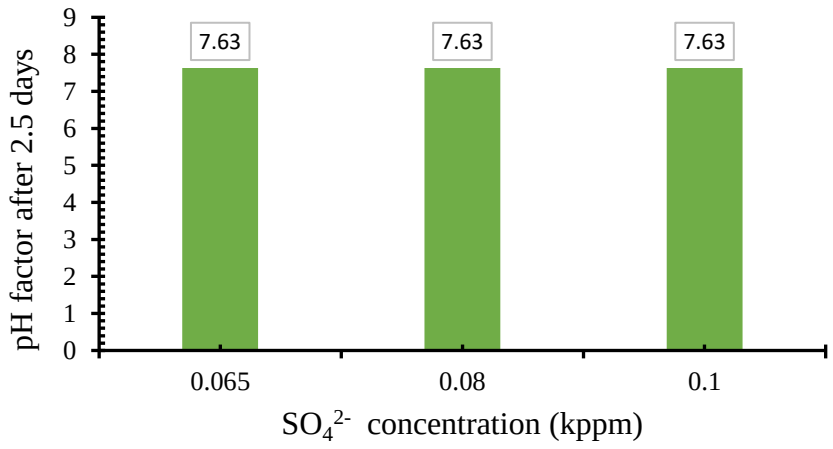

Figure 3.20: pH change in carbonates in terms of SO_4^{2-}

$$H_2O_{aq} + CaCO_{3_s} \leftrightarrow H^+_{aq} + HCO^{2-}_{3\ aq} + Ca^{2+}_{aq} \quad (3.18)$$

Hence the resultant increase in pH during LSWI for carbonates is only about ±1 units for every ±10000ppm increase or reduction of salinity. Thus, pH has no predominant effect on altering interfacial tension in carbonate reservoirs so that it does not appreciably contribute to change in the total oil recovery.

Effect of LSWI on Mineral Dissolution and Precipitation. Figures 3.21 and 3.22 depict property distance plots to demonstrate the calcite precipitation and dolomite dissolution, respectively, during LSWI through a cross-section of (1, 1, 1 – 25, 1, 1) along I- direction. It should be noted that the sign convention, used by CMG, is -ve for precipitation and +ve for dissolution. Low salinity favors more precipitation as seen in Figure 21. This behaviour/mechanism is further explained by the following equation:

$$\text{Calcite} + H^+ \leftrightarrow Ca^{++} + HCO^{2-}_3 \quad (3.19)$$

During the low salinity injection and in the presence of CO_2, the gas will be favorably dissolved into water and HCO_3^{2-} is formed when Ca^{2+} ions are surplus. It shifts Equation (3.19) to the left side, causing precipitation of calcite. According to Figure 3.21, the amount of precipitated calcite is very small. Even though the equilibrium rate cannot be measured by CMG during the simulation run, there was evidence of precipitation in the property distance plot. This phenomenon should not be overlooked as the precipitation of calcites in some cases might occur faster in the presence of catalytic ions in the formation water, resulting in considerable influence on porosity, permeability, and total oil recovery.

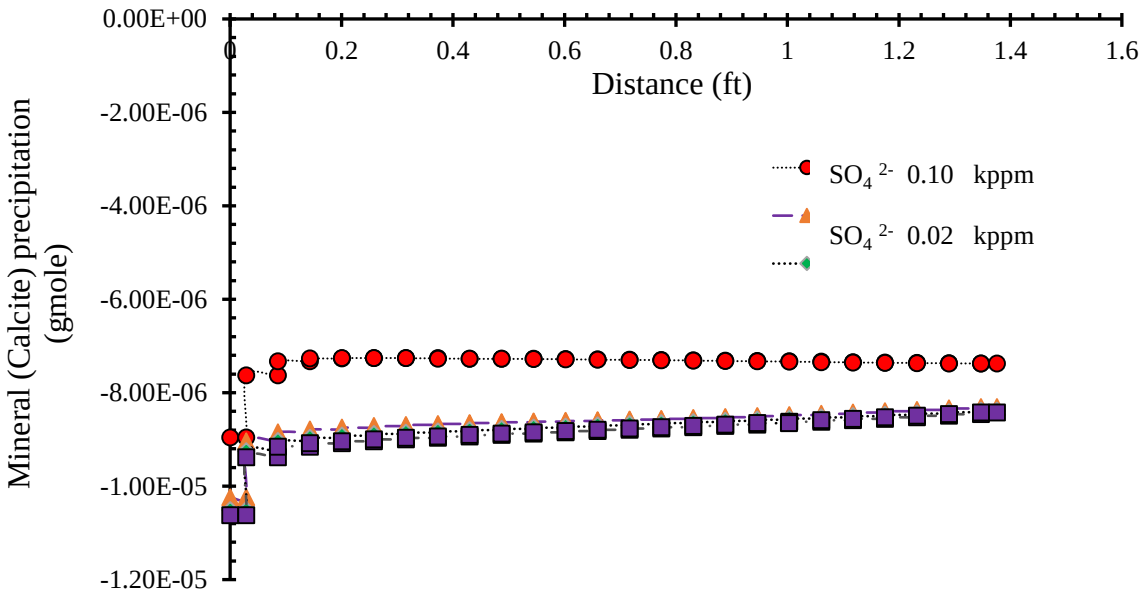

Figure 3.21: Effect of LSWI on mineral (calcite) precipitation in carbonates.

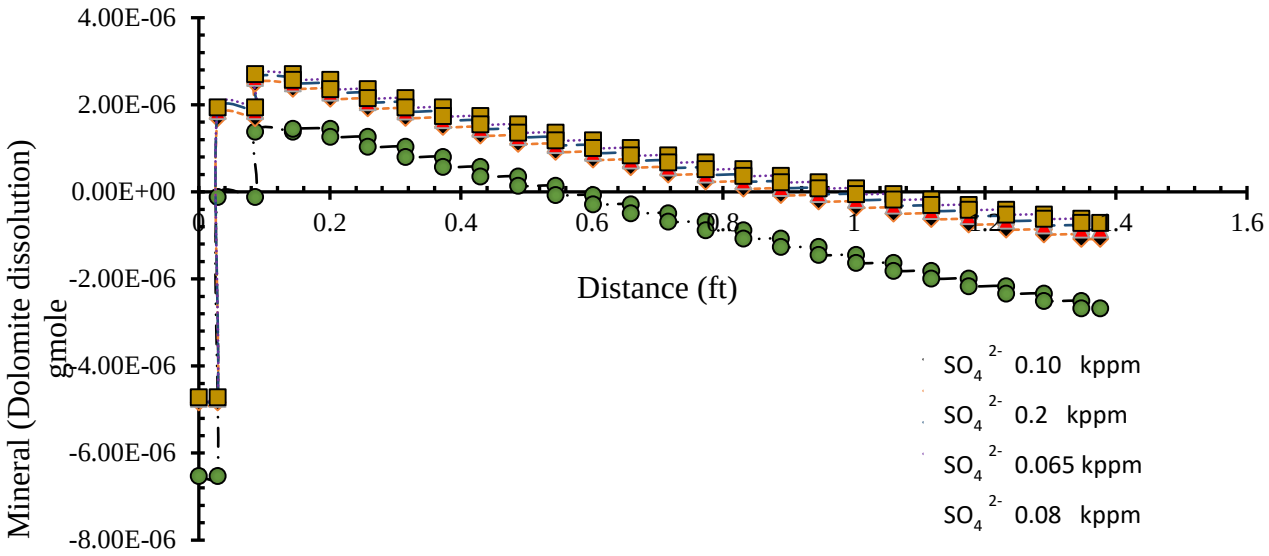

Figure 3.22: Influence of LSWI on mineral (dolomite) dissolution in carbonates

Similarly, Figure 3.22 demonstrates the dolomite dissolution in the carbonate system as low salinity favors dissolution of dolomite. This behaviour is illustrated by the following reaction:

$$\text{Dolomite} + 2H^{+} \leftrightarrow Ca^{++} + 2HCO_3^{2-} + Mg^{++} \tag{3.20}$$

Based on Equation (3.20), there is surplus of H^{+} ions, but there is deficiency of HCO_3^{2-} and Ca^{++}. The deficiency and surplus cause that the reaction moves to the right side to dissolve more dolomite. The equilibrium rate of this reaction is not known as this parameter cannot be measured with CMG. However, Figure 3.22 reveals the occurrence of the dissolution process in carbonate cases.

LSWI is identified as a prominent EOR technique where microscale investigation of this process is needed to capture the important recovery mechanisms that result in considerable changes in oil saturation distribution and oil and rock properties. To further understand the detailed physics at both micro and micro scales, the systematic experimental and modeling works seem necessary.

This study provides further insight of the LSWI process through conducting numerical simulation of LSWI as an EOR method. CMG-GEM is only capable of modelling low salinity water injection in sandstones by using Na^+ as an interpolant between the low salinity relative permeability curve and high salinity relative permeability curve. Only Ca^{2+} or SO_4^{2-} can be used as an interpolant for modelling in carbonates. Therefore, during this study, the main challenge was to capture LSWI using a different ion aside Na^+, Ca^{2+} or SO_4^{2-} as an interpolant. However, to a large extent, it gives considerably good results when compared to experimental and other numerical commercial simulators such as PHREEQC. PHREEQC is a computer program for simulating chemical reactions and transport processes in natural or polluted water, in laboratory experiments, or in industrial processes

In this study, we confirm that wettability alteration is one of the dominant mechanisms for additional recovery during LSWI process. Furthermore, we conclude that an increase in pH represents another important mechanism for additional oil recovery in sandstone reservoirs. Most importantly, it was found that there are two vital phenomena including mineral dissolution and precipitation occurring in sandstone and carbonates over LSWI, respectively which are capable of changing the reservoir properties and causing flow assurance problems (pore throat plugging), consequently leading to further operating expenditures during production operations.

3.5 **Acknowledgements**

The financial assistance offered by Memorial University (NL, Canada), Natural Sciences and Engineering Research Council of Canada (NSERC), InnovateNL (formerly RDC), and Statoil Canada is greatly acknowledged.

3.6 **Conclusions**

LSWI as an EOR technique leads to an improvement in conventional water flooding processes. Moreover, it exhibits more advantages, compared to other chemical EOR Process in terms of its relatively low capital cost, environmental impact, and relative ease of field implementation. This research work presents modeling simulation of LSWI for sandstones and carbonates to investigate variation of pH, calcite precipitation, dolomite dissolution, recovery mechanisms, and oil recovery factor over the production process. The following conclusions are drawn based on the results:

- A decrease in salinity content for a sandstone reservoir offers a considerable increase in the oil recovery factor until a critical salinity below which no significant change occurs in the recovery factor.

- Analyzing the recovery data of carbonate reservoirs, there is an optimum salinity which gives the maximum oil recovery; further decrease behind this particular salinity lowers the recovery factor.

- The impact of the local pH (while increasing this parameter) is more noticeable in sandstone reservoirs, compared to carbonates. This factor coupled with wettability alteration provides effective/higher driving force for LSWI operation in sandstones. It is known that an increase in pH reduces the oil-water interfacial tension and consequently the residual oil saturation (S_{or}), leading to a greater oil recovery.

- No considerable improvement in oil recovery from carbonates is noticed with increasing local pH, due to the formation of bicarbonates HCO_3^{2-} which neutralizes the proton H^+. Hence, the main driving force causing higher oil recovery with low salinity injection in carbonates is the wettability alteration. This occurs due to the release of divalent ions which cause a shift in the oil-water relative permeability curve towards more water wet porous system.

- The effect of mineral reactions including both precipitation of calcite and dissolution of dolomite is important during LSWI even though the reaction rate is low. Nevertheless, under favorable conditions in the presence of catalytic ions, the mineral dissolution and precipitation can occur at a much faster rate which can appreciably change reservoir properties and hence affect oil recovery.

- Further modelling and experimental investigations are recommended to systematically study the influence of mineral reactions as this may be a dominant factor affecting oil recovery in the presence of bicarbonates and other catalytic ions in the formation water.

Nomenclatures

Acronyms

API	American Petroleum Institute
BHP	Bottom Hole Pressure
CEC	Cation Exchange Capacity
Ca	Calcium
Ca^{2+}	Calcium ion
CMG	Computer Modelling Group
CO_2	Carbon dioxide
CCE	Constant Composition Expansion
CVD	Constant Volume Depletion
DL	Differential Liberation
EOR	Enhanced Oil Recovery
EoS	Equation of State
FVF	Formation Volume Factor
GOR	Gas Oil Ratio
kppm	kilo parts per million
LSWI	Low Salinity Water Injection
Mg^{2+}	Magnesium ion
mD	milli Darcy
Na	Sodium
Na^{+}	Sodium ion
N_2	Nitrogen gas
Psat	Saturation Pressure
R.F	Recovery Factor
$R\text{-}COO^{-}$	Carboxylic components
ROV	Relative Oil Volume
SO_4^{2-}	Sulphate ion
TDS	Total Dissolved Salt

Variables and parameters

a	Activity
D	Diffusivity
f	fugacity (-)
g	Acceleration due to gravity
h	height
K	Equilibrium constant
K_{row}	Oil water relative permeability
K’	Selectivity coefficient
M	Molality
na	Aqueous component
P	Pressure (Psia)

q_i	Injection and production rate of
R	Reaction rate (moles/m^3)
T	Transmissibility
u	Darcy velocity (ft/day)
V	Grid block volume (m^3)
$VR_{i,aq}^{n+1}$	Intra aqueous reaction rate
$VR_{i,mn}^{n+1}$	Mineral dissolution/precipitation
X	Exchanger
y	mole fraction

Greek letters

ρ	Mass density ($\frac{Kg}{m^3}$)
μ	Viscosity (centipoise)
ϕ	Porosity (-)
γ_i	Activity coefficient
Δ	Difference operator

Subscripts

aq	Aqueous
w	Water
mn	Mineral component

Superscripts

u =n	Explicit time step for grid block
n+1	Implicit time step for grid block

References

[1] Al-Shalabi EW, Sepehrnoori K, Delshad M. Does the double layer expansion mechanism contribute to the LSWI effect on hydrocarbon recovery from carbonate rocks? SPE Reserv Characterisation Simul Conf Exhib New Approaches Characterisation Model Complex Reserv RCSC 2013 2013;1:319–35. doi:10.2118/165974-MS.

[2] Zhang Y, Morrow NR. Comparison of Secondary and Tertiary Recovery with Change in Injection Brine Composition for Crude Oil/ Sandstone Combinations. SPE/DOE Symp Improv Oil Recover 2006:1–15. doi:10.2523/99757-MS.

[3] Sheng JJ. Critical review of low-salinity waterflooding. J Pet Sci Eng 2014;120:216–24. doi:10.1016/j.petrol.2014.05.026.

[4] Koleini MM, Mehraban MF, Ayatollahi S. Effects of low salinity water on calcite/brine interface: A molecular dynamics simulation study. Colloids Surfaces A Physicochem Eng Asp 2018;537:61–8. doi:10.1016/J.COLSURFA.2017.10.024.

[5] Xie Q, Brady P V., Pooryousefy E, Zhou D, Liu Y, Saeedi A. The low salinity effect at high temperatures. Fuel 2017;200:419–26. doi:10.1016/J.FUEL.2017.03.088.

[6] Shalabi EW Al, Sepehrnoori K, Delshad M. Mechanisms behind low salinity water injection in carbonate reservoirs. Fuel 2014;121:11–9. doi:10.1016/J.FUEL.2013.12.045.

[7] Dang C, Nghiem L, Nguyen N, Chen Z, Nguyen Q. Mechanistic modeling of low salinity water flooding. J Pet Sci Eng 2016;146:191–209. doi:10.1016/J.PETROL.2016.04.024.

[8] Sharma H, Mohanty KK. An experimental and modeling study to investigate brine-rock interactions during low salinity water flooding in carbonates. J Pet Sci Eng 2017. doi:10.1016/J.PETROL.2017.11.052.

[9] Al-Shalabi EW, Sepehrnoori K. A comprehensive review of low salinity/engineered water injections and their applications in sandstone and carbonate rocks. J Pet Sci Eng 2016;139:137–61. doi:10.1016/J.PETROL.2015.11.027.

[10] Kilybay A, Ghosh B, Chacko Thomas N. A Review on the Progress of Ion-Engineered Water Flooding. J Pet Eng 2017;2017:1–9. doi:10.1155/2017/7171957.

[11] Zhang Y, Xie X, Morrow NR. Waterflood Performance By Injection Of Brine With Different Salinity For Reservoir Cores. SPE Annu. Tech. Conf. Exhib., Society of Petroleum Engineers; 2007. doi:10.2118/109849-MS.

[12] Al-Attar HH, Mahmoud MY, Zekri AY, Almehaideb RA, Ghannam MT. Low Salinity Flooding in a Selected Carbonate Reservoir: Experimental Approach. EAGE Annu. Conf. Exhib. Inc. SPE Eur., Society of Petroleum Engineers; 2013. doi:10.2118/164788-MS.

[13] Peimao Zhang *, Medad T. Tweheyo and, Austad T. Wettability Alteration and Improved Oil Recovery in Chalk: The Effect of Calcium in the Presence of Sulfate 2006. doi:10.1021/EF0600816.

[14] Nasralla RA, Nasr-El-Din HA. Double-Layer Expansion: Is It A Primary Mechanism of Improved Oil Recovery by Low-Salinity Waterflooding? SPE Improv. Oil Recover. Symp., Society of Petroleum Engineers; 2012. doi:10.2118/154334-MS.

[15] Yousef AA, Al-Saleh S, Al-Jawfi MS, Al-Salehsalah SH, Al-Jawfi MS. New recovery method for carbonate reservoirs through tuning the injection water salinity: Smart WaterFlooding. 73rd Eur Assoc Geosci Eng Conf Exhib 2011 Unconv Resour Role Technol Inc SPE Eur 2011 2011;4:2814–30. doi:10.2118/143550-MS.

[16] Austad T, Strand S, Høgnesen EJ, Zhang P. Seawater as IOR Fluid in Fractured Chalk. 2005 SPE Int Symp Oilf Chem 2005:1–10. doi:10.2118/93000-MS.

[17] Austad T, Rezaeidoust A, Puntervold T. Chemical Mechanism of Low Salinity Water Flooding in Sandstone Reservoirs. SPE Improv. Oil Recover. Symp., 2010. doi:10.2118/129767-MS.

[18] Fathi SJ, Austad T, Strand S. “Smart Water” as a Wettability Modifier in Chalk: The Effect of Salinity and Ionic Composition. Energy & Fuels 2010;24:2514–9. doi:10.1021/ef901304m.

[19] Experimental and theoretical study of wettability alteration during low salinity water flooding-an state of the art review. Colloids Surfaces A Physicochem Eng Asp 2017;520:622–39. doi:10.1016/J.COLSURFA.2017.02.006.

[20] Strand S, Austad T, Puntervold T, Høgnesen EEJ, Olsen M, Barstad SMF. “Smart water” for oil recovery from fractured limestone: a preliminary study. Energy & 2008;21:3126–33. doi:10.1021/ef800062n.

[21] Austad T. Enhanced Oil Recovery Field Case Studies. Gulf Professional Publishing; 2013. doi:10.1016/B978-0-12-386545-8.00013-0.

[22] Standnes DC, Austad T. Wettability alteration in chalk. J Pet Sci Eng 2000;28:111–21. doi:10.1016/S0920-4105(00)00083-8.

[23] Fathi SJ, Austad T, Strand S. Effect of Water-Extractable Carboxylic Acids in Crude Oil on Wettability in Carbonates 2011. doi:10.1021/ef200302d.

[24] Hassenkam T, Mitchell AC, Pedersen CS, Skovbjerg LL, Bovet N, Stipp SLSS, et al. Low Salinity Effect at Pore Scale: Probing Wettability Changes in Middle East Limestone. Energy & Fuels 2016;30:3768–75. doi:10.1021/acs.energyfuels.5b02562.

[25] Altahir M, Yu M, Hussain F. LOW SALINITY WATER FLOODING IN CARBONATE ROCKS – DISSOLUTION EFFECT 2017:1–8.

[26] Vajihi F, Diaz P, Sagbana I, Zabihi H, Farhadi A, Sherhani S. Effect of Low Salinity Water Injection on Capillary Pressure and Wettability in Carbonates 2017:1–9.

[27] Didier M, Chaumont A, Joubert T, Bondino I, Hamon G. Contradictory Trends for Smart Water Injection Method : Role of Ph and Salinity From Sand / Oil / Brine Adhesion Maps. Sca 2015:1–12.

[28] Hassenkam T, Mitchell AC, Pedersen CS, Skovbjerg LL, Bovet N, Stipp SLS. The low salinity effect observed on sandstone model surfaces. Colloids Surfaces A Physicochem Eng Asp 2012;403:79–86. doi:10.1016/j.colsurfa.2012.03.058.

[29] Tong Z, Xie X, Morrow NR. Crude Oil Composition and the Stability of Mixed Wettability in Sandstones 2003;44:233–42.

[30] Mahani H, Keya AL, Berg S, Bartels W-BW-B, Nasralla R, Rossen W. Driving mechanism of low salinity flooding in carbonate rocks. Eur 2015 2015:210–36. doi:10.2118/174300-MS.

[31] Yousef AA, Al-Saleh SH, Al-Kaabi A, Al-Jawfi MS. Laboratory investigation of the impact of injection-water salinity and ionic content on oil recovery from carbonate reservoirs. SPE Reserv Eval Eng 2011;14:578–93. doi:10.2118/137634-PA.

[32] Lager A, Webb KJ, Black CJJ, Singleton M, Sorbie KS. Low Salinity Oil Recovery - An Experimental Investigation 2008:0–12.

[33] Zhang Y, Xie X, Morrow NR. Waterflood performance by injection of brine with different salinity for reservoir cores. Proc - SPE Annu Tech Conf Exhib 2007;2:1217–28. doi:10.2523/109849-MS.

[34] Bennion DB, Bennion DW, Thomas FB, Bietz RF. Injection Water Quality-A Key Factor to Successful Waterflooding. J Can Pet Technol 1998;37. doi:10.2118/98-06-06.

[35] Sheng JJ. Formation damage in chemical enhanced oil recovery processes. Asia-Pacific J Chem Eng 2016;11:826–35. doi:10.1002/apj.2035.

[36] Nasralla R a, Nasr-el-din H a. Double-Layer Expansion: Is It A Primary Mechanism of Improved Oil Recovery by Low-Salinity Waterflooding? Eighteenth SPE Improv Oil Recover Symp 2012:1–17. doi:10.2118/154334-MS.

[37] Yu L, Standnes DC, Skjaeveland SM. Wettability Alteration of Chalk by Sulphate Containing Water, Monitored by Contact Angle Measurement. Int Symp Soc Core Anal 2007:1–12.

[38] Ahmadi P, Riazi M, Malayeri MR. Investigation of wettability alteration of carbonate rock in presence of sulfate, calcium 2017:1–9.

[39] Alhammadi M, Mahzari P, Sohrabi M. NEW EXPERIMENTAL EVIDENCE ON THE DOMINANT MECHANISM OF OIL RECOVERY BY LOW SALINITY 2017:1–12.

[40] Hiorth A, Cathles LM, Kolnes J, Vikane O, Lohne A, Korsnes RI, et al. A Chemical Model for the Seawater-CO2 - Carbonate System – Aqueous and Surface Chemistry. Soc Core Anal 2008:1–12.

[41] Gachuz-muro H, Sohrabi M. Prediction , Control and Validation of Rock Dissolution During Smart Water Injection and Its Impact on Waterflood Performance 2017:1–12.

[42] Austad T, Strand S, Puntervold T. Is Wettability Alteration of Carbonates By Seawater Caused By Rock Dissolution ? Changes 2009;3:1–6.

[43] Fathi SJ, Austad T, Strand S. “smart water” as a wettability modifier in chalk: The effect of salinity and ionic composition. Energy and Fuels 2010;24:2514–9. doi:10.1021/ef901304m.

[44] Austad, T., Strand, S., & Puntervold T. Is wettability alteration of carbonates by seawater caused by rock dissolution. . Proc. SCA Int. Symp. Noordwijk, Netherlands, 2009, p. 2009–43.

[45] Zhang P, Tweheyo MT, Austad T. Wettability alteration and improved oil recovery by spontaneous imbibition of seawater into chalk: Impact of the potential determining ions Ca2+, Mg2+, and SO42-. Colloids Surfaces A Physicochem Eng Asp 2007;301:199–208. doi:10.1016/j.colsurfa.2006.12.058.

[46] Computer Modelling Group 2017

[47] Dang, C., et al., Modeling and Optimization of Low Salinity Waterflood. Vol. 1. 2015. 55-73.

[48] Appelo, C.A.J., and D. Postma. 2005. Geochemistry, groundwater and pollution,.2nd ed.

Amsterdam, the Netherlands.

Chapter 4 **Modelling Strategy for Carbonated Water Injection for EOR and Co_2 Sequestration**

ABSTRACT

Carbonated water injection (CWI) has been well investigated to improve oil recovery when compared to other enhanced oil recovery (EOR) techniques both in the secondary and tertiary modes. Extra oil recovery percent and CO_2 sequestration associated with CWI have been studied through several experimental studies. There are not adequate number of modelling studies about the CWI operation in the open sources because of the complex multi-physics involved with the fluid-fluid and fluid-rock interactions during CWI processes. Hence, further experimental and modelling investigations are needed to be conducted on CWI to systematically capture and comprehend the governing physics and complex displacement mechanisms. This research work will focus on the analysis of vital aspects such as oil recovery amount (and mechanisms), fluids distribution, and effects of operational parameters and well placement on the performance of CWI EOR and CWI for CO_2 sequestration. To achieve these objectives, a 3-D heterogenous reservoir is developed using the experimental data reported in the recent literature. A new approach of using the grid local pressure to model CWI is adopted where the moles of CO_2/water are controlled by their injection rates. The dissolution of CO_2 in water is modeled by the Henry's law for each subsequent grid local pressure. In this research, it is found that through CWI, an additional oil recovery can be achieved when compared to plain (conventional) waterflooding (WF) in the secondary recovery mode. A subsequent increase in the injection pressure leads to more dissolution of CO_2 and enhancement of the overall performance of CWI. There is an optimum injector rate, which ensures an effective mass transfer across phases. An optimal well orientation will also give a better recovery performance during CWI. The amount of CO_2 stored is also illustrated in this work as an additional benefit in the CWI processes.

Keywords: Carbonated Water Injection (CWI); Grid Local Pressure; CO_2 Storage; Oil Recovery Factor; Well placement

4.1 **Introduction**

The depletion of reservoirs has motivated researchers to develop new recovery methods that improve oil recovery factor to meet the ever-increasing energy demands. Normally, after primary

oil recovery stage, 75 %, 95 %, and 100 % of the original oil in place (OOIP) remain as the residual fluid in the reservoir for light oil, heavy oil, and tar sands, respectively [1]. Enhanced oil recovery (EOR) methods are usually implemented to considerably reduce the residual oil saturation in the reservoir especially after primary and secondary processes. For EOR processes, the desired oil recovery for light oil, heavy oil, and tar sands is estimated to be 45 %, 90 %, and 100 %, respectively [1]. After conventional water injection (WI) or water flooding (WF), the injection of CO_2 is normally conducted in most reservoirs to reduce the residual oil saturation. Gas injection (GI) has been commonly employed in various fields as a suitable EOR method, though it is associated with some demerits [2]. For example, a poor sweep efficiency attributed to the high mobility of CO_2 gas, has been reported during CO_2 injection. This poor displacement process is due to the large contrast between the fluid densities (oil and gas) and hence high mobility of CO_2 gas, compared to oil [2]. Gravity segregation (override) is another issue where the injected CO_2 migrates to the top of the reservoir leaving behind a large amount of unswept zones because of early gas breakthrough in the production wells. To overcome the problems associated with pure CO_2 injection, alternative EOR methods such as CO_2 foam flooding, water alternating gas (WAG), polymer flooding, and low salinity water injection have been developed at the laboratory, pilot, and field scales. Esene et al. [32] recently performed a modelling investigation on low salinity water injection (LSWI) in sandstone and carbonate reservoirs. In their research, it was reported that oil recovery is improved in the LSWI process when compared to the plain/conventional water flooding. However, there was a high mobility ratio because of the considerable difference between the densities of low saline water and oil, leading to viscous fingering. Gas (e.g., CO_2) injection is still commonly used in the oil industry because of a relatively easy procedure and its availability for implementation [3, 4]. Carbon dioxide is essentially regarded as the gas with the highest potential to cause greenhouse effects, compared to other gases. CO_2 gas accounts for about two third of global warming potential, which gradually increases the earth's temperature [5]. Global warming and climate change associated with the greenhouse effects have been primarily attributed to the increased concentration of CO_2 in the atmosphere [6-8]. However, finding efficient ways to reduce the concentration of CO_2 in the atmosphere is a major concern to researchers, engineers, and environmentalists.

Carbonated water injection (CWI) is a proven EOR method, which can enhance the oil recovery of reservoirs that are in their secondary or tertiary stage of oil production [9, 10]. A secondary

advantage, which is associated with CWI, is the ability to store anthropogenic CO_2 gas in the reservoir pore spaces [11]. Practically, during CWI, CO_2 is dissolved into the water and then injected into the reservoir as a single-phase fluid. Theoretically, after injection, mass transfer occurs between the CW and the oil. When the CO_2 gas moves from CW to the oil phase, it leads to a reduction in the oil viscosity, causes oil swelling, and increases the oil mobility towards the production well. Several researchers have studied and reported their findings about CWI complex processes as a promising EOR technique especially through experimental and simulation approaches [9, 12-25]. CWI has been studied experimentally to better understand the displacement mechanisms [13]. For instance, Miller and Jones [26] concluded based on a laboratory work that oil density is reduced in the presence of CO_2 to a certain degree which is dependent on the oil type, pressure, and temperature conditions. In another experimental investigation, it was shown that the density of pure water is much lower than that of CWI. Thus, CO_2 transition from carbonated water to the oil phase changes the density of both oil and water during a core flooding test [11, 27]. Sohrabi et al. [16, 22] conducted a series of CW flooding experiments at reservoir conditions. It was found that through CWI injection, a higher oil recovery is achieved, compared to the conventional water flooding. A portion of injected CO_2 was also stored in the core. In another sand pack experimental set up of CW flooding for a light oil sample, additional oil recovery and CO_2 storage were also reported when implemented in the secondary mode [15]. A comparative analysis was investigated through a core flooding strategy. It was concluded that more CO_2 is stored in the porous media through a more stable scheme, compared to conventional pure CO_2 injection [19]. Riazi et al.[12, 28] performed a micro-model investigation. Based on their results, a significant oil swelling occurred during CWI process, which contributed to the additional oil recovery during implementation of this EOR strategy. Mahdavi and James[29] performed a series of experiments on CWI in a fractured porous medium. It was reported that there is a stable oil displacement and saturation front even in the presence of fractures. It was reported that fractures aid in draining oil mostly through film flow, since oil is displaced from the matrix to matrix, and matrix to fracture. As fractures are more permeable, they observed an increase in the oil recovery in their laboratory investigation [29].

CWI processes through modelling and simulation approaches have not been comprehensively studied. This is because of the complexities involved in the physical and chemical phenomena attributed to the CWI processes. A three-phase black oil simulator was developed by Ramesh and

Dixon, where CO_2 can be dissolved in both water and oil phases [30]. However, their model did not consider the conventional CWI process either as a black oil or compositional mode. A compositional simulator was developed by Mansoori on the basis of the instantaneous equilibrium assumption [23]. In their model, the solubility of CO_2 in water was determined by the Henry's law. Kechut et al.[17] used ECLIPSE300 (E300) compositional simulator to investigate several laboratory experiments on CWI. In their work, E300 notably over-predicted the oil recovery factor when compared with their tests results. It was hypothesized that the disparity is due to the assumption of instantaneous equilibrium made by E300 as the transfer of CO_2 across the phases (oil and water) during CWI process is time-dependent. Ahmadi et al.[11] investigated CWI in the secondary and tertiary oil recovery modes using E300 for a southern Iranian oil field. According to their investigation, CWI provided a higher extent of oil recovery when compared to conventional water injection. However, it was not reported how the model was developed and/or how they simulated the mass transfer of CO_2 between the phases (water and oil), which is predominantly based on the CO_2 solubility gradient in the two fluids. Nevers [25] developed a mathematical model to forecast the performance of carbonated water injection based on the theory proposed by Buckley–Leveret. Gravity terms as well as capillary forces were not included in their modelling approach. Also, their model assumed that the pressure remains constant in all areas of the reservoir. These assumptions flawed their modelling work, as in the real case scenarios pressure is not always constant in the reservoir. A comprehensive review of carbonated water injection for enhanced oil recovery was conducted by Esene et al.[31]. In their review, the mechanisms of CWI process, fluid-fluid interactions, fluid-rock interactions, phase behaviors of fluids (CO_2, oil, and water), and the challenges (both theoretical and practical) involved with implementing CWI process were reported.

In this paper, an extracted sub model representing a North Sea field is used for modelling of CWI to investigate this efficient secondary EOR process in terms of performance and environmental prospects. The secondary oil recovery from CWI is analyzed for a 3-D anisotropic reservoir. We study various aspects of CWI for secondary EOR such as influences of operational parameters and well orientation on the recovery performance as well as geological sequestration/ storage of CO_2. The fluid model is constructed to ensure that the model is matched with experimental data from the open sources [32]. The resultant matched fluid is coupled into the field model. Water flooding is first simulated in the full field reservoir model and the quality check is performed by history

matching the field rates (liquid, oil and water) to the simulated rates. After the developed field model was history matched, a sub model is extracted to investigate CWI. The injection rate of both fluids (CO_2 and water) is utilized to determine the mole ratios between injected fluids (CO_2 and water). The solubility of CO_2 in the water is governed by the Henry's law for all pressure variations in the grid for the *i-j-k* plane. This approach will improve the past underlying assumption of instantaneous equilibrium made by other researchers. The developed model can be readily used to study two- phase (carbonated water-oil) in porous media.

4.2 **Manuscript Organization**

The organization of this research paper is as follows. The introductory section is followed by a theoretical analysis and description of CWI process in Section 3. The vital aspect / work flow of this research study is shown in Figure 4.1. A fluid model is first constructed with the aid of experimental data from open sources [32]. The matched fluid is then coupled into the field model. Water flooding is first simulated in the full field reservoir model and quality check is carried out by history matching the field rates (liquid, oil and water) to the simulated/model rates. After the developed field model is history matched, a sub model is extracted to investigate CWI.

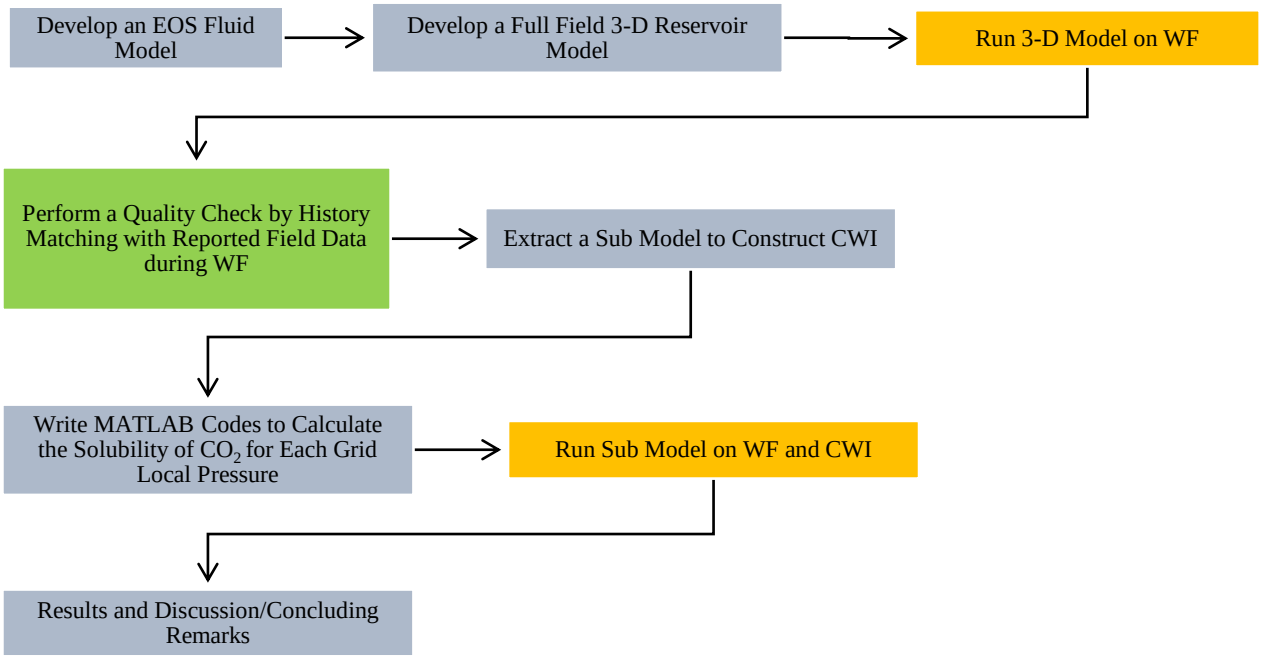

Figure 4.1: Research work flow in the current study

The development of an EOS fluid model and development of a full field 3-D reservoir model used in this study are discussed in the methodology section. Boundary condition, CO_2 solubility modelling, and sub model extraction are also included in the methodology section. The obtained results are discussed in Section 5 and finally, the concluding remarks on modelling investigation of CWI process are listed, based on the research findings.

4.3 **Theoretical Analysis**

In mathematical modelling of carbonated water injection, there are two approaches that can be adopted which are either the black oil model or the compositional model. The black oil model is characterized by a two-phase (carbonated water and oil) system and even when there is a mass transfer from carbonated water into the oil, it is assumed that there is no free CO_2 in the system. The compositional model is characterized by the pressure and dissolution rate such that at a certain pressure drop, CO_2 gas can exsolve from the solution and exhibit itself as a free gas. According to the numerical and experimental studies, both methods have been successful to a fair extent in capturing the complex phenomena of the CWI process, though the compositional model appears to be more efficient (and general). Figure 4.2 depicts a schematic representation of CWI process, which shows a stable front at the phase interface during the displacement process. This is because of a very low interfacial tension between carbonated water and oil due to having almost the same fluid density [15].

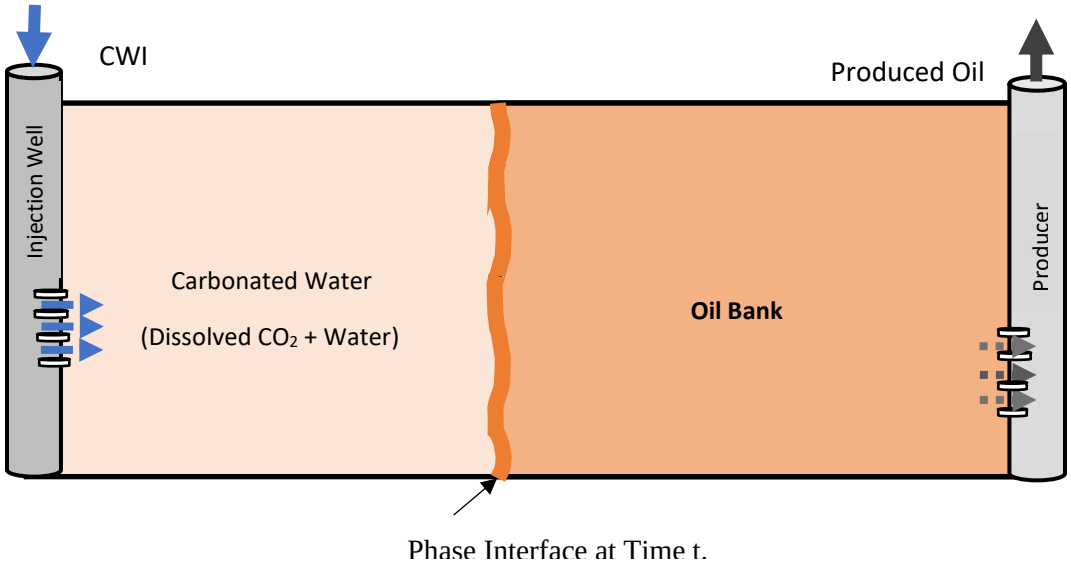

Figure 4.2: Schematic 2-D representation of CWI process.

When the injected carbonated water (CW) reaches the fluid interface, mass transfer due to CO_2 dissolution occurs because of the concentration gradient between the two fluids (CW and oil). This phenomenon causes oil swelling, oil viscosity reduction, and oil density reduction that consequently improves oil mobility towards the production well. Figure 4.3 illustrates a three-dimensional flow in x, y, and z directions to describe the material balance of 2-phase (CW and oil) containing 3-component (CO_2, water, and oil) system.

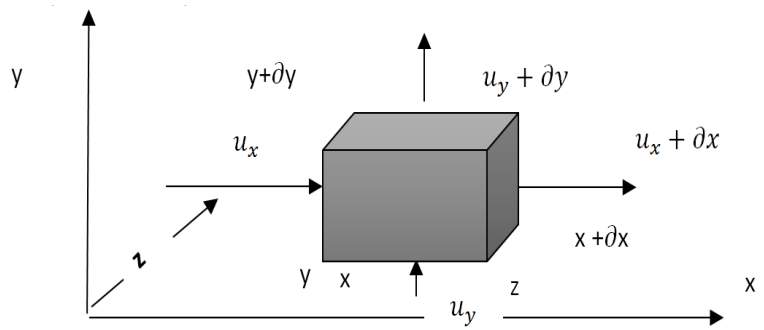

Figure 4.3: A schematic representation of an x, y and z directional flow for a control volume/element [32].

According to the control volume shown in Figure 4.3, the material balance equations for water, CO_2, and oil that captures the CWI process are a set of coupled partial non-linear differential equations, as expressed below by Equation (4.1) in x-direction.

The mass balance for a component I in phase α, which is displaced through a porous medium in x direction by the convection and diffusion mechanisms [13, 33], is written as follows:

$$\frac{\phi\,\partial(\rho_\alpha s_\alpha \omega_\alpha^{I})}{\partial t} = -\frac{\partial(\rho_\alpha u_\alpha \omega_\alpha^{I})}{\partial x} + \frac{\partial}{\partial x}\left(\phi s_\alpha D_{(I-\alpha)} \quad \frac{\partial}{\partial x}(\rho_\alpha \omega_\alpha^{I})\right) + U \tag{4.1}$$

where ω_α^I represents the mass fraction of the component I in the phase α. s_α and ρ_α denote the saturation and density of phase α, respectively. u_α , D, U, and ϕ stand for the Darcy velocity of phase α, diffusion coefficient, mass transfer term, and the porosity of the porous system, respectively. Making some reasonable assumptions (such as neglecting dispersion since CO_2 gas

continually remains dissolved in water), the following mass balance equations can be given for oil, water, and CO_2 as the existing components:

$$\frac{\phi\,\partial(\rho_o s_o \omega_o^o)}{\partial t} = -\frac{\partial(\rho_o u_o \omega_o^o)}{\partial x} \tag{4.2}$$

$$\frac{\phi\,\partial\left(\rho_o s_o \omega_o^{CO_2}\right)}{\partial t} = -\frac{\partial\left(\rho_o u_o \omega_o^{CO_2}\right)}{\partial x} + U \tag{4.3}$$

$$\frac{\phi\,\partial(\rho_w s_w \omega_w^w)}{\partial t} = -\frac{\partial(\rho_w u_w \omega_w^w)}{\partial x} \tag{4.4}$$

$$\frac{\phi\,\partial\left(\rho_w s_w \omega_w^{CO_2}\right)}{\partial t} = -\frac{\partial\left(\rho_w u_w \omega_w^{CO_2}\right)}{\partial x} - U \tag{4.5}$$

Equation (4.2) represents the mass balance of the oil phase in the finite form, Equation (4.3) introduces the mass balance of the oil phase where CO_2 transfer into the oil is modelled as a "source", which is characterized by the addition of the mass transfer term U. Equation (4.4) refers to the mass balance of the water component and Equation (4.5) describes the mass balance of the water phase, where CO_2 transfer from the water is modelled as a "sink" term. Other constitutive equations needed to simplify and to solve for pressure and saturation profiles of each phase in Equations (4.1) to (4.5) are listed below in Equations (4.6) to (4.10). Equation (4.6) states that the total saturation of fluids in the model is unity, which is necessary to solve the equations and avoid numerical errors. Equation (4.7) represents the Darcy velocity as a function of the fluid mobility and pressure drop. Equation (4.8) is the fluid mobility of each phase, which is strongly dependent on the relative permeability of each phase and the flux of each phase. Equation (4.9) relates the pressure difference between the wetting and non-wetting phases. This is a driving force for the

fluid flow, which is known as the capillary pressure. Capillary pressure is a strong function of the fluid saturation.

$$S_o + S_{cw} = 1 \tag{4.6}$$

$$u_\alpha = -\frac{\lambda_\alpha \partial p_\alpha}{\partial_x} \tag{4.7}$$

$$\lambda_\alpha = \frac{K k_{r_\alpha}}{u_\alpha} \tag{4.8}$$

$$P_c = P_o - P_{cw} = \int (S_w) \tag{4.9}$$

The mass transfer term as shown in Equation (4.10) governs the CO_2 distribution between the oil and water phases, which is defined as follows [13, 34]:

$$U = M_{TC} \times (C_{cw}^{CO_2} - k_{eq} C_o^{CO_2}) \tag{4.10}$$

where S_o, S_w, λ, P_o, P_{cw}, P_c, k_{r_α}, K, M_{TC}, $C_{cw}^{CO_2}$, $C_o^{CO_2}$, and k_{eq} stand for the oil saturation, water saturation, mobility, oil pressure, water pressure, capillary pressure, relative permeability of phase α, absolute permeability, mass transfer coefficient, CO_2 concentration in the water phase, CO_2 concentration in the oil phase, and CO_2 partition coefficient, respectively. The mass transfer coefficient is obtained through core flooding experiments or through history matching [18, 33].

The above relationships (Equations (1) to (10)) typically describe the overall physics that governs CWI in a porous medium. The equations are further discretized by finite differencing (central) for

linearization and then solved with the iterative Newton's method to obtain stable solutions for pressure and saturations for each phase.

4.4 **Modeling Methodology/Stages**

Developing an EOS Fluid Model.

Laboratory data from constant composition expansion (CCE), constant volume depletion (CVD), and differential liberation (DL) experiments are available for a North Sea fluid, as shown in Table 4.1. Experimental and theoretical values of fluid properties/parameters such as saturation pressure (P^s), formation volume factor (FVF), gas oil ratio (GOR), and API are reported in Table 4.2 [32]. These fluid properties are tuned to develop an EOS fluid model to be used in this study.

Table 4.1: North Sea fluid compositional analysis [32]

Pure	Mole %
CO_2	11.83
N_2	0.16
C_1	11.54
C_2	6.00
C_3	6.48
i-C_4	2.22
n-C_4	4.76
i-C_5	3.28
n-C_5	3.70
C_6	6.51
C_7+	43.52

Table 4.2: Measured and modelled properties of oil [32]

Parameter	Measured	Before Regression	After Regression	Percentage Error
P^s, (psi)	740	740.04	736.70	0.40 %
FVF, (bbl/stb)	1.18	1.14	1.16	1.70 %
GOR, (scf/stb)	247	240.00	248.88	0.40%
API (-)	40.00	41.00	40.00	0.00%

Developing a 3-D Black Oil Reservoir Model. An anisotropic model representing a North Sea field is developed with the help of CMG package using a corner point grid system. 26, 26, and 9 grids used in the *i*, *j*, and *k* directions respectively are shown in Figure 4.4. The average grid thickness for the 1st to the 8th layer ranges from 8 ft -15 ft and the 9th layer has a grid thickness of 100 ft. The Porosity of the reservoir ranges from 0.19 to 0.229, the permeability varies from 230 mD to 2298 mD and the oil has a viscosity of 0.77 cp. The 3-D model is assumed to have 320 million barrels of oil original in place, a total of 6084 grid blocks, 2052 view blocks, and 2288 exterior faces where the simulation run time is 9 hrs when fully loaded on 4 processors.

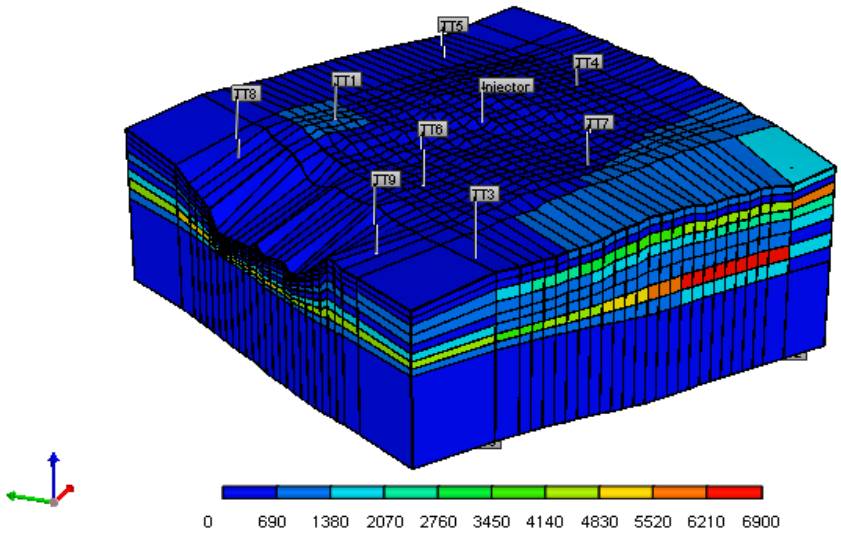

Figure 4.4: A 3-D anisotropic reservoir model.

The depth of the reservoir, water oil contact, reservoir pressure, and rock compressibility are 6000ft, 5990 ft, 3500 psi, and 4 $\times 10^{-6}$ psi^{-1}, respectively. The aquifer is at the bottom of the reservoir and it is modeled using the fetkovitch method. The field currently has 7 producer wells with an average rate of 1500 bbl/day and one injector well which is responsible for water flooding. The rock-fluid properties for water-oil and gas -oil relative permeability curves used for this study are based on experimental data from literature [35] and are shown in Figure 4.5 and Figure 4.6, respectively.

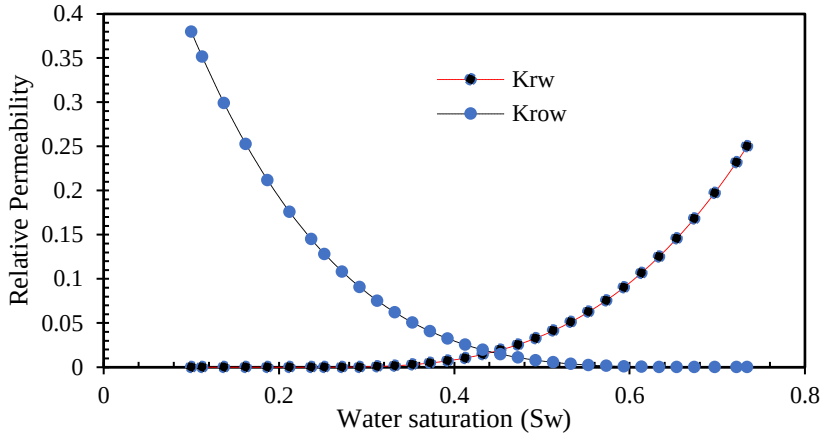

Figure 4.5: Water-Oil relative permeability [35]

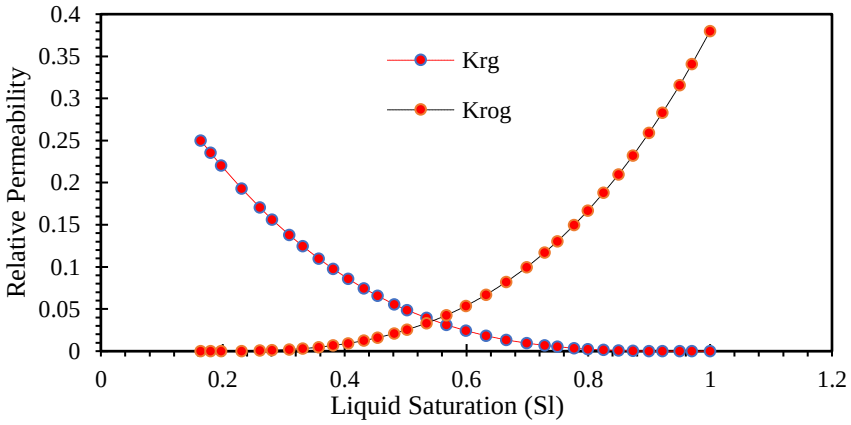

Figure 4.6: Gas-Oil relative permeability [35]

The developed EOS fluid model and 3-D reservoir model are coupled to simulate the water flooding process, which is validated with the reported North Sea field data.

Boundary Conditions and Well Models. To solve the coupled partial differential equations involved in the fluid flow in porous media, initial and boundary conditions are required [32]. In this research, we adopt the Dirchelet and Neuman boundary conditions, which are also called no flow and constant pressure boundary conditions. In this modelling investigation, two types of constraints, which serve as a part of the constitutive equations needed to solve the overall mass/ momentum conservation equations, are the rate constraints and pressure constraints. For the injector well, a primary rate constraint is used to determine the time dependent solutions for the

injector pressure profile. For the producer well, a pressure dependent constraint is set to calculate the time dependent surface oil flow rate through employing Equations (4.11) to (4.14). These equations are corrected by Peaceman [39] whose theorem demonstrates that the pressure in the grid/node containing the well can be approximated as the actual flowing pressure at a radial distance of approximately 0.2078Δx from the well, as given below:

$$P_{wf} = P_i + \left(\frac{q_{cwi}\mu B_w}{2\pi Kh}\right) ln(\frac{0.2078\Delta x}{r_w}\ ) \tag{4.11}$$

Equation (11) is simplified to the following expression:

$$P_{wf} = P_i + \frac{q_{cwi}}{J_i} \tag{4.12}$$

where

$$q_{cwi} = \ -\frac{2\pi kh}{\mu B_w\ ln\left(\frac{0.20708\Delta x}{r_w}\right)}\ (P_i - P_{wf}) \tag{4.13}$$

Equation (13) turns to:

$$q_{cwi} = \ -J_i(P_i - P_{wf}) \tag{4.14}$$

.

where P_{wf}, P_i, q_{cwi}, μ, B_w, Δx, K, h, and J_i represent the bottom hole pressure, initial reservoir pressure, viscosity, formation volume factor, grid size, absolute permeability, reservoir thickness, and initial productivity index, respectively. These relationships satisfy the total transmissibility equations to describe the flow in the porous media involving CO_2, water, and oil which are solved by CMG with the Newton iterative method. The initial pressure for this reservoir is 3500 psi, which is bounded (no flux) around all sides.

CO_2 Solubility Modelling. To maintain a thermodynamic equilibrium, the chemical potential of a component in all involved phases should be the same. In other words, the equation for the phase

equilibrium is the equality of the fugacity of each component in the gas mixture and aqueous solution as follows:

$$f_{ig} = f_{iw} \tag{4.15}$$

where f_{ig} and f_{iw} represent the fugacity of component i in the gaseous and aqueous system, respectively. The fugacity of the gaseous components is determined from an equation of state [36, 37]. The fugacity of a component in the aqueous phase is calculated using the Henry's law in this study [38]. The latter is only applicable in this research work due to low solubility of gas components (e.g., CO_2), as given below:

$$f_{co_2,w} = y_{co_2,w} \times H_{CO_2} \tag{4.16}$$

in which, $y_{co_2,w}$ and H_{CO_2} denote the mole fraction of CO_2 in the aqueous phase and Henry's constant of CO_2, respectively. The Henry's constant [38] at any pressure is determined by the following equation to obtain CO_2 solubility in this modelling study.

$$ln\, H_{co_2} = lnH^* + \frac{v_{co_2}(P - P^*)}{RT} \tag{4.17}$$

where v_{co_2} stands for the molar volume of CO_2 in the aqueous component, which is determined at a given temperature by the Winprop module. H^*, $R, T,$ and P are the Henry's constant at the reference pressure, universal gas constant, temperature, and pressure, respectively. The above approach assumes that the salinity and temperature remain constant in the reservoir. Hence, each Henry's constant is evaluated at a defined reservoir temperature but a variable pressure. This strategy is only suitable for thin reservoirs, where the temperature variation is insignificant from the top to the bottom of the reservoir. In this work, a more general equation is implemented, which considers that the temperature change for a thick aquifer is substantial and the salinity of the aquifer may change due to CWI. Therefore, equations based on Henry's law [38] as shown in equation (4.18), (4.19), and (4.20) which are more suitable, are employed to calculate the Henry's constant as a function of temperature, salinity, and pressure, as given below:

$$\begin{aligned} ln\, H^s_{co_2} = ln\, p^s_{H_20} + A\left(T_{(r,H20)}\right)^{-1} + B\left(1 - T_{(r,H_2O)}\right)^{0.335}\left(T_{(r,H_20)}\right)^{-1} \\ + C\left[exp\left(1 - T_{r,H_2O}\right)\right]\left(T_{r,H_20}\right)^{-0.41} \end{aligned} \tag{4.18}$$

$$ln\, H_{co_2} = ln\, H^{s}_{co_2} + ln\frac{1}{RT}\int_{p_{H_2O}}^{p} v_{co_2} dP \tag{4.19}$$

where H_i^s, $T_{(r,H20)}$, and $p^s_{H_20}$ are the Henry's constant of CO_2 at the saturation pressure of H_2O, reduced temperature of H_2O, and saturation pressure of H_2O at a temperature, T(K). A, B, and C are the constants for the Henry's correlation for the CO_2 solute.

To model the effect of salinity on the solubility of CO_2, the following correlation is utilized:

$$ln\,(\frac{H_{salt,CO_2}}{H_{CO_2}}) = K_{salt,co_2}\, M_{salt} \tag{4.20}$$

In Equation (20), $H_{salt,}$ H_{CO_2},K_{salt}, and M_{salt} stand for the Henry's constant of CO_2 in brine, Henry's constant of CO_2 with zero salinity, salting out coefficient of CO_2, and molality of dissolved salt, respectively. It should be noted that Equations (18) to (20) are used in this modelling work to determine the solubility of CO_2 in the aqueous, which is dependent on temperature, pressure, and salinity. The modelling of CWI is performed using the CMG compositional simulator, which takes input from a MALTAB script designed to calculate the solubilities of CO_2 for every grid, pressure, and timestep.

Sub Model Extraction for CWI Investigation. To construct a model for studying CWI process, a sub model is extracted from the parent reservoir to reduce run time/computational costs. The sub model retains the reservoir properties, rock-fluid characteristics, and well configuration of the parent model with 15, 12, and 9 grids in the *i*, *j*, and *k* directions, respectively. As seen in Figure 4.7, the extracted model closely mimics a 5 spot well patterns of 4 producer and 1 injector having a simulation run time of 1.5 hrs.

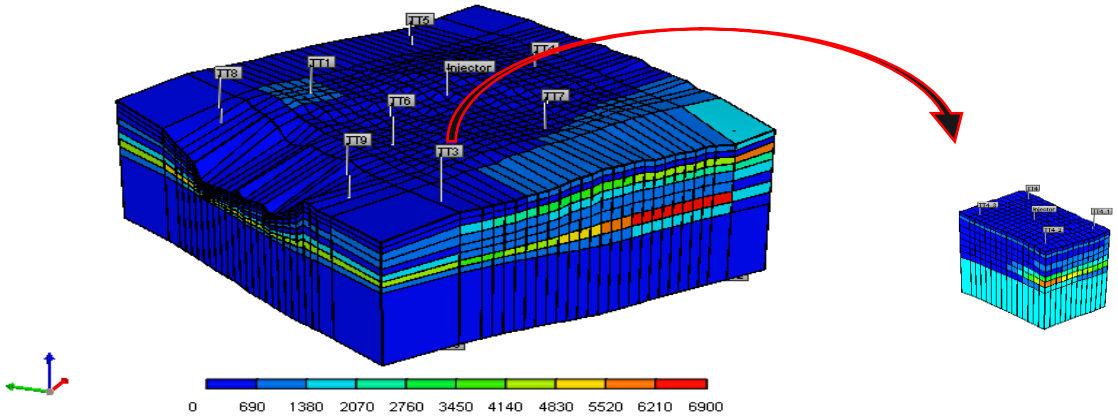

Figure 4.7: Extracted sub model with 15,12, and 9 grids in i, j, and k directions respectively.

4.5 **Results and Discussion**

In this section, the validation stage and the results of CWI to investigate various aspects such secondary EOR, effect of injection rates, effect of injection pressure, well orientation, and CO_2 storage will be discussed.

Quality Check/Validation of 3-D Model by History Matching. The developed model is validated with the measured field data for two producer wells namely TT4 and TT6, which were reported during water flooding. The relative permeability curves and the capillary pressure of the developed model are tuned to match the liquid rates, oil rates, and water cut with the real data. The validation phase and quality check of the developed model are demonstrated in Figure 4.8 and

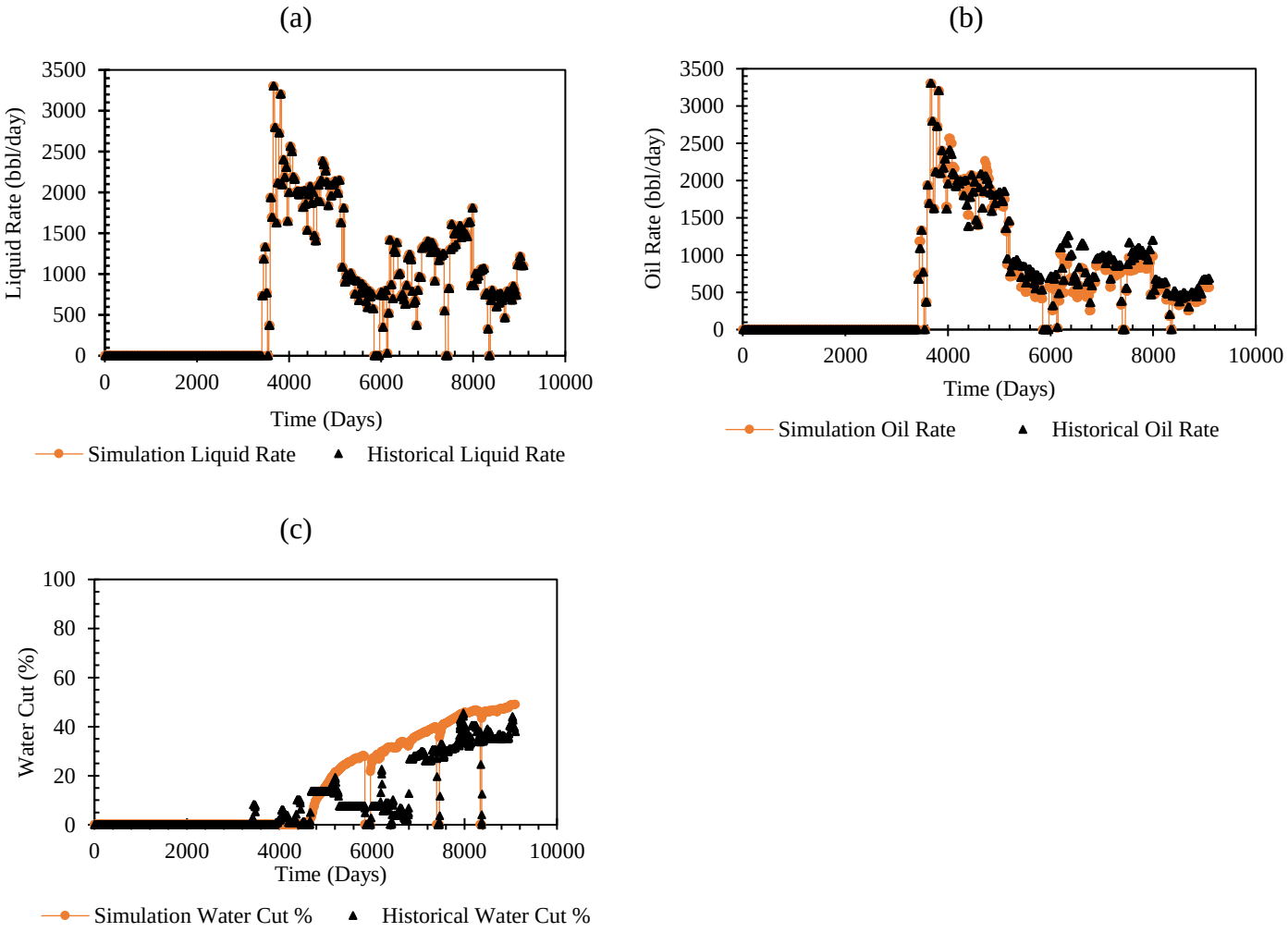

Figure 4.8: Comparing simulation and historical results at well TT4: (a) Liquid rates, (b) Oil rates, and (c) Water cut % versus time

Figure 4.9, which compare the simulation results to historical field results for the water flooding operation.

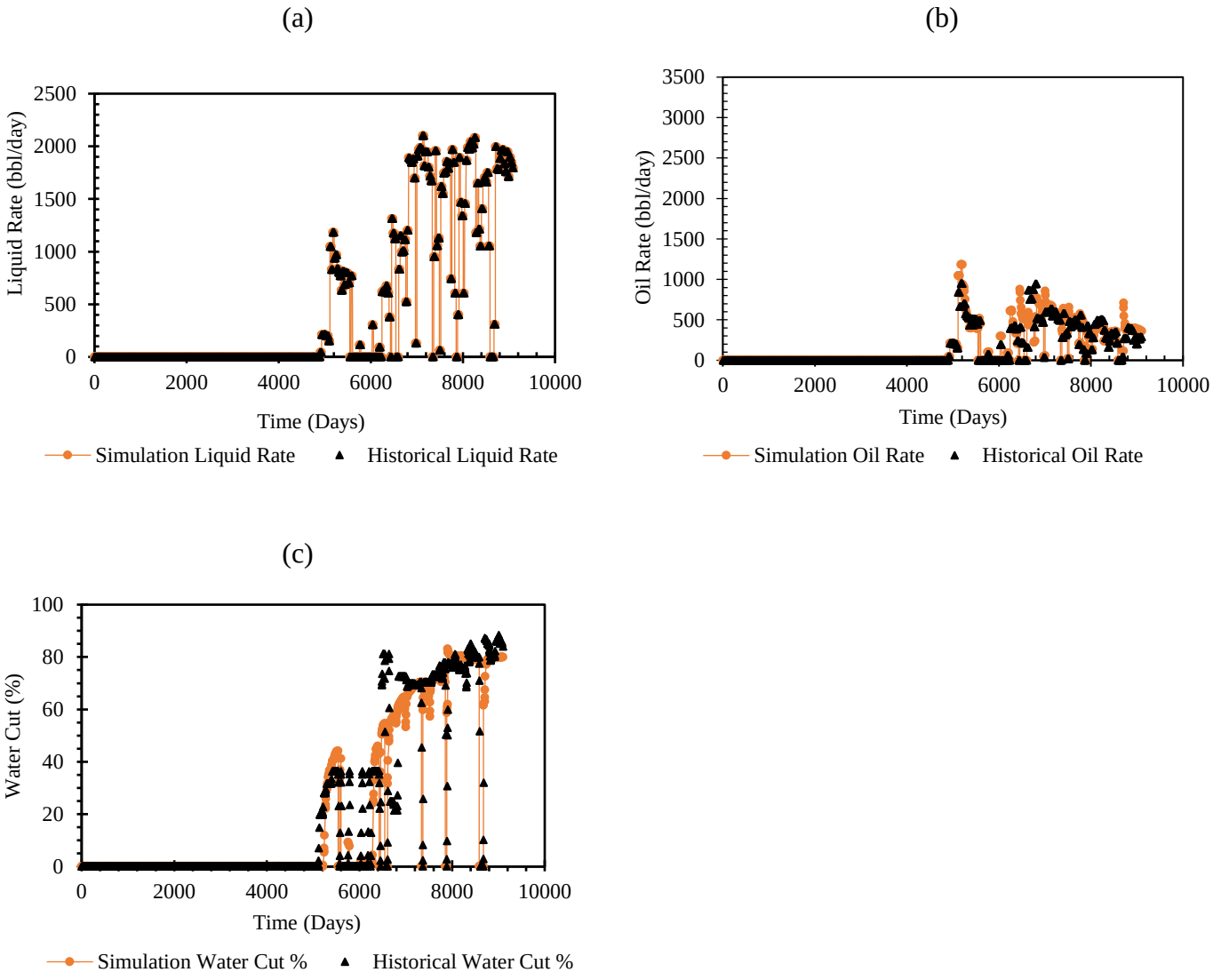

Figure 4.9: Comparing simulation and historical results at well TT6: (a) Liquid rates, (b) Oil rates, and (c) Water cut % versus time

According to Figures 4.8 and 4.9, there is a satisfactory agreement between the modeling results and field data. The little variations/mismatch in the water cut % prediction can be improved by using a local grid refinement around the producer wells or using an end mobility injection strategy. However, this model can be further analyzed to conduct a parametric sensitivity analysis to attain the research objectives with focus on CWI.

Oil Recovery. When compared to plain water flooding as shown in Figure 4.10, CWI gives a higher recovery factor by injecting at 3500 bbl/day. Unlike plain water flooding, the mass transfer of CO_2 associated with CWI changes the oil viscosity, causes oil swelling, and improves the mobility ratio and sweep efficiency.

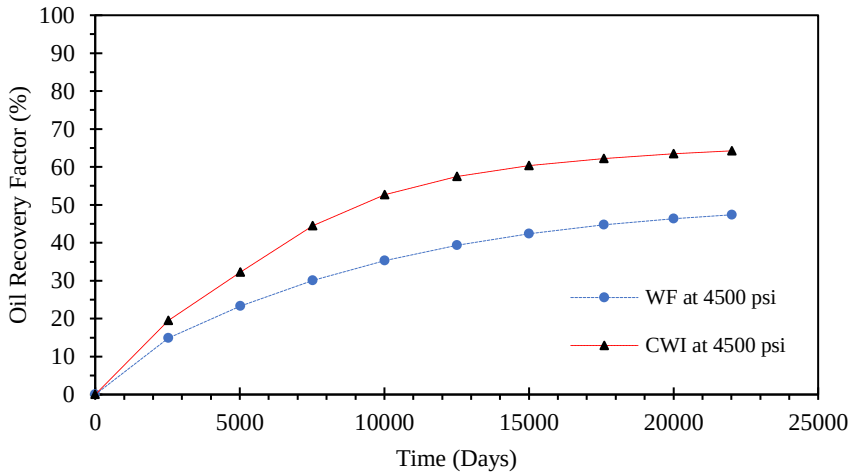

Figure 4.10: Oil recovery comparison for WF and CWI at 4500 psi

These alterations of oil properties during CWI invariably improves the recovery factor. In Figure 4.10, breakthrough of plain water flooding occurs at 7520 days with a recovery factor of 30.06 % due to high mobility between the plain water and oil. High mobility ratio is caused by the contrasting differences in fluid densities between oil and plain water. However, during displacement process it causes viscous fingering, which leads to several zones in the reservoir to be unswept during plain water flooding.

Also, in Figure 4.10, the breakthrough of CWI is delayed because of the very low mobility ratio between CW and oil. The breakthrough of CWI occurs at 10000 days with a recovery factor of 52.60 % , which is attributed to the stable displacement achieved during CWI. At the end of the simulation period, the ultimate recovery factor for both plain WF and CWI is 47.3 % and 67.20 % respectively.

Effect of Injection Rate. Sensitivity analysis is performed to investigate the effect of injection rate at 5500 psi on the oil recovery factor during carbonated water injection. Figure 4.11 and Table

4.3 show the oil recovery profiles at injection rates of 500, 1000,2500, and 3500 bbl/day with their corresponding days.

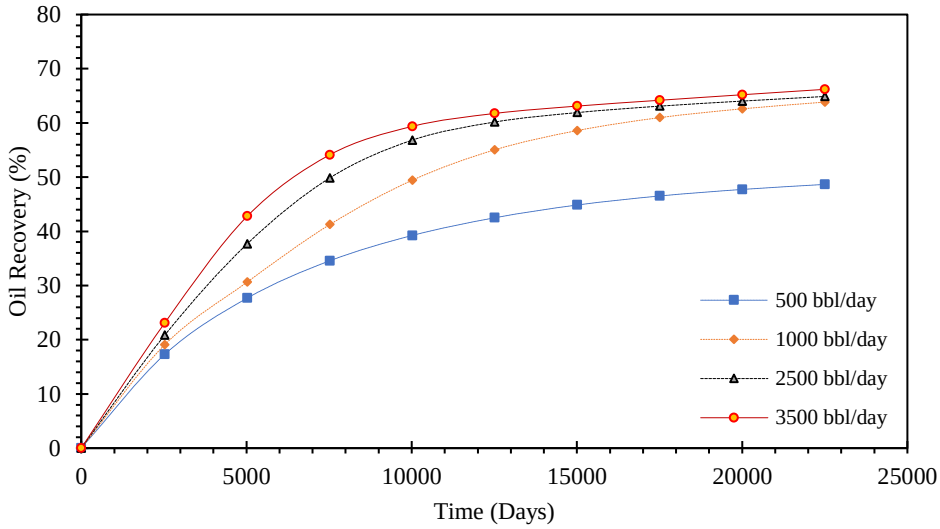

Figure 4.11: Effect of injection rates on CWI performance

Table 4.3: Recovery for different injection rates during CWI

Rate (bbl/day)	B.T *Recovery (%)	Days	U.T *Recovery (%)	Days
500	27.68	5022	48.65	
1000	49.24	10015	63.83	22502
2500	49.84	7520	64.88	
3500	54.51	7520	66.19	

*B.T stands for the breakthrough time and U.T represents the ultimate time.

As can be seen in Table 4.3, at 1000 bbl/day, there is a sustained period of constant oil production with 49.24 % recovery until 10015 days when compared to 2500 bbl/day injection with a breakthrough of 49.84 % recovery at 7250 days. This is attributed to the fact that during CWI, there is a critical injection rate that ensures the maximum contact time between CW and oil, leading to a proper mass transfer across the fluid phases. However before selecting an injection rate, a detailed sensitivity analysis should be carried out based on economic aspects that include the maximum allowable water cut and cost of separation facilities.

Effect of Injection Pressure. Based on Henry's law, the mole fraction of gas soluble in the water is directly proportional to the pressure applied on the solution as given below:

$$x = P \times K_c \tag{4.21}$$

where,

$$\frac{1}{K_c} = H \tag{4.22}$$

$$x = \frac{P}{H} \tag{4.23}$$

in which, x, P, K_c, and H denote the mole fraction of CO_2 in the water, pressure, proportionality constant, and Henry's constant, respectively.

Therefore, large injection pressure values result in lower values for the Henry's constant (see Equations (21)-(23)) and high extent for the mole fraction of gas soluble in water. It can be seen from Figure 4.12 that the recovery factor after 10000 days for 3500 psi, 4000 psi, 4500 psi and 5000 psi are 28 %, 31% ,35 %, and 39 %, respectively. A high solubility of CO_2 is achieved at 4500 and 5000 psi. According to Figure 4.12, the CWI at those pressure results in a high ultimate oil recovery of 48 %.

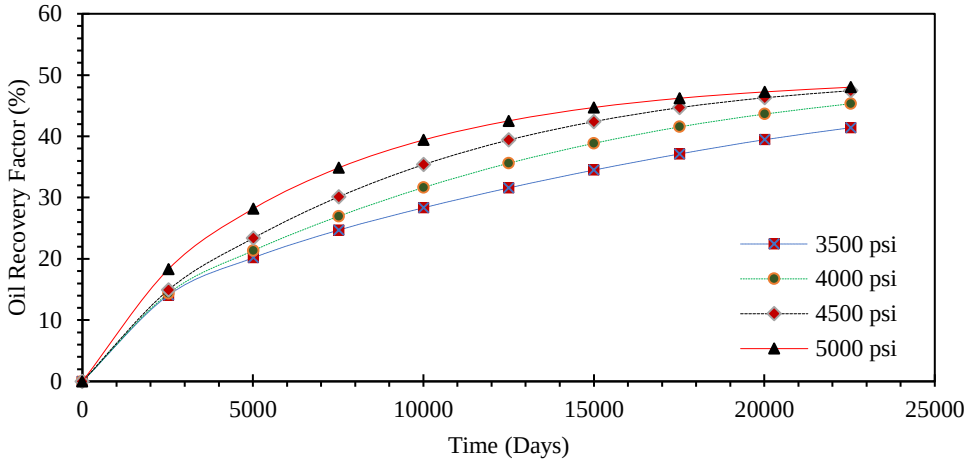

Figure 4.12: Effect of injection pressure on CWI performance at 500 bbl/day

Effect of Well Orientation. The type of well orientation used during an EOR process is dependent on a variety of reservoir properties such as horizontal permeability (K_H), vertical permeability (K_V), and pay zone thickness. In this research, different scenarios of well orientation are investigated as shown in Figure 4.13 through Figure 4.16 and their performances in terms of oil recovery factor are compared.

Figure 13 (a) illustrates the use of vertical injector well and vertical producer well perforated in layers 3, 4, and 5 in the k- direction. Also, Figure 13 (b) shows the horizontal injection well perforated in the layer 4 in k -direction that is simulated through 2,3 4, and 5 grids in the *i*-direction.

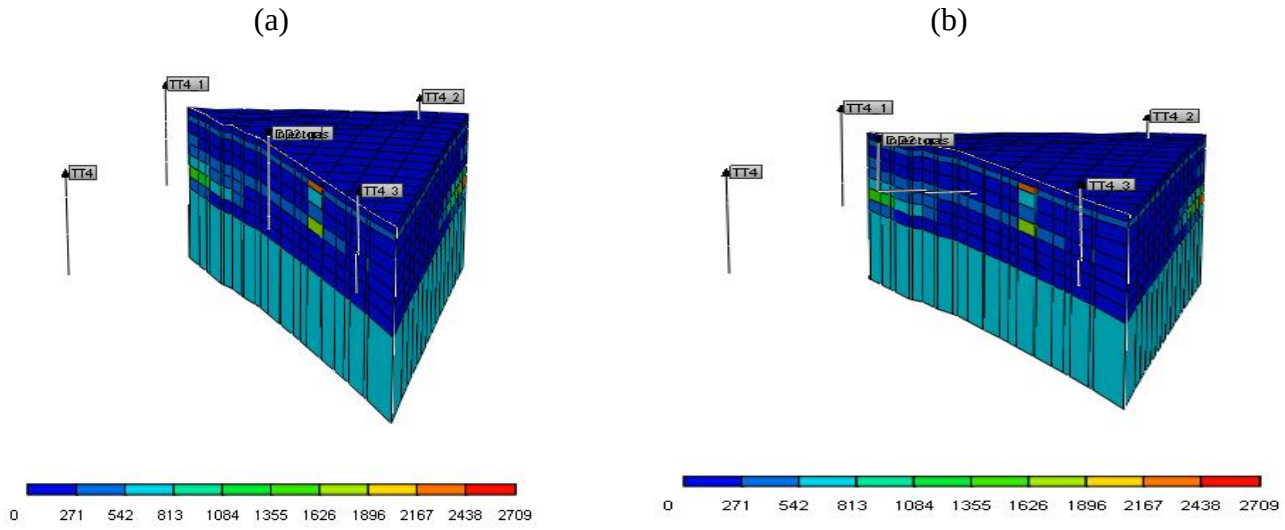

Figure 4.13: Schematic of well orientation for (a) the case of vertical injectors-vertical producer wells and (b) the case of horizontal injector-vertical producer wells

The production history results of the cases (shown in Figure 4.13) with various well orientations are shown in Figure 4.14.

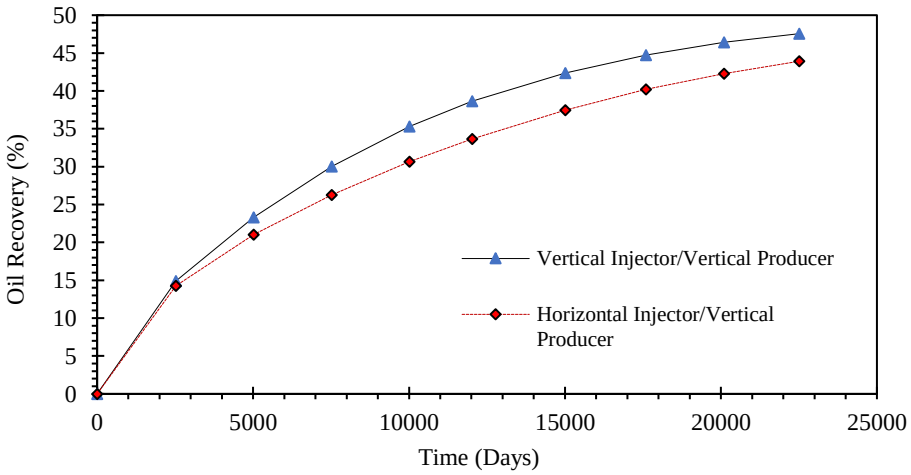

Figure 4.14: Effect of injector well orientation on CWI

The ultimate oil recovery factors achievable in these two well orientations are 47.6 and 43.9 % for the vertical injector -vertical producers case and the horizontal injectors- vertical producers case,

respectively. The difference in the oil recovery is attributed to the fact that a better sweep is achieved by the vertical injection due to the maximum well contact area in all the layers as well as favourable horizontal permeability (K_H) in layers 3, 4, and 5. In contrary, for the horizontal injector well, there is only one contact layer (layer 4) with the reservoir. Therefore, the performance of the horizontal injection well in terms of sweep efficiency is lower than that of vertical injection for this reservoir. Figure 4.15 (Panels a and b) illustrate the use of the vertical injector well and horizontal producer well as well as horizontal injector and horizontal producer, respectively.

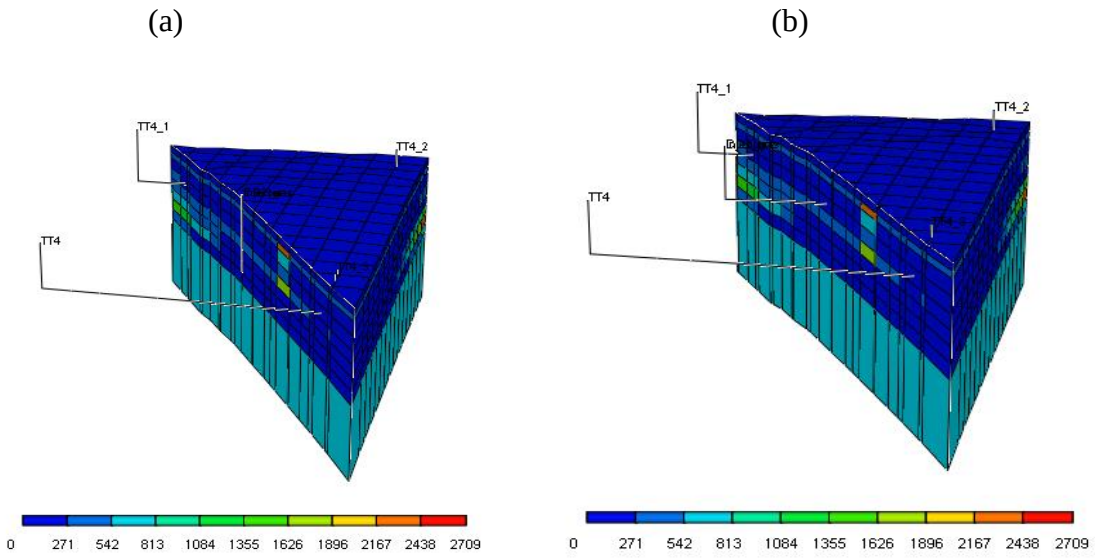

Figure 4.15: Schematic of well orientation for (a) vertical injectors-horizontal producer wells and (b) horizontal injector-horizontal producer wells cases

The performance of the vertical injector-horizontal producer case and the horizontal injector-horizontal producer case is reported in Figure 4.16. It is found that there is no considerable difference between these different well placements because the horizontal well can only producer from one layer and the contribution of the vertical permeability for the horizontal producer well remains unchanged, regardless of the orientation of the injector wells.

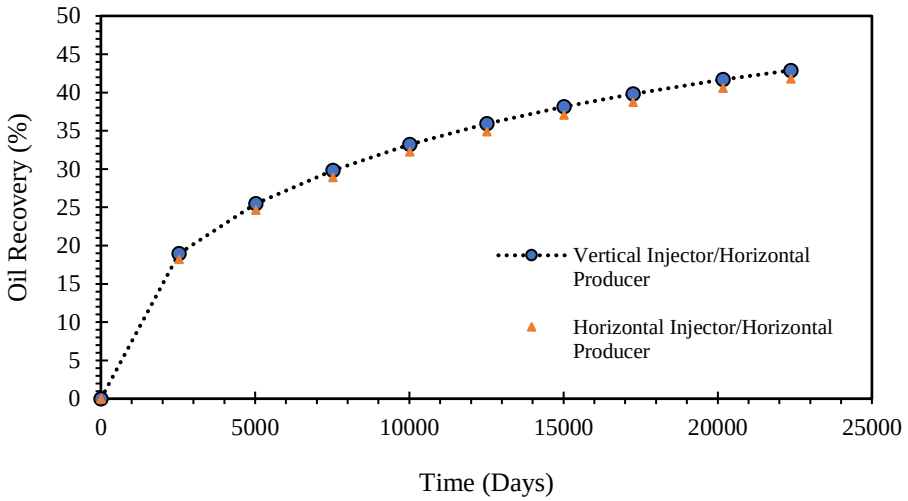

Figure 4.16: Effect of well orientation on CWI oil recovery

CO_2 Storage during CWI. CO_2 storage potential is a secondary benefit associated with CWI. The amount of stored CO_2 varies with the injection pressure as clearly described in Table 4.4 at a temperature of 189 ^oF. Table 4.4 lists the amount of injected CO_2 and the amount of stored CO_2 at 189 ^oF, but different pressures; including 3000 psi, 4000 psi, and 4500 psi.

The amount of stored CO_2 varies with increasing solubility of CO_2 in aqueous phase and pressure (see Equations (21), (22), and (23)).

Table 4.4: Number of moles of CO_2 stored after 22509 days for different pressures at 189 ^{o} F.

Pressure (psia)	CO_2 Injected (moles)	CO_2 Stored (moles)	Moles % of CO_2 Stored
3000	8500	3626.95	42.67
4000		5308.25	62.45
5500		7017.60	82.56

For CO_2 gas to be continually stored in the reservoir pore spaces, it must be ensured that the injection pressure is operated below the limit of reservoir fracture pressure (5700 psi) to minimize the risk of gas leak to the surface. Based on the results related to CO_2 storage pattern during CWI, it is found that there is a positive step towards minimizing the quantity of anthropogenic CO_2 gas in the atmosphere to maintain a green and sustainable environment through implementation of CWI.

4.6 Conclusions

CWI is an improved EOR method when compared to conventional CO_2 injection, water flooding, and water alternating gas (WAG) in terms of sweep efficiency and total recovery. Moreover, it exhibits an additional benefit of CO_2 storage/sequestration in the reservoirs when implemented. This research work presents modeling/simulation of CWI to investigate fluid distribution during CWI, CO_2 storage aspect, the effects of operational parameters and well orientation. Based on the results from this research, the following conclusions are made:

- There is a stable and piston-like displacement of oil by CWI because of similarities of fluid densities and low mobility ratio. Therefore, there are no problems such as gravity override and viscous fingering with CWI, which are associated with pure gas injection and conventional water flooding.
- A higher recovery factor is achieved with CWI when compared to WF because of the changes in the oil properties associated with the mass transfer of CO_2 into oil.
- More CO_2 is dissolved in water during high injection pressure according to the Henry's law, which improves the overall performance of CWI.
- There is a critical injection rate to ensure a maximum contact time between the fluids (CW and oil) for effective mass transfer across phases.
- A secondary benefit associated with implementing CWI is its high potential for anthropogenic carbon dioxide storage. The amount of CO_2 stored is strongly dependent on the operational injection pressure.
- The choice of well placement is strongly dependent on the vertical and horizontal permeabilities in the reservoir.
- Further modelling and laboratory studies are recommended to investigate the rate of reaction of carboxylic acid ($HC0_3^{2-}$) as the influence of CW on the extent of permeability and porosity will be of great interest.
- Advanced laboratory experiments are recommended to generate the relative permeability of oil as function of carbonated water will help to improve the understanding of phase movement (CW and oil) during the displacement process and improve other modelling works.

- This modelling work was able to simulate CWI in the black oil mode. In cases where random compositional variations exist, the model may not be able to accurately predict recovery factors and other displacement mechanisms.

Acknowledgements

The financial assistance offered by Memorial University (NL, Canada), Natural Sciences and Engineering Research Council of Canada (NSERC), InnovateNL (formerly RDC), and Statoil Canada is greatly acknowledged.

Nomenclatures

Acronyms

API	American Petroleum Institute
BHP	Bottom Hole Pressure
CMG	Computer Modelling Group
CO_2	Carbon Dioxide
CCE	Constant Composition Expansion
CVD	Constant Volume Depletion
CWI	Carbonated Water Injection
CW	Carbonated Water
DL	Differential Liberation
EOR	Enhanced Oil Recovery
EOS	Equation of State
E300	Eclipse 300
FVF	Formation Volume Factor
GOR	Gas Oil Ratio
GI	Gas Injection
kppm	kilo parts per million
LSWI	Low Salinity Water Injection
mD	milli Darcy
OOIP	Original Oil in Place
P^s	Saturation Pressure
RF	Recovery Factor
SWAG	Simultaneous Water Alternating Gas
UT	Ultimate
WAG	Water Alternating Gas
WF	Water Flooding
WI	Water Injection

Variables and Parameters

B	Formation volume factor
D	Diffusion coefficient
f	Fugacity (-)
g	Acceleration due to gravity
h	Thickness
H	Henry's constant
H^*	Reference Henry's constant
J	Productivity index
k_{rog}	Oil gas relative permeability
k_{row}	Oil water relative permeability
k_{rg}	Gas relative permeability
k_{rw}	Water relative permeability
K_c	Proportionality constant
M	Molality
M_{TC}	Mass transfer coefficient
P	Pressure
P^*	Reference pressure
P^s	Saturation pressure
q	Injection and production rate
R	Universal gas constant
s	Saturation
r_w	Wellbore radius
T	Temperature
U	Mass transfer term
u	Darcy velocity
v	Molar volume
Δx	Grid size
y	Mole fraction

Greek Letters

ρ	Density ($\frac{Kg}{m^3}$)
μ	Viscosity (cP)
ϕ	Porosity (-)
Δ	Difference operator
ω	Mass fraction
α	Phase α
λ	Mobility

Subscripts

CO_2	Carbon dioxide
cwi	Carbonated water injection
g	Gas
i	Initial
r	Reduced
c	capillary
w	Water
o	Oil

Superscripts

o	Oil
s	Saturation
w	Water

References

1. S. Thomas, Enhanced Oil Recovery - An Overview. Oil & Gas Science And Technology 2007.
2. S.G. Ghedan, Global Laboratory Experience Of Co2-Eor Flooding. Society Of Petroleum Engineers, 2009.
3. M.M. Kulkarni,D.N. Rao, Experimental Investigation Of Miscible And Immiscible Water-Alternating-Gas (Wag) Process Performance. Journal Of Petroleum Science And Engineering, 2005. **48**(1): P. 1-20.
4. W. Ampomah,R. Balch,R. Will,M. Cather,D. Gunda,Z. Dai, Co-Optimization Of Co2-Eor And Storage Processes Under Geological Uncertainty. Energy Procedia, 2017. **114**: P. 6928-6941.
5. F.K.Y. Cinar, Co-Optimizing Enhanced Oil Recovery And Co2 Storage By Simultaneous Water And Co2 Injection. Energy Exploration & Exploitation, 2013.
6. Ippc, The Physical Science Basis. Contribution Of Working Group I To The Fourth Assessment Report Of The Intergovernmental Panel On Climate Change. 2007.
7. F. Abbas,M.P. C., Prospects For Subsurface Co2 Sequestration. Aiche Journal, 2010. **56**(6): P. 1398-1405.
8. F.M. Orr, Jr., Storage Of Carbon Dioxide In Geologic Formations. 2004.

9. N.I. Kechut,M. Jamiolahmady,M. Sohrabi, Numerical Simulation Of Experimental Carbonated Water Injection (Cwi) For Improved Oil Recovery And Co2 Storage. Journal Of Petroleum Science And Engineering, 2011. **77**(1): P. 111-120.
10. R.J. Christensen, Carbonated Waterflood Results--Texas And Oklahoma, In Annual Meeting Of Rocky Mountain Petroleum Engineers Of Aime. 1961, Society Of Petroleum Engineers: Farmington, New Mexico.
11. M.A. Ahmadi,M.Z. Hasanvand,S.S. Behbahani,A. Nourmohammad,A. Vahidi,M. Amiri,G. Ahmadi, Effect Of Operational Parameters On The Performance Of Carbonated Water Injection: Experimental And Numerical Modeling Study. The Journal Of Supercritical Fluids, 2016. **107**: P. 542-548.
12. M. Riazi,M. Sohrabi,M. Jamiolahmady,S. Ireland,C. Brown, Oil Recovery Improvement Using Co2-Enriched Water Injection, In Europec/Eage Conference And Exhibition. 2009, Society Of Petroleum Engineers: Amsterdam, The Netherlands.
13. J. Foroozesh,M. Jamiolahmady,M. Sohrabi, Mathematical Modeling Of Carbonated Water Injection For Eor And Co2 Storage With A Focus On Mass Transfer Kinetics. Fuel, 2016. **174**: P. 325-332.
14. Z. Li,A. Firoozabadi, Cubic-Plus-Association Equation Of State For Water-Containing Mixtures: Is "Cross Association" Necessary? Aiche Journal, 2009. **55**(7): P. 1803-1813.
15. N. Mosavat,F. Torabi, Performance Of Secondary Carbonated Water Injection In Light Oil Systems. Industrial & Engineering Chemistry Research, 2014. **53**(3): P. 1262-1273.
16. M. Sohrabi,N.I. Kechut,M. Riazi,M. Jamiolahmady,S. Ireland,G. Robertson, Safe Storage Of Co2 Together With Improved Oil Recovery By Co2-Enriched Water Injection. Chemical Engineering Research And Design, 2011. **89**(9): P. 1865-1872.
17. N.I. Kechut,M. Riazi,M. Sohrabi,M. Jamiolahmady, Tertiary Oil Recovery And Co2 Sequestration By Carbonated Water Injection (Cwi), In Spe International Conference On Co2 Capture, Storage, And Utilization. 2010, Society Of Petroleum Engineers: New Orleans, Louisiana, Usa.
18. S. Embid,O. Rivas, Simulation Of Miscible Displacement With Interphase Mass Transfer Resistance. 1994.
19. M. Tavakolian,M. Sohrabi,M. Jami,S. Ireland, Significant Improvement In Oil Recovery And Co2 Storage By Carbonated Water Injection (Cwi). 2012.
20. M. Seyyedi,M. Sohrabi,A. Sisson,S. Ireland, Quantification Of Oil Recovery Efficiency, Co2 Storage Potential, And Fluid-Rock Interactions By Cwi In Heterogeneous Sandstone Oil Reservoirs. Journal Of Molecular Liquids, 2018. **249**: P. 779-788.
21. N. Mosavat,F. Torabi, Micro-Optical Analysis Of Carbonated Water Injection In Irregular And Heterogeneous Pore Geometry. Fuel, 2016. **175**: P. 191-201.
22. M. Sohrabi,N. Kechut,M. Riazi,M. Jamiolahmady,S. Ireland,C. Brown,G. Robertson, Coreflooding Studies To Investigate The Potential Of Carbonated Water Injection As An Injection Strategy For Improved Oil Recovery And Co2 Storage. Vol. 91. 2009.
23. J. Mansoori, Compositional Modeling Of Co2 Flooding And The Effect Of Co2 Water Solubility. 1982, Society Of Petroleum Engineers.

24. Y.-B. Chang,B.K. Coats,J.S. Nolen, A Compositional Model For Co2 Floods Including Co2 Solubility In Water. Spe Reservoir Evaluation & Engineering, 1998. **1**(02): P. 155-160.
25. N. De Nevers, A Calculation Method For Carbonated Water Flooding. Society Of Petroleum Engineers Journal, 1964. **4**(01): P. 9-20.
26. J.S. Miller,R.A. Jones, A Laboratory Study To Determine Physical Characteristics Of Heavy Oil After Co2 Saturation, In Spe/Doe Enhanced Oil Recovery Symposium. 1981, Society Of Petroleum Engineers: Tulsa, Oklahoma.
27. A. Hebach,A. Oberhof,N. Dahmen, Density Of Water + Carbon Dioxide At Elevated Pressures: Measurements And Correlation. Journal Of Chemical & Engineering Data, 2004. **49**(4): P. 950-953.
28. M. Riazi,M. Sohrabi,M. Jamiolahmady, Experimental Study Of Pore-Scale Mechanisms Of Carbonated Water Injection. Vol. 86. 2011. 73-86.
29. L.A.J. Sedigheh Mahdavi, Investigation Of Water Flooding And Carbonated Water Injection (Cwi) In A Fractured Porous Media. 2017.
30. A.B. Ramesh,T.N. Dixon, Numerical Simulation Of Carbonated Waterflooding In A Heterogeneous Reservoir, In Spe Symposium On Numerical Simulation Of Reservoir Performance. 1973, Society Of Petroleum Engineers: Houston, Texas.
31. C. Esene,N. Rezaei,A. Aborig,S. Zendehboudi, Comprehensive Review Of Carbonated Water Injection For Enhanced Oil Recovery. Fuel, 2019. **237**: P. 1086-1107.
32. C. Esene,D. Onalo,S. Zendehboudi,L. James,A. Aborig,S. Butt, Modeling Investigation Of Low Salinity Water Injection In Sandstones And Carbonates: Effect Of Na+ And So42−. Fuel, 2018. **232**: P. 362-373.
33. H. Valiollahi,Z. Ziabakhsh,P.L.J. Zitha, Mathematical Modeling Of Chemical Oil-Soluble Transport For Water Control In Porous Media. Computers & Geosciences, 2012. **45**: P. 240-249.
34. J.T. Geller,J.R. Hunt, Mass Transfer From Nonaqueous Phase Organic Liquids In Water-Saturated Porous Media. Water Resources Research, 1993. **29**(4): P. 833-845.
35. C.M. Group, Co2 Modelling Using Gem. 2017.
36. D.-Y. Peng,D.B. Robinson, A New Two-Constant Equation Of State. Industrial & Engineering Chemistry Fundamentals, 1976. **15**(1): P. 59-64.
37. G. Soave, Equilibrium Constants From A Modified Redlich-Kwong Equation Of State. Chemical Engineering Science, 1972. **27**(6): P. 1197-1203.
38. L. Yau-Kun,N.L. X., Phase Equilibria Of Oil, Gas And Water/Brine Mixtures From A Cubic Equation Of State And Henry's Law. The Canadian Journal Of Chemical Engineering, 1986. **64**(3): P. 486-496.
39. D.W. Peaceman, Interpretation Of Well-Block Pressures In Numerical Reservoir Simulation. Society Of Petroleum Engineers Journal, 1978.

Chapter 5 **Effect of Operational Parameters and Rock Dissolution on Performance of Carbonated Water Injection: Core Scale Tests and Computational Modeling**

ABSTRACT

Oil recovery is expected to increase considerably by implementation of carbonated water injection (CWI) particularly in the secondary mode according to various experimental and modeling research works. There have been a few modelling studies and core flooding tests reported on CWI in open sources. This inadequacy fuels the objectives of this paper. This study includes core scale experiments and computational fluid dynamic (CFD) modeling. To effectively capture the physics involved during CWI, the Navier-Stokes, mass balance equations, and reaction equations are solved for the same computational domains of CO_2, water, and oil. The modeling results are validated by the core scale experimental data of carbonated water injection in its secondary application. It is found that there is a good agreement between modeling results and real data; thus, the introduced CFD model can adequately simulate the CWI process. The developed model is also used to investigate the effect of operational parameters/conditions and rock dissolution during CWI. Based on the research results, an increase in the injection rate from 0.2 ml/min to 0.8 ml/min gives an additional oil recovery of 6 %. There is an optimum injection rate above which there is no significant change in the oil recovery. Increasing the injection pressure leads to a more dissolution of CO_2, which improves the overall performance of CWI such that the oil recovery increases by an additional 16 % upon an increase in the injection pressure from 1500 psi to 3500 psi. There is no evidence of rock dissolution based on the results attributed to permeability changes in a property-distance plot.

***Keywords*:** Carbonated water injection; Navier Stokes; Computational fluid dynamics; Rock dissolution; Core scale tests

5.1 Introduction

Carbonated water injection (CWI) is a promising oil recovery technique as the quantity of oil in reserves continually declines. CO_2 storage potential of CWI is another interesting benefit associated with this recovery technique especially when compared with water injection, CO_2 injection, water alternating gas, and other related enhanced oil recovery (EOR) methods. Although conventional CO_2 injection and plain water flooding (WF) have been successful and easy to implement, some problems associated with them as EOR methods have been reported in the literature [1-4]. Due to the appreciable difference in fluid densities while conducting CO_2 injection or plain WF, several serious issues including, viscous fingering and gravity segregation are expected during these EOR operations that may lead to considerable unswept zones and early breakthrough of CO_2 [2].

CWI has the potential to perform better when compared to other EOR methods in reducing the residual oil saturation because of the density similarities that exist between carbonated water (CW) and oil. Additional oil recovery factor (RF) have been reported during CWI based on several experimental investigations in sand packs and core samples, ranging between 2 – 30 % [5-9]. Mcfarlane et al. found that during CWI there is a further reduction between 33-48 % of residual oil saturation after WF [6]. In the K&S field where CWI has been implemented, an additional oil recovery of 10 % was achieved when compared to WF [10]. Various research and engineering activities related to CWI (as an EOR technique) have also been reported even though the complex process involved have not been well understood [7, 11]. During CWI, there is a transfer of CO_2 from the water phase to the oil phase which is controlled by the solubility gradient between the phases. The transfer of CO_2 into the oil phase causes oil swelling, which is one of the main mechanisms that contributes to an increase in oil recovery percentage [2, 5, 11]. Another vital factor for the increased RF during CWI is a reduction in oil viscosity caused by the dissolution of CO_2. Variations in interfacial tension, oil density, and fluid rock wettability have also been studied through experimental approach and reported to contribute to the overall performance of CWI [11-14].

There have been several attempts to understand the complex physics involved in CWI process through experimental and modelling studies [5, 7, 11-21]. The first study to model CWI was by

De Nevers [18] based on Buckley Leveret theory to simulate CWI operation. Although the capillary and gravity terms were ignored, the model was able to consider oil swelling and viscosity reduction as CO_2 moves across phases. The reactive and diffusive terms, which are also part of complex physics during CWI were ignored. A three- phase flow mathematical model was developed by Dixon et al.[22]. In their model, an implicit method for pressure and an explicit approach for saturation were used to investigate the displacement mechanisms of CWI and oil recovery. Their model did not include the reaction effect. Mansoori [20] developed a model to simulate the displacement process of CWI in 1-D and 2-D, however, this researcher also did not take into account the gravity, reactive, and diffusive terms, which may play important roles to the performance of carbonated water injection. A pore network model was developed by Zhao and Ioannidis[23]. Their developed model was used to investigate important aspects particularly mass transfer in the gas phase. Several other modelling and simulation work have been used to investigate carbonated water injection with a focus on displacement mechanisms and recovery factor [7, 21, 24, 25]. It has been reported that, through validation of developed models with experimental data, there is an overprediction of the recovery factor. The reason for this disparity has been hypothesized to the inherent assumption of instantaneous equilibrium during CWI. Several modelling works have overlooked the effect of coupling of the reaction, diffusive as well as gravity terms to the overall mass and momentum equations representing CWI. A few experimental studies have been performed on CWI. In a laboratory work conducted by Miller and Jones [26], it was concluded that depending on the operational parameters such as temperature, pressure, and oil type, the density of oil is reduced to a certain degree. Sohrabi et al.[11, 19] perfomed several experiments and reported extra oil recovery achieved through CWI and an additional benefit such as CO_2 storage. In another experimental study [13], the recovery mechanism and the storage capability of CO_2 during CWI were compared with plain or conventional CO_2 injection approach. It was found that CWI offers a more stable displacement process and a suitable means to safely store anthropogenic CO_2. In a micro model investigation performed by Riazi et al [5, 27], oil swelling was reported to be a major driving mechanism contributing to the additional RF during CWI. CWI for EOR purpose was investigated by Mahdavi and James through experimental and modeling studies [28]. It their research work, CWI led to a greater oil recovery when compared to plain WF. It was also concluded that the presence of fractures does not considerably affect the displacement process during CWI. Esene et al. published

a comprehensive review of CWI, highlighting key aspects such as fluid- fluid interactions, fluid rock interactions, and effect of operating condition on the production performance during CWI. As mentioned earlier, the previous modelling and experimental approaches confirm that CWI is a well-established method to decrease the residual oil saturation during an EOR process with an additional benefit of CO_2 storage. In a recent modeling study, Esene et al.[29] investigated CWI in a 3-D heterogenous reservoir (Norne field) for EOR where the effects of operational parameters and CO_2 storage in the CWI process were analysed. Their model did not consider rock dissolution due to the formation of carboxylic acid that may alter the rock porosity and permeability. Also, there was no adequate available data of CWI on a field scale to properly validate their model. In most of the modelling approaches for CWI, the reactive, diffusive, and gravity terms have been overlooked by other researchers [29, 30]. The inclusion of these terms would lead to a better generalization and understanding of the complex process involved in CWI process.

In this paper, a more general equation representing CWI is solved through using COMSOL Multiphysics. Navier-Stokes, mass balance equation, and reaction equation are solved for the same computational domain assigned for CO_2, water, and oil. The developed model is validated with experimental data [28] and the developed model is used to conduct sensitivity analysis.

After the introductory section of the manuscript, the experimental set up and the rock/fluid properties and conditions are presented in section 2. The governing equations to capture the physics of CWI are discussed is section 3. The limitations of the developed model are listed in section 4 and the obtained results and corresponding discussions are provided section 4. The vital conclusions and recommendations are included in the last section.

.

5.2 **Experimental Study**

Set up and operational conditions. The core flood experimental study on CWI performed in Memorial University EOR laboratory is shown in Figure 5.1. The experimental set up includes core, oven, core holder, back pressure regulator, amplified transducer, three double capped piston accumulators, gasometers, O-rings, and sleeves

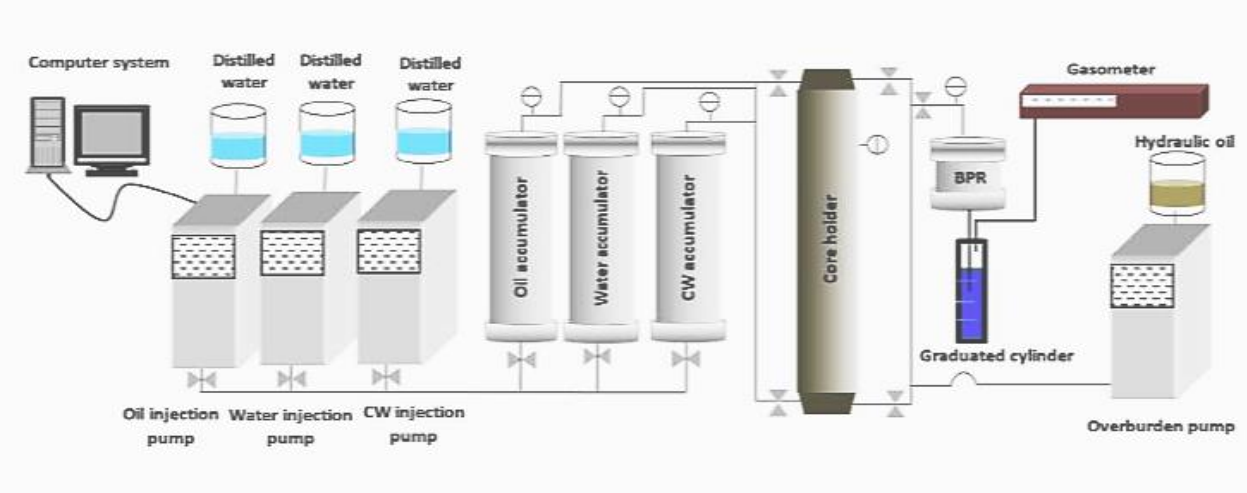

Figure 5.1 : Schematic representation of core flood experiments for carbonated water injection process.

The experiments are performed in a tri-axial Hassler-type core holder. All areas/surfaces of the core in the core holder experience compressive load in three axes (two radial, and one longitudinal). The core is a vertical oriented sandstone as shown in Figure 5.1. The operating conditions for this experimental study are 185 ^{o}F, 4500 psia, and 35,987 ppm for the temperature, pressure, and initial formation brine saturation, respectively. A connate water of 0.27 and an injection rate of 0.2 ml/min are other operating conditions for this experimental study.

As can be seen in Table 5.1, a summary of all the input data/operating condition for the experimental study of CWI is presented. This information is used in the modelling work to simulate the experiments.

Table 5.1: Summary of experimental conditions

Parameter	Value
Initial Pressure	4500 psi
Rock Permeability	345 mD
Rock Porosity	22 %
Length of core	10.88 cm
Temperature	185 ^{o}F
Salinity	35,987 ppm
Oil viscosity	6.82 cP
Connate water saturation	0.27
Wettability	Water wet
Rate constant	0.039 s^{-1}

Rock properties. In the experimental study, a Berea 2 rock with a length of 10.88 cm, a diameter of 3.83 cm, a porosity of 22 %, and a permeability of 345 mD is used to investigate the secondary CWI.

Fluid properties. The fluid properties are 252 g/mol, 877 g/m^3, 6.82 cP that represent its molecular weight, density, and viscosity, respectively. Using the gas chromatography, the compositional analysis of the fluid is listed in Table 5.2.

Table 5.2: Compositional analysis of fluid at 15.5 ^{o}C and 0.101 MPa [29].

Component	Mole %	Component	Mole %
C6	0.07	C19	3.14
C7	1.58	C20	2.65
C8	6.27	C21	2.38
C9	8.55	C22	2.13
C10	8.11	C23	1.95
C11	7.31	C24	1.74
C12	6.49	C25	1.69
C13	6.26	C26	1.44
C14	5.7	C27	1.41
C15	4.8	C28	1.27
C16	4.11	C29	1.27
C17	3.54	C30+	12.81
C18	3.33	MW of $C30^{+}$ = 642g/mol	
		Density of $C30^{+}$ = 0.994 kg/m^3	

5.3 **Mathematical Modeling Phase**

To model the CWI, the generalized form of equation for flow in 3-D for any specie is given below.

$$\frac{\varphi\partial(\rho_\alpha s_\alpha \omega_\alpha^x)}{\partial t} + \nabla(u_\alpha \rho_\alpha \omega_\alpha - s_\alpha D_\alpha^x \nabla\omega_\alpha) = U + \varphi s_\alpha R_\alpha^x \tag{5.1}$$

where *x* represents the species; α refers to the phase; φ denotes the porosity; ρ is the density; ω symbolizes the mass fraction; u resembles the Darcy velocity; U is the mass transfer; s is the saturation; and R stands for the reaction term. The compound terms on the left-hand side of Equation (5.1) are the accumulation term, convective terms, and dispersion term, respectively. The terms on the right-hand side of Equation (5.1) are the mass transfer term and the reactive term, respectively.

The Navier-Stokes equation, mass conservation equation, and reaction equation are all solved for the same computational domain as shown in Figure 5.2 in the *z-x* plane. The mass conservation equation and the reaction equation are coupled by adding the Darcy law interface and transport of diluted species interface in COMSOL Multiphysics.

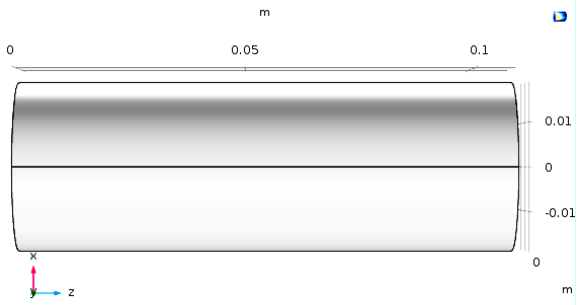

Figure 5.2: Core model representation in the z-x plane.

Two-phase Darcy law. Carbonated water is being modelled in a black oil mode using the COMSOL Multiphysics. Two-phase flow interfaces for carbonated water and oil are defined for the principal domain to represent wetting phase and non-wetting phase as follows:

$$(\varphi_s - \varphi_r)\frac{\partial Se_{cw}}{\partial_t} + \nabla.\left[-\frac{k_{int}k_{r,w}}{\mu_{cw}}\nabla\left(p_{cw} + \rho_{cw}g\nabla Z\right)\right] = 0 \quad (5.2)$$

$$(\varphi_s - \varphi_r)\frac{\partial Se_o}{\partial_t} + \nabla.\left[-\frac{k_{int}k_{r,o}}{\mu_o}\nabla\left(p_o + \rho_o g\nabla Z\right)\right] = 0 \quad (5.3)$$

in which, φ_s introduces the total porosity; φ_r is the residual volume fraction; and the resultant difference is the available pore space for the phase to move. The effective saturation is represented by $Se.\, k_{int},\ k_{r,}\ \mu, p, \rho$, g, and Z represent the intrinsic or absolute permeability, relative permeability, viscosity, pressure, density, gravity, and coordinate of the vertical elevation.

Auxiliary equations. The capillary pressure (P_C) and the effective phase saturation equations are needed to solve the governing equations, as shown below:

$$P_C = P_{nw} - P_w \quad (5.4)$$

$$Se_{nw} + Se_w = 1 \quad (5.5)$$

Equations (5.2) to (5.5) are coupled together to solve for pressure and saturation of carbonated water and oil phases.

Carbonated water injection consists of low concentration of CO_2; hence the Fickian approach for the diffusion term in the mass transport is valid. The reaction taking place in the porous medium during CWI is governed by the convective- diffusion equation as listed below:

$$\nabla.(-D_i\nabla c_i + c_i u) = R_i \quad (5.6)$$

where D is the diffusivity; c denotes the concentration, and R represents the reaction rate for the resultant specie (HCO_3^{2-})

Boundary and initial conditions. The initial conditions for the system of two-phase flow in porous medium are shown in Equations (5.7) to (5.9). The inlet of the core is assumed to have a

constant velocity as shown in Equation (5.7) and the volumetric flow rate is obtained by an inlet surface integration using COMSOL Multiphysics. In Equation (5.8), the inlet concentration of CO_2 is assumed fixed. This condition eliminates the need for a fix flux at the outlet boundary, since the convection mechanism dominates at the outlet (see Equation (5.9)).

$$u = u_{in} \tag{5.7}$$

$$c_i = c_{iinlet} \tag{5.8}$$

$$n.(-D_i \nabla c_i + c_i u) = n.c_i u \tag{5.9}$$

Additionally, van Genuchten retention model [31] is employed to characterize the phase movement and hydraulic properties relative to the wetting phase, as given by the following expressions:

$$k_{r,w} = Se_w^L \left(1 - \left(1 - Se_w^{\frac{1}{m}}\right)^m\right)^2 \tag{5.10}$$

$$k_{r,nw} = (1 - Se_w)^L \left(1 - Se_w^{\frac{1}{m}}\right)^m \tag{5.11}$$

where α, n, m, and L are the constants based on the characteristics of the porous medium. k_{rw} and $k_{r,nw}$ resemble the relative permeabilities of wetting and non wetting phases (water and oil), respectively.

Model discretization and mesh geometry. Triangular elements are used as the geometry for meshes in this study**.** The quality of meshing is determined by physics-controlled strategy, which is the default in COMSOL multiphysics. The size of the elements of the core is selected to be fine, as seen in Figure 5.3. The edges and surface areas of the core are selected to be extra fine mesh. This approach is applied to capture the phase movement along those areas during simulation.

Figure 5.3: Fine element size -Mesh in a 1-D geometry.

The maximum mesh size is 0.000598 m, the minimum mesh size is 0.000043 m, the curvature factor of 0.4 is considered. This meshing uses a computation time of 15 mins with a set algebraic error of 1×10^{-6} to enable an appropriate convergence during simulation. In the selection of meshing type, the finer the mesh sizes, the more accurate the results would be but at the cost of a longer simulation time.

Flowchart. COMSOL Multiphysics is a powerful tool that can be used for modeling different transport phenomena. It exhibits a wide range of applications in the medical, electrical, mechanical, chemical, and environmental engineering and science sectors. Regardless of the phenomenon/process to be investigated, using COMSOL Multiphysics follows a similar workflow or procedure, as depicted in Figure 5.4.

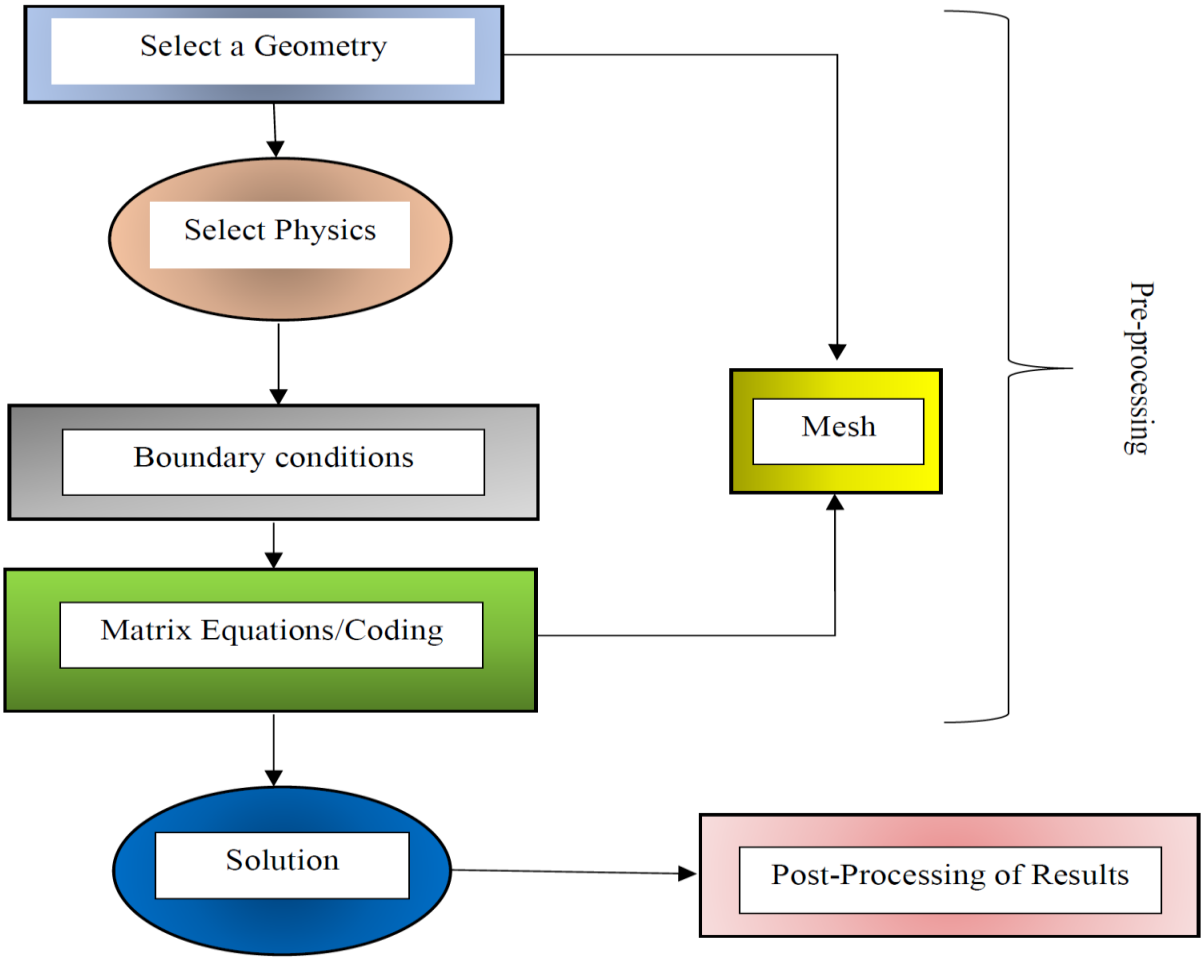

Figure 5.4: Main steps to conduct modeling simulation while using COMSOL Multiphysics.

As shown in Figure 5.4, in developing a core scale CWI model with COMSOL Multiphysics, the first step is to select a 1-D cylindrical geometry using the dimensions of the core that were utilized in the laboratory experiment. Two-phase Darcy law and transport of diluted species are selected as the governing physics to represent CWI in the black oil mode. Boundary conditions for a stable solution of partial differential equations are chosen for each computational domain in COMSOL Multiphysics. According to Figure 5.4, meshing step is conducted after the matrix equations are all selected and defined appropriately for each domain. The solution of the overall physics is based on a time dependent scheme, which is preceded by the post processing of CWI results.

5.4 **Limitations**

- COMSOL Multiphysics is able to accurately model a core scale but might not be very efficient in scenarios where reservoir heterogeneities in terms of permeability and wettability exist.
- Building a model in COMSOL Multiphysics requires an in-depth understanding of the physics involved as well as the equations. It is time consuming to understand the overall governing equation of a particular physical phenomenon.
- The rock-fluid data is required to be implemented on each domain, which might be very time consuming and requires a huge effort for accuracy.
- The gas non-ideality and non-elementary reactions might not well captured using COMSOL simulator package.
- Modeling transport phenomena in the interface within porous systems is challenging in terms of gridding and selecting proper governing equation while employing this simulation strategy.

5.5 **Results and Discussion**

In this research, a core scale model for CWI is developed using COMSOL multiphysics. The validation of the model, parametric sensitivity analysis of the model at various condition, and the effect of rock dissolution are presented in this section where adequate justifications and discussions on the results are provided.

Model Validation. The core model developed in COMSOL is validated by laboratory experiment on CWI reported in the literature [30]. Figure 5.5 (a) shows the fluid distribution of CW in a core originally saturated with oil with a connate water of 0.3. Figure 5.5 (b) shows the comparison of the developed model results and the experimental result.

(a) (b)

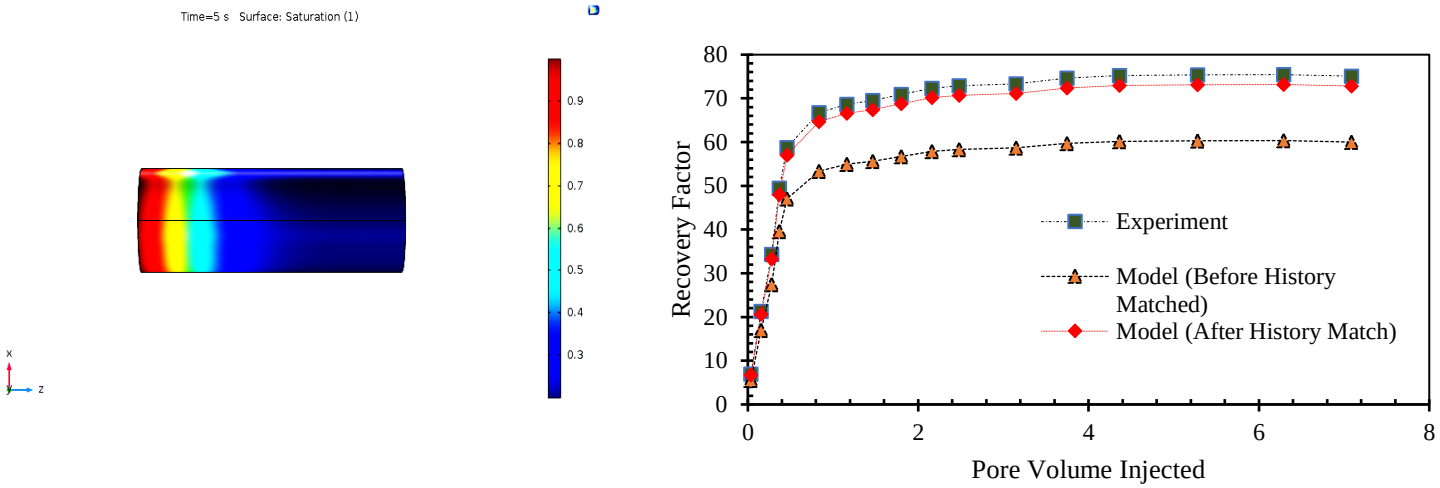

Figure 5.5: (a) Carbonated water displacement profile, and (b) Oil recovery results based on experimental and modeling works.

Based on Figure 5.5 (b), there is a satisfactory agreement between the results from the developed model and the experimental data. The oil recovery predictions initially have a large deviations when compared to the experimental result as can be seen from Figure 5.5 (b); but after a tuning (history matching) of the relative permeabilities, exponents, and capillary function, the error is greatly reduced.

Parametric sensitivity analysis. Parametric analysis is performed to investigate the response of the model at different conditions. Effects of injection rate, injection pressure, salinity, oil viscosity, reservoir permeability, temperature, and rock dissolution on the CWI performance are presented in this section.

The influence of injection rate is investigated at 3000 psi to determine the performance of CWI in terms of oil recovery by gradually increasing the injection rate based on a core scale. As demonstrated in Figure 5.6, the ultimate oil recovery is increased by 2 % when the injection rate increases from 0.2 ml/min to 0.4 ml/min after injecting 7 pore volume of CW. According to the results, the performance of CWI is greatly influenced by the injection rate as the sweep efficiency is improved upon an increase in injection rate.

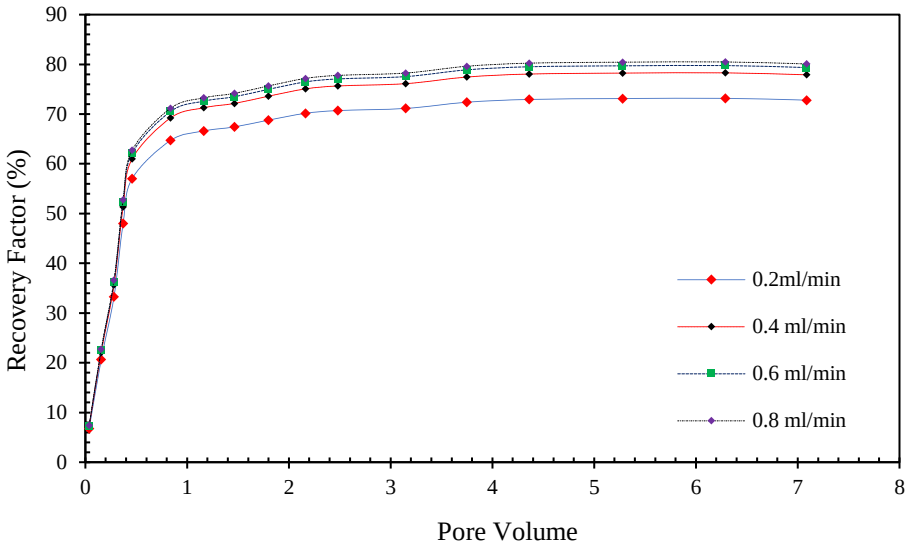

Figure 5.6: Effect of Injection Rate on CWI performance at 3000 psi.

A further increase from 0.4 ml/min to 0.8 ml/min offers no significant improvement in the oil recovery because of the core size or because the maximum displacement efficiency has been reached by a flow rate of 0.4 ml/min. Increasing the flow rate of CW is expected to give similar trend in the field case as well until the injection well shut in time has been reached. Well shut-in is normally performed to control the economic limit of the maximum allowable water production in the producer well(s).

The effect of injection pressure on CWI performance in terms of oil recovery is investigated based on the core characteristics, as illustrated in Figures 5.7 and 5.8. Based on Figure 5.7, an increase in the injection pressure improves the performance of CWI. By increasing injection pressure from 1500 psi to 3500 psi, an additional 16 % ultimate oil recovery is achieved.

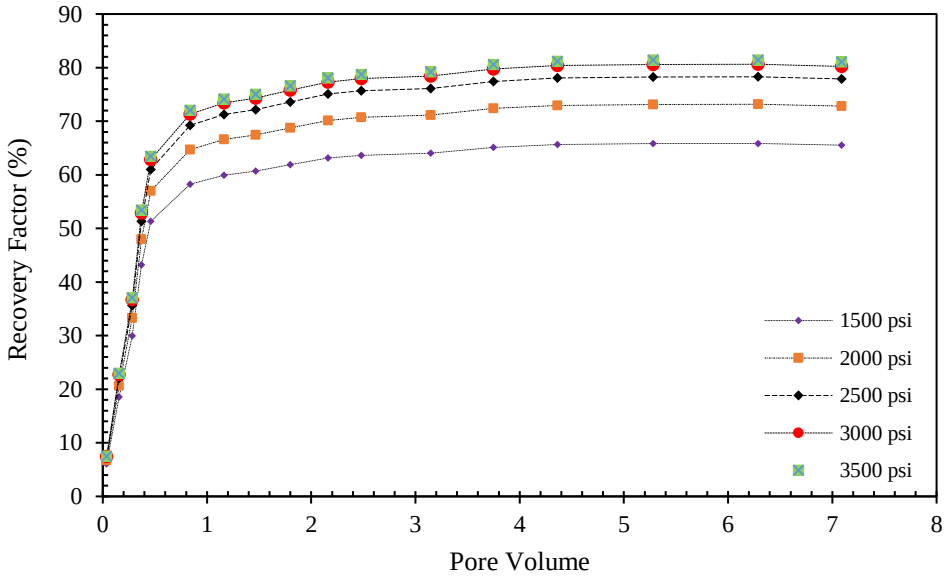

Figure 5.5: Effect of pressure on CWI performance at 0.4 ml/min injection rate.

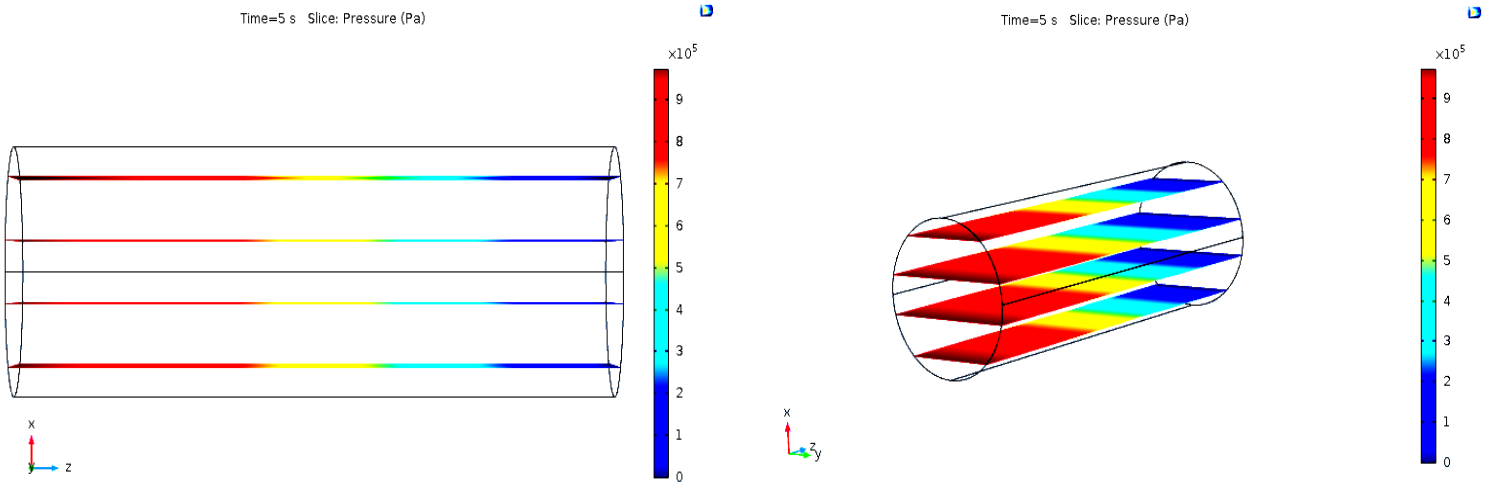

z-x direction x-y direction

Figure 5.6: Pressure profile along the (a) z-x and (b) x-y direction.

This substantial improvement is because of the enhancement of the CW; as more CO_2 is dissolved in water upon an increase in pressure. The injection pressure should be maintained below the fracture pressure of the reservoir rock to prevent CO_2 gas leakage to the surface through fractures

that are unnaturally created due to the high injection pressures. Figure 5.8 (panels (a) and (b)) shows the model numerical stability through an evenly distributed pressure pattern in the z-x direction and across the 4 planar slides in the x-y direction. As the simulation time elapses, the pressure count increases numerically until it reaches the set pressure in COMSOL Multiphysics.

The effect of salinity on the CWI performance in terms of oil recovery is studied. At a pressure of 3000 psi and an injection rate of 4ml/min, the salinities of 1000 ppm, 35987 ppm, 60000 ppm, and 100000 ppm are examined as shown in Figure 5.9.

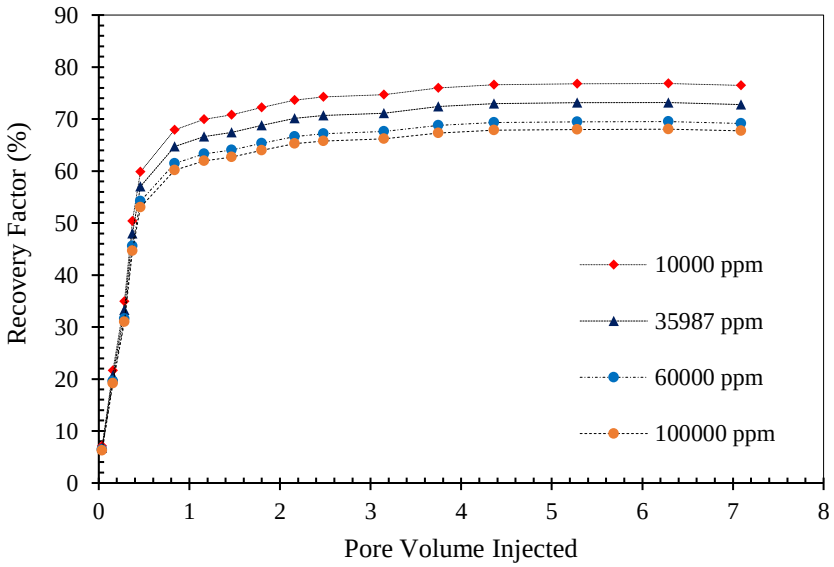

Figure 5.7: Effect of salinity on oil recovery at 3000 psi and 4 ml/min.

A reduction in dissolution of CO_2 occurs with increasing the water salinity. This behavior influences the performance of carbonated water injection. As depicted in Figure 5.9, the CWI exhibits the greatest RF when the magnitude of salinity is minimal. For instance, the salinities of 10000 ppm, 35987 ppm, 60000 ppm, and 100000 ppm yield the ultimate RF values of 76.44 % , 72. 80 %, 69. 10 % and 67.7 %, respectively. Therefore, it is recommended to determine the critical salinity for attaining an optimum dissolution of CO_2 in water during CWI.

The CWI operation is studied while using different oil types with various viscosities. The oil viscosities of 1 cP, 6.28 cP, 20 cP, and 40 cP are considered in this investigation as demonstrated

in Figure 5.10. Based on the modeling results, the ultimate RF values for the various oil viscosities are 83.72 %, 72.80 %, 65.52 % and 62.60 %, respectively.

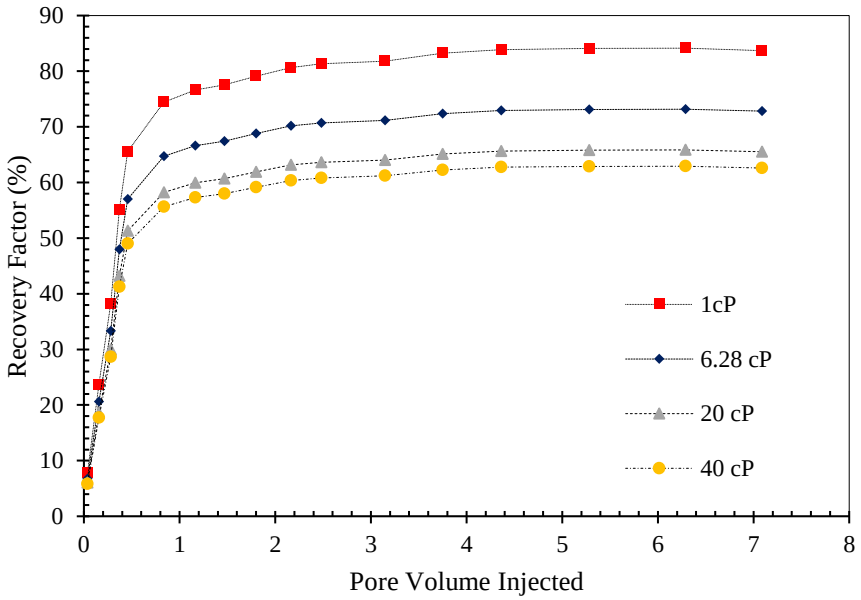

Figure 5.8: Effect of oil viscosity on oil recovery at 3000 psi and 4 ml/min.

The CWI performance for oil with a viscosity of 1 cP is much better than the case having an oil of 20 cP as the oil with a higher viscosity. This is because the solubility of CO_2 in lighter oil is greater than that in the heavier oil. Therefore, it improves the overall performance of CWI when applied to light oil. The mass transfer of CO_2 from carbonated water across phases into lighter oil components is faster when compared to the case with heavier oil components. CWI integrated with thermal methods may be applied to heavy oil reservoir to accelerate mass transfer. The performance of CWI in a heavy oil reservoir can be also improved by using a very low injection rate to sustain a slow and effective mass transfer across phases (carbonated water and oil).

CWI simulations are performed on cores with different permeabilities of 100 mD, 345 mD, 1000 mD, and 1200 mD. The performance of CWI at various permeability conditions is studied in terms of RF, as depicted in Figure 5.11.

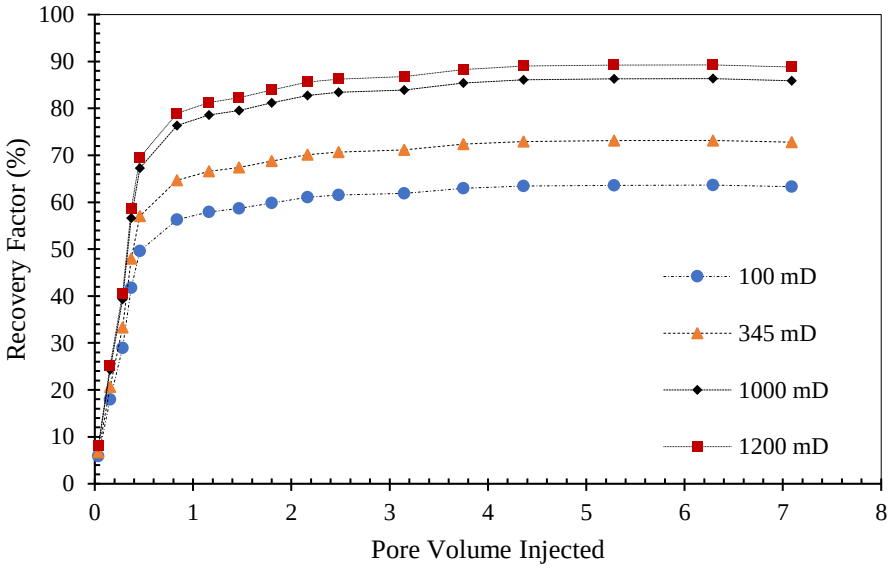

Figure 5.9: Effect of permeability on CWI oil recovery at 3000 psi and 4 ml/min.

According to Figure 5.11, the highest ultimate recovery factor is obtained for the core with the maximum permeability, 1200 mD. CWI offers a very low mobility ratio and a piston-like displacement due to the similarities in the densities between the displacing fluid (CW) and displaced fluid (oil). Hence, an increase in the core permeability consistently increases the RF as seen in the Figure 5.11. For instance, the permeabilities of 100 mD, 345 mD,1000 mD, and 1200 mD result in RF of 63.33 %, 72.80 %, 86.33 %, and 88.81%, respectively

The performance of CWI in terms of oil recovery is also studied at various temperatures of 100 ^{o}F, 185 ^{o}F, 250 ^{o}F, and 300 ^{o}F (see Figure 5.12).

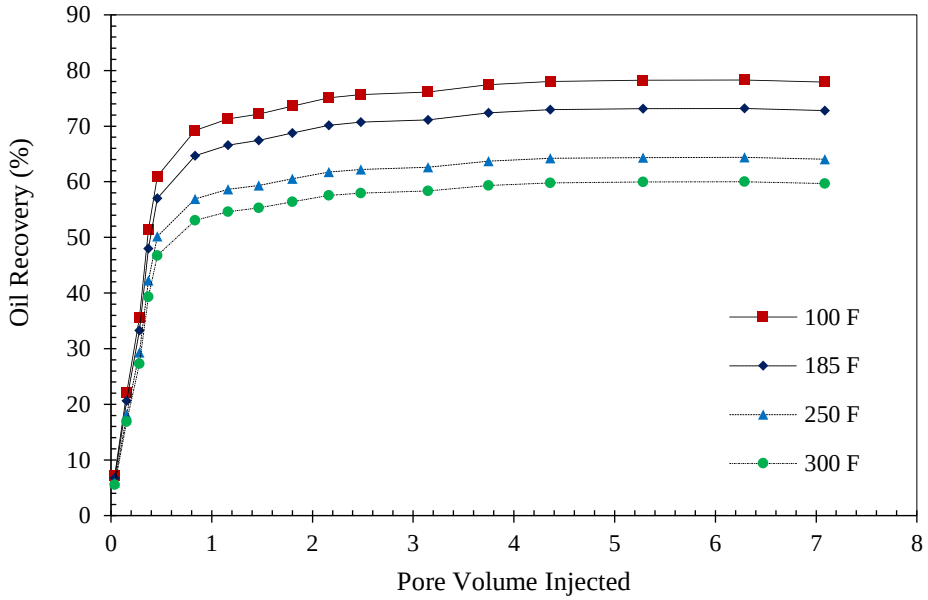

Figure 5.10: Effect of Temperature on oil recovery at 3000 psi and 4 ml/min.

As the temperature increases, the solubility of CO_2 in water lowers, as expected. According to Figure 5.12, the CWI leads to the highest RF at a temperature of 100 F when compared to the RF at higher temperatures. Hence, the performance of CWI in high temperature reservoirs will be considerably lower than that in conventional reservoirs. We can also investigate the performance of CWI in reservoirs with various thicknesses/depths as the temperature varies with depth.

The impact of rock dissolution on the medium permeability is studied a long the length of the core, as shown in Figure 5.13.

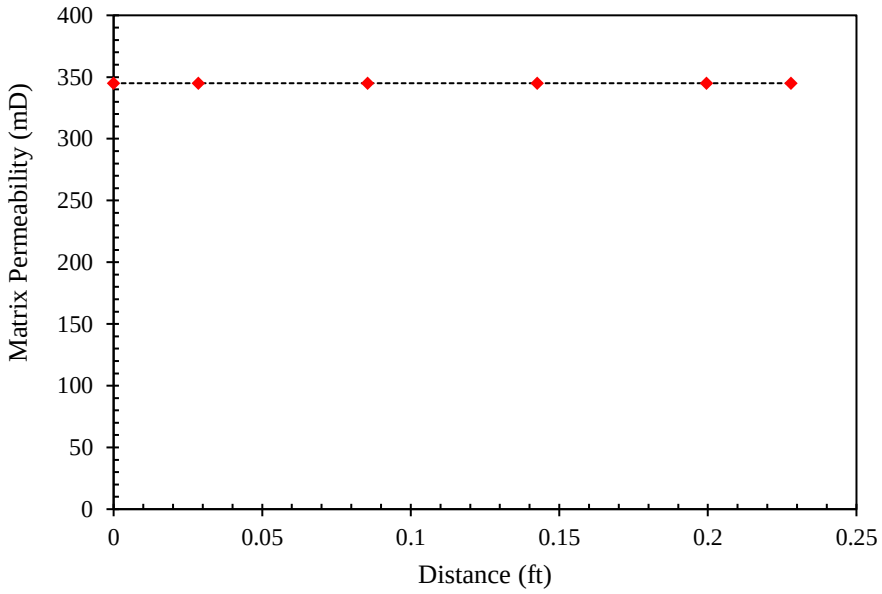

Figure 5.11: Effect of CWI on rock dissolution and consequently matrix permeability.

According to Figure 5.13, the permeability of the core remains constant, through there is formation of carboxylic acid through the interaction of CO_2 and water during CWI. This behaviour indicates that there is no considerable change in reservoir petrophysical properties during CWI. This conclusion can change in the presence of certain ions and catalytic reservoir conditions which may result in various reactions.

This research demonstrates an experimental and modelling approach of carbonated water injection where core scale set up and COMSOL Multiphysics are utilized. The developed model captures more robust physics when compared to earlier modelling methods. The accuracy of the developed model is validated with available experimental data. The model is then used to carry out parametric sensitivity analysis. Carbonated water injection is recognized as an improved method, when compared to other CO_2-EOR related techniques. Thus, the need of a model that captures the important displacement mechanisms is inevitable. With the use of the developed model, core scale simulation studies of CWI can be performed accurately and upscaled into field scale for CWI-EOR projects. It is expected that a precise model can assist researchers and engineers make proper technical and economic decisions in in the pre-developmental stages of CWI projects.

5.6 **Conclusions**

Carbonated water injection (CWI) is a viable option to further decrease the fraction of residual oil saturation. Upon application in the core scale or field scale, a secondary benefit of CO_2 sequestration is also achieved. This research work presents core scale analysis of CWI in terms of oil recovery at various process conditions. Based on the obtained results, the following conclusions can be drawn:

- There is a stable displacement during CWI which improves the sweep efficiency due to the low mobility ratio that results from small difference between densities of the displacing fluid (CW) and displaced oil. According to the core scale results, the predominant problems (viscous fingering and early breakthrough) associated with conventional water injection are mitigated while employing CWI.
- In the core scale, a recovery factor (60 % - 78 %) is achieved with CWI when compared to WF (30 % - 45 %) due to change in the fluid properties as well as the mass transfer of CO_2 into oil. This range of RF is expected in a full scale case (reservoir), though it is strongly dependent on the reservoir petrophysical properties, oil characteristics, and operational conditions.
- An increase in injection pressure leads to an improvement in the overall performance of CWI. The main reason is that more CO_2 is dissolved in water at high injection pressure according to the Henry's law.
- The performance of CWI in a light oil case is much better, compared to a more viscous or heavy oil case due to variations in solubility.
- The performance of CWI in a high temperature reservoir is lower, compared to medium temperature reservoir. This is because increasing the temperature lowers the CO_2 solubility in water.
- An increase in salinity decreases the solubility of CO_2 in water. Therefore, it has an adverse effect on the performance of CWI technique.
- Based on the funding of sensitivity analysis, there is an optimum or critical injection rate, which gives a maximum (effective) performance of CWI in terms of oil recovery. This particular injection rate rate ensures a maximum contact time that leads to a greater mass transfer between carbonated water and oil.

- Although there is a potential formation of carboxylic acid (HCO_3^{2-}) from the interaction of CO_2, water, and a favorable salinity content, no rock dissolution during CWI is confirmed. The dissolution of the core is investigated by observing the changes in matrix permeability in a property distance plot. Based on the results, the matrix permeability remains constant in the core, which reflects no considerable alteration in the rock properties over CWI.

The development of a field scale model is recommended to better investigate CWI in terms of theoretical, environmental, and economic aspects.

ACKNOWLEDGEMENTS

We would like to acknowledge the Natural Sciences and Engineering Research Council of Canada (NSERC), Memorial University, Equinor Canada, and InnovateNL for supporting this research project.

NOMENCLATURES

Acronyms

API	American Petroleum Institute
BHP	Bottom Hole Pressure
CO_2	Carbon dioxide
CWI	Carbonated Water Injection
CW	Carbonated Water
EOR	Enhanced Oil Recovery
mD	milli Darcy
P^s	Saturation Pressure
RF	Recovery Factor
UT	Ultimate
WF	Water Flooding

Variables and Parameters

D	Diffusion coefficient
c	Concentration
g	Acceleration due to gravity
K_{int}	Intrinsic permeability
$k_{r,w}$	Water relative permeability
$k_{r,0}$	Oil relative permeability
P	Pressure
q	Injection and production rate

R	Reaction Rate
Se	Effective Saturation
T	Temperature
U	Mass transfer term
u	Darcy velocity
v	Molar volume

Greek Letters

ρ	Mass density ($\frac{Kg}{m^3}$)
μ	Viscosity (cP)
ϕ_s	Total Porosity (-)
ϕ_r	Residual Porosity
Δ	Difference operator
ω	Mass fraction
α	Phase
λ	Mobility

Subscripts

CO_2	Carbon dioxide
cw	Carbonated water injection
nw	Non-wetting
w	Wetting
g	Gas
i	Initial
r	Reduced
c	capillary
w	Water
o	Oil

Superscripts

o	Oil
s	Saturation
w	Water

REFERENCES

1. Riazi M.,Jamiolahmady M.,Sohrabi M., Theoretical investigation of pore-scale mechanisms of carbonated water injection. Journal of Petroleum Science and Engineering, 2011. **75**(3): p. 312-326.

2. Esene C.,Rezaei N.,Aborig A.,Zendehboudi S., Comprehensive review of carbonated water injection for enhanced oil recovery. Fuel, 2019. **237**: p. 1086-1107.
3. Ghedan S. G., Global laboratory experience of CO_2-EOR flooding, in In: SPE/EAGE reservoir characterization and simulation conference. 12-19 October 2009, Society of Petroleum Engineer: Abu Dhabi.
4. Kulkarni M. M. R., Dandina N., Experimental investigation of miscible and immiscible water-alternating-gas (WAG) process performance. Journal of Petroleum Science and Engineering, 2005. **48**(1): p. 1-20.
5. Riazi M.,Sohrabi M.,Jamiolahmady M.,Ireland S.,Brown c., Oil recovery improvement using CO_2-enriched water injection, in EUROPEC/EAGE Conference and Exhibition. 8-11 June 2009, Society of Petroleum Engineers: Amsterdam, The Netherlands.
6. McFarlane R.,Breston J.,Neil D., Oil recovery from cores when flooded with carbonated water and liquid CO_2. Producers Monthly, 1952: p. 23-35.
7. Foroozesh J.,Jamiolahmady M.,Sohrabi M., Mathematical modeling of carbonated water injection for EOR and CO_2 storage with a focus on mass transfer kinetics. Fuel, 2016. **174**: p. 325-332.
8. Li Z.,Firoozabadi A., Cubic-plus-association equation of state for water-containing mixtures: Is "cross association" necessary? AIChE Journal, 2009. **55**(7): p. 1803-1813.
9. Mosavat N.,Torabi F., Application of CO_2-saturated water flooding as a prospective safe CO_2 storage strategy. Energy Procedia, 2014. **63**: p. 5619-5630.
10. Hickok C. W.,Ramsay H. J., Jr., Case histories of carbonated waterfloods in dewey-bartlesville field, in SPE Secondary Recovery Symposium. 1962, Society of Petroleum Engineers: Wichita Falls, Texas. p. 24.
11. Sohrabi M.,Kechut N. I.,Riazi M.,Jamiolahmady M.,Ireland S.,Robertson G., Safe storage of CO_2 together with improved oil recovery by CO_2-enriched water injection. Chemical Engineering Research and Design, 2011. **89**(9): p. 1865-1872.
12. Mosavat N.,Torabi F., Performance of secondary carbonated water injection in light oil systems. Industrial & Engineering Chemistry Research, 2014. **53**(3): p. 1262-1273.
13. Tavakolian M.,Sohrabi M.,Jami M.,Ireland S., Significant improvement in oil recovery and CO_2 storage by carbonated water injection (cwi), in Third EAGE CO_2 Geological Storage Workshop. 26-27 March 2012, EAGE Publishing BV: Edinburgh, United Kingdom. p. 147-149.
14. Mosavat N.,Torabi F., Micro-optical analysis of carbonated water injection in irregular and heterogeneous pore geometry. Fuel, 2016. **175**: p. 191-201.
15. Kechut N. I.,Riazi M.,Sohrabi M.,Jamiolahmady M., Tertiary oil recovery and CO_2 sequestration by carbonated water injection (cwi), in SPE International Conference on CO_2 Capture, Storage, and Utilization. 10-12 November 2010, Society of Petroleum Engineers: New Orleans, Louisiana, USA.
16. Foroozesh J.,Jamiolahmady M., Simulation of carbonated water injection coreflood experiments: An insight into the wettability effect. Fuel, 2016. **184**: p. 581-589.
17. Seyyedi M.,Sohrabi M.,Sisson A.,Ireland S., Quantification of oil recovery efficiency, CO_2 storage potential, and fluid-rock interactions by CWI in heterogeneous sandstone oil reservoirs. Journal of Molecular Liquids, 2018. **249**: p. 779-788.
18. De Nevers N., A calculation method for carbonated water flooding. Society of Petroleum Engineers Journal, 1964. **4**(01): p. 9-20.
19. Sohrabi M.,Kechut N.,Riazi M.,Jamiolahmady M.,Ireland S.,Brown C.,Robertson G., Coreflooding studies to investigate the potential of carbonated water injection as an injection strategy for improved oil recovery and CO_2 storage. Transport in Porous Media, 2009. **91**(1): p. 101-121.
20. Mansoori J., Compositional modeling of CO_2 flooding and the effect of CO_2 water solubility. 24 September 1982, Society of Petroleum Engineers.

21. Chang Y.-B.,Coats B. K.,Nolen J. S., A compositional model for CO_2 floods including CO_2 solubility in water. SPE Reservoir Evaluation & Engineering, 1998. **1**(02): p. 155-160.
22. Ramesh A. B.,Dixon T. N., Numerical simulation of carbonated waterflooding in a heterogeneous reservoir, in SPE Symposium on Numerical Simulation of Reservoir Performance. 11-12 January, 1973, Society of Petroleum Engineers: Houston, Texas.
23. Zhao W.,Ioannidis M., Gas exsolution and flow during supersaturated water injection in porous media: I. Pore network modeling. Vol. 34. 2011. 2-14.
24. Kechut N. I.,Jamiolahmady M.,Sohrabi M., Numerical simulation of experimental carbonated water injection (cwi) for improved oil recovery and CO_2 storage. Journal of Petroleum Science and Engineering, 2011. **77**(1): p. 111-120.
25. Ahmadi M. A.,Hasanvand M. z.,Behbahani S. S.,Nourmohammad A.,Vahidi A.,Amiri M.,Ahmadi G., Effect of operational parameters on the performance of carbonated water injection: Experimental and numerical modeling study. The Journal of Supercritical Fluids, 2016. **107**: p. 542-548.
26. Miller J. S. J., Ray A., A laboratory study to determine physical characteristics of heavy oil after co2 saturation, in SPE/DOE Enhanced Oil Recovery Symposium. 5-8 April 1981, Society of Petroleum Engineers: Tulsa, Oklahoma.
27. Riazi M.,Sohrabi M.,Jamiolahmady M., Experimental study of pore-scale mechanisms of carbonated water injection. Transport in Porous Media, 2011. **86**(1): p. 73-86.
28. Sedigheh Mahdavi L. A. J., Investigation of water flooding and carbonated water injection (cwi) in a fractured porous media, in International Symposium of the Society of Core Analysts 27 August - 1 September 2017: Vienna Austria.
29. Esene C.,Zendehboudi S.,Aborig A.,Shiri H., A modeling strategy to investigate carbonated water injection for EOR and CO_2 sequestration. Fuel, 2019. **252**: p. 710-721.
30. Sedigheh Mahdavi L. A. J., Investigation of carbonated water injection (cwi) for enhanced oil recovery in; pore-scale, core scale and simulation study. Doctoral Theses, 2018.
31. Van Genuchten M. T., A closed form equation for predicting the hydraulic conductivity of unsaturated soils. Soil Science Society of America Journal, 1980(44): p. 892-898.

Chapter 6 **Deterministic Tools to Predict Recovery Performance of Carbonated Water Injection**

Abstract

Carbonated water injection (CWI) is an efficient oil recovery method, which provides solution to the drawbacks of existing related recovery techniques such as water flooding and pure CO_2 injection. The recovery factor achieved from CWI is considerably higher than that for related CO_2-enhanced oil recovery (EOR) methods, due to effective transport phenomena involved in the displacement process. Additionally, the sequestration of anthropogenic CO_2 makes CWI even more attractive for practical implications. Although CWI has been experimentally proven to be an efficient technique, simulation/mathematical models to capture detailed CWI physics have been unreliable because of the complex recovery mechanisms associated with CWI. A majority of models have been developed based on unrealistic assumptions. Thus, existing models become doubtful and the confidence to apply CWI in the larger scales such as pilot plants becomes low. In this research work, smart methods such as artificial neural network (ANN), least squares support vector machine (LSSVM), and gene expression programming (GEP) are suggested to avoid the impractical and inconclusive assumptions. The connectionist techniques (e.g., ANN, LSSVM, and GEP) relate the recovery factor (RF) to the key input parameters such as pressure, temperature, viscosity, permeability, and injection rate based on pattern recognition without detailed knowledge about the process as well as use of the governing equations. The performance of the deterministic models is evaluated through using statistical parameters such as mean squared error (MSE), maximum absolute percentage error (MAAPE), minimum absolute percentage error (MIAPE), and goodness of fit (R^2). The results reveal that the ANN model has the lowest MSE (0.35), MIAPE (0.001), MAAPE (2.47), and the highest R^2 (0.99) in the testing phase. Based on the sensitivity analysis, pressure is recognized as the most important parameter, while temperature has the least rank in terms of significance. The findings of this research study can assist to provide a reasonable estimation of RF achievable from CWI, which can be an asset in better management and planning of CWI processes toward optimal conditions in terms of technical, economic, and environmental prospects.

Keywords: Carbonated Water Injection; Prediction Tools; Optimization; Recovery Factor; Sensitivity Analysis

6.1 Introduction

There are a variety of recovery and production strategies such as gas injection, low salinity water injection, polymer flooding, and carbonated water injection (CWI) that can enhance oil recovery rate and cumulative oil recovery, depending on rock and fluid properties [1-14]. CWI is an efficient oil recovery technique to further reduce residual oil saturation [1-2]. The major problems normally associated with water flooding and CO_2 injection such viscous fingering, early breakthrough, and CO_2 leakage can be mitigated by implementing CWI as an enhanced oil recovery (EOR) technique [15-20]. Additional oil recovery obtained during CWI has been investigated through several experimental and numerical studies. The secondary benefit associated with CWI is carbon storage [7, 15-17]. During CWI, complex transport phenomena occur where the main mechanisms to improve oil recovery during this process are mass transfer, oil swelling, viscosity reduction, and wettability. The mass transfer of CO_2 from water phase to oil phase is driven by the concentration gradient between the two fluids (oil and carbonated water) [1, 21, 22]. There is a subsequent decrease in the viscosity of oil and the rock wettability tends to be more water wet [6, 17, 22].

Experimental and modelling studies have been performed on CWI to understand the complex physics during CWI [6, 16, 17, 21-34] and to investigate the performance of CWI. The effects of operational parameters on CWI recovery factor were studied through an experimental work conducted by Miller and Jones [35]. It was reported that oil properties such as oil density and viscosity might change at particular operating conditions over CWI operation [35]. Several experiments have been also performed by other researchers to figure out the recovery mechanisms involved in CWI as well as to examine carbon storage potential of CWI [2, 21, 22, 26]. According to the literature, CWI would further reduce the residual oil saturation (and/or improve RF), compared to water flooding (WF); CO_2 storage capability was also confirmed upon implementing CWI [21, 22, 26]. Riazi et al. [33] performed laboratory tests in a micro model and reported that the oil swelling is the main mechanism that happens during CWI. In another experimental work, it was found that CWI offers a stable displacement pattern even in the presence of fractures due to the low mobility ratio [25]. Zhao and Ioannidis [30] carried out an experimental study on CWI to investigate the mass transfer phenomenon during CWI. The literature confirms that CWI leads to an additional oil recovery factor, compared to conventional water and CO_2 injection processes. However, the modeling works were not successful enough to well simulate the experimental tests

due to complex recovery mechanisms of CWI. Using the Buckley Leveret theory, De Nevers [25] simulated CWI in the secondary recovery mode. Although the capillary and gravity terms were ignored, the model was able to adequately capture the oil swelling and viscosity reduction. It is believed that neglecting the capillary and gravity terms causes considerable errors in modeling and calculations. In another 3-phase flow model introduced by Dixon et al. [29], the reaction term was not incorporated in their model. A 2-D model was also developed by Mansoori [28] to forecast the recovery factor during CWI. In their work, the diffusion, gravity, and reaction terms were not taken into account. Esene et al. [8] performed a modelling study on CWI in the field scale to investigate the influence of operational parameters, well orientation, and CO_2 storage during CWI. It was found that there is an optimum injection rate that leads to optimal performance of CWI. However, the reaction term was not important in their modelling work [8]. Most numerical modelling works regarding CWI suffer from serious drawbacks in terms of physics and applicability [17, 27, 31, 32]. Thus, the results obtained from the modelling approach might not well match with the experimental results. One of the reasons for this mismatch might be corresponded to the instantaneous equilibrium assumption in a majority of modelling studies [1]. The difficulty to accurately capture the entire physics involved during CWI (as an EOR technique) leads to the practical drawback. These limitations negate the application of CWI specifically in the pilot scale as the process has not been fully understood or modelled. Some of available models do not effectively and realistically simulate/model CWI as keys aspects such as reaction, gravity, diffusive terms, and oil swelling are overlooked, resulting in an over prediction or under prediction of CWI recovery factor. Hence, the accuracy of the CWI modelling results is limited.

The deterministic methods such as artificial neural network (ANN), least square support vector machine (LSSVM), response surface method (RSM), and gene expression programming (GEP) have proven to be reliable for prediction of target parameter(s) based on pattern recognition. The deterministic tools help to develop fast, simple, and accurate models by making connections between the input and output parameters without the involvement of governing equations [36]. The deterministic methods have been successfully applied in the oil and gas industry particularly in the prediction of oil recovery factor attained from EOR techniques. Ansari et al.[37] developed an ANN model to obtain the recovery performance of steam assisted gravity drainage (SAGD) as an EOR approach. It was reported that the model is able to accurately forecast the oil recovery factor of selected EOR projects with less than 10% error. Panja et al.[38] employed three smart

predictive techniques (ANN, RSM, and LSSVM) to estimate the hydrocarbon production from shales. Their model networks were constructed by using 80 % of the collected data for training and 20 % for testing. Their models were evaluated by determining the coefficient of determination and the normalized root mean square error. Based on the statistical analysis, there was a very good match between the modeling outputs and real data. Thus, the connectionist (smart) tools can serve as a proxy model to predict RF. It has been also proven that the ANN has strong potential to accurately estimate the recovery factor of CO_2-foam as an EOR technique where the recovery factor was measured from the laboratory CO_2-foam flooding tests [39]. Si and Bo [40] introduced a three-layer ANN model to obtain the magnitude of recovery factor during CO_2-WAG. Their model yielded a determination coefficient (R^2) of 98 % and a root mean square error of 3.2 %. Based on their research results, it was concluded that ANN is a proper predictive tool for the recovery assessment of most EOR projects for the purposes of project management and optimization. In addition, Zendehboudi et al. [41] employed a hybridized connectionist model, artificial neural network (ANN) combined with particle swarm optimization (PSO), to calculate RF and cumulative steam-to-oil ratio (CSOR) of SAGD in homogeneous and fracture reservoirs. Their model was validated through statistical parameters including mean squared error, coefficient of correlation, and average absolute deviation. It was concluded that ANN-PSO offers a reliable and accurate method to forecast recovery performance during SAGD with limited or unavailable experimental data. There are several studies in the open sources that discuss about conventional and hybrid smart models and their use for prediction of various important variables in chemical and petroleum engineering [42-51]. However, there are no adequate research works in the literature that utilize a variety of deterministic tools to investigate the recovery performance and optimization during CWI. Hence, the current research work aims to bridge this gap.

The main objective of this paper is to present efficient predictive methods to accurately estimate RF over CWI where data driven techniques are employed. The models are presented to build a network for pattern recognition based on significant relevant input parameters contributing to CWI to assess the recovery performance. Artificial neural network (ANN), least square support vector machine (LSSVM), and gene expression programming (GEP) approaches are selected where several experimental and numerical modelling data are used for the model construction. The effectiveness of the models is evaluated on the basis of statistical criteria such as mean squared error (MSE), goodness of fit (R^2), minimum absolute percentage error (MIAPE), and maximum

absolute percentage error (MAAPE). This current research will provide a forecasting tool for the RF over CWI without the need of the governing equations and complex multi-physics involved in CWI. The developed deterministic tools work based on the direct link between the inputs and output.

This paper is structured as follows. After the introductory section, the fundamentals/theory of deterministic tools (ANN, LSSVM, and GEP) are presented in section 6.2. The methodology and structure of the smart models are described in section 6.3. Section 6.4 lists the advantages and limitations of each method. The results and discussion are provided in section 6.5. The summary and research conclusions are given in the last section.

6.2 Theory of Deterministic Tools

In this section, a brief theory on ANN, LSSVM, and GEP as deterministic models is presented.

Artificial neural network. Artificial neural network (ANN) is a smart tool, which is used for a non-linear multivariate regression and pattern recognition between the inputs and output without considering governing equations. During the network construction, the training is achieved through a set of given input data and known outputs [36, 52]. Typically, the training phase can be supervised or unsupervised for pattern adaptation to the structured features of the input parameters [42-45, 53-55]. ANN was first demonstrated in 1950s for pattern recognition and since then, ANN has been implemented in several science and engineering fields such as transportation, telecommunication, aerospace, military, medical, and manufacturing [36, 47-55]. The schematic network of ANN is depicted in Figure 6.1. According to Figure 6.1, generally, the neural network architecture consists of an input layer, a hidden layer(s), and an output layer.

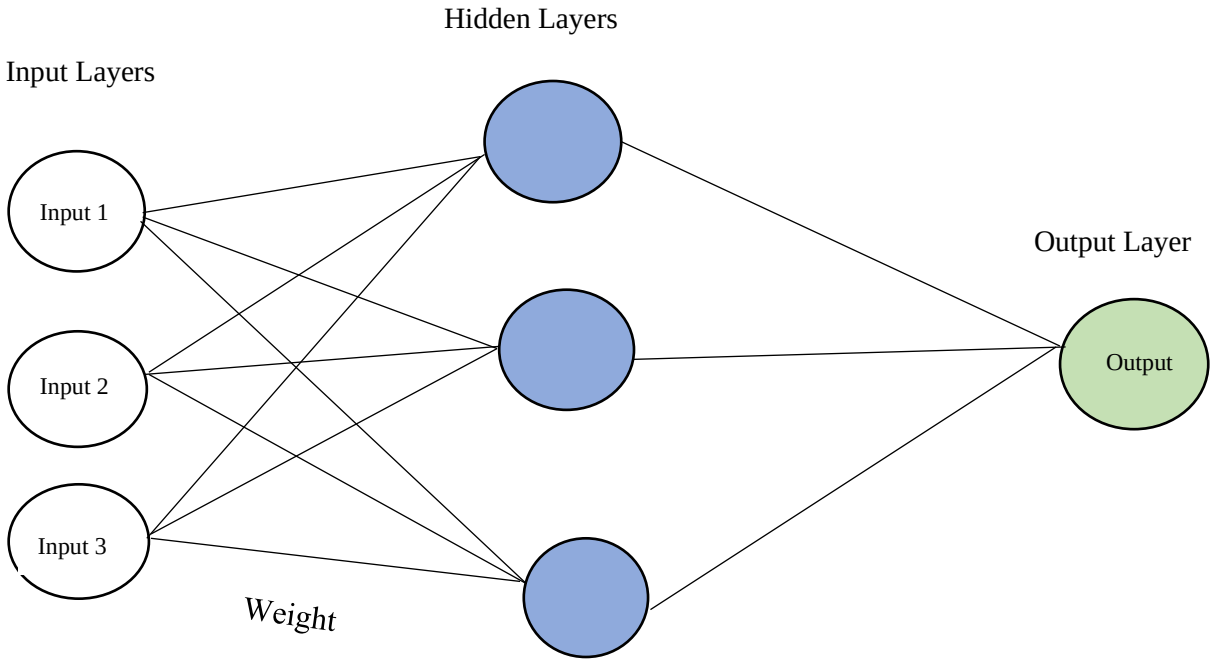

Figure 6.1: A schematic of a neural network architecture.

The hidden layer is characterized by several number of computation units called neurons and the selection of number of neurons and hidden layers depend on the non linearity of the problem [36]. As seen in Figure 6.1, the input layer is linked to the hidden layer by a certain weight, which is constantly being adjusted by an algorithm based on the real data. The hidden layer and the output layer are all connected/linked together in a forward direction.

Least squares support vector machine. least squares support vector machine (LSSVM) is a modified version of support vector machine (SVM) developed by Suykens and Vandewalle [56], which has considerably reduced the complexity, run time, and computational effort associated with the former version [36]. Figure 6.2 illustrates a simple architecture of the LSSVM strategy. In the modified LSSVM algorithm, the hyperplanes are optimized by using equality constraint instead of inequality constraint as well as the use of slack variables and a minimizing command [36, 47, 57] as shown in Equations (6.1) and (6.2).

$$Minimize \frac{1}{2} |\omega^2| + \frac{1}{2} \gamma \Sigma_{i=1}^{n} = \xi^2 \quad (6.1)$$

$$y_i = \left(\omega \phi (x_i)\right) + b + \xi_i \quad (6.2)$$

where ω, ξ, ϕ, and b represent the weight, slack variable, non-linearity function, and bias, respectively. γ is the constant that determines the trade-off between the minimum error and maximum margin [36, 47,48,57]. In this work, due to strong mapping ability and wide convergence domain, we adopt the radial basis kernel function (RBF) where the convergence speed is strongly dependent on the regularization parameter (γ) and RBF kernel width (σ^2). The kernel function, K (x_i,x_j), is determined by the following equation [47, 57]:

$$K\left(x_i, x_j\right) = \exp\left(-\frac{\left(\left|\left|x_i - x_j\right|\right|\right)^2}{\sigma^2}\right) \quad (6.3)$$

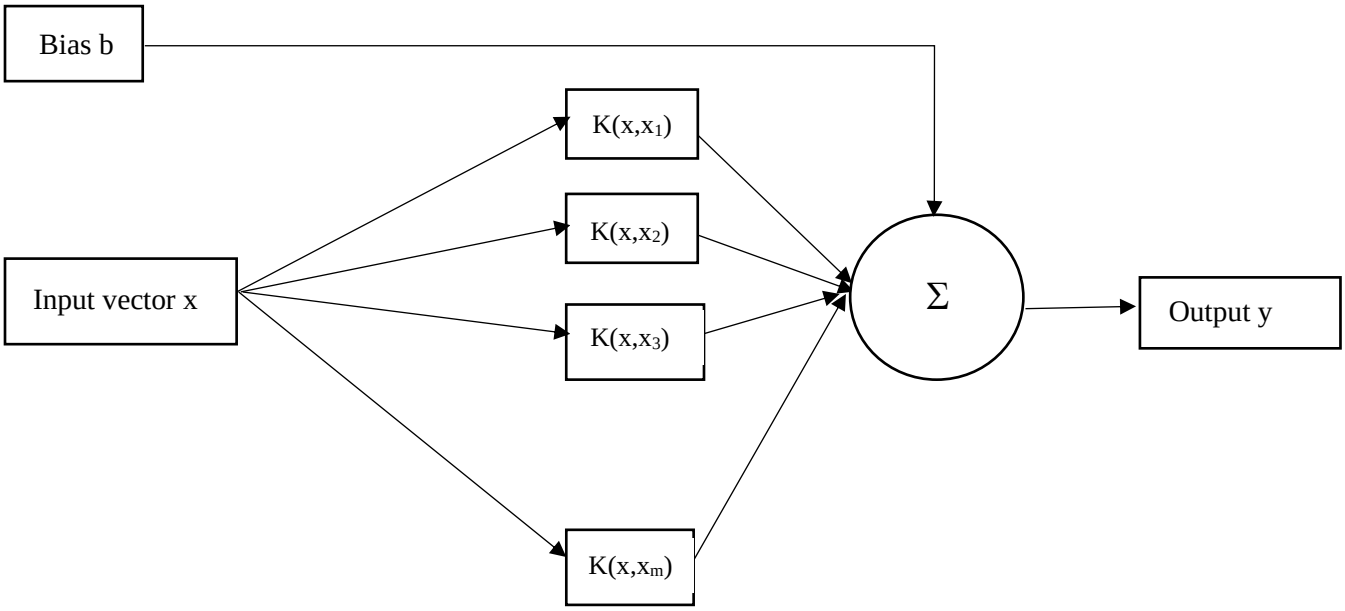

Figure 6.2: Simple structure of the least square support vector machine (modified after Neeraj) [58].

Unlike the ANN approach, a large amount of data is not required in the LSSVM method. This useful technique is not associated with a complex design structure and it exhibits a higher prediction accuracy based on data type.

Gene expression programming. As an artificial intelligence-based technique, gene expression programming (GEP) method was developed in 2001 by Ferreria [59]. The structure of GEP is based on the Darwin's theory of reproduction, mutation, and crossover [36, 60]. Similar to the Darwin's theory, the chromosomes become genes, which are characterised by tail terminals; and head functions aid in coding of any program necessary for effective solutions. As demonstrated in Figure 6.3, there is a schematic representation of a typical structure of chromosomes, head functions, and terminals such as (Q, -,× and /) and (x, y and z), respectively.

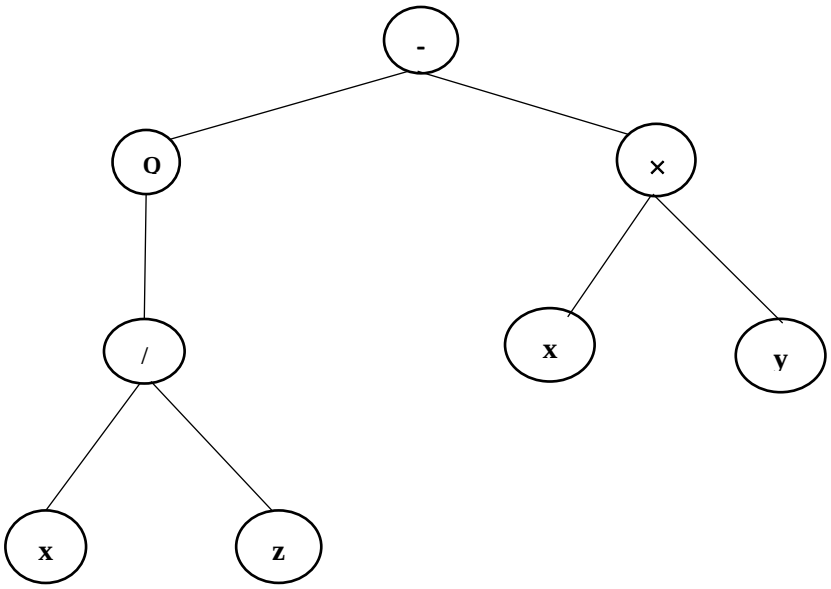

Figure 6.3: A simple configuration of an expression tree in GEP (modified after Hamideh et al.) [36].

Based on Figure 6.3, the mathematical expression is written from top to bottom and from left to right in the following form:

$$(\sqrt{x}/z) - (x \times y) \qquad (6.4)$$

Unlike the ANN models, the outputs of GEP appear in simple or complex mathematical functions without the influence of weight matrices, topology, and iteration choices [36].

6.3 **Methodology**

The objective of this research is to employ three different models such as ANN, LSSVM, and GEP to examine the performance of secondary CWI. The modeling results and real data are then compared for the validation purpose. The general workflow of developing ANN, LSSVM, and GEP models is mainly classified into data screening, selection of modeling tool, and statistical evaluation.

Data screening. To introduce proper deterministic models, an extensive amount of literature data and/or experimental results are collected from the open sources. Esene et al.[1] published a comprehensive review on CWI that discusses about the effects of various operational parameters, rock characteristics, and oil properties on the recovery performance of CWI based on several research studies in the literature. In their work, it was found that the CWI recovery performance is strongly dependent on injection pressure (p), injection rate (q), oil viscosity (μ), and rock characteristics such as permeability (K) and wettability [7, 16, 23, 24, 26-29, 31-33, 61-66]. The input and output data are normalized between 1 and -1 to attain convergence and to avoid numerical overflow [36], by the following equation:

$$\hat{x} = \frac{2(x_i - x_{min})}{(x_{max} - x_{min})} - 1 \tag{6.5}$$

In Equation (6.5), $\hat{x}$ is the normalized value of x_i; and x_{min} and x_{max} are the minimum and maximum magnitudes of x_i, respectively.

Selection of modeling tool. The tool box available in the MATLAB version of R2017a was utilized to implement the ANN modeling. It is recommended that a multi layered perceptron (MLP) back propagation training approach is used to achieve a proper ANN algorithm [36, 43, 57]. Appropriate MATLAB codes are also run to conduct LSSVM and GEP methods as the second and third deterministic tools in this research work.

Model statistical evaluation. After developing the ANN, LSSVM, and GEP models, the reliability and accuracy of the models are evaluated with statistical standards. The statistical parameters used for the assessment include the mean squared error (MSE), goodness of fit (R^2),

minimum absolute percentage error (MIAPE), and maximum absolute percentage error (MAAPE). The mathematical representations of these statistical evaluation parameters are given below:

$$MSE = \frac{1}{n}\sum\left(y_t^{(i)} - y_p^{(i)}\right)^2 \tag{6.6}$$

$$R^2 = 1 - \frac{\Sigma_{i=1}^{n}\left(y_t^{(i)} - y_p^{(i)}\right)^2}{\Sigma_{i=1}^{n}\left(y_t^{(i)} - \hat{y}\right)^2} \tag{6.7}$$

$$MIIPE = Max \mid \frac{y_{t-}^{(i)} y_p^{(i)}}{y_t^{(i)}} \mid \times 100 \tag{6.8}$$

$$MAAPE = Min \mid \frac{y_{t-}^{(i)} y_p^{(i)}}{y_t^{(i)}} \mid \times 100 \tag{6.9}$$

in which, $y_p^{(i)}, y_t^{(i)}, \hat{y}$, and n resemble the predictive value, real value, average of predicted outputs, and number of data points, respectively.

Data ranges. The required data are collected from the previous research studies available in the open sources [7, 16, 23, 24, 26-29, 31-33, 61-66]. The minimum and maximum values of the vital input parameters are listed in Table 6.1.

Table 6.1: Ranges of input data for predictive tools.

Parameter	**Minimum value**	**Maximum value**
Pressure	104.7 psia	6900 psia
Injection rate	0.01 cm^3/h	30 cm^3/h
Temperature	25 ^{o} C	142 ^{o} C
Viscosity	0.83 cP	289 cP
Permeability	500 mD	5700 mD

Before performing modeling approaches, the collected data are randomly divided into three subcategories so that we consider 70 % for training, 20 % for testing, and 10 % for validation steps. The training process is terminated when the statistical errors (MSE, MAAPE, and MIAPE) are minimal and the R^2 value is close to 1. The testing/validation datasets are used to check the reliability and accuracy of the models developed in the training phase. The precision and

appropriateness of introduced deterministic strategies are strongly dependent on the quantity and quality of dataset used to simulate system behaviors and pattern recognition.

6.4 **Pros and Cons of Deterministic Tools**

The smart models are simple, fast, and effective ways for prediction of an output variable(s). They generally offer a high computational speed and efficiency in pattern recognition and variable estimation without adequate knowledge of complex process physics and governing relationships. The main advantages and drawbacks of the ANN, LSSVM, and GEP techniques are presented in Table 6.2.

Table 6.2: Advantages and disadvantages of predictive models.

Deterministic approach	**Advantages**	**Limitations**
ANN	✓ ANN models generally provide a high prediction accuracy in most cases. ✓ ANN presents an efficient black box model for modelling of non-linear processes without defining certain link between inputs and output(s). ✓ It is flexible and highly adaptable. ✓ It can efficiently model randomly changing variables with a non-constant variance. ✓ ANN offers a more convenient modeling approach, compared to analytical, numerical, and hybrid strategies.	✓ With a small databank, ANN models offer less accurate results. ✓ ANN has slow convergence speed. ✓ It might be trapped at local minima with overfitting problems. ✓ The sensitivity or importance of input parameters cannot be analysed. ✓ ANN models provide a less generalization performance.
LSSVM	✓ LSSVM generally offers a good generalization performance.	✓ LSSVM uses sum square errors that may lead to less

	✓ It exhibits a good prediction accuracy. ✓ LSSVM does not require a high data range for estimation purpose. ✓ Complex structural design is not needed. ✓ There are no over fitting or under fitting issues with LSSVM. ✓ No local minima are experienced in LSSVM.	robust prediction without regularization. ✓ There is a lack of sparsity, which might limit LSSVM application for large-scale problems.
GEP	✓ Sensitivity analysis is possible using GEP to determine variable importance. ✓ A proper data visualization can be provided by GEP. ✓ GEP has a good iteration speed. ✓ GEP is able to generate a general mathematical formula based on gene expressions.	✓ The GEP method needs a considerable amount of data points to build a reliable and precise model.

6.5 **Results and Discussion**

In this research study, three powerful models; namely, ANN, LSSVM, and GEP are employed for prediction of oil recovery factor (RF) during carbonated water injection (CWI). The statistical analysis is performed to examine the effectiveness of the developed models. Additionally, a parametric sensitivity analysis is carried out to determine the importance of each input variable. The performance of the models in forecasting RF is also compared in this section.

ANN model performance. To investigate the appropriateness of ANN multilayer perceptron (MLP), the Levenberg -Marquardt back propagation algorithm is selected to train the network using the ANN tool box available in MATLAB 2017a. The collected data samples are split into training, testing, and validation parts. In this research, 70 % of the data is used for training, 20 % for testing, and 10 % for validation. One hidden layer with 10 neurons is enough for the case with 4 input parameters. According to Figure 6.4 and Table 6.1, the values of R-squared (R^2) for the training and testing phases are 0.9988 and 0.9937, respectively, while using the ANN-MLP. As clear from Figure 6.5, the predicted and target values (real data) follow an identical pattern. It implies that the developed model is able to simulate the real behaviour of the process. Conducting statistical evaluation, the magnitudes of MSE, MAAPE, and MIAPE for the training and testing phases are reported to be (1.10, 5.66, 2.91) and (0.35, 2.47, 0.001), respectively, as listed in Table 6.3

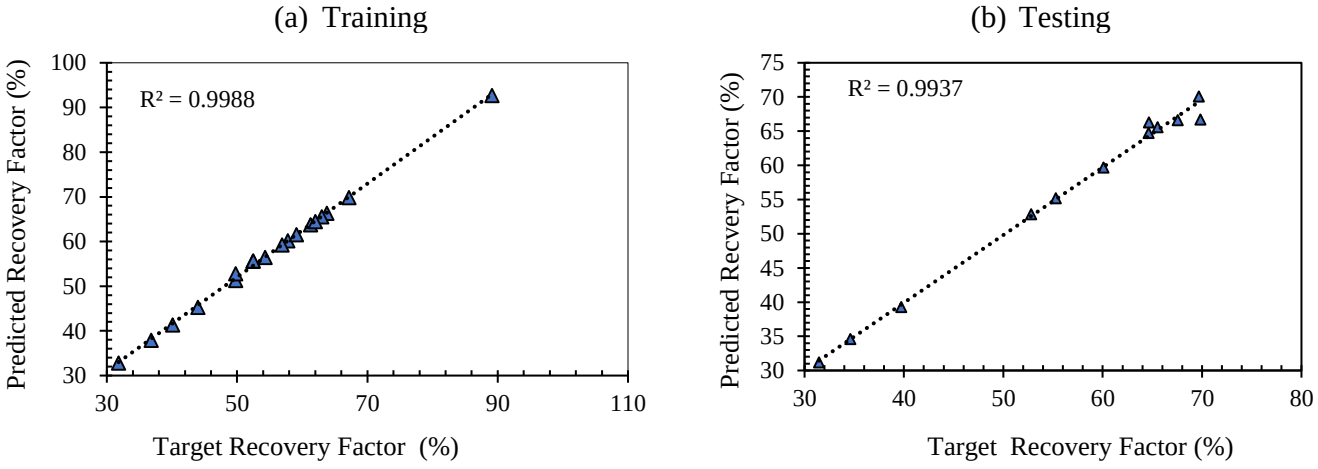

Figure 6.4: Performance of ANN model: (a) Training and (b) Testing.

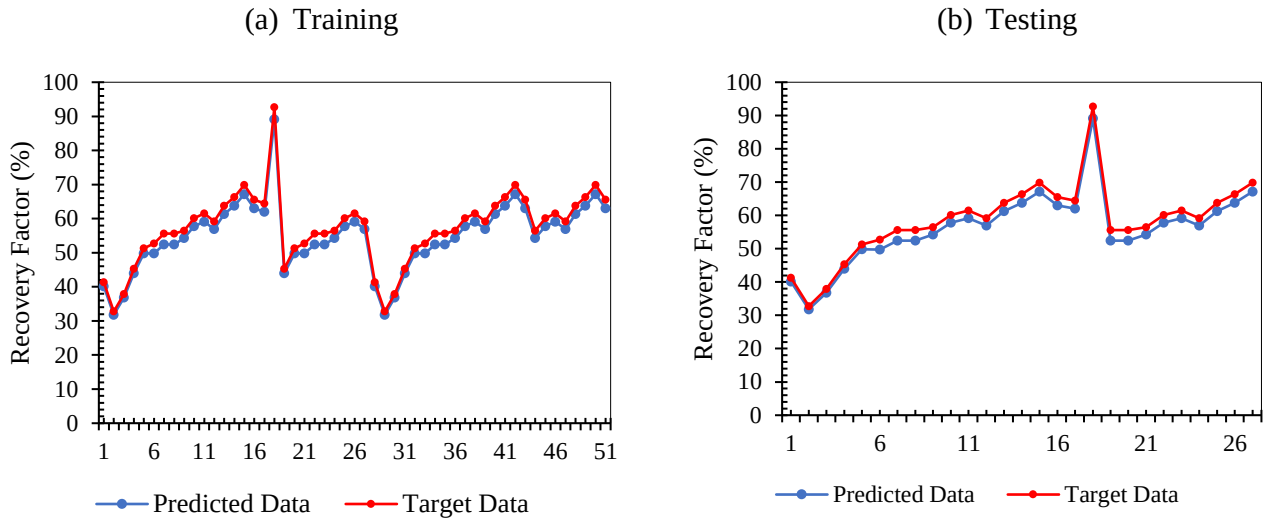

Figure 6.5: Predictions versus real data: (a) Training and (b) Testing.

Table 6.3: Statistical evaluation of the ANN deterministic model.

Parameter	ANN-MLP	
	Training	Testing
R^2	0.9988	0.9937
MSE	1.10	0.35
MAAPE	5.66	2.47
MIAPE	2.91	0.001

Based on the statistical analysis of the ANN-MLP model, there is very good agreement between the modeling results and literature data. Hence, the ANN-MLP can be used to determine the RF of CWI with a high accuracy in the absence of complicated and comprehensive numerical modeling strategies.

LSSVM model performance. The radial kernel function is used in the LSSVM model. The optimum values of σ^2 and γ are needed for the accurate prediction of RF. To obtain the optimum values, an R-squared value close to unity and a very small extent of MSE are the selection criteria. In this study, the optimum values of RBF kernel width (σ^2) and regularization parameter (γ) are 1.56×10^4 and 254.47, respectively. The outcomes of training and testing phases in the LSSVM

technique are depicted in Figure 6.6 (panels a and b). Table 6.4 also reports the values of statistical parameters obtained from the training and testing stages.

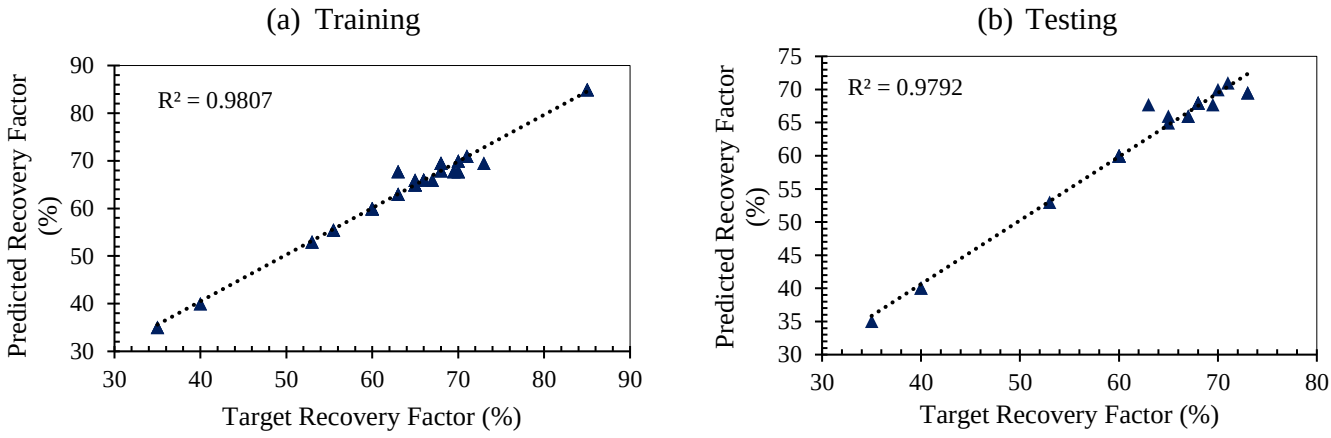

Figure 6.6: Performance of LSSVM method: (a) Training and (b) Testing.

Table 6.4: Statistical assessment of LSSVM for estimation of RF.

Parameter	**LSSVM**	
	Training	**Testing**
R^2	0.9807	0.9792
MSE	1.964	2.303
MAAPE	7.00	7.00
MIAPE	0.0011	0.0048

As it is clear from Figure 6.6 and Table 6.4, the values of R^2 are high (close to one) and all error percentages hold small values in both training and testing, indicating suitability and accuracy of the LSSVM method.

Figure 6.7 shows the estimated RF values versus the targeted values for both training and testing stages. Again, a good match is noticed between the predicted and real values. It also confirms that LSSVM is a proper deterministic model to simulate the CWI process in terms of recovery/production behaviour.

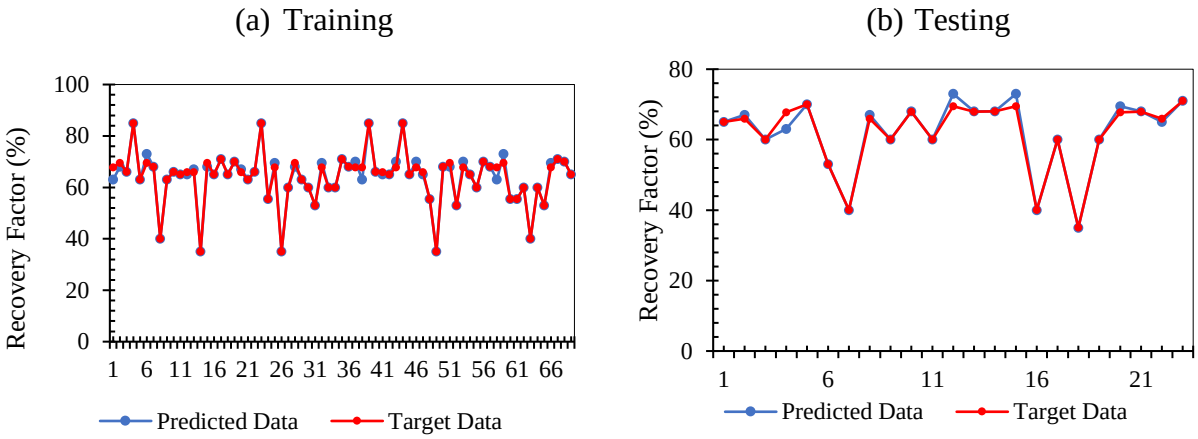

Figure 6.7: Comparison between the predicted RF and literature data: (a) Training and (b) Testing.

GEP performance. The performance of gene expression programming (GEP) is also evaluated using statistical parameters such as R^2, MSE, MAAPE, and MIAPE for both training and testing stages. According to Figure 6.8 (a) and Figure 6.8 (b), the R^2 values for training and testing are 0.82 and 0.51, respectively. Figure 6.9 shows the relationship/closeness degree of predicted values and real data. It can be concluded based on Figures 6.8 and 6.9 that GEP is not able to accurately predict RF of CWI at some points due to the limited number of data and complex nature of CWI process. Figure 6.10 illustrates the gene expression of the developed model and an overall predictive equation, which is deduced from the expression tree moving from bottom to top and from left to right, as introduced by Equations (6.9) – (6.12).

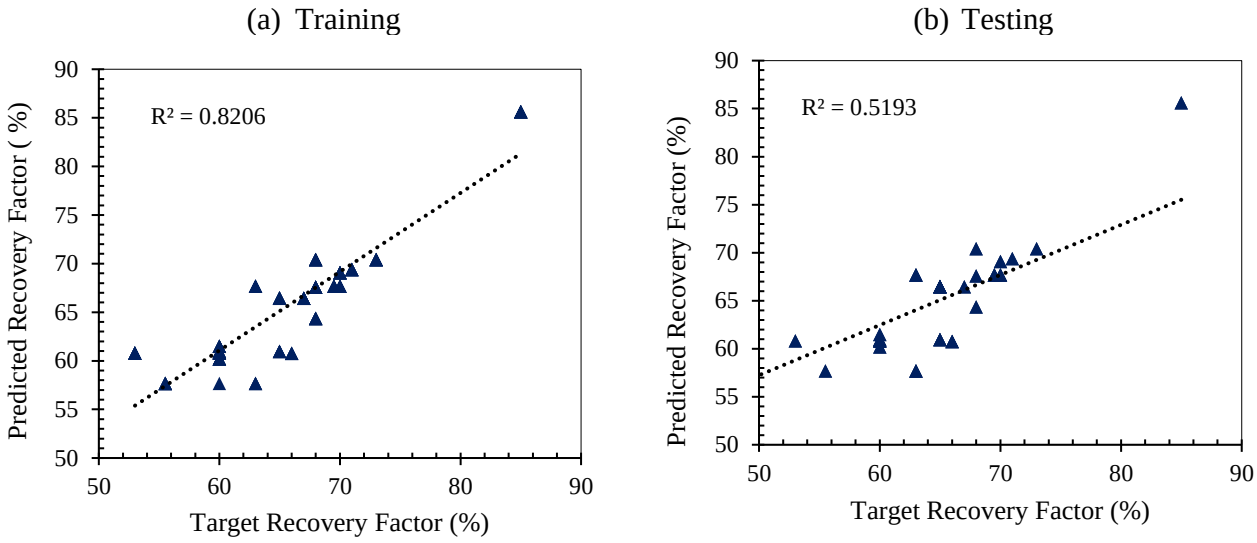

Figure 6.8: Performance of GEP model: (a) Training and (b) Testing.

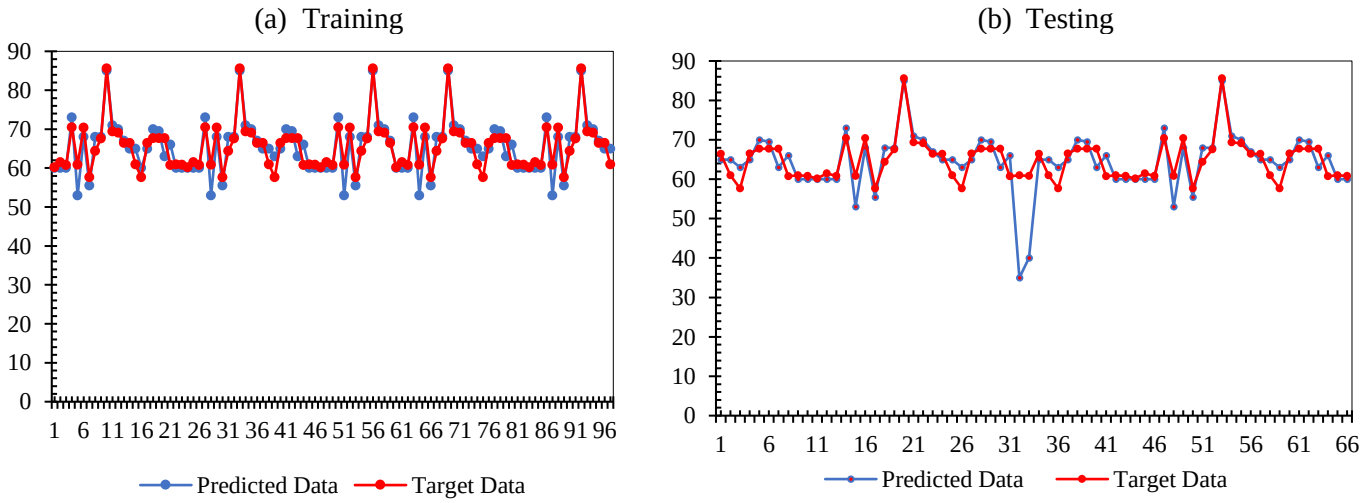

Figure 6.9: Predicted versus target RF data based on GEP approach: (a) Training and (b) Testing.

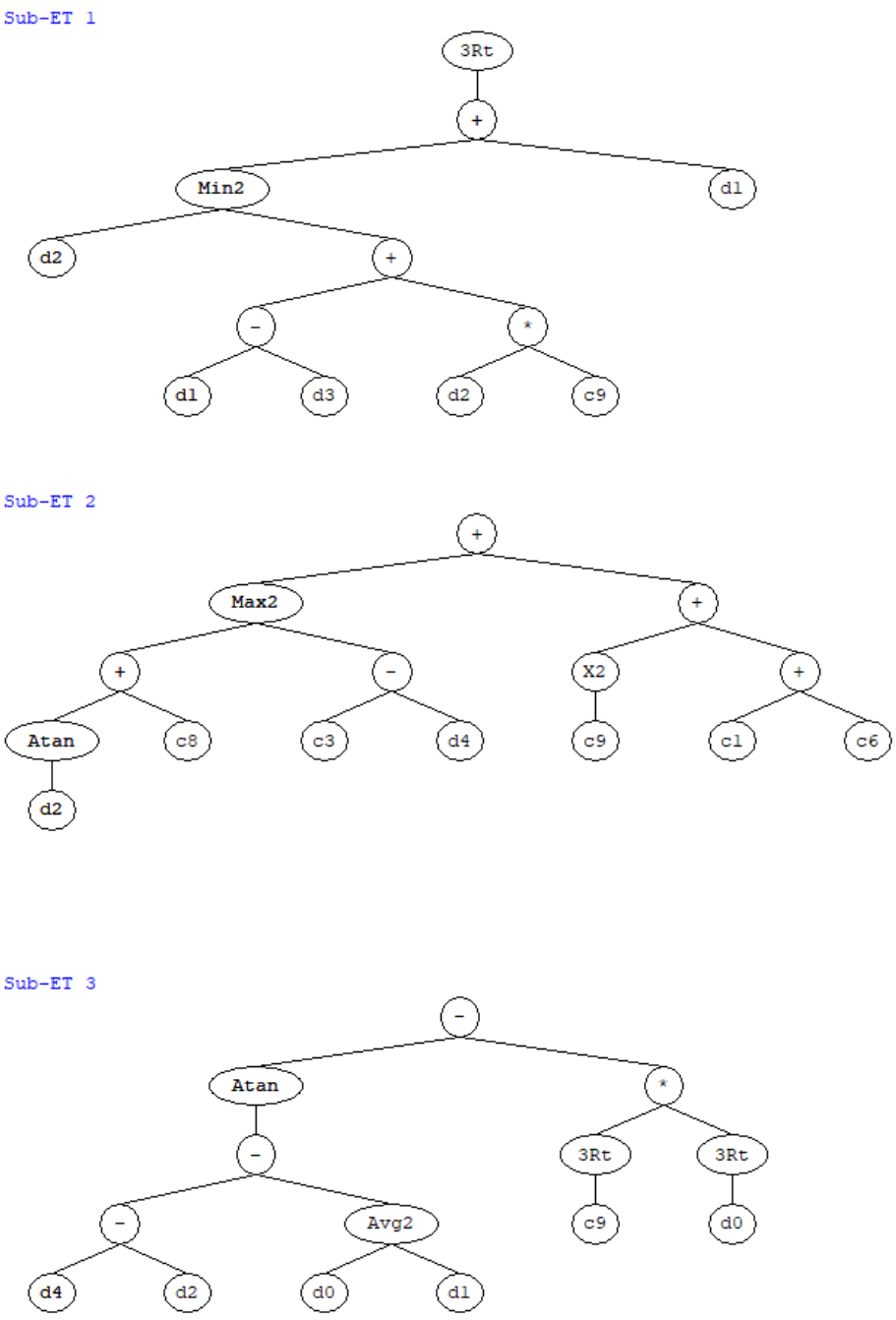

Figure 6.10: Expression trees of the developed GEP model.

The RF expression for the CWI process is given as follows:

Recovery factor = f(pressure (P), oil viscosity (μ), injection rate (Inj), permeability (K), Temperature (T))

$$y = a + b + c \tag{6.9}$$

$$a = 3Rt((\min(d(Inj)((d(T)\text{-}d(\mu)) + (d(Inj)*G1C9))) + d(T))); \tag{6.10}$$

$$b = a + (\max((\operatorname{atan}(d(Inj)) + G2C8), (G2C3 - d(K))) + ((G2C9\text{^}2) + (G2C1 + G2C6))); \tag{6.11}$$

$$c = b + (\operatorname{atan}(((d(K) - d(Inj)) - ((d(P) + d(T))/2.0))) - (3Rt(G3C9) * 3Rt(d(P)))); \tag{6.12}$$

where the constants of the above expressions are listed below:

$G1C9 = -1.32185644093142;\ G2C8 = 4.28788415173803;\ G2C3 = 9.00551741080966;$

$G2C9 = 8.17865535447249;\ G2C1 = 8.68805238863194;\ G2C6 = -8.78716914975432;$ and $G3C9 = 0.396876643392133$

The GEP model shows a low performance in estimating RF during CWI at some conditions as reflected in the low R^2 value associated with the testing phase as well as the high values of MSE, MAAPE, and MIAPE, as reported in Table 6.5.

Table 6.5: Statistical evaluation of the GEP model while determining RF.

Parameter	GEP	
	Training	**Testing**
R^2	0.8206	0.5193
MSE	8.425	25.967
MAAPE	12.85	74.14
MIAPE	0.33	0.33

Parametric sensitivity analysis. Although the GEP model is not as effective as other methods in this study to predict RF, it is a useful approach to identify the importance of input variables related to CWI through a systematic parametric sensitivity analysis (see Figure 6.11 and Table 6.6). The significance of each input variable toward predicting the RF during CWI is evaluated in this subsection, as presented in Table 6.6

(a) Pressure

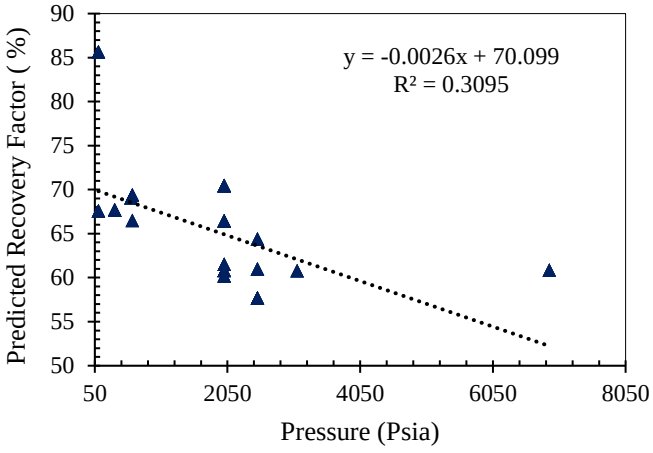

(b) Injection rate

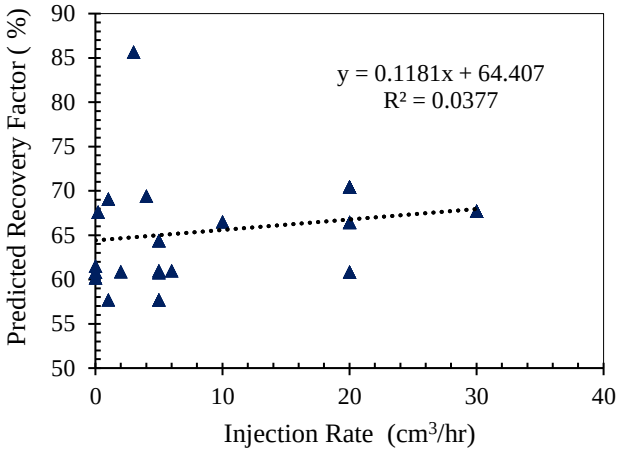

(c) Oil viscosity

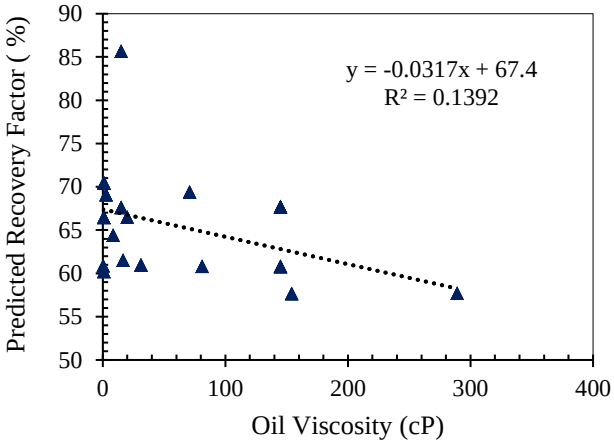

(d) Permeability

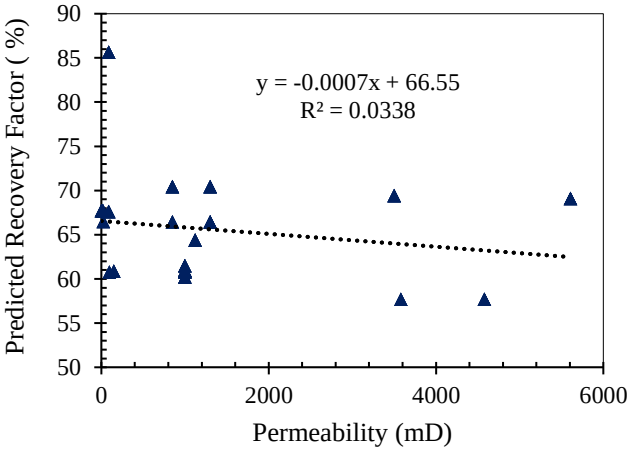

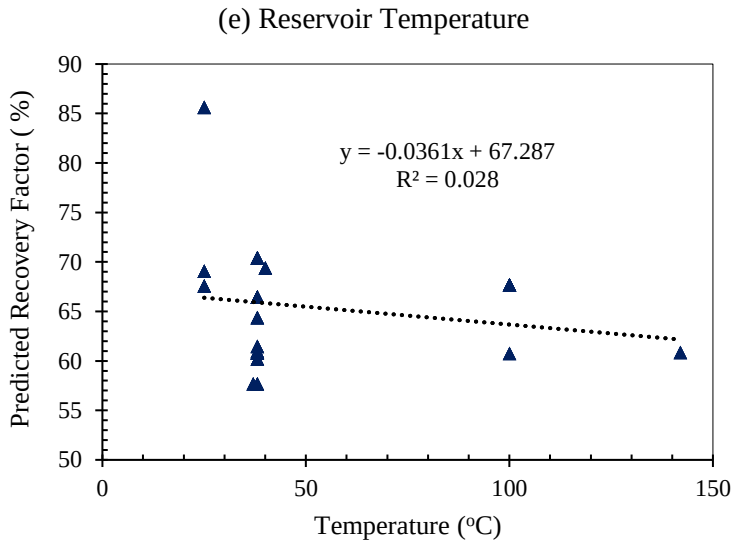

Figure 6.11: Significance of input variables for predicting RF of CWI while utilizing the GEP model: (a) Pressure, (b) Injection rate, (c) Oil viscosity, (d) Permeability, and (e) Temperature.

Table 6.6: Importance of input variables contributing to RF of CWI.

Input Variable	**R^2**
Pressure	0.3095
Injection rate	0.0377
Oil viscosity	0.1392
Permeability	0.033
Temperature	0.028

Based on Table 6.6, a high value of R^2 for an input parameter is an indicator of high importance of that input variable. Pressure with an R^2 value of 0.3095 has the highest level of importance, while the temperature has the least significance among the parameters (see Table 6.6). This is also confirmed by previous research works where the effects of operational parameters on CWI recovery factor were studied [1, 8]. The higher the pressure the more the solubility of CO_2 in water and consequently the overall performance of CWI is improved. The sensitivity analysis performed to determine the importance of input variables is useful to design proper experiments, model the process, and optimize the recovery operation. Also, the GEP provides several functions/equations

to determine the RF of CWI based on each input variable as seen in Figures 6.10 and 6.11. However, considering only one input parameter to obtain the target variable causes significant errors if other input variables have different values at various magnitudes of that included input parameter that seems logical. In general, the GEP model provides fair estimation of the objective function.

Comparison of models performance. Table 6.7 reports the values of statistical parameters such as R^2, MSE, MAAPE, and MIAPE to assess the overall performance of all deterministic tools introduced in this study. According to Table 6.7, the ANN model exhibits the best performance in terms of RF prediction, compared to LSSVM and GEP models, since the ANN has the highest value of R^2 and the minimum values of MSE, MAAPE, and MIAPE. However, the GEP model exhibits the lowest accuracy while forecasting RF of the CWI process.

Table 6.7: Prediction performance of smart models in the testing phase while obtaining RF.

Model	R^2	MSE	MAAPE	MIAPE
ANN	0.99	0.35	2.47	0.001
LSSVM	0.97	2.303	7.00	0.0048
GEP	0.51	25.96	74.14	0.33

This research introduces smart, easy, fast, and efficient methods to estimate RF during CWI without the need of complex theoretical governing equations. The reliability and quality check of the deterministic models are evaluated based on a statistical analysis.

Although CWI has been proven to be an effective EOR strategy, no pilot and field scales of this recovery approach have been reported in the recent years. This is due to the practical and theoretical limitations associated with model formulations and implication of CWI. With the use of developed deterministic tools, a quick prediction can be made on the amount of recoverable oil percentage based on the input operational parameters. This is possible without building sophisticated models or running complex reservoir simulation runs. The utilization of deterministic tools (ANN, LSSVM, and GEP) will help save resources, make fast and appropriate economic decisions, and optimize various stages of CWI projects.

6.6 **Summary and Conclusions**

Although CWI is an efficient and a promising EOR technique, accurate models that capture the complicated physics and recovery mechanisms of this recovery method are rare. In this research work, three different types of data driven models including ANN-MLP, LSSVM, and GEP are developed to predict the RF of CWI process. A considerable amount of data available in the open sources are collected and the input and output parameters are identified based on previous related experimental and modeling investigations. The effectiveness of the developed models is examined using the statistical parameters of R^2, MSE, MIAPE, and MAAPE. On the basis of the research results, the following conclusions can be drawn;

- The ANN-MLP model exhibits a better performance to obtain the RF during CWI with the limited available data, compared to the LSSVM and GEP models. For instance, the mean square error (MSE) of the ANN-MLP is considerably lower than that for LSSVM and GEP techniques.
- The optimum values of the RBF kernel width and regularization parameter to predict RF using the LSSVM model are 1.54×10^{4} and 254.47, respectively.
- One hidden layer that includes 10 neurons can well estimate the objective function while employing the ANN-MLP model.
- Deterministic tools such as ANN-MLP and LSSVM are efficient and powerful to offer a good prediction of the recovery factor attained from CWI as an EOR process. This is solely based on pattern recognition without the need of mathematical equations representing the physics and transport phenomenon of CWI.
- The GEP model is not able to precisely obtain RF with pattern recognition but this method can fairly categorize the importance of operational input variables. For example, it is found based on the GEP that the injection pressure is the most important parameter among the input parameters.
- The reliability and performance of the developed models will be greatly enhanced with the availability of more sample data related to the CWI process.

The limitation of the smart models is mainly resulted from unavailability of large dataset. As the interest in CWI in terms of research and practical implication prospects continues to grow, further

experimental, modelling, and reported field data will become available. Thus, more generalized and reliable deterministic tools for RF prediction can be developed in the near future.

ACKNOWLEDGEMENTS

The authors would like to acknowledge the Natural Sciences and Engineering Research Council of Canada (NSERC), Memorial University, InnovateNL, and Equinor Canada for supporting this research project.

NOMENCLATURES

Acronyms

ANN	Artificial Neural Network
CO_2	Carbon dioxide
CWI	Carbonated Water Injection
CW	Carbonated Water
EOR	Enhanced Oil Recovery
GEP	Gene Expression Programming
LSSVM	Least Square Support Vector Machine
mD	milli Darcy
MSE	Mean Square Error
MAAPE	Maximum Absolute Percentage Error
MIAPE	Minimum Absolute Percentage Error
MLP	Multi Layered Peceptron
RBF	Radial Basis Kernel Function
RSM	Root Square Mean
R^2	Coefficient of Determination
SAGD	Steam Assisted Gravity Drainage
SVM	Support Vector Machine
WF	Water Flooding

Variables and Parameters

b	bias
p	Injection pressure
K	Permeability
q	Injection rate
$\hat{x}$	Normalized value
x_{min}	Minimum magnitude
x_{max}	Maximum Magnitude
y_p	Predicted value

y_t	Real value
y	Average number of predicted
n	Data points

Greek Letters

μ	Viscosity (cP)
γ	Trade off
ξ	Slack variable
ω	weight
ϕx	Non-linearity function
σ	Kernel width

Subscripts

min	Minimum
max	Maximum
p	Predicted
t	Target

References

1. Esene C.,Rezaei N.,Aborig A.,Zendehboudi S., Comprehensive review of carbonated water injection for Enhanced Oil Recovery. Fuel, 2019. **237**: p. 1086-1107.
2. Riazi M.,Jamiolahmady M.,Sohrabi M., Theoretical investigation of pore-scale mechanisms of carbonated water injection. Journal of Petroleum Science and Engineering, 2011. **75**(3): p. 312-326.
3. Ghedan S. G., Global laboratory experience of CO_2-EOR flooding, in In: SPE/EAGE reservoir characterization and simulation conference. 12-19 October 2009, Society of Petroleum Engineer: Abu Dhabi.
4. Kulkarni M. M. R., Dandina N., Experimental investigation of miscible and immiscible water-alternating-gas (wag) process performance. Journal of Petroleum Science and Engineering, 2005. **48**(1): p. 1-20.
5. Mosavat N.,Torabi F., Micro-optical analysis of carbonated water injection in irregular and heterogeneous pore geometry. Fuel, 2016. **175**: p. 191-201.
6. Mosavat N.,Torabi F., Performance of secondary carbonated water injection in light oil systems. Industrial & Engineering Chemistry Research, 2014. **53**(3): p. 1262-1273.
7. Mosavat N.,Torabi F., Application of CO_2-saturated water flooding as a prospective safe CO_2 storage strategy. Energy Procedia, 2014. **63**: p. 5619-5630.
8. Esene C.,Zendehboudi S.,Aborig A.,Shiri H., A modeling strategy to investigate carbonated water injection for EOR and CO_2 sequestration. Fuel, 2019. **252**: p. 710-721.
9. Olayiwola S.,Dejam M., A comprehensive review on interaction of nanoparticles with low salinity water and surfactant for enhanced oil recovery in sandstone and carbonate reservoirs. Fuel, 2019. **241**: p. 1045-1057.

10. Olayiwola S.,Dejam M., Mathematical modelling of surface tension of nanoparticles in electrolyte solutions. Chemical Engineering Science, 2019. **197**: p. 345-356.
11. Rostami P.,Mehraban M. F.,Sharifi M.,Dejam M.,Ayatollahi S., Effect of water salinity on oil/brine interfacial behaviour during low salinity waterflooding: A mechanistic study. Petroleum, 2019.
12. Amirian E.,Dejam M.,Chen Z., Performance forecasting for polymer flooding in heavy oil reservoirs. Fuel, 2018. **216**: p. 83-100.
13. Saboorian-Jooybari H.,Dejam M.,Chen Z., Heavy oil polymer flooding from laboratory core floods to pilot tests and field applications: Half-century studies. Journal of Petroleum Science and Engineering, 2016. **142**: p. 85-100.
14. Mashayekhizadeh V.,Kord S.,Dejam M., Eor potential within iran. Special Topics Reviews in Porous Media: An International Journal, 2014. **5**: p. 325-354.
15. McFarlane R.,Breston J.,Neil D., Oil recovery from cores when flooded with carbonated water and liquid co2. Producers Monthly, 1952: p. 23-35.
16. Foroozesh J.,Jamiolahmady M., Simulation of carbonated water injection coreflood experiments: An insight into the wettability effect. Fuel, 2016. **184**: p. 581-589.
17. Foroozesh J.,Jamiolahmady M.,Sohrabi M., Mathematical modeling of carbonated water injection for EOR and CO_2 storage with a focus on mass transfer kinetics. Fuel, 2016. **174**: p. 325-332.
18. Li Z.,Firoozabadi A., Cubic-plus-association equation of state for water-containing mixtures: Is "cross association" necessary? AIChE Journal, 2009. **55**(7): p. 1803-1813.
19. Dejam M.,Hassanzadeh H., The role of natural fractures of finite double-porosity aquifers on diffusive leakage of brine during geological storage of CO_2. International Journal of Greenhouse Gas Control, 2018. **78**: p. 177-197.
20. Dejam M.,Hassanzadeh H., Diffusive leakage of brine from aquifers during CO_2 geological storage. Advances in Water Resources, 2018. **111**: p. 36-57.
21. Riazi M.,Sohrabi M.,Jamiolahmady M.,Ireland S.,Brown c., Oil recovery improvement using CO_2-enriched water injection, in EUROPEC/EAGE Conference and Exhibition. 8-11 June 2009, Society of Petroleum Engineers: Amsterdam, The Netherlands.
22. Sohrabi M.,Kechut N. I.,Riazi M.,Jamiolahmady M.,Ireland S.,Robertson G., Safe storage of CO_2 together with improved oil recovery by CO_2-enriched water injection. Chemical Engineering Research and Design, 2011. **89**(9): p. 1865-1872.
23. Kechut N. I.,Riazi M.,Sohrabi M.,Jamiolahmady M., Tertiary oil recovery and CO_2 sequestration by carbonated water injection (cwi), in SPE International Conference on CO_2 Capture, Storage, and Utilization. 10-12 November 2010, Society of Petroleum Engineers: New Orleans, Louisiana, USA.
24. Seyyedi M.,Sohrabi M.,Sisson A.,Ireland S., Quantification of oil recovery efficiency, CO_2 storage potential, and fluid-rock interactions by CWI in heterogeneous sandstone oil reservoirs. Journal of Molecular Liquids, 2018. **249**: p. 779-788.
25. De Nevers N., A calculation method for carbonated water flooding. Society of Petroleum Engineers Journal, 1964. **4**(01): p. 9-20.
26. Sohrabi M.,Kechut N.,Riazi M.,Jamiolahmady M.,Ireland S.,Brown C.,Robertson G., Coreflooding studies to investigate the potential of carbonated water injection as an injection strategy for improved oil recovery and CO_2 storage. Transport in Porous Media, 2009. **91**(1): p. 101-121.
27. Chang Y.-B.,Coats B. K.,Nolen J. S., A compositional model for CO_2 floods including CO_2 solubility in water. SPE Reservoir Evaluation & Engineering, 1998. **1**(02): p. 155-160.
28. Mansoori J., Compositional modeling of CO_2 flooding and the effect of CO_2 water solubility. 24 September 1982, Society of Petroleum Engineers.
29. Ramesh A. B.,Dixon T. N., Numerical simulation of carbonated waterflooding in a heterogeneous reservoir, in SPE Symposium on Numerical Simulation of Reservoir Performance. 11-12 January, 1973, Society of Petroleum Engineers: Houston, Texas.

30. Zhao W.,Ioannidis M., Gas exsolution and flow during supersaturated water injection in porous media: I. Pore network modeling. Vol. 34. 2011. 2-14.
31. Kechut N. I.,Jamiolahmady M.,Sohrabi M., Numerical simulation of experimental carbonated water injection (CWI) for improved oil recovery and CO_2 storage. Journal of Petroleum Science and Engineering, 2011. **77**(1): p. 111-120.
32. Ahmadi M. A.,Hasanvand M. z.,Behbahani S. S.,Nourmohammad A.,Vahidi A.,Amiri M.,Ahmadi G., Effect of operational parameters on the performance of carbonated water injection: Experimental and numerical modeling study. The Journal of Supercritical Fluids, 2016. **107**: p. 542-548.
33. Riazi M.,Sohrabi M.,Jamiolahmady M., Experimental study of pore-scale mechanisms of carbonated water injection. Transport in Porous Media, 2011. **86**(1): p. 73-86.
34. Sedigheh Mahdavi L. A. J., Investigation of water flooding and carbonated water injection (CWI) in a fractured porous media, in International Symposium of the Society of Core Analysts 27 August - 1 September 2017: Vienna Austria.
35. Miller J. S. J., Ray A., A laboratory study to determine physical characteristics of heavy oil after CO_2 saturation, in SPE/DOE Enhanced Oil Recovery Symposium. 5-8 April 1981, Society of Petroleum Engineers: Tulsa, Oklahoma.
36. Hamedi H.,Ehteshami M.,Mirbagheri S. A.,Zendehboudi S., New deterministic tools to systematically investigate fouling occurrence in membrane bioreactors. Chemical Engineering Research and Design, 2019. **144**: p. 334-353.
37. Ansari A.,Heras M.,Nones J.,Mohammadpoor M.,Torabi F., Predicting the performance of steam assisted gravity drainage (sagd) method utilizing artificial neural network (ann). Petroleum, 2019.
38. Panja P.,Velasco R.,Pathak M.,Deo M., Application of artificial intelligence to forecast hydrocarbon production from shales. Petroleum, 2018. **4**(1): p. 75-89.
39. Seyedeh Raha Moosavi D. A. W., Mohammad Ali Ahmadi,Abouzar Choubineh, Ann-based prediction of laboratory-scale performance of CO_2-foam flooding for improving oil recovery. Natural Resources Research, 2019: p. 1-19.
40. Le Van S.,Chon H. B., Applicability of an artificial neural network for predicting water-alternating-CO_2 performance. Energies, 2017. **10**(7).
41. Zendehboudi S., Rajabzadeh A.R., Bahadori A., Chatzis I., Dusseault M. B., Elkamel A., Lohi A., Fowler M., Connectionist model to estimate performance of steam-assisted gravity drainage in fractured and unfractured petroleum reservoirs: enhanced oil recovery implications. Industrial & Engineering Chemistry Research 2014, 53 (4), 1645-1662.
42. Kamari A., Bahadori A., Mohammadi A.H., Zendehboudi S. New tools predict monoethylene glycol injection rate for natural gas hydrate inhibition. Journal of Loss Prevention in the Process Industries 2015, 33, 222-231.
43. Kamari A., Mohammadi A.H., Bahadori A., Zendehboudi S. Prediction of air specific heat ratios at elevated pressures using a novel modeling approach. Chemical Engineering & Technology 2014, 37 (12), 2047-2055.
44. Arabloo M., Bahadori A., Ghiasi M.M., Lee M., Abbas A., Zendehboudi S. A novel modeling approach to optimize oxygen–steam ratios in coal gasification process. Fuel 2015, 153, 1-5.
45. Chamkalani A., Zendehboudi S., Bahadori A., Kharrat R., Chamkalani R., James L., Chatzis I. Integration of LSSVM technique with PSO to determine asphaltene deposition. Journal of Petroleum Science and Engineering 2014, 124, 243-253.
46. Kamari A., Bahadori A., Mohammadi A.H., Zendehboudi S. Evaluating the unloading gradient pressure in continuous gas-lift systems during petroleum production operations. Petroleum Science and Technology 2014, 32 (24), 2961-2968.
47. Zendehboudi S., Rezaei N., Lohi A. Applications of hybrid models in chemical, petroleum, and energy systems: A systematic review. Applied energy 2018, 228, 2539-2566.

48. Ghiasi M.M., Arabloo M., Bahadori A., Zendehboudi S. Prediction of methanol loss in liquid hydrocarbon phase during natural gas hydrate inhibition using rigorous models. Journal of Loss Prevention in the Process Industries 2015, 33, 1-9.
49. Rajabzadeh A.R., Ruzich N., Zendehboudi S., Rahbari M. Biomass leachate treatment and nutrient recovery using reverse osmosis: experimental study and hybrid artificial neural network modeling. Energy & Fuels 2012, 26 (12), 7155-7163.
50. Chamkalani A., Zendehboudi S., Amani M., Chamkalani R., James L., Dusseault, M.B. Pattern recognition insight into drilling optimization of shaly formations. Journal of Petroleum Science and Engineering 2017, 156, 322-339.
51. Dashti A., Raji M., Razmi A., Rezaei N., Zendehboudi S., Asghari M. Efficient hybrid modeling of CO2 absorption in aqueous solution of piperazine: Applications to energy and environment. Chemical Engineering Research and Design 2019, 144, 405-417.
52. Hornik K.,Stinchcombe M.,White H., Universal approximation of an unknown mapping and its derivatives using multilayer feedforward networks. Neural Networks, 1990. **3**(5): p. 551-560.
53. Soleimani R.,Shoushtari N. A.,Mirza B.,Salahi A., Experimental investigation, modeling and optimization of membrane separation using artificial neural network and multi-objective optimization using genetic algorithm. Chemical Engineering Research and Design, 2013. **91**(5): p. 883-903.
54. Ghiasi M. M.,Bahadori A.,Zendehboudi S., Estimation of the water content of natural gas dried by solid calcium chloride dehydrator units. Fuel, 2014. **117**: p. 33-42.
55. Zendehboudi S.,Shafiei A.,Bahadori A.,James L. A.,Elkamel A.,Lohi A., Asphaltene precipitation and deposition in oil reservoirs – technical aspects, experimental and hybrid neural network predictive tools. Chemical Engineering Research and Design, 2014. **92**(5): p. 857-875.
56. Suykens J. A. K.,Vandewalle J., Least squares support vector machine classifiers. Neural Processing Letters, 1999. **9**(3): p. 293-300.
57. Fayazi A.,Arabloo M.,Mohammadi A. H., Efficient estimation of natural gas compressibility factor using a rigorous method. Journal of Natural Gas Science and Engineering, 2014. **16**: p. 8-17.
58. Neeraj Dhanraj Bokde A. E. F., Daniel Villanueva,K.D. Kulat, A review on hybrid empirical mode decomposition models for wind speed and wind power prediction. Energies, 2019. **12**(2): p. 1-42.
59. C.Ferreria, Gene expression programming; a new adaptive algorithm for solving problems. Complex syst, 2001. **13**.
60. Roy S.,Ghosh A.,Das A. K.,Banerjee R., Development and validation of a GEP model to predict the performance and exhaust emission parameters of a crdi assisted single cylinder diesel engine coupled with egr. Applied Energy, 2015. **140**: p. 52-64.
61. Alizadeh A. H.,Khishvand M.,Ioannidis M. A.,Piri M., Multi-scale experimental study of carbonated water injection: An effective process for mobilization and recovery of trapped oil. Fuel, 2014. **132**: p. 219-235.
62. Dong Y.,Dindoruk B.,Ishizawa C.,Lewis E. J.,kubicek T., An experimental investigation of carbonated water flooding, in SPE Annual Technical Conference and Exhibition. 2011, Society of Petroleum Engineers: Denver, Colorado, USA. p. 16.
63. Kilybay A.,Ghosh B.,Chacko Thomas N.,Sulemana N., Hybrid eor technology: Carbonated water-smart water flood improved recovery in oil wet carbonate formation: Part-ii. 2017.
64. Mahzari P.,Tsolis P.,Farzaneh S. A.,Sohrabi M.,Enezi S.,Yousef A. A.,Eidan A. A., A comprehensive experimental study of pore-scale and core-scale processes during carbonated water injection under reservoir conditions, in SPE Kingdom of Saudi Arabia Annual Technical Symposium and Exhibition. 2017, Society of Petroleum Engineers: Dammam, Saudi Arabia. p. 27.
65. Sohrabi M.,Emadi A.,Farzaneh S. A.,Ireland S., A thorough investigation of mechanisms of enhanced oil recovery by carbonated water injection, in SPE Annual Technical Conference and Exhibition. 2015, Society of Petroleum Engineers: Houston, Texas, USA. p. 33.

66. Al Mesmari A.,Mahzari P.,Sohrabi M., Modelling formation of a new fluid phase during carbonated water injection, in International Petroleum Technology Conference. 2016, International Petroleum Technology Conference: Bangkok, Thailand. p. 13.
67. Mirbagheri S. A.,Bagheri M.,Bagheri Z.,Kamarkhani A. M., Evaluation and prediction of membrane fouling in a submerged membrane bioreactor with simultaneous upward and downward aeration using artificial neural network-genetic algorithm. Process Safety and Environmental Protection, 2015. **96**: p. 111-124.
68. Samanta B., Gear fault detection using artificial neural networks and support vector machines with genetic algorithms. Mechanical Systems and Signal Processing, 2004. **18**(3): p. 625-644.
69. Le-Clech P.,Chen V.,Fane T. A. G., Fouling in membrane bioreactors used in wastewater treatment. Journal of Membrane Science, 2006. **284**(1): p. 17-53.
70. Diez V.,Ezquerra D.,Cabezas J. L.,García A.,Ramos C., A modified method for evaluation of critical flux, fouling rate and in situ determination of resistance and compressibility in mbr under different fouling conditions. Journal of Membrane Science, 2014. **453**: p. 1-11.

Chapter 7 **Summary Conclusion and Recommendation**

Carbonated water injection is an effective means to recovery oil as already been investigated in several research experimental studies. Modelling approaches of CWI found in open sources have so many limitations and this thesis addresses those limitations and presents a novel method for developing CWI models. This thesis in chapter 2, presents a comprehensive overview of CWI, in the pore scale, core scale and field scale. Fluid-fluid, Fluid-rock interactions, the effects of important variables on CWI performance (fluid properties, reservoir properties, and operating conditions) are also extensively studied and summarized for the field, experimental, and modelling approaches of CWI. In chapter 3, this thesis presents an investigation of how to determine a critical salinity necessary for EOR and optimum for the solubility of CO_2 which will enhance the performance of CWI models. A unique modelling strategy that captures most of the physics during CWI and relaxing past assumptions is presented in chapter 4. The effect of reaction term as a constitutive physics during CWI was considered in a core scale investigation which is presented in chapter 5. Chapter 6 presents the use of artificial intelligence and other deterministic tools to predict the R.F during carbonated water injection which solely relies on a black box model without the need of equations governing the physical/chemical system.

7.1 **Conclusion**

The major conclusions of this manuscript-based thesis are presented below in this section

- Although CWI is assumed to be a single-phase injection of completely dissolved CO_2 in water, the effect of gas exsolution can occur as the pressure drops. This phenomenon will provide an additional energy for the displacement of oil along the gas growth path, leading to an additional oil recovery.

- The reservoir heterogeneity does not reduce the performance of CWI as CW was able to sustain a stable front even along the fractured channels or zones.

- CO_2 storage capacity appears to be an additional benefit during the implementation of CWI. There are many research and industrial projects ongoing in the area of carbon management where CWI is proposed for EOR and CO_2 sequestration purposes.
- A decrease in salinity content for a sandstone reservoir offers a considerable increase in the oil recovery factor until a critical salinity below which no significant change occurs in the recovery factor.
- Analyzing the recovery data of carbonate reservoirs, there is an optimum salinity which gives the maximum oil recovery; further decrease behind this salinity lowers the recovery factor.
- There is a stable and piston-like displacement of oil by CWI because of similarities of fluid densities and low mobility ratio. Therefore, there are no problems such as gravity override and viscous fingering with CWI, which are associated with pure gas injection and conventional water flooding.
- A higher recovery factor is achieved with CWI when compared to WF because of the changes in the oil properties associated with the mass transfer of CO_2 into oil.
- More CO_2 is dissolved in water during high injection pressure according to the Henry's law, which improves the overall performance of CWI.
- There is a critical injection rate to ensure a maximum contact time between the fluids (CW and oil) for effective mass transfer across phases.
- A secondary benefit associated with implementing CWI is its high potential for anthropogenic carbon dioxide storage. The amount of CO_2 stored is strongly dependent on the operational injection pressure
- In the core scale a recovery factor (60 % - 78 %) is achieved with CWI when compared to WF (30 % - 45 %) because of the changes in the oil properties associated with the mass transfer of CO_2 into oil. This R.F of CWI is expected in a full reservoir after upscaling although is largely dependent of the reservoir petro-physical properties, oil properties and operational parameters
- The increase in pressure leads to an improvement in the overall performance of CWI. More CO_2 is dissolved in water during high injection pressure according to the Henry's law.
- The performance of CWI in light oil is much better when applied to a more viscous heavy oil due to variations in solubility gradient.

- The performance of CWI in a high temperature reservoir is lower comparatively to medium temperature reservoir. This is because at high temperatures the CO_2 gas possesses a high kinetic energy which reduces its solubility in water.
- ANN-MLP model exhibits a better performance to predict the R.F during CWI with the limited data that was used when compared to the LSSVM and GEP models. The mean square error of ANN-MLP is considerably lower than that obtained from the LSSVM and GEP models specifically to this research.
- The optimum values to predict R.F using the LSSVM model are obtained based on 1.54×10^4 and 254.47 for the RBF kernel width and regularization parameter respectively.
- Ten neurons with one hidden layer is adequate to develop a predictive ANN-MLP model
- Deterministic tool such as ANN-MLP and LSSVM models are exceptional tools to give a good prediction of the obtainable recovery factor of CWI during an EOR process. This is solely based on pattern recognition without the need of mathematical equations representing the physical phenomenon of CWI.
- The GEP model was not able to accurately predict R.F with pattern recognition but was able to fairly categorize the importance of operational input variable and identifies pressure to be the most important parameter.
- The reliability and performance of the developed model will be greatly enhanced with the availability of more sample data relating to CWI necessary for modelling of deterministic tools.

7.2 **Recommendations**

Although considerable effort has been made in this thesis to develop model that can be used to investigate CWI, future recommendations are presented in this section to aid in consistent and progressive improvement of CWI as an oil recovery technique.

- Advanced laboratory experiments are recommended to generate the relative permeability of oil as function of carbonated water will help to improve the understanding of phase movement (CW and oil) during the displacement process and improve other modelling works.
- The occurrence of asphaltene precipitation during CWI operations has not been highlighted in several research works, while it is expected to occur during the CO_2 exsolution resulted

from the pressure drop. Advanced experimental studies are needed to investigate asphaltene occurrence.

- Further modelling and experimental investigations are recommended to systematically study the influence of mineral reactions as this may be a dominant factor affecting oil recovery in the presence of bicarbonates and other catalytic ions in the formation water
- The development of a field scale model is recommended using COMSOL Multiphysics to investigate CWI following the procedure/approach highlighted in this paper. This will account for reservoir heterogeneities for a more robust model to predict R.F during CWI
- As the interest in CWI studies continues to grow, the availability of more experimental, modelling and reported field data will increase and become available. When more data becomes readily available, it is recommended that deterministic tools for R.F prediction should be re-developed to enhance model accuracy during CWI.